HAL
open science

Les fondements neurophysiologiques de la latéralisation motrice : le paradigme des mouvements en miroir

Quentin Welniarz

▶ **To cite this version:**

Quentin Welniarz. Les fondements neurophysiologiques de la latéralisation motrice : le paradigme des mouvements en miroir. Neurosciences [q-bio.NC]. Université Pierre et Marie Curie - Paris VI, 2016. Français. NNT : 2016PA066235 . tel-01839462

HAL Id: tel-01839462

https://theses.hal.science/tel-01839462v1

Submitted on 15 Jul 2018

HAL is a multi-disciplinary open access archive for the deposit and dissemination of scientific research documents, whether they are published or not. The documents may come from teaching and research institutions in France or abroad, or from public or private research centers.

L'archive ouverte pluridisciplinaire **HAL**, est destinée au dépôt et à la diffusion de documents scientifiques de niveau recherche, publiés ou non, émanant des établissements d'enseignement et de recherche français ou étrangers, des laboratoires publics ou privés.

Université Pierre et Marie Curie

Ecole doctorale Cerveau-Cognition-Comportement (ED3C)

Inserm, U1127, CNRS, UMR 7225, Institut du Cerveau et de la moelle épinière

Equipe Mouvements anormaux et ganglions de la base : physiopathologie et thérapeutique expérimentale, Pr Vidailhet et Pr Lehéricy

Les fondements neurophysiologiques de la latéralisation motrice : le paradigme des mouvements en miroir

Par Quentin Welniarz

Thèse de doctorat en neurosciences

Codirigée par Emmanuel Flamand-Roze et Isabelle Dusart

Présentée et soutenue publiquement le 13 Juillet 2016

Devant un jury composé de :

Dr. Patricia Gaspard, directrice de recherche, Présidente du jury

Dr. Sonia Garel, directrice de recherche, Rapporteure

Pr. Julie Duqué, Professeure à l'université de Louvain, Rapporteure

Pr. Pascal Derkinderen, PU-PH, Examinateur

Pr. Emmanuel Flamand-Roze, PU-PH, Directeur de thèse

Dr. Isabelle Dusart, directrice de recherche, Directrice de thèse

This work is licensed under a Creative Commons Attribution-NonCommercial 4.0 International License.

TABLE DES MATIERES

TABLE DES MATIERES 3

REMERCIEMENTS 7

ABREVIATIONS 11

LISTE DES FIGURES 13

INTRODUCTION 15

I. Les mouvements en miroir congénitaux : un paradigme pour l'étude des bases neurophysiologiques de la latéralisation motrice 16

A. Préambule : comprendre le normal par le pathologique 16

B. Mouvements en miroir congénitaux 17

1) Définition et description clinique 17

2) Autres pathologies associées aux mouvements en miroir 19

3) Génétique des mouvements en miroir congénitaux 20

C. Revue de la littérature 1 : Applaudir d'une main, la latéralisation du contrôle moteur 27

D. Problématique et objectifs de la thèse 40

II. Evolution, anatomie, développement et pathologies du corps calleux et du faisceau corticospinal 43

A. Evolution, anatomie, développement et pathologies du corps calleux 43

1) Le corps calleux au sein de l'évolution 43

2) Anatomie et organisation du corps calleux 47

3) Développement comparé du corps calleux chez les euthériens 50

4) Génération des neurones calleux au cours du développement chez la souris 53

5) Développement des structures nécessaires à la formation du corps calleux 62

6) Guidage des axones calleux au cours du développement 64

7) Pathologies développementales du corps calleux chez l'humain 75

B. Revue de la littérature 2 : Le faisceau corticospinal, évolution, développement et pathologies humaines (soumis) 78

C. Développement comparé du système nerveux central chez différents mammifères .. 118

III. Latéralisation du contrôle moteur au cours de la préparation du mouvement ... 120

A. MM et préparation motrice 120

B. Exécution de mouvements latéralisés 122

1) L'exécution d'un mouvement unimanuel est associée à l'activation latéralisée du système moteur 122

2) Interactions inter-hémisphériques et latéralisation de l'activité corticale lors de la réalisation d'un mouvement unimanuel. 126

C. Préparation de mouvements latéralisés 129

1) La préparation d'un mouvement unimanuel est associée à une activation latéralisée du système moteur 129

2) Interactions inter-hémisphériques et latéralisation de l'activité corticale lors de la préparation d'un mouvement unimanuel. 132

D. Le rôle de l'AMS dans la préparation des mouvements latéralisés 134

1) Anatomie et localisation de l'AMS 134

2) L'AMS est impliquée dans la préparation des mouvements 134

3) L'AMS est impliquée dans la production de mouvements bimanuels 136

RESULTATS 139

I. Article 1 : Le rôle de DCC dans le guidage du faisceau corticospinal n'est pas cellule-autonome (soumis) 140

II. Résultats complémentaires : Rôle de *Netrin-1* dans le guidage du FCS à la ligne médiane 185

III. Article 2 : Des mutations du gène *NETRIN1* sont responsables du syndrome des mouvements en miroir congénitaux (soumis) 191

IV. Article 3 : Etude du rôle de RAD51 dans le développement du système moteur (en préparation) 217

V. Article 4 : L'aire motrice supplémentaire intervient dans la préparation des mouvements latéralisés en modulant les interactions inter-hémisphériques (soumis) 253

DISCUSSION 279

I. Les mouvements en miroir congénitaux : un modèle pour comprendre la latéralisation motrice 281

A. Des causes génétique hétérogènes aboutissant à un phénotype commun 281

B. Importance relative du CC et du FCS dans la physiopathologie des MMC 283

C. Vers d'autres acteurs et mécanismes responsables des MMC ? 285

II. Le couple NETRIN1-DCC joue un rôle crucial dans le développement du système moteur 288

III. Conclusion 291

REFERENCES 295

REMERCIEMENTS

Je souhaite remercier Sonia Garel, Julie Duqué, Pascal Derkinderen et Patricia Gaspard de me faire l'honneur de faire partie de mon jury de thèse.

Je remercie profondément Emmanuel Roze et Isabelle Dusart. Leur gentillesse et leur bienveillance à mon égard ont grandement participé à mon épanouissement au cours de ses années de thèse. Leur curiosité, leur enthousiasme et leur rigueur scientifique à tous deux a été pour moi un modèle que j'espère avoir suivi au cours de mon travail.

Je remercie Cécile Gallea pour tout ce qu'elle m'a apporté : je lui dois l'ensemble de mes connaissances en IRM, et nos discussions m'ont plus d'une fois inspiré et motivé. Son écoute attentive, sa gentillesse et son amitié ont été des atouts précieux qui m'ont accompagné au cours de ces quatre ans.

Je remercie Maire-Pierre Morel, qui m'a tout appris sur la souris, notamment à être patient pendant le comportement (c'est malheureusement le seul point de son enseignement vis-à-vis duquel je suis resté réticent). Je la remercie aussi, avec Oriane Trouillard, d'avoir effectué le nombre colossal de génotypages qu'a demandé ce projet.

Je remercie Sabine Meunier de m'avoir initié à l'électrophysiologie humaine et de m'en avoir donné le goût. Je la remercie aussi pour l'ensemble du travail conceptuel qu'elle a fourni pour ce projet, qui n'aurait pas été le même sans elle.

Je remercie Jean-Charles Lamy d'avoir partagé avec moi de longues de heures de manipulation TMS, dont j'ai tiré un grand bénéfice grâce à nos riches discussions.

Je remercie Aurélie Méneret, ancienne étudiante d'Emmanuel, qui m'a dit tant de bien de cette équipe, de ce projet, et qui avait raison.

Je remercie Sophien Mehdi, Frédéric Humbert, Antoine Burgos et Mélanie Didier, qui furent présents avec moi au cours des centaines d'heures d'IRM et de TMS du protocole MOMIC2.

Je remercie Marie Vidailhet et Stéphane Lehéricy de m'avoir accueilli dans leur équipe, ainsi que pour leur bienveillance et leur disponibilité. Je remercie l'ensemble des membres de leur équipe, notamment Marta, Cécile, Aliénor, Sophie et Elodie.

Je remercie Alain Trembleau pour son accueil au sein de l'équipe DPRN ainsi que ses membres présents et passés de cette dernière: Laura, Isabelle, Caroline, Coralie, Oriane, Vidji, Rosine, Lamia, Alexandre et Maxime. Je remercie en particulier Laura et Oriane d'avoir partagé à de nombreuses reprises mes footings en bord de Seine.

Au cours de ces quatre années, j'aurai passé beaucoup de temps à faire des aller-retours entre Jussieu et l'ICM : je remercie donc les Velibs de la ville de Paris, qui m'ont permis d'effectuer ces quelques 2700 kilomètres en un temps record.

Je remercie les nombreuses personnes qui m'ont aidé à Jussieu, que ce soit par leurs compétences techniques ou par leur oreille attentive : Mohamed Doulazmi, Marc Dos Santos, Sebastian Jara, Juliette Piquet, Fabio Marti, Philippe Faure, Malou Dongelmans, Steve Didienne, Samir Takillah, Antoine Bergel, Jérémie Naude, Benjamin Lassus, Pauline Vaur, Jamilé Hazan, Coralie Fassier, Nicolas Jardin.

Je remercie Alain Chédotal, dont la contribution matérielle et intellectuelle à ce travail fut décisive. Je remercie aussi les membres de son équipe : François, Chloé, Morgane, Heike, Yvrick, Kim, ainsi que David pour les acquisitions à l'ultramicroscope et au nanozoomer.

Je remercie Xavier Nicol, mon tuteur de l'école doctorale, pour sa gentillesse, sa disponibilité et ses conseils.

Je remercie l'ensemble de l'équipe de l'animalerie de l'ICM : Béatrice, Mélanie, Mélanie et Erwan.

Je remercie Magali et Marika pour leurs conseils précieux concernant les tests comportementaux moteurs.

Je remercie Alexis Brice et les membres de son équipe, notamment Hamid, pour leurs discussions enrichissantes et leur soutien matériel.

Je remercie ma famille et mes amis pour tous les moments passés ensemble en dehors du laboratoire.

Je remercie Claire, pour les quatre merveilleuses années que j’ai passées avec elle, et pour celles qui nous attendent.

ABREVIATIONS

AgCC : agénésie du corps calleux

AMS : aire motrice supplémentaire

BDA : biotinulated dextran amine

CA : commissure antérieure

CC : corps calleux

CH : commissure hippocampique

DCC : deleted in colorectal cancer

EX : jour de développement embryonnaire X

FCS : faisceau corticospinal

EEG : électro-encéphalogramme

FGF : fibroblast growth factor

GW : glial wedge

HS : héparane sulfate

IHH : inhibition inter-hémisphérique

IHH_c/IHH_i : IHH dirigée vers le cortex moteur contralatéral/ipsilatéral

IRM : imagerie par résonnance magnétique

M1 : cortex moteur primaire

$M1_c$/$M1_i$: M1 contralatéral/M1 ipsilatéral

MM : mouvements en miroir

MMC : mouvements en miroir congénitaux

MZG : midline zipper glia

OI : olive inférieure

PEM : potentiel évoqué moteur

PM : cortex prémoteur

PMd : cortex prémoteur dorsal

PX : jour post-natal X

S1/S2 : cortex somatosensoriel primaire/secondaire

SC : stimulation conditionnante

SCS : subcallosal sling

SHH : sonic hedgehog

SMT : stimulation magnétique transcrânienne

ST : stimulation test

ZV/ZSV : zone ventriculaire/zone sub-ventriculaire

Notes sur la nomenclature des gènes et des protéines

Tout au long de ce manuscrit, nous utiliserons la convention suivante :

*DCC (*en majuscule et en italique) désigne le gène humain

Dcc (en minuscules et en italiques) désigne le gène murin

DCC (en majuscule) désigne la protéine

LISTE DES FIGURES

Introduction

Figure 1. Mutations et variants répertoriés dans les gènes *DCC* et *RAD51* chez des patients atteints de MMC (p. 21)

Figure 2. Phénotype des mutants *Dcc*$^{-/-}$ chez la souris (p. 23)

Figure 3. Mécanisme de réparation des cassures double brin de l'ADN par recombinaison homologue (p. 25)

Figure 4. Phylogénie des mammifères (p. 44)

Figure 5. Anatomie comparée des commissures du cerveau antérieur chez les mammifères (p. 46)

Figure 6. Organisation tangentielle, laminaire et topographique du corps calleux (p. 49)

Figure 7. Maturation des connexions calleuses au cours du développement post-natal chez le chat (p. 52)

Figure 8. Les différents types de neurones à projection du néocortex (p. 55)

Figure 9. Génération séquentielle des différentes couches néocorticales (p. 58)

Figure 10. *Satb2* intervient dans la spécification des neurones calleux chez la souris (p. 61)

Figure 11. Molécules impliquées dans la spécification et le guidage des neurones calleux (p. 68)

Figure 12. Différentes anomalies développementales du corps calleux chez l'humain (p. 76)

Figure 13. Préparation motrice anormale chez les patients MMC lors de mouvements unimanuels de la main droite (dominante) (p. 121)

Figure 14. Le principe de la stimulation double-pulse : l'inhibition inter-hémisphérique (p. 124)

Figure 15. Modulation de l'excitabilité des cortex moteurs primaires lors de la réalisation de mouvements unimanuels chez des sujets sains et chez des patients atteints de MMC (p. 128)

Figure 16. Interactions inter-hémisphériques entre PMd et M1 et entre les deux M1 au cours de la préparation d'un mouvement unimanuel (p. 133)

Figure 17. Organisation anatomique et rôle fonctionnel de l'AMS (p. 135)

Résultats

Figure 18. L'anatomie du FCS est anormale chez les souris Shh::cre;Netrin$^{lox/lox}$ (p. 186)

Figure 19. Organisation anormale du FCS dans la moelle chez les mutants Shh::cre;Netrin1$^{lox/lox}$ (p. 187)

Figure 20. *Netrin-1* est impliquée dans la génération de mouvements asymétriques des membres antérieurs (p. 189)

INTRODUCTION

I. Les mouvements en miroir congénitaux : un paradigme pour l'étude des bases neurophysiologiques de la latéralisation motrice

A. Préambule : comprendre le normal par le pathologique

Comme l'indique le titre de cette thèse, le travail que j'ai effectué avait pour but d'étudier une situation pathologique, celle de mouvements anormaux appelés « mouvements en miroir », afin d'approfondir nos connaissances sur cette maladie, mais aussi sur le fonctionnement du système moteur dans le cas dit « normal ». Cette démarche s'inscrit dans une tradition datant du XIXe siècle pouvant être simplement résumée : comprendre le normal par le pathologique. Bien que cette approche soit aujourd'hui extrêmement naturelle et qu'il nous semblerait absurde de remettre en cause son bien-fondé scientifique, j'aimerais revenir brièvement sur son histoire afin de mettre en avant les présupposés qu'elle implique.

Dans *Le normal et le pathologique* (1966), Georges Canguilhem rappelle que cette approche scientifique qui a jeté les bases de la physiologie moderne est principalement due à deux scientifiques français : Auguste Comte et Claude Bernard. Auguste Comte reprend à son compte et généralise un principe énoncé par Broussais, selon lequel il n'existe pas de différence de nature, mais seulement une différence de degré, entre le fonctionnement normal d'un organisme et son état pathologique. Autrement dit, les mécanismes mis en jeux dans des tissus sains et malades sont fondamentalement les mêmes : ils ne diffèrent que d'un point de vue quantitatif, du fait d'un trop plein ou d'un trop peu d'excitation, mais pas d'un point de vue qualitatif. Comte affirme dans la 40e leçon du *Cours de philosophie positive* (1838) : « […] l'état pathologique ne diffère point radicalement de l'état physiologique, à l'égard duquel il ne saurait constituer, sous un aspect quelconque, qu'un simple prolongement plus ou moins étendu des limites de variation soit supérieures soit inférieures, propres à chaque

phénomène de l'organisme normal, sans pouvoir jamais produire de phénomènes vraiment nouveaux, qui n'auraient point, à un certain degré, leurs analogues purement physiologiques ». Claude Bernard adhère à cette idée que la pathologie ne consiste qu'en une dérégulation des phénomènes normaux, physiologiques. Nous citons ici un extrait des *Leçons sur le diabète et la glycogenèse animale* (1877) : « Physiologie et pathologie se confondent et sont au fond une seule et même chose. […] Toute maladie a une fonction normale correspondante dont elle n'est qu'une expression troublée, exagérée, amoindrie ou annulée. Si nous ne pouvons pas aujourd'hui expliquer tous les phénomènes des maladies, c'est que la physiologie n'est pas encore assez avancée et qu'il y a encore une foule de fonctions normales qui nous sont inconnues ».

C'est en vertu de cette homogénéité, de cette continuité entre le phénomène normal et le phénomène pathologique que nous pouvons prétendre expliquer le premier – en l'occurrence la latéralisation motrice – par l'étude du second – les mouvements en miroir. Cette approche est donc très puissante, mais son présupposé n'est peut être pas si évident : la pathologie est-elle véritablement incapable de « produire des phénomènes vraiment nouveaux » ?

B. Mouvements en miroir congénitaux

Dans cette partie, nous nous intéresserons à la description clinique des mouvements en miroir congénitaux et à leurs causes génétiques. La physiopathologie de ces mouvements anormaux sera abordée dans la section suivante.

1) Définition et description clinique

Les comportements moteurs d'un organisme sont la résultante d'un ensemble de contractions musculaires finement coordonnées qui sont contrôlées par le système nerveux.

Les humains possèdent un répertoire de mouvements extrêmement diversifié, notamment en ce qui concerne les mouvements manuels. Nous appellerons mouvement latéralisé (des mains) tout mouvement impliquant une asymétrie de contraction musculaire entre les mains droite et gauche. En ce sens, les mouvements latéralisés comprennent les mouvements strictement unimanuels (impliquant le mouvement d'une seule des deux mains tandis que l'autre est au repos) et les mouvements bimanuels asymétriques. La capacité de réaliser des mouvements latéralisés est un aspect crucial de nos activités quotidiennes. Taper à l'ordinateur, jouer d'un instrument de musique, ouvrir un bocal de confiture, faire de l'escalade, sont autant de gestes qui nécessitent de produire des mouvements asymétriques avec nos deux mains.

Les mouvements en miroir (MM) sont des mouvements involontaires d'une main qui miment et accompagnent les mouvements volontaires de la main opposée. Des MM sont fréquemment observés chez les jeunes enfants de moins de sept ans, et sont considérés comme des manifestations de l'immaturité du système nerveux central, en particulier du corps calleux (Koerte et al., 2010; Beaule et al., 2012). Leur persistance au-delà de cet âge définit leur caractère pathologique (Bonnet et al., 2010). Les MM touchent majoritairement les extrémités distales des membres supérieures (les mains et les doigts). Ils sont généralement d'amplitude inférieure aux mouvements volontaires contralatéraux et sont d'intensité variable d'un patient à l'autre. La sévérité des MM est évaluée avec l'échelle de Woods et Teuber (Woods and Teuber, 1978) comme suit : 0 : pas de MM ; 1 : MM à peine discernables mais répétés ; 2 : MM discrets mais soutenus ; 3 : MM importants, soutenus et répétés ; 4 : MM égaux à ceux qui sont observés sur la main en mouvement volontaire. Les individus atteints ne peuvent donc pas réaliser de mouvements unimanuels ou de mouvements bimanuels asymétriques.

Le syndrome des Mouvements en Miroir Congénitaux (MMC) constitue une pathologie développementale rare, souvent familiale à transmission autosomique dominante,

mais il existe aussi des cas sporadiques (Meneret et al., 1993; Peng and Charron, 2013; Meneret et al., 2014a). Dans ce syndrome, les MM ne sont pas associés à d'autres anomalies neurologiques. Les MMC constituent donc une atteinte extrêmement pure du système de la latéralisation motrice. Dans cette pathologie, les MM apparaissent tôt dans la petite enfance, puis restent stables au cours de la vie. C'est une pathologie très rare, avec une prévalence estimée à moins de 1/1 000 000 (Orphanet #238722), mais la maladie est probablement sous-diagnostiquée.

2) Autres pathologies associées aux mouvements en miroir

Les MM d'origine développementale (par opposition aux formes acquises, qui seront brièvement évoquées à la fin de ce paragraphe) peuvent aussi être associés à d'autres symptômes dans le cadre de syndromes complexes.

Syndrome de Kallmann : le syndrome de Kallmann est caractérisé par l'association d'hypogonadisme hypogonadotrope et d'anosmie. La présence de MM dans ce symptôme est majoritairement associée aux mutations du gène *KAL1*, mutations responsables de la forme liée à l'X de la pathologie (Quinton et al., 1996; Royal et al., 2002; Dode and Hardelin, 2010).

Syndrome de Klippel-Feil : ce syndrome est caractérisé par une fusion des vertèbres cervicales, et inclut un cou court, une mobilité cervicale réduite, une implantation basse des cheveux. Des MM sont fréquemment observés chez ces patients (Bauman, 1932; Baird et al., 1967; Royal et al., 2002).

Syndrome de Joubert : ce syndrome est une entité hétérogène, caractérisée par les malformations du vermis cérébelleux et du tronc cérébral. Les manifestations phénotypiques peuvent inclure faiblesses musculaires, respiration et mouvements oculomoteurs anormaux, maladresse, retards cognitifs, comportement autistique et des dysfonctions variables de

différents organes (principalement les reins, la rétine, le foie et le squelette) (Romani et al., 2013). Des MM sont parfois associés à ce tableau clinique (Ferland et al., 2004).

Syndrome de Möbius : ce syndrome inclut une faiblesse faciale non évolutive associée à une abduction limitée des yeux (Verzijl et al., 2003). Une étude récente a décrit le cas de trois patients atteints du syndrome de Möbius ayant des MM (Webb et al., 2014).

Syndrome de Gorlin : ce syndrome est caractérisé par une association de carcinomes, de kystes de la mâchoire et de malformations squelettiques (Gorlin and Goltz, 1960). Le cas d'un patient présentant un syndrome de Gorlin et des MM a été récemment décrit (Sag et al., 2016).

Syndrome de Seckel : ce syndrome associe une microcéphalie primaire à des retards de croissance et une déficience intellectuelle. Un patient atteint de ce syndrome et présentant des mouvements en miroir a été décrit (Thapa and Mukherjee, 2010).

Mouvements en miroir acquis : dans le cas des MM acquis, l'âge de début des MM est bien plus tardif. La présence de MM est souvent associée à d'autres pathologies du mouvement, et ce symptôme peut être retrouvé dans la maladie de Parkinson, le syndrome corticobasal, le tremblement essentiel, la dystonie miroir, le syndrome de Creutzfeldt-Jacob, la maladie de Huntington (Cox et al., 2012). L'apparition de MM a aussi été décrite chez un patient à la suite d'un infarctus touchant l'aire motrice supplémentaire (Chan and Ross, 1988).

3) Génétique des mouvements en miroir congénitaux

Les mouvements en miroir congénitaux sont souvent une pathologie héréditaire à transmission autosomique dominante. Deux gènes responsables des MMC ont été identifiés sans ambiguïté à ce jour : *DCC* et *RAD51* (Figure 1) (Srour et al., 2010; Depienne et al., 2011; Depienne et al., 2012; Peng and Charron, 2013; Meneret et al., 2014a). *DNAL4* est potentiellement impliqué, mais des mutations de ce gène n'ont été identifiées que dans ne

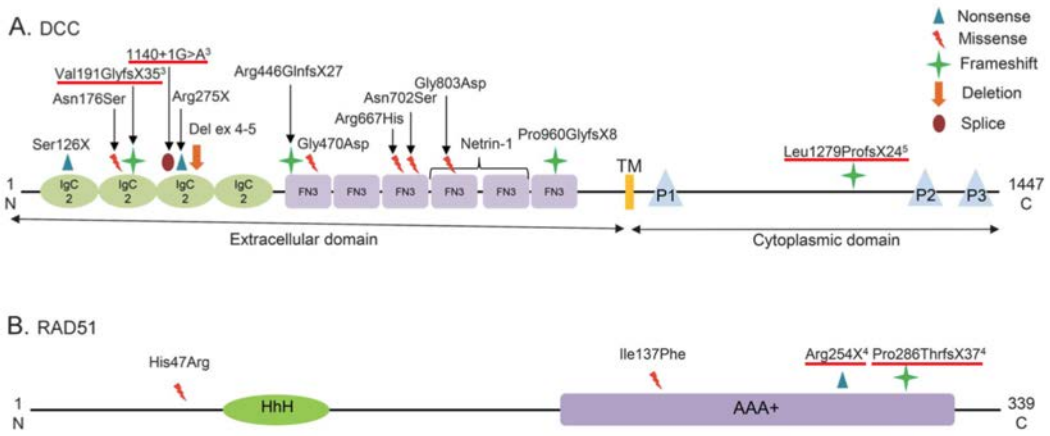

Figure 1. Mutations et variants répertoriés dans les gènes *DCC* et *RAD51* chez des patients atteints de MMC. (A) Mutations et variants répertoriés dans le gène *DCC*. (B) Mutations et variants répertoriés dans le gène *RAD51*. Les formes familiales de MMC sont associées à des mutations hétérozygotes tronquantes de RAD51 ou DCC (soulignées en rouge). La première mutation décrite de *DCC* (A : 1140 + 1G >A) aboutit à une protéine tronquée après l'exon 5, dont la plupart des domaines fonctionnels sont absents et qui ne peut pas interagir avec son ligand NETRIN-1. Les autres mutations aboutissent probablement à une diminution de la quantité de protéine fonctionnelle produite. Adapté de (Meneret et al, 2014).

seule famille (Ahmed et al., 2014; Meneret et al., 2014b). *RAD51* et *DCC* à eux seuls ne rendent pas compte de l'ensemble des cas familiaux et MMC, ce qui signifie que d'autres gènes, pour le moment inconnus, sont associés à cette pathologie. Les mutations de *RAD51* et *DCC* identifiées dans les familles de patients MMC sont hétérozygotes et leur pénétrance est de 50%. La première mutation décrite de DCC aboutit à la formation d'une protéine tronquée, ne pouvant pas interagir avec son ligand NETRIN-1 (Srour et al., 2010). Il a été proposé que les autres mutations tronquantes soient responsables d'une diminution de la quantité de protéine fonctionnelle produite (ou haploinsuffisance) du fait de la dégradation de l'ARN messager anormal (Depienne et al., 2011; Depienne et al., 2012; Meneret et al., 2014a). Cependant cette hypothèse n'a pas été testée directement, et la possibilité que certaines de ces mutations soient responsables d'effets dominants négatifs ne peut pas être exclue.

DCC assure différentes fonctions au cours du développement. Il joue un rôle important dans la survie cellulaire et dans le contrôle de la prolifération en tant que récepteur à dépendance : en l'absence de son ligand, NETRIN-1, il enclenche un programme de mort cellulaire (Mehlen et al., 1998). En lien avec ce rôle de suppresseur de tumeurs, des mutations de DCC ont été initialement associées à des cancers colorectaux (d'où son nom, DCC signifiant « Deleted in Colorectal Cancer ») (Fearon et al., 1990; Krimpenfort et al., 2012). DCC est aussi impliqué dans le guidage des axones commissuraux (c'est-à-dire des axones qui croisent la ligne médiane du corps) au cours du développement. Dans la moelle épinière, les axones exprimant le récepteur DCC à la membrane de leur cône de croissance sont attirés par leur ligand NETRIN-1, molécule qui est sécrétée au niveau de la ligne médiane par les cellules de la plaque du plancher (Kennedy et al., 1994; Keino-Masu et al., 1996). Cette interaction permet aux axones commissuraux de franchir la ligne médiane, pour ensuite poursuivre leur trajet et contacter leurs cibles dans l'hémi-moelle opposée. Par la suite, DCC s'est révélé être impliqué dans le développement de nombreuses commissures (Figure 2),

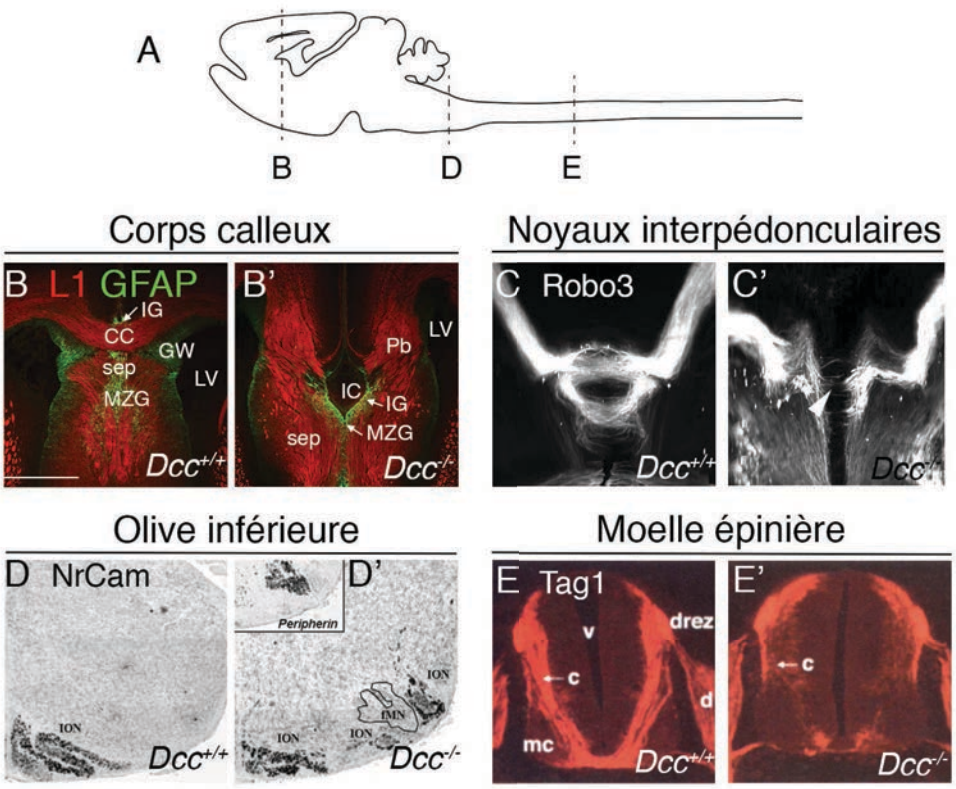

Figure 2. Phénotype des mutants *Dcc*$^{-/-}$ chez la souris. (A) Schéma représentant le système nerveux central d'une souris à P0 en vue sagittale et indiquant le niveau des différentes coupes. (B, B') Coupes coronales du corps calleux (CC) de souris *Dcc*$^{+/+}$ et *Dcc*$^{-/-}$ à P0 avec immuno-marquage anti-L1 (marquage du CC) et anti-GFAP (marquage des populations gliales). CC : corps calleux ; IG : indusium griseum ; GW : glial wedge ; sep : septum ; MZG : midline zipper glia ; IC : kyste inter-hémisphérique ; LV : lateral ventricule. (Données personnelles). (C, C') Visualisation du fasciculus retroflexus par immuno-marquage anti-ROBO3 combiné à une procédure de clarification 3DISCO chez des souris *Dcc*$^{+/+}$ et *Dcc*$^{-/-}$ à E16 (Extrait de Belle et al, 2014). (D, D') Coupes coronales de souris *Dcc*$^{+/+}$ et *Dcc*$^{-/-}$ à P0 avec une hybridation *in-situ* dirigée contre NrCam et contre la peripherin. ION : neurones de l'olive inférieure (Extrait de Marcos et al, 2009). (E, E') Coupes coronales de moelles épinières d'embryons de souris *Dcc*$^{+/+}$ et *Dcc*$^{-/-}$ à E11.5 avec immuno-marquage anti-Tag1. c : axones commissuraux; mc : colonne motrice ; v : ventricule ; d : ganglion de la racine dorsale ; drez : zone d'entrée du ganglion de la racine dorsale (Extrait de Fazeli et al, 1997).

notamment les commissures du cerveau antérieur (commissure antérieure, commissure hippocampique et corps calleux) (Fazeli et al., 1997; Fothergill et al., 2014), le fasciculus retroflexus (qui relie l'habenula aux noyaux inter-pédonculaires du pont) (Belle et al., 2014), les fibres grimpantes de l'olive inférieure (Marcos et al., 2009), les interneurones commissuraux de la moelle épinière (Rabe Bernhardt et al., 2012) et le faisceau corticospinal (Finger et al., 2002).

RAD51 est une protéine connue essentiellement pour son rôle dans la réparation de l'ADN. Il s'agit de l'homologue du gène *RecA*, bien connu chez les bactéries. RAD51 assure le maintien de la stabilité génomique au cours de la prolifération cellulaire. En effet, RAD51 intervient dans la réparation des cassures double brin de la molécule d'ADN par un processus de recombinaison homologue (Figure 3) (Thacker, 2005; Jasin and Rothstein, 2013). Alors que des mutations de nombreux partenaires de RAD51 impliqués la voie de réparation de l'ADN sont associées à un risque accru de cancer, aucune mutation dans la séquence codante de *RAD51* n'a été associée de manière causale au cancer (Lose et al., 2006; Moynahan and Jasin, 2010). Les seules mutations familiales dans la séquence codante de *RAD51* publiées à ce jour sont celles associées au syndrome des mouvements en miroir congénitaux (Depienne et al., 2012; Meneret et al., 2014a; Franz et al., 2015), ce qui peut sembler surprenant à plusieurs égards. Premièrement, RAD51 étant exprimée de façon ubiquitaire dans les cellules progénitrices pendant les phases de proliférations au cours du développement, il est étonnant qu'un déficit de la fonction de réparation d'ADN conduise à un phénotype aussi spécifique que celui des MM. Deuxièmement, RAD51 intervenant dans la réparation des cassures d'ADN par recombinaison homologue, cela signifie qu'elle utilise la chromatide sœur du chromosome lésé pour procéder à la réparation. Ce procédé n'est donc possible que dans les cellules ayant des chromosomes à deux chromatides, autrement dit des cellules dont le cycle cellulaire comprend une phase G2 (post réplication). Ce n'est pas le cas des neurones qui sont

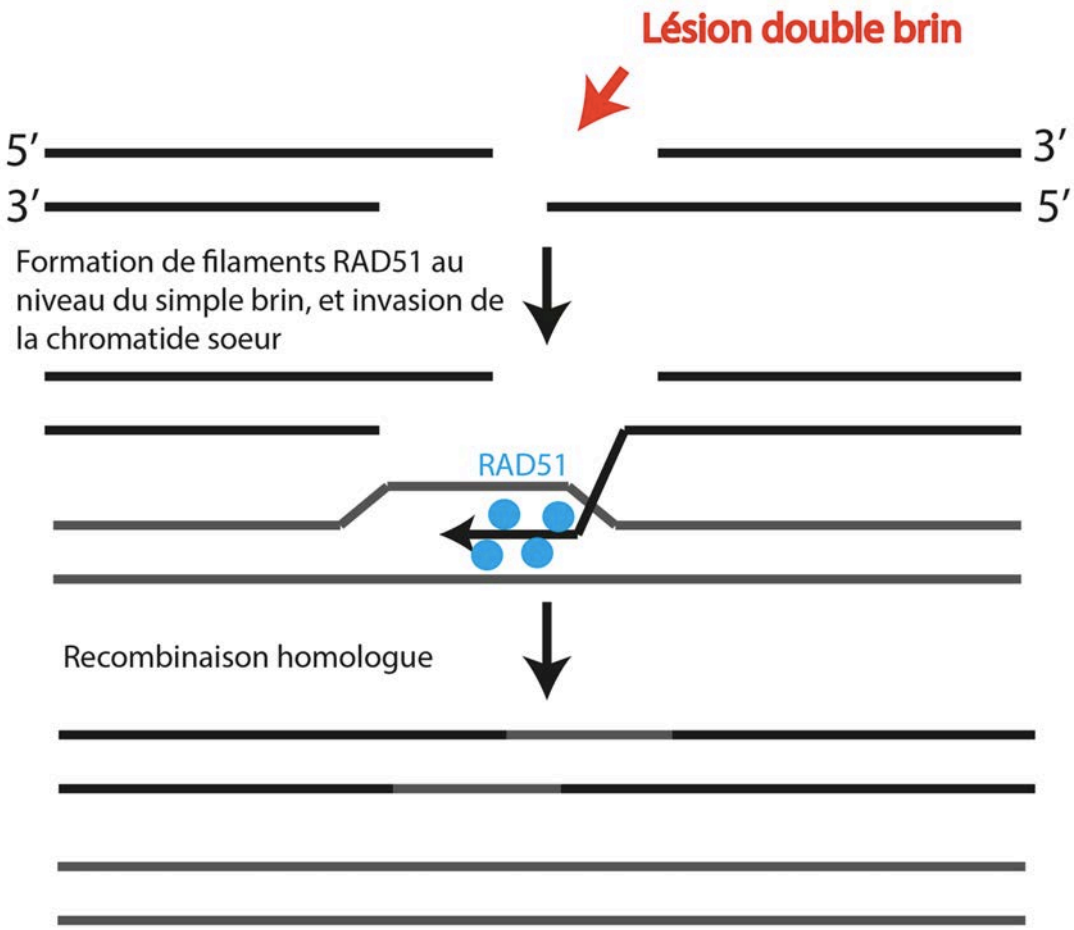

Figure 3. Mécanisme de réparation des cassures double brin de l'ADN par recombinaison homologue. A la suite d'une cassure double brin de l'ADN, RAD51 forme un filament au niveau d'un simple brin d'ADN de la chromatide lésée. A la suite de cette étape, L'ADN double brin intact de la chromatide sœur est utilisé comme matrice, permettant ainsi la réparation de la lésion. Adapté de (Thacker, 2005).

des cellules quiescentes, et présentent donc des chromosomes à une chromatide. Pour ces différentes raisons, il est probable que RAD51 joue un rôle encore inconnu au cours du développement du système nerveux central, et que ce soit la perturbation de cette fonction qui soit responsable du syndrome des MMC.

L'anémie de Fanconi est une pathologie héréditaire caractérisée par une hyper-sensibilité aux lésions de l'ADN, et associée à des symptômes incluant de multiples anomalies congénitales et hématologiques, ainsi qu'une augmentation de la prédisposition aux cancers (Auerbach, 2009). Récemment, deux études ont décrit le cas de patients présentant une anémie de Fanconi associée à une mutation faux-sens hétérozygote du gène *RAD51*. Ces mutations *de novo* aboutissaient à la formation d'une forme dominante négative de la protéine qui interfère avec ses fonctions normales (Ameziane et al., 2015; Wang et al., 2015). Dans un des deux cas décrit, l'anémie de Fanconi est une forme atypique associée à des troubles neurologiques (microcéphalie, hydrocéphalie, retard mental) (Ameziane et al., 2015).

Comment les mutations de *RAD51* et *DCC* aboutissent-elles aux MMC ? Tandis que le rôle connu de DCC dans le développement du système moteur chez la souris fournit à première vue une explication satisfaisante pour les MMC causés par des mutations de *DCC*, le rôle de RAD51 dans le développement du système moteur est complètement inconnu. Dans la partie suivante, la présentation de la physiopathologie des MMC permettra de mieux comprendre les mécanismes nécessaires à la production de mouvements latéralisés. Les liens entre les mutations des gènes *DCC* et *RAD51* et la physiopathologie des MMC ont fait l'objet d'une partie de mon travail de thèse et seront abordés dans le chapitre des résultats.

C. Revue de la littérature 1 : Applaudir d'une main, la latéralisation du contrôle moteur

Comprendre le fonctionnement normal d'un organisme par l'étude d'une situation pathologique est une approche scientifique puissante. Dans cette perspective, la compréhension des mécanismes neurophysiologiques sous-tendant la latéralisation motrice a beaucoup à gagner de l'étude de situations pathologiques associées à une perte de la capacité à réaliser des mouvements latéralisés. Dans cette revue, nous nous sommes intéressés aux corrélats neurophysiologiques de deux situations pathologiques qui sont, à notre connaissance, les seules à être associées à l'incapacité de produire des mouvements latéralisés : les mouvements en miroir chez l'humain, et le « hopping gait » chez la souris.

Cette analyse souligne le rôle crucial de commissures situées à différents niveaux du système nerveux central dans la latéralisation motrice. Les commissures, en tant que structures permettant la mise en relation des deux hémicorps, sont en effet les principaux acteurs de la latéralisation du contrôle moteur. Nous identifions trois populations de neurones commissuraux d'une importance primordiale pour la production de mouvements latéralisés :

- les neurones formant le corps calleux (CC), principale commissure assurant la communication entre les deux hémisphères cérébraux
- les neurones formant le faisceau corticospinal (FCS), l'un des principaux effecteurs de la commande motrice volontaire
- les neurones commissuraux de la moelle épinière

Le CC et le FCS sont les deux principales structures impliquées dans la neurophysiologie des MM, ce qui souligne leur rôle dans la production de mouvements asymétriques des mains. Le CC et le FCS semblent n'avoir pas d'impact sur la latéralisation motrice durant la locomotion (quadrupède), ce rôle étant essentiellement assuré par les axones commissuraux de la moelle.

frontiers in Neuroanatomy

REVIEW
published: 02 June 2015
doi: 10.3389/fnana.2015.00075

One hand clapping: lateralization of motor control

*Quentin Welniarz[1,2], Isabelle Dusart[1], Cécile Gallea[2] and Emmanuel Roze[2,3]**

[1] Neuroscience Paris Seine, CNRS UMR8246, Inserm U1130, Sorbonne Universités, UPMC UM119, Paris, France, [2] Inserm U1127, CNRS UMR 7225, Sorbonne Universités, UPMC UMR S1127, Institut du Cerveau et de la Moelle épinière, ICM, Paris, France, [3] Département des Maladies du Système Nerveux, AP-HP, Hôpital Pitié Salpêtrière, Paris, France

Lateralization of motor control refers to the ability to produce pure unilateral or asymmetric movements. It is required for a variety of coordinated activities, including skilled bimanual tasks and locomotion. Here we discuss the neuroanatomical substrates and pathophysiological underpinnings of lateralized motor outputs. Significant breakthroughs have been made in the past few years by studying the two known conditions characterized by the inability to properly produce unilateral or asymmetric movements, namely human patients with congenital "mirror movements" and model rodents with a "hopping gait". Whereas mirror movements are associated with altered interhemispheric connectivity and abnormal corticospinal projections, abnormal spinal cord interneurons trajectory is responsible for the "hopping gait". Proper commissural axon guidance is a critical requirement for these mechanisms. Interestingly, the analysis of these two conditions reveals that the production of asymmetric movements involves similar anatomical and functional requirements but in two different structures: (i) lateralized activation of the brain or spinal cord through contralateral silencing by cross-midline inhibition; and (ii) unilateral transmission of this activation, resulting in lateralized motor output.

Keywords: mirror movement, hopping gait, corticospinal tract, corpus callosum, spinal cord, axon guidance

OPEN ACCESS

Edited by:
Yun-Qing Li,
The Fourth Military Medical University, China

Reviewed by:
José A. Armengol,
University Pablo de Olavide, Spain
Yu-Qiang Ding,
Tongji Unversity, China

***Correspondence:**
Emmanuel Roze,
Département des Maladies du Système Nerveux, AP-HP, Hôpital Pitié Salpêtrière, 47–83 boulevard de l'Hôpital, 75013 Paris, France
emmanuel.flamand-roze@psl.aphp.fr

Received: *31 March 2015*
Accepted: *17 May 2015*
Published: *02 June 2015*

Citation:
Welniarz Q, Dusart I, Gallea C and Roze E (2015) One hand clapping: lateralization of motor control. Front. Neuroanat. 9:75. doi: 10.3389/fnana.2015.00075

Introduction

Lateralization of motor control is required for a variety of coordinated movements, including skilled bimanual tasks and locomotion. To our knowledge, only two conditions are associated with the inability to produce asymmetric movements in mammals: human "mirror movements" and rodent "hopping gait".

Mirror movements are involuntary symmetrical movements of one side of the body that mirror voluntary movements of the other side. The affected individuals are unable to perform purely unimanual movements and have difficulties to perform tasks requiring independent actions with the two hands such as holding a cup while filling it with water, opening a jar or playing a musical instrument. During these tasks, the effectors produce different motor outputs that are usually bound together by a shared, object-directed goal.

Quadrupedal locomotion is characterized by coordinated, alternating bilateral activation of limb muscles, in which effectors repeatedly produce similar motor outputs in a specific temporal order. A "hopping gait" is a switch from alternate to synchronous activity of the limbs during locomotion that is observed in rodent mutants with impaired axonal guidance.

Here we discuss the neuroanatomical substrates and pathophysiological underpinnings of lateralized motor output through the study "mirror movements" and "hopping gait". Whereas mirror movements are associated with altered interhemispheric connectivity and abnormal corticospinal projections, abnormal spinal cord interneurons trajectory is responsible for the "hopping gait". Interestingly, the analysis of these two conditions indicates that the production of asymmetric movements involves similar anatomical and functional requirements but in two different structures, the cerebral cortex and the spinal cord, and it emphasizes the importance of proper commissural axon guidance in this process.

The "Mirror Movement" Paradigm: Inability to Produce Asymmetric Skilled Hand Movements

Humans have a greater ability than other species to produce purposeful handling movements, most of them being asymmetric. With training, we can master highly complex skills ranging from the fluid movements of the virtuoso pianist to the precise life-saving gestures of the heart surgeon. In humans, execution of unimanual movements requires lateralized activation of the primary motor cortex (M1), which then transmits the motor command to the contralateral hand through the crossed corticospinal tract (CST; **Figure 1A**; Chouinard and Paus, 2010; Galléa et al., 2011).

Loss of this lateralization results in mirror movements (MM), which consist of involuntary symmetrical movements of one side of the body that mirror voluntary movements of the other side. Congenital mirror movement disorder (CMM) is a rare genetic disorder transmitted in autosomal dominant manner in which mirror movements are the only clinical abnormality. These mirror movements predominate in the distal upper limbs, leaving affected individuals unable to perform independent actions with the two hands or to perform purely unimanual movements. They usually have hand clumsiness and pain in the upper limbs during sustained manual activities. The two main culprit genes are *Dcc* (deleted in colorectal cancer) and *Rad51* (Srour et al., 2010; Depienne et al., 2011, 2012; Méneret et al., 2014a). A third gene, *Dnal4*, might also be involved (Ahmed et al., 2014; Méneret et al., 2014b). *Dcc* plays a key role in CST midline crossing (Finger et al., 2002), while *Rad51* is well known for its role in DNA repair and may also have a major role in motor system development (Depienne et al., 2012; Gallea et al., 2013). In addition to isolated congenital mirror movements caused by *Dcc* or *Rad51* mutations, syndromic forms of MM may be accompanied by numerous other symptoms, in disorders such as Dandy walker syndrome, Joubert's syndrome, X-linked Kallmann syndrome, Klippel Feil syndrome and congenital hemiparesis (Vulliemoz et al., 2005; Galléa et al., 2011; Peng and Charron, 2013).

CMM provides a unique paradigm for studying the lateralization of motor control (Carson, 2005; Galléa et al., 2011; Peng and Charron, 2013). Two main non exclusive mechanisms may account for MM: (i) abnormal interhemispheric communication resulting in bilateral activation of primary motor areas (**Figures 1B,C**); and (ii) a corticospinal tract abnormality leading to bilateral downstream transmission of the motor command (**Figures 1D,E**; Gallea et al., 2013).

Interhemispheric Connectivity and Motor Lateralization

In humans, the default set-up of motor behavior is probably a mirror program (Chan and Ross, 1988; Meyer et al., 1995; Cincotta and Ziemann, 2008). Unilateral and bilateral voluntary movements are preceded by slow negativity on EEG recordings, known as the *Bereitschaftpotential* (Shibasaki and Hallett, 2006), which starts 2 s before movement onset and is distributed over the two hemispheres. This *Bereitschaftpotential* may reflect bilateral activation of the supplementary motor areas (SMA) and dorsal premotor cortices (dPMC) during motor planning. Just before movement onset, cortical activity is restricted to the primary motor cortex and dPMC contralateral to the intended movement (Shibasaki and Hallett, 2006). An active mechanism is required to restrict motor activation to one hemisphere during execution of a pure unimanual movement.

Our current understanding of this "non mirror transformation" derives mainly from the study of "physiological" mirror movements. Healthy subjects have a default tendency to produce minimal mirror movements when performing highly complex and effortful unimanual tasks (Koerte et al., 2010; Sehm et al., 2010; Beaulé et al., 2012). Activation of the mirror M1 (ipsilateral to the voluntary movement) is the main explanation for this tendency (Mayston et al., 1999; Cincotta et al., 2004; Zijdewind et al., 2006; Hübers et al., 2008). In order to achieve this "non mirror transformation", the active M1 (contralateral to the intended movement) inhibits the mirror M1 via fibers that pass through the corpus callosum (transcallosal tract, TCT), thereby restricting the motor output to the active M1. This inhibition of one motor cortex by the other is called interhemispheric inhibition (IHI). IHI is thought to rely on transcallosal glutamatergic connections to inhibitory interneurons that in turn innervate pyramidal cells in the receiving hemisphere (Meyer et al., 1995; Reis et al., 2008). Several lines of evidence support the importance of TCT-mediated IHI in the lateralization of motor control. For example, the gradual disappearance of minimal MM frequently observed in young children correlates with the degree of TCT myelination and with the level of IHI (Koerte et al., 2010; Beaulé et al., 2012). Also, experimental modulation of IHI directed from the active M1 to the mirror M1 affects mirror activity: a transient increase in IHI is associated with a decrease in mirror activity, and *vice versa* (Hübers et al., 2008).

IHI between the two primary motor cortices is modulated differently during the different phases of unimanual movements. IHI is balanced between the two motor cortices at the onset of movement preparation, then shifts towards the ipsilateral M1 (ipsilateral to the voluntary movement) at the end of movement preparation and at movement onset (Murase et al.,

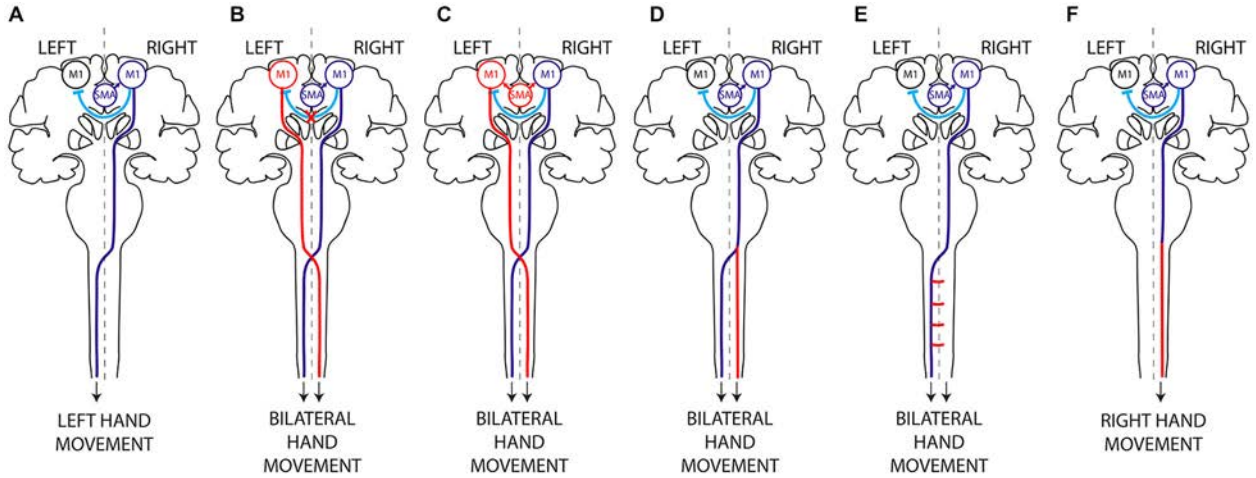

FIGURE 1 | Hypothetical mechanisms of mirror movements. (A) In humans, execution of a unilateral left hand movement requires both lateralized activation of the right primary motor cortex (M1) by interhemispheric inhibition (IHI) and proper motor planning and then transmission of the motor command to the contralateral (left) hand alone, through a crossed corticospinal tract. There are two main mechanisms underlying MM: (i) abnormal IHI **(B)** or abnormal delivery of the motor plan from the supplementary motor area (SMA) to M1 **(C)**, resulting in bilateral activation of the primary motor cortices; and (ii) abnormal decussation of the CST **(D)** or abnormal branching of the CST in the spinal cord **(E)**, resulting in bilateral transmission of the motor command to the spinal cord. Mirror movements have not been described in horizontal gaze palsy with progressive scoliosis (HGPPS), despite the absence of CST decussation in these patients **(F)**. This suggests that MM are related to the presence of bilateral spinal cord projections arising from a single primary motor cortex rather than to abnormal decussation of the CST *per se*. Dark Blue, normal mechanism; Red, abnormal mechanism; Light blue, IHI.

2004; Duque et al., 2007). In parallel, IHI of the contralateral M1 decreases during movement preparation and shifts towards facilitation at movement onset (Murase et al., 2004; Perez and Cohen, 2008). These subtle time-dependent bilateral variations of IHI are necessary to avoid premature execution (Duque and Ivry, 2009), and to prevent mirror activity in the ipsilateral M1 (Giovannelli et al., 2009). Impairment of IHI may thus result in bilateral M1 activation and transmission of the motor command to both hands through the two crossed CSTs.

In patients with CMM and X-linked Kallmann syndrome, several studies have revealed abnormal, bilateral M1 activation during voluntary unimanual movements and have confirmed that activation of the mirror M1 is not a sensory consequence of the mirror movement but rather participates actively in the mirroring motor activity (Shibasaki and Nagae, 1984; Cohen et al., 1991; Mayer et al., 1995; Cincotta et al., 1996; Krams et al., 1997; Verstynen et al., 2007). However, studies based on indirect methods have failed to demonstrate consistent impairment of IHI mechanisms in CMM patients (Cincotta et al., 1996, 2002; Papadopoulou et al., 2010). Using dual-site transcranial magnetic stimulation (TMS), a more direct method (Perez and Cohen, 2008), we found that CMM patients with *Rad51* mutations had abnormal IHI between the primary motor cortices at rest, together with morphological abnormalities of the TCT (**Figure 1B**; Gallea et al., 2013). It has been proposed that this impaired IHI is due to an abnormal input of the transcallosal glutamatergic connections onto the inhibitory interneurons in the receiving hemisphere. It is noteworthy that most individuals lacking a corpus callosum do not exhibit mirror movements, suggesting that the absence of the corpus callosum and interhemispheric connections alone might not be sufficient to generate MM. Finally, a study of a CMM patient with complete agenesis of the corpus callosum concluded that the absence of TCT played little part in the pathophysiology of MM (Lepage et al., 2012).

Interhemispheric pathways are not limited to direct M1-M1 interactions and IHI but also include circuits linking secondary motor areas (SMA and PMd) to contralateral motor areas. These circuits might be involved in restricting the generation of motor output to the active hemisphere during movement preparation. For these reasons it has been proposed that abnormal motor planning and/or abnormal transmission of the motor plan from the secondary motor areas to the primary motor areas might also be involved in MM generation (Chan and Ross, 1988; Cincotta et al., 2004; Duque et al., 2010; Galléa et al., 2011; Gallea et al., 2013). Evidence of abnormal motor planning associated with MM was first obtained through studies of two CMM patients and a patient with Kallmann's syndrome, who showed an abnormal, bilateral (instead of unilateral) distribution of the *Bereitschaftpotential* during movement preparation (Shibasaki and Nagae, 1984; Cohen et al., 1991). However, two other studies argued against a role of abnormal movement planning in MM: the first showed that movement-related cortical EEG potentials were identical (that is to say, lateralized and not bilateral) in healthy volunteers and in six CMM patients (Mayer et al., 1995), while the second study, a case report, showed normal, unilateral cortical activation during fMRI imaging of imagined movements

closely related to motor planning (Verstynen et al., 2007). More recently, we found that the SMA activation pattern and connectivity are abnormal during both unimanual and bimanual movements in *Rad51*-mutated CMM patients (**Figure 1C**; Gallea et al., 2013) This suggested that cortical activation and connectivity might be modified in CMM patients during movement preparation, resulting in inappropriate delivery of the motor program from the SMA to both primary motor cortices.

Together, these results suggest that interhemispheric connectivity is critical for lateralized activation of the motor cortex when a unilateral movement is intended.

The Corticospinal Tract and Motor Lateralization

The CST is a crossed tract that transmits the motor command from one motor cortex to the contralateral spinal cord. The CST first appeared in mammals and was likely critical for the development of voluntary skilled movements through evolution (Vulliemoz et al., 2005). Selective lesions of the CST in humans, non human primates and rodents impair skilled digit movements such as reaching (Schieber, 2007). The CST is massively crossed in humans. About 70–95% of all CST axons cross the midline at the junction between the medulla and the spinal cord, forming the so-called "pyramidal decussation", and establish direct contacts with the motor neurons located in the anterior horn of the spinal cord (Vulliemoz et al., 2005). The approximately 10% of CST axons that do not decussate at the medulla remain ipsilateral, and this ipsilateral tract is mainly located in the ventral part of the spinal cord in both humans and rodents (Brösamle and Schwab, 1997; Vulliemoz et al., 2005). The ipsilateral CST component does not target motor neurons innervating distal limb muscles but rather motor neurons innervating the proximal or axial musculatures (Bawa et al., 2004; Vulliemoz et al., 2005). In humans, cats and rodents, the CST initially establishes strong bilateral projections to the spinal cord. The ipsilateral projections consist of uncrossed CST axons (Joosten et al., 1992; Brösamle and Schwab, 1997; Eyre et al., 2001), and/or of normally crossed CST axons that recross the midline within the spinal cord (Li and Martin, 2000; Rosenzweig et al., 2009). This CST projection pattern is refined during early post-natal development, resulting in the elimination of the majority of the ipsilateral projections (Joosten et al., 1992; Eyre et al., 2000, 2001; Li and Martin, 2000). This refinement of the ipsilateral projections is an activity-dependent process of competition with the crossed CST fibers originating from the contralateral motor cortex (Martin and Lee, 1999; Eyre et al., 2001; Eyre, 2003; Martin et al., 2004; Friel and Martin, 2007; Friel et al., 2014).

Human MM could result from the presence of CST projections to both the ipsilateral and contralateral spinal cord. In patients with CMM, Kallmann syndrome, Klippel-Feil syndrome or congenital hemiparesis, unilateral stimulation of the primary motor cortex hand area at rest by TMS elicits bilateral hand muscle responses with identical latencies, whereas in healthy volunteers the muscle response is strictly contralateral to the stimulated hemisphere (Nass, 1985; Farmer et al., 1990; Benecke et al., 1991; Mayston et al., 1997; Alagona et al., 2001; Staudt et al., 2002; Cincotta et al., 2003; Bawa et al., 2004; Srour et al., 2010; Depienne et al., 2011; Gallea et al., 2013). This reveals the presence of fast-conducting corticospinal projections from the hand area of one primary motor cortex to both sides of the spinal cord in CMM patients and suggests an anatomic-functional link between anomalies in the CST trajectory and the inability to produce lateralized movements.

Bilateral corticospinal projections to the spinal cord could be due to: (i) abnormal pyramidal decussation resulting in an aberrant uncrossed ipsilateral CST (**Figure 1D**); or (ii) aberrant branching of crossed CST axons in the spinal cord (**Figure 1E**). In both cases, the aberrant CST projection pattern could result from abnormal guidance of the CST axons or from an abnormal persistence of the ipsilateral CST projections that are normally eliminated during development. An elegant TMS study of two CMM patients supports the existence of a separate uncrossed ipsilateral CST (Cincotta et al., 2003). Diffusion tensor imaging (DTI) was used to study the precise anatomy of the pyramidal decussation in *Rad51*-mutated patients, confirming abnormal CST decussation (Gallea et al., 2013), although *Dcc*-mutated CMM patients have yet to be studied. *Rad51* expression pattern in the mouse central nervous system (Depienne et al., 2012), and the known role of *DCC* in commissural axons guidance (Kennedy et al., 1994; Serafini et al., 1994; Keino-Masu et al., 1996; Finger et al., 2002), suggest that abnormal axonal guidance rather than impaired CST maturation is responsible for the bilateral CST projections observed in *Rad51*- and *Dcc*-mutated patients. Electrophysiological studies also support the existence of an aberrant uncrossed CST in X-linked Kallmann patients (Mayston et al., 1997; Farmer et al., 2004). In patients with congenital hemiparesis, MM may be explained by an abnormal maturation of the CST due to the unequal activity between the affected and unaffected motor cortices (Eyre et al., 2001; Eyre, 2003; Friel et al., 2014). This would lead to the maintenance and reinforcement of the ipsilateral CST from the unaffected motor cortex, combined with aberrant branching of corticospinal fibers in the spinal cord (Benecke et al., 1991; Alagona et al., 2001; Staudt et al., 2002; Galléa et al., 2011; Friel et al., 2014). Mirror movements have not been described in patients with horizontal gaze palsy with progressive scoliosis (HGPPS), despite their lack of CST decussation. HGPPS is linked to mutations in the axon guidance receptor ROBO3 (Jen et al., 2004). The CST is completely uncrossed in HGPPS patients, and each hemisphere thus projects in a strictly ipsilateral manner to the spinal cord (**Figure 1F**). Together, these findings suggest that MM are related to the presence of bilateral spinal cord projections arising from a single primary motor cortex rather than to abnormal decussation of the CST *per se*.

Study of MM patients enlightened the critical importance of two mechanisms for the generation of asymmetric movements: (i) lateralized activation of the brain through contralateral silencing by IHI and proper motor planning; and (ii) unilateral transmission of the motor command to the contralateral spinal cord via the CST. Both abnormal interhemispheric connectivity

and an altered CST trajectory could be responsible for MM, but the respective importance of each factor is unclear.

Control of Left-Right Alternation During Locomotion: New Insights from Genetically Modified Mice with Developmental Motor System Anomalies

Quadrupedal locomotion requires repeated coordinated activity of each limb in a specific temporal sequence. Alternating left-right activity of the forelimbs and hindlimbs is observed at low locomotor frequencies (walking and trotting), while synchronized activity of the homologous limbs is observed at high locomotor frequencies (galloping) in mice, cats, horses and dogs (Forssberg et al., 1980; Dickinson et al., 2000; Serradj and Jamon, 2009). Lateralized motor output is thus a crucial aspect of locomotion, especially at low motor frequencies. In the past decade, careful analysis of genetically modified mice with a "hopping gait" has shed light on the respective contributions of the corticospinal tract and spinal central pattern generators (CPG) to left-right alternation during mouse locomotion.

The Corticospinal Tract and Left-Right Alternation During Locomotion

The CST forms a crossed (lateralized) motor circuit controlling voluntary movements of the four limbs. In rodents, the CST is composed of neurons originating from cortical layer V, projecting mainly to the contralateral side of the spinal cord and eventually connecting to motor neurons via a multisynaptic pathway (**Figure 2**; Canty and Murphy, 2008). A role of the CST in the control of alternating left-right activity during mouse locomotion was initially suggested by the "hopping gait" described in mice with genetically induced alterations of CST projections (mice with mutations of the EphA4 signaling pathway and kanga mice). EphA4 (a member of the Eph family of tyrosine-kinase receptors) and its ligand ephrinB3 are involved in axonal guidance of the CST during development. Deletion of EphA4, Ephrin-B3 or proteins involved in the EphA4 downstream signaling pathway (α2-chimaerin, Nck, RhoA) results in a hopping-gait phenotype (Dottori et al., 1998; Kullander et al., 2001a,b; Yokoyama et al., 2001; Beg et al., 2007; Fawcett et al., 2007; Iwasato et al., 2007; Mulherkar et al., 2013). In EphA4 and EphrinB3 knockout mice, the CST trajectory is normal from the cortex to the pyramidal decussation. In the spinal cord, CST axons re-cross the midline, resulting in bilateral innervation of the spinal cord by each of the two hemispheres. In wild-type animals, EphA4-expressing CST axons are repelled by ephrin-B3 secreted at the midline, deterring them from re-crossing the midline at the spinal level (Dottori et al., 1998; Kullander et al., 2001a,b; Yokoyama et al., 2001). These findings suggested that the hopping gait might be explained by transmission of motor commands to both sides of the spinal cord through abnormally re-crossed CST axons. Similarly to mice with genetic alterations of the EphA4 signaling pathway, a mutant mouse line carrying a viable mutation of the DCC receptor have a "kangaroo-like" hopping gait phenotype and are thus named "kanga" (Finger et al., 2002). The DCC ligand Netrin-1 belongs to the netrin family of extracellular guidance molecules. Netrin-1 has an attractive effect on growth cones when it interacts with the DCC receptor (Keino-Masu et al., 1996). This attraction allows commissural axons to approach and cross the midline (Kennedy et al., 1994; Serafini et al., 1994). DCC is expressed within the main forebrain descending tracts during their development (Shu et al., 2000). In kanga mice, the CST fails to cross the midline at the pyramidal decussation and projects exclusively to the ipsilateral side of the spinal cord (Finger et al., 2002).

However, other experimental findings do not support a major contribution of the CST to alternating left-right activity during locomotion. Indeed, abnormal CST midline crossing is not systematically associated with synchronized activity of the limbs during locomotion: mutants for L1 (Cohen et al., 1998; Jakeman et al., 2006), NCAM (Rolf et al., 2002), Sema6A and PlexinA3/PlexinA4 (Faulkner et al., 2008; Runker et al., 2008), exhibit normal locomotion despite having an abnormal CST. In rodents, a lateralized lesion of the cortex or CST, occurring during the first week of life, leads to sprouting of the remaining CST across the midline and thus to bilateral spinal cord projections (Leong and Lund, 1973; Kartje-Tillotson et al., 1987). This results in altered skilled forelimb movements without affecting left-right alternation during locomotion (Kunkel-Bagden et al., 1992; Whishaw et al., 1993; Whishaw, 2000; Metz and Whishaw, 2002; Tennant and Jones, 2009). Thus, abnormal CST projections do not necessarily induce a hopping gait.

It is important to recall that the genetic alterations induced in EphA4, ephrin-B3 and DCC kanga mutant mice not only impact CST development but also affect commissural cell populations expressing these proteins, such as pre-cerebellar commissural neurons (Hashimoto et al., 2012), and commissural spinal cord interneurons (Kullander et al., 2003; Beg et al., 2007; Iwasato et al., 2007; Rabe Bernhardt et al., 2012). This implies that the hopping gait observed in these mice is not necessarily due to their CST abnormalities. Two recent studies took advantage of the conditional knockout mouse Emx1::cre;EphA4$^{flox/flox}$ in which genetic deletion of EphA4 is restricted to the forebrain. These mice exhibit normal stereotypical locomotion despite bilateral CST projections to the spinal cord (Borgius et al., 2014; Serradj et al., 2014). Together, these results show that proper CST wiring is not necessary for stereotypic left-right alternation.

Supra-spinal control plays a critical role in voluntary movements and adaptive locomotion when sensory-motor integration is required (for example when stepping over an obstacle). Emx1::cre;EphA4$^{flox/flox}$ mice with bilateral CST projections to the spinal cord exhibit symmetric voluntary movements under conditions when asymmetric limbs movements are normally produced (Borgius et al., 2014; Friel et al., 2014; Serradj et al., 2014). These results emphasize the role of the CST in voluntary asymmetric movements.

In addition to the CST, supra-spinal structures playing an important role in the control of gait are located in the cerebral cortex, the cerebellum and in the brainstem, and constitute an interconnected network. There is no clear evidence implicating a supra-spinal control for left-right alternation and lateralization

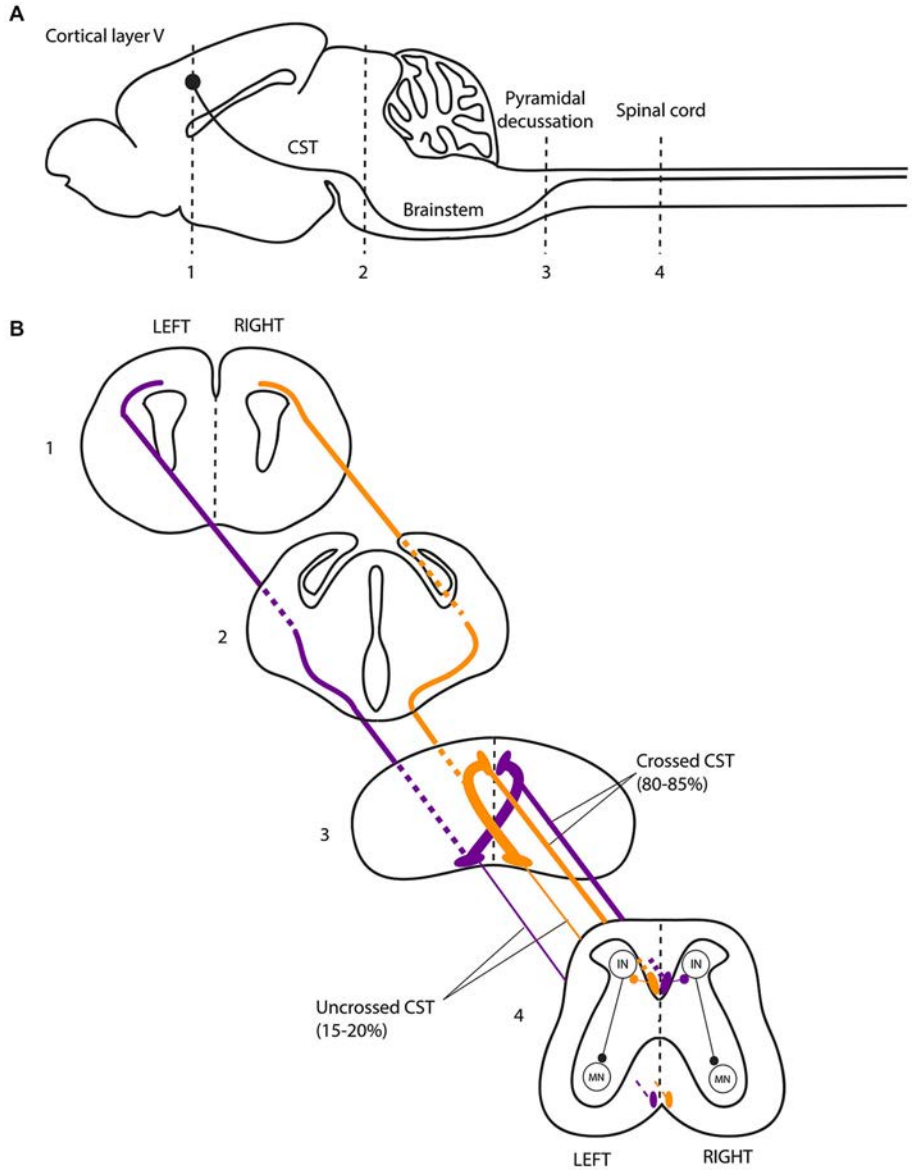

FIGURE 2 | The corticospinal tract forms a crossed motor system in mice. **(A)** Sagittal view of the mouse central nervous system and corticospinal tract (CST). **(B)** Coronal views of the CST trajectory. The level of each coronal schematic section is indicated in figure A. At the junction between the hindbrain and the spinal cord (pyramidal decussation, level 3), the vast majority (80–85%) of corticospinal tract (CST) axons cross the midline and continue their trajectory through the most ventral part of the dorsal funiculus within the half of the spinal cord contralateral to their hemisphere of origin. In the spinal cord, the CST undergoes collateral branching principally at the level of the cervical and lumbar enlargement, eventually transmitting motor commands to the forelimb and hindlimb muscles, respectively, via a multisynaptic pathway involving interneurons mainly located in the dorsal horn of the spinal cord. CST, corticospinal tract; IN, interneurons; MN, motor neurons.

of motor control during gait. Among the locomotor centers with direct spinal projections, the mesencephalic locomotor region (MLR) is of particular interest for our purpose. Electrical stimulation of the brainstem in decerebrate cats placed on a treadmill recapitulates normal alternate locomotion without the need of descending commands from the cortex (Shik et al., 1966, 1967). The MLR, which comprises the pedunculopontine (PPN) and cuneiform (CN) nuclei, sends outputs to the basal ganglia, the cerebellar and the cerebral locomotor areas. The MLR plays a major role in gait initiation and in internal generation of adaptive lower limb movement during the automated gait cycle (Alam et al., 2011; Grabli et al., 2012). The MLR could be involved in the control of gait cadence (Piallat et al., 2009; Karachi et al., 2010), but this involvement is more likely related to higher-order functions during faster gait rather than basic motor control as suggested by rodent models (Winn, 2008). Dysfunction of the MLR and cerebral locomotor centers is observed in patients with Parkinson disease and freezing of

gait (Fling et al., 2013, 2014), which is the inability to move the feet despite the effort to overcome the motor block and move forward. These patients exhibit alteration of gait rhythm, gait symmetry and bilateral coordination in stepping (Plotnik and Hausdorff, 2008; Plotnik et al., 2008). However, freezing of gait and bilateral coordination problems are triggered by particular circumstances, when adaptive locomotion is needed (Grabli et al., 2012). In addition, freezing also occurs during writing and speech, although the MLR is not involved in such tasks. MPTP monkeys with selective loss of cholinergic neurons in the PPN have gait impairments but no specific problem in the alternation of lower limb movements (Karachi et al., 2010). In cats, electrical stimulation of the PPN suppresses postural muscle tone, whereas CN stimulation elicits locomotor movements (Takakusaki et al., 2003). In humans, activity of the PPN seems to be modulated during rhythmical stepping, but the increased demands of postural control and attention during stepping could not be cancelled out (Fraix et al., 2013). Therefore, the structures constituting the MLR might play different roles in gait control, but none of them is known to be specifically involved in left-right alternation of the lower limbs.

In non mammalian vertebrates the descending motor pathways are mainly composed of reticulospinal tracts originating from the hindbrain (Vulliemoz et al., 2005). In zebrafish, descending motor pathways include Mauthner cells and other reticulospinal neurons (MiD2cm, MiD3cm and MiD3cl). This crossed network plays a critical role in adaptive locomotor activity such as escape behavior: a stimulus delivered to one side of the head results first in tail bending towards the opposite side, followed by a counter-bend that enables efficient propulsion (Kohashi and Oda, 2008; Jain et al., 2014). *DCC* mutations, leading to midline guidance defects of MiD2cm and MiD3cm neurons that project bilaterally instead of contralaterally, cause an abnormal counter-bend in the same direction as the first. Escape behavior of these mutant zebrafish is thereby compromised. This phenotype is rescued by ablation of the aberrantly projecting MiD2cm and MiD3cm neurons, demonstrating that supra-spinal pathways predominate over spinal circuitry during adaptive locomotion (Jain et al., 2014).

Altogether, these results suggest that supra-spinal control plays a critical role in motor lateralization during voluntary movements and adaptive locomotion but is not involved in left-right alternation during stereotypic locomotion.

Spinal Control of Left-Right Alternation During Locomotion

The importance of local spinal circuitry in locomotion is supported by "fictive locomotion" experiments performed *in vitro*. Exposure of isolated rodent spinal cords to neurotransmitter agonists such as serotonin and dopamine produces rhythmic activity at the lumbar level lasting several hours. This activity is characterized by alternating ipsilateral flexor-extensor activity and alternating left-right activity (Smith and Feldman, 1987; Kiehn and Kjaerulff, 1996). Successful replication of left-right alternation in spinal cords isolated from the forebrain strongly suggests that the spinal neuronal network plays a critical role in locomotion. This network is called the central pattern generator (CPG), and its role in swimming and walking has been extensively studied (Grillner, 2003; Goulding, 2009; Kiehn et al., 2010; Kiehn, 2011). The CPG generates rhythm, ipsilateral flexor-extensor alternation, and left-right alternation. Spinal commissural interneurons (CIN), mostly located in the ventromedial spinal cord (lamina VIII), play a key role in left-right alternation (Stokke et al., 2002). Fictive locomotion experiments *in vitro* have shown that removal of the dorsal part of the spinal cord does not affect left-right alternation, whereas sectioning of the ventral spinal cord commissure completely abolishes it (Kjaerulff and Kiehn, 1996). When inhibitory GABAa or glycinergic CIN are neutralized by the use of antagonists, spinal left-right alternating activity switches to synchronous activity, demonstrating that this cross-midline inhibition is critical for lateralized motor activity (Cowley and Schmidt, 1995). Conversely, suppression of glutamatergic excitatory transmission in the spinal cord of Vglut2 mutants does not affect the generation of left-right alternation or locomotor rhythms (Gezelius et al., 2006; Wallén-Mackenzie et al., 2006).

The specific characteristics and fate of spinal cord interneurons are determined by the progenitor subtype from which they originate. During the early phases of CNS development, transcription-factor gradients result in dorsoventral patterning of spinal neurons. There are 11 progenitor domains in the spinal cord, six dorsal (dI1-dI6) and five ventral (V0, V1, V2, motor neurons and V3 interneurons, in dorsal-to-ventral order; Jessell, 2000; Arber, 2012). Delineation of the CPG circuitry through the use of mutant mice improved our understanding of spinal alternating left-right activity.

By connecting the two sides of the spinal cord, CIN determine the excitatory/inhibitory balance over the midline. Most CIN involved in left-right coordination originate from the ventral spinal cord, from V0 and V3 progenitors (Kiehn, 2011; Chédotal,

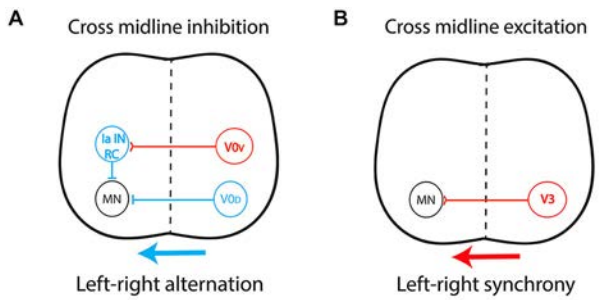

FIGURE 3 | Central pattern generator circuitry underlying left-right coordination during locomotion. **(A)** The dual inhibitory pathway (glycinergic/GABAergic) is composed of V0-derived interneurons including: (i) a group of dorsal inhibitory commissural interneurons (CIN) that project monosynaptically to contralateral motor neurons ($V0_D$); and (ii) a group of ventral glutamatergic CIN ($V0_V$) which provide indirect inhibition via a multisynaptic pathway with ipsilateral inhibitory interneurons such as Renshaw cells (RC) and Ia inhibitory interneurons (Ia IN). This system produces cross-midline inhibition that allows contralateral silencing during left-right alternation, in a frequency-dependent manner. **(B)** The excitatory pathway is composed of glutamatergic CIN (V3) projecting directly to contralateral motor neurons, providing the support for left-right synchronicity. Red, excitatory interneurons; Blue, inhibitory interneurons.

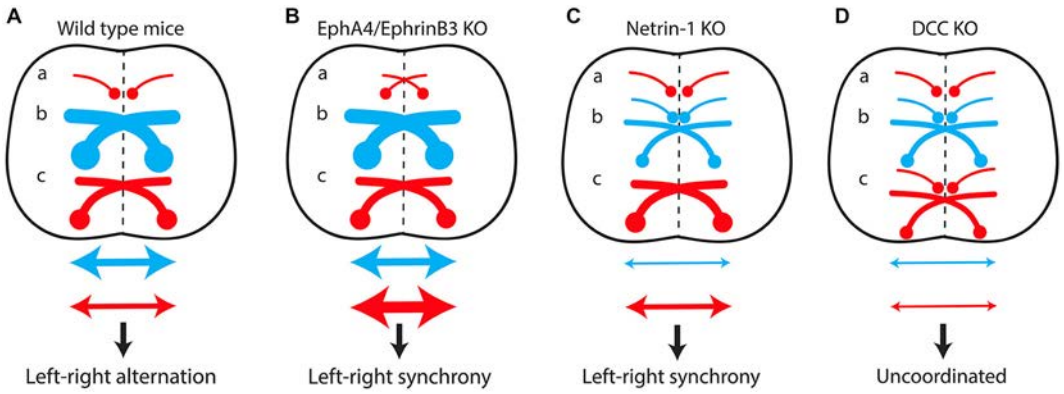

FIGURE 4 | The excitatory/inhibitory balance over the midline in the spinal cord determines the lateralization of motor output. **(A)** In wild-type mice, predominant recruitment of the dual-inhibitory pathway at low locomotor frequencies produces cross-midline inhibition resulting in left-right alternating activity. A switch from alternating to synchronous left-right activity results from increased cross-midline excitation due to the formation of "pseudo-commissural" excitatory neurons (a) in EphA4/EphrinB3 knockout mice **(B)** or to misguidance of several populations of inhibitory commissural interneurons (b) in Netrin-1 knockout mice **(C)**. Conversely, the loss of both inhibitory (b) and excitatory commissural interneurons (c) in DCC mutants **(D)** produces uncoordinated left-right activity. (a) Excitatory ipsilateral interneurons. (b) Inhibitory commissural interneurons. (c) Excitatory commissural interneurons. Red arrow, cross-midline excitation; Blue arrow, cross-midline inhibition.

2014), but the role of dorsally derived interneurons was recently highlighted (Andersson et al., 2012; Vallstedt and Kullander, 2013). Cross-midline inhibition relies on a dual inhibitory pathway (**Figure 3A**) composed mainly of V0-derived CIN and comprising: (i) a group of dorsal inhibitory CIN ($V0_D$) that project monosynaptically to contralateral motor neurons; and (ii) a group of ventral glutamatergic CIN ($V0_V$) which provide indirect inhibition via multisynaptic connections with ipsilateral inhibitory interneurons such as Renshaw cells (RC) and Ia inhibitory interneurons (Moran-Rivard et al., 2001; Pierani et al., 2001; Lanuza et al., 2004; Goulding, 2009; Kiehn et al., 2010). This system allows contralateral silencing during left-right alternation, in a frequency-dependent manner (Talpalar et al., 2013). In contrast, an excitatory pathway (**Figure 3B**) composed of glutamatergic CIN derived from V3 progenitors and projecting directly to contralateral motor neurons provides support for left-right synchrony (Zhang et al., 2008; Rabe et al., 2009; Borowska et al., 2013). This organization has been described in rodents (Quinlan and Kiehn, 2007; Restrepo et al., 2009) and cats (Jankowska et al., 2009). Additionally, ipsilaterally projecting interneurons are key components of multisynaptic pathways that provide indirect cross-midline inhibition and, as such, also participate in left-right alternation (Crone et al., 2008, 2009).

Mutant mice with commissural axon guidance defects have been critical for studying the spinal locomotor circuitry (**Figure 4**). Spinal CIN cross the midline at the floor plate, a structure located in the ventral spinal cord that secretes several molecules such as Ephrin-B3 and Netrin-1 involved in commissural axon guidance (Nawabi and Castellani, 2011). EphA4 and Ephrin-B3 knockout mice both have a hopping-gait phenotype (Dottori et al., 1998; Kullander et al., 2001b; Yokoyama et al., 2001). Fictive locomotion was studied with isolated spinal cords from EphA4 and ephrin-B3 null mutants aged between post-natal day 0 (P0) and P5, a period when the CST has not yet reached the lumbar spinal cord (Gianino et al., 1999). A switch from left-right alternating activity to synchronous activity was observed, together with an increased number of CIN in the ventral spinal cord. Reinforcement of cross-midline inhibition by GABA/glycine uptake blockers completely reversed this effect (Kullander et al., 2003). It was postulated that EphA4 is expressed in a population of excitatory interneurons projecting ipsilaterally, and that loss of EphA4 or ephrin-B3 leads to aberrant midline crossing of this population, resulting in "pseudo-commissural" excitatory connections. This would push the excitatory/inhibitory balance over the midline towards excitation (**Figure 4B**). In keeping with this hypothesis, specific deletion of EphA4 in the spinal cord or in glutamatergic interneurons is sufficient to induce a hopping gait both *in vivo* and *in vitro* (Borgius et al., 2014).

Netrin-1 knockout mice lack several inhibitory CIN populations, whereas their excitatory CIN are unaffected (Rabe et al., 2009). The inhibitory/excitatory balance over the midline is therefore shifted toward excitation, resulting in synchronous left-right locomotor activity *in vitro* (**Figure 4C**; Rabe et al., 2009). Surprisingly, suppression of the expression of DCC, the Netrin-1 receptor, leads to a different phenotype. DCC knockout mice exhibit uncoordinated left-right activity *in vitro*, reflecting the preservation of the excitatory/inhibitory balance over the midline, due to the loss of both inhibitory and excitatory CIN populations (**Figure 4D**; Rabe Bernhardt et al., 2012).

A hopping gait has also been described in Nkx mutant mice (Holz et al., 2010). Nkx transcription factors are involved in the development of the floor plate. The misguidance of V0 and dI6 CIN might be responsible for the phenotype of Nkx mutant mice (Holz et al., 2010).

Lateralization of motor output between the two sides of the spinal cord during stereotypic locomotion mainly relies on the excitatory/inhibitory balance over the midline. Recruitment of inhibitory pathways results in cross-midline inhibition and

left-right alternation, whereas recruitment of the excitatory pathway results in a shift toward excitation and left-right synchrony. Supra-spinal control and descending pathways (CST in mammals, reticulospinal tracts in non mammalian vertebrates) do not participate in stereotypic left-right alternation but rather contribute to motor lateralization during voluntary movements and adaptive locomotion.

Conclusion

The study of human "mirror movements" and rodent "hopping gait" reveals analogous mechanisms underlying the generation of asymmetric movements. Lateralized activation of the brain or spinal cord is first achieved through contralateral silencing by cross-midline inhibition. In the brain, this inhibition relies on excitatory neurons of the transcallosal tract that connect to inhibitory interneurons in the receiving hemisphere, while in the spinal cord both direct and indirect inhibition is involved during locomotion. Unilateral transmission of these activations results in lateralized motor output. When commissural axon guidance is compromised during development, the formation of projections to both sides of the spinal cord results in bilateral motor output. In mice, the formation of aberrant crossed excitatory connections in the spinal cord induces a hopping gait, while abnormal guidance of the CST in humans results in mirror movements.

Author's Role

QW, ID, CG and ER drafted the manuscript. QW, CG produced the figures. QW, ID, CG and ER critically reviewed the manuscript.

References

Ahmed, I., Mittal, K., Sheikh, T. I., Vasli, N., Rafiq, M. A., Mikhailov, A., et al. (2014). Identification of a homozygous splice site mutation in the dynein axonemal light chain 4 gene on 22q13.1 in a large consanguineous family from pakistan with congenital mirror movement disorder. *Hum. Genet.* 133, 1419–1429. doi: 10.1007/s00439-014-1475-8

Alagona, G., Delvaux, V., Gérard, P., De Pasqua, V., Pennisi, G., Delwaide, P. J., et al. (2001). Ipsilateral motor responses to focal transcranial magnetic stimulation in healthy subjects and acute-stroke patients. *Stroke* 32, 1304–1309. doi: 10.1161/01.str.32.6.1304

Alam, M., Schwabe, K., and Krauss, J. K. (2011). The pedunculopontine nucleus area: critical evaluation of interspecies differences relevant for its use as a target for deep brain stimulation. *Brain* 134, 11–23. doi: 10.1093/brain/awq322

Andersson, L. S., Larhammar, M., Memic, F., Wootz, H., Schwochow, D., Rubin, C. J., et al. (2012). Mutations in DMRT3 affect locomotion in horses and spinal circuit function in mice. *Nature* 488, 642–646. doi: 10.1038/nature11399

Arber, S. (2012). Motor circuits in action: specification, connectivity and function. *Neuron* 74, 975–989. doi: 10.1016/j.neuron.2012.05.011

Bawa, P., Hamm, J. D., Dhillon, P., and Gross, P. A. (2004). Bilateral responses of upper limb muscles to transcranial magnetic stimulation in human subjects. *Exp. Brain Res.* 158, 385–390. doi: 10.1007/s00221-004-2031-x

Beaulé, V., Tremblay, S., and Théoret, H. (2012). Interhemispheric control of unilateral movement. *Neural Plast.* 2012:627816. doi: 10.1155/2012/627816

Beg, A. A., Sommer, J. E., Martin, J. H., and Scheiffele, P. (2007). α2-Chimaerin is an essential EphA4 effector in the assembly of neuronal locomotor circuits. *Neuron* 55, 768–778. doi: 10.1016/j.neuron.2007.07.036

Benecke, R., Meyer, B. U., and Freund, H. J. (1991). Reorganisation of descending motor pathways in patients after hemispherectomy and severe hemispheric lesions demonstrated by magnetic brain stimulation. *Exp. Brain Res.* 83, 419–426. doi: 10.1007/bf00231167

Borgius, L., Nishimaru, H., Caldeira, V., Kunugise, Y., Löw, P., Reig, R., et al. (2014). Spinal glutamatergic neurons defined by EphA4 signaling are essential components of normal locomotor circuits. *J. Neurosci.* 34, 3841–3853. doi: 10.1523/JNEUROSCI.4992-13.2014

Borowska, J., Jones, C. T., Zhang, H., Blacklaws, J., Goulding, M., and Zhang, Y. (2013). Functional subpopulations of V3 interneurons in the mature mouse spinal cord. *J. Neurosci.* 33, 18553–18565. doi: 10.1523/JNEUROSCI.2005-13.2013

Brösamle, C., and Schwab, M. E. (1997). Cells of origin, course and termination patterns of the ventral, uncrossed component of the mature rat corticospinal tract. *J. Comp. Neurol.* 386, 293–303. doi: 10.1002/(SICI)1096-9861(19970922)386:2%3C293::AID-CNE9%3E3.0.CO;2-X

Canty, A. J., and Murphy, M. (2008). Molecular mechanisms of axon guidance in the developing corticospinal tract. *Prog. Neurobiol.* 85, 214–235. doi: 10.1016/j.pneurobio.2008.02.001

Carson, R. G. (2005). Neural pathways mediating bilateral interactions between the upper limbs. *Brain Res. Brain Res. Rev.* 49, 641–662. doi: 10.1016/j.brainresrev.2005.03.005

Chan, J. L., and Ross, E. D. (1988). Left-handed mirror writing following right anterior cerebral artery infarction: evidence for nonmirror transformation of motor programs by right supplementary motor area. *Neurology* 38, 59–63. doi: 10.1212/wnl.38.1.59

Chédotal, A. (2014). Development and plasticity of commissural circuits: from locomotion to brain repair. *Trends Neurosci.* 37, 551–562. doi: 10.1016/j.tins.2014.08.009

Chouinard, P. A., and Paus, T. (2010). What have we learned from "Perturbing" the human cortical motor system with transcranial magnetic stimulation? *Front. Hum. Neurosci.* 4:173. doi: 10.3389/fnhum.2010.00173

Cincotta, M., Borgheresi, A., Balestrieri, F., Giovannelli, F., Rossi, S., Ragazzoni, A., et al. (2004). Involvement of the human dorsal premotor cortex in unimanual motor control: an interference approach using transcranial magnetic stimulation. *Neurosci. Lett.* 367, 189–193. doi: 10.1016/j.neulet.2004.06.003

Cincotta, M., Borgheresi, A., Balzini, L., Vannucchi, L., Zeloni, G., Ragazzoni, A., et al. (2003). Separate ipsilateral and contralateral corticospinal projections in congenital mirror movements: neurophysiological evidence and significance for motor rehabilitation. *Mov. Disord.* 18, 1294–1300. doi: 10.1002/mds.10545

Cincotta, M., Borgheresi, A., Boffi, P., Vigliano, P., Ragazzoni, A., Zaccara, G., et al. (2002). Bilateral motor cortex output with intended unimanual contraction in congenital mirror movements. *Neurology* 58, 1290–1293. doi: 10.1212/wnl.58.8.1290

Cincotta, M., Lori, S., Gangemi, P. F., Barontini, F., and Ragazzoni, A. (1996). Hand motor cortex activation in a patient with congenital mirror movements: a study of the silent period following focal transcranial magnetic stimulation. *Electroencephalogr. Clin. Neurophysiol.* 101, 240–246. doi: 10.1016/0924-980x(96)95621-0

Cincotta, M., and Ziemann, U. (2008). Neurophysiology of unimanual motor control and mirror movements. *Clin. Neurophysiol.* 119, 744–762. doi: 10.1016/j.clinph.2007.11.047

Cohen, L. G., Meer, J., Tarkka, I., Bierner, S., Leiderman, D. B., Dubinsky, R. M., et al. (1991). Congenital mirror movements. Abnormal organization of motor pathways in two patients. *Brain* 114(Pt. 1B), 381–403. doi: 10.1093/brain/114.1.381

Cohen, N. R., Taylor, J. S., Scott, L. B., Guillery, R. W., Soriano, P., and Furley, A. J. (1998). Errors in corticospinal axon guidance in mice lacking the neural cell adhesion molecule L1. *Curr. Biol.* 8, 26–33. doi: 10.1016/s0960-9822(98)70017-x

Cowley, K. C., and Schmidt, B. J. (1995). Effects of inhibitory amino acid antagonists on reciprocal inhibitory interactions during rhythmic motor activity in the *in vitro* neonatal rat spinal cord. *J. Neurophysiol.* 74, 1109–1117.

Crone, S. A., Quinlan, K. A., Zagoraiou, L., Droho, S., Restrepo, C. E., Lundfald, L., et al. (2008). Genetic ablation of V2a ipsilateral interneurons disrupts left-right locomotor coordination in mammalian spinal cord. *Neuron* 60, 70–83. doi: 10.1016/j.neuron.2008.08.009

Crone, S. A., Zhong, G., Harris-Warrick, R., and Sharma, K. (2009). In mice lacking V2a interneurons, gait depends on speed of locomotion. *J. Neurosci.* 29, 7098–7109. doi: 10.1523/JNEUROSCI.1206-09.2009

Depienne, C., Bouteiller, D., Méneret, A., Billot, S., Groppa, S., Klebe, S., et al. (2012). RAD51 haploinsufficiency causes congenital mirror movements in humans. *Am. J. Hum. Genet.* 90, 301–307. doi: 10.1016/j.ajhg.2011.12.002

Depienne, C., Cincotta, M., Billot, S., Bouteiller, D., Groppa, S., Brochard, V., et al. (2011). A novel DCC mutation and genetic heterogeneity in congenital mirror movements. *Neurology* 76, 260–264. doi: 10.1212/WNL.0b013e318207b1e0

Dickinson, M. H., Farley, C. T., Full, R. J., Koehl, M. A., Kram, R., and Lehman, S. (2000). How animals move: an integrative view. *Science* 288, 100–106. doi: 10.1126/science.288.5463.100

Dottori, M., Hartley, L., Galea, M., Paxinos, G., Polizzotto, M., Kilpatrick, T., et al. (1998). EphA4 (Sek1) receptor tyrosine kinase is required for the development of the corticospinal tract. *Proc. Natl. Acad. Sci. U S A* 95, 13248–13253. doi: 10.1073/pnas.95.22.13248

Duque, J., Davare, M., Delaunay, L., Jacob, B., Saur, R., Hummel, F., et al. (2010). Monitoring coordination during bimanual movements: where is the mastermind? *J. Cogn. Neurosci.* 22, 526–542. doi: 10.1162/jocn.2009.21213

Duque, J., and Ivry, R. B. (2009). Role of corticospinal suppression during motor preparation. *Cereb. Cortex* 19, 2013–2024. doi: 10.1093/cercor/bhn230

Duque, J., Murase, N., Celnik, P., Hummel, F., Harris-Love, M., Mazzocchio, R., et al. (2007). Intermanual differences in movement-related interhemispheric inhibition. *J. Cogn. Neurosci.* 19, 204–213. doi: 10.1162/jocn.2007.19.2.204

Eyre, J. A. (2003). Development and plasticity of the corticospinal system in man. *Neural Plast.* 10, 93–106. doi: 10.1155/np.2003.93

Eyre, J. A., Miller, S., Clowry, G. J., Conway, E. A., and Watts, C. (2000). Functional corticospinal projections are established prenatally in the human foetus permitting involvement in the development of spinal motor centres. *Brain* 123(Pt. 1), 51–64. doi: 10.1093/brain/123.1.51

Eyre, J. A., Taylor, J. P., Villagra, F., Smith, M., and Miller, S. (2001). Evidence of activity-dependent withdrawal of corticospinal projections during human development. *Neurology* 57, 1543–1554. doi: 10.1212/wnl.57.9.1543

Farmer, S. F., Harrison, L. M., Mayston, M. J., Parekh, A., James, L. M., and Stephens, J. A. (2004). Abnormal cortex-muscle interactions in subjects with X-linked Kallmann's syndrome and mirror movements. *Brain* 127, 385–397. doi: 10.1093/brain/awh047

Farmer, S. F., Ingram, D. A., and Stephens, J. A. (1990). Mirror movements studied in a patient with Klippel-Feil syndrome. *J. Physiol.* 428, 467–484. doi: 10.1113/jphysiol.1990.sp018222

Faulkner, R. L., Low, L. K., Liu, X. B., Coble, J., Jones, E. G., and Cheng, H. J. (2008). Dorsal turning of motor corticospinal axons at the pyramidal decussation requires plexin signaling. *Neural Dev.* 3:21. doi: 10.1186/1749-8104-3-21

Fawcett, J. P., Georgiou, J., Ruston, J., Bladt, F., Sherman, A., Warner, N., et al. (2007). Nck adaptor proteins control the organization of neuronal circuits important for walking. *Proc. Natl. Acad. Sci. U S A* 104, 20973–20978. doi: 10.1073/pnas.0710316105

Finger, J. H., Bronson, R. T., Harris, B., Johnson, K., Przyborski, S. A., and Ackerman, S. L. (2002). The netrin 1 receptors Unc5h3 and Dcc are necessary at multiple choice points for the guidance of corticospinal tract axons. *J. Neurosci.* 22, 10346–10356.

Fling, B. W., Cohen, R. G., Mancini, M., Carpenter, S. D., Fair, D. A., Nutt, J. G., et al. (2014). Functional reorganization of the locomotor network in Parkinson patients with freezing of gait. *PLoS One* 9:e100291. doi: 10.1371/journal.pone.0100291

Fling, B. W., Cohen, R. G., Mancini, M., Nutt, J. G., Fair, D. A., and Horak, F. B. (2013). Asymmetric pedunculopontine network connectivity in parkinsonian patients with freezing of gait. *Brain* 136, 2405–2418. doi: 10.1093/brain/awt172

Forssberg, H., Grillner, S., Halbertsma, J., and Rossignol, S. (1980). The locomotion of the low spinal cat. II. Interlimb coordination. *Acta Physiol. Scand.* 108, 283–295. doi: 10.1111/j.1748-1716.1980.tb06534.x

Fraix, V., Bastin, J., David, O., Goetz, L., Ferraye, M., Benabid, A. L., et al. (2013). Pedunculopontine nucleus area oscillations during stance, stepping and freezing in Parkinson's disease. *PLoS One* 8:e83919. doi: 10.1371/journal.pone.0083919

Friel, K. M., and Martin, J. H. (2007). Bilateral activity-dependent interactions in the developing corticospinal system. *J. Neurosci.* 27, 11083–11090. doi: 10.1523/jneurosci.2814-07.2007

Friel, K. M., Williams, P. T., Serradj, N., Chakrabarty, S., and Martin, J. H. (2014). Activity-based therapies for repair of the corticospinal system injured during development. *Front. Neurol.* 5:229. doi: 10.3389/fneur.2014.00229

Galléa, C., Popa, T., Billot, S., Méneret, A., Depienne, C., and Roze, E. (2011). Congenital mirror movements: a clue to understanding bimanual motor control. *J. Neurol.* 258, 1911–1919. doi: 10.1007/s00415-011-6107-9

Gallea, C., Popa, T., Hubsch, C., Valabregue, R., Brochard, V., Kundu, P., et al. (2013). RAD51 deficiency disrupts the corticospinal lateralization of motor control. *Brain* 136, 3333–3346. doi: 10.1093/brain/awt258

Gezelius, H., Wallén-Mackenzie, A., Enjin, A., Lagerström, M., and Kullander, K. (2006). Role of glutamate in locomotor rhythm generating neuronal circuitry. *J. Physiol. Paris* 100, 297–303. doi: 10.1016/j.jphysparis.2007.05.001

Gianino, S., Stein, S. A., Li, H., Lu, X., Biesiada, E., Ulas, J., et al. (1999). Postnatal growth of corticospinal axons in the spinal cord of developing mice. *Brain Res. Dev. Brain Res.* 112, 189–204. doi: 10.1016/s0165-3806(98)00168-0

Giovannelli, F., Borgheresi, A., Balestrieri, F., Zaccara, G., Viggiano, M. P., Cincotta, M., et al. (2009). Modulation of interhemispheric inhibition by volitional motor activity: an ipsilateral silent period study. *J. Physiol.* 587, 5393–5410. doi: 10.1113/jphysiol.2009.175885

Goulding, M. (2009). Circuits controlling vertebrate locomotion: moving in a new direction. *Nat. Rev. Neurosci.* 10, 507–518. doi: 10.1038/nrn2608

Grabli, D., Karachi, C., Welter, M. L., Lau, B., Hirsch, E. C., Vidailhet, M., et al. (2012). Normal and pathological gait: what we learn from Parkinson's disease. *J. Neurol. Neurosurg. Psychiatry* 83, 979–985. doi: 10.1136/jnnp-2012-302263

Grillner, S. (2003). The motor infrastructure: from ion channels to neuronal networks. *Nat. Rev. Neurosci.* 4, 573–586. doi: 10.1038/nrn1137

Hashimoto, M., Ito, R., Kitamura, N., Namba, K., and Hisano, Y. (2012). Epha4 controls the midline crossing and contralateral axonal projections of inferior olive neurons. *J. Comp. Neurol.* 520, 1702–1720. doi: 10.1002/cne.23008

Holz, A., Kollmus, H., Ryge, J., Niederkofler, V., Dias, J., Ericson, J., et al. (2010). The transcription factors Nkx2.2 and Nkx2.9 play a novel role in floor plate development and commissural axon guidance. *Development* 137, 4249–4260. doi: 10.1242/dev.053819

Hübers, A., Orekhov, Y., and Ziemann, U. (2008). Interhemispheric motor inhibition: its role in controlling electromyographic mirror activity. *Eur. J. Neurosci.* 28, 364–371. doi: 10.1111/j.1460-9568.2008.06335.x

Iwasato, T., Katoh, H., Nishimaru, H., Ishikawa, Y., Inoue, H., Saito, Y. M., et al. (2007). Rac-GAP alpha-chimerin regulates motor-circuit formation as a key mediator of EphrinB3/EphA4 forward signaling. *Cell* 130, 742–753. doi: 10.1016/j.cell.2007.07.022

Jain, R. A., Bell, H., Lim, A., Chien, C. B., and Granato, M. (2014). Mirror movement-like defects in startle behavior of zebrafish dcc mutants are caused by aberrant midline guidance of identified descending hindbrain neurons. *J. Neurosci.* 34, 2898–2909. doi: 10.1523/JNEUROSCI.2420-13.2014

Jakeman, L. B., Chen, Y., Lucin, K. M., and McTigue, D. M. (2006). Mice lacking L1 cell adhesion molecule have deficits in locomotion and exhibit enhanced corticospinal tract sprouting following mild contusion injury to the spinal cord. *Eur. J. Neurosci.* 23, 1997–2011. doi: 10.1111/j.1460-9568.2006.04721.x

Jankowska, E., Bannatyne, B. A., Stecina, K., Hammar, I., Cabaj, A., and Maxwell, D. J. (2009). Commissural interneurons with input from group I and II muscle afferents in feline lumbar segments: neurotransmitters, projections and target cells. *J. Physiol.* 587, 401–418. doi: 10.1113/jphysiol.2008.159236

Jen, J. C., Chan, W. M., Bosley, T. M., Wan, J., Carr, J. R., Rüb, U., et al. (2004). Mutations in a human ROBO gene disrupt hindbrain axon pathway crossing and morphogenesis. *Science* 304, 1509–1513. doi: 10.1126/science.1096437

Jessell, T. M. (2000). Neuronal specification in the spinal cord: inductive signals and transcriptional codes. *Nat. Rev. Genet.* 1, 20–29. doi: 10.1038/35049541

Joosten, E. A., Schuitman, R. L., Vermelis, M. E., and Dederen, P. J. (1992). Postnatal development of the ipsilateral corticospinal component in rat spinal cord: a light and electron microscopic anterograde HRP study. *J. Comp. Neurol.* 326, 133–146. doi: 10.1002/cne.903260112

Karachi, C., Grabli, D., Bernard, F. A., Tandé, D., Wattiez, N., Belaid, H., et al. (2010). Cholinergic mesencephalic neurons are involved in gait and postural disorders in Parkinson disease. *J. Clin. Invest.* 120, 2745–2754. doi: 10.1172/JCI42642

Kartje-Tillotson, G., O'Donoghue, D. L., Dauzvardis, M. F., and Castro, A. J. (1987). Pyramidotomy abolishes the abnormal movements evoked by intracortical microstimulation in adult rats that sustained neonatal cortical lesions. *Brain Res.* 415, 172–177. doi: 10.1016/0006-8993(87)90283-6

Keino-Masu, K., Masu, M., Hinck, L., Leonardo, E. D., Chan, S. S., Culotti, J. G., et al. (1996). Deleted in Colorectal Cancer (DCC) encodes a netrin receptor. *Cell* 87, 175–185. doi: 10.1016/s0092-8674(00)81336-7

Kennedy, T. E., Serafini, T., de la Torre, J. R., and Tessier-Lavigne, M. (1994). Netrins are diffusible chemotropic factors for commissural axons in the embryonic spinal cord. *Cell* 78, 425–435. doi: 10.1016/0092-8674(94)90421-9

Kiehn, O. (2011). Development and functional organization of spinal locomotor circuits. *Curr. Opin. Neurobiol.* 21, 100–109. doi: 10.1016/j.conb.2010.09.004

Kiehn, O., Dougherty, K. J., Hägglund, M., Borgius, L., Talpalar, A., and Restrepo, C. E. (2010). Probing spinal circuits controlling walking in mammals. *Biochem. Biophys. Res. Commun.* 396, 11–18. doi: 10.1016/j.bbrc.2010.02.107

Kiehn, O., and Kjaerulff, O. (1996). Spatiotemporal characteristics of 5-HT and dopamine-induced rhythmic hindlimb activity in the *in vitro* neonatal rat. *J. Neurophysiol.* 75, 1472–1482.

Kjaerulff, O., and Kiehn, O. (1996). Distribution of networks generating and coordinating locomotor activity in the neonatal rat spinal cord *in vitro*: a lesion study. *J. Neurosci.* 16, 5777–5794.

Koerte, I., Eftimov, L., Laubender, R. P., Esslinger, O., Schroeder, A. S., Ertl-Wagner, B., et al. (2010). Mirror movements in healthy humans across the lifespan: effects of development and ageing. *Dev. Med. Child Neurol.* 52, 1106–1112. doi: 10.1111/j.1469-8749.2010.03766.x

Kohashi, T., and Oda, Y. (2008). Initiation of Mauthner- or non-Mauthner-mediated fast escape evoked by different modes of sensory input. *J. Neurosci.* 28, 10641–10653. doi: 10.1523/jneurosci.1435-08.2008

Krams, M., Quinton, R., Mayston, M. J., Harrison, L. M., Dolan, R. J., Bouloux, P. M., et al. (1997). Mirror movements in X-linked Kallmann's syndrome II. A PET study. *Brain* 120(Pt. 7), 1217–1228. doi: 10.1093/brain/120.7.1217

Kullander, K., Butt, S. J., Lebret, J. M., Lundfald, L., Restrepo, C. E., Rydström, A., et al. (2003). Role of EphA4 and EphrinB3 in local neuronal circuits that control walking. *Science* 299, 1889–1892. doi: 10.1126/science.1079641

Kullander, K., Croll, S. D., Zimmer, M., Pan, L., McClain, J., Hughes, V., et al. (2001a). Ephrin-B3 is the midline barrier that prevents corticospinal tract axons from recrossing, allowing for unilateral motor control. *Genes Dev.* 15, 877–888. doi: 10.1101/gad.868901

Kullander, K., Mather, N. K., Diella, F., Dottori, M., Boyd, A. W., and Klein, R. (2001b). Kinase-dependent and kinase-independent functions of EphA4 receptors in major axon tract formation *in vivo*. *Neuron* 29, 73–84. doi: 10.1016/s0896-6273(01)00181-7

Kunkel-Bagden, E., Dai, H. N., and Bregman, B. S. (1992). Recovery of function after spinal cord hemisection in newborn and adult rats: differential effects on reflex and locomotor function. *Exp. Neurol.* 116, 40–51. doi: 10.1016/0014-4886(92)90174-o

Lanuza, G. M., Gosgnach, S., Pierani, A., Jessell, T. M., and Goulding, M. (2004). Genetic identification of spinal interneurons that coordinate left-right locomotor activity necessary for walking movements. *Neuron* 42, 375–386. doi: 10.3410/f.1019388.218551

Leong, S. K., and Lund, R. D. (1973). Anomalous bilateral corticofugal pathways in albino rats after neonatal lesions. *Brain Res.* 62, 218–221. doi: 10.1016/0006-8993(73)90630-6

Lepage, J. F., Beaulé, V., Srour, M., Rouleau, G., Pascual-Leone, A., Lassonde, M., et al. (2012). Neurophysiological investigation of congenital mirror movements in a patient with agenesis of the corpus callosum. *Brain Stimul.* 5, 137–140. doi: 10.1016/j.brs.2011.02.004

Li, Q., and Martin, J. H. (2000). Postnatal development of differential projections from the caudal and rostral motor cortex subregions. *Exp. Brain Res.* 134, 187–198. doi: 10.1007/s002210000454

Martin, J. H., Choy, M., Pullman, S., and Meng, Z. (2004). Corticospinal system development depends on motor experience. *J. Neurosci.* 24, 2122–2132. doi: 10.1523/jneurosci.4616-03.2004

Martin, J. H., and Lee, S. J. (1999). Activity-dependent competition between developing corticospinal terminations. *Neuroreport* 10, 2277–2282. doi: 10.1097/00001756-199908020-00010

Mayer, M., Bötzel, K., Paulus, W., Plendl, H., Pröckl, D., and Danek, A. (1995). Movement-related cortical potentials in persistent mirror movements. *Electroencephalogr. Clin. Neurophysiol.* 95, 350–358. doi: 10.1016/0013-4694(95)00100-d

Mayston, M. J., Harrison, L. M., Quinton, R., Stephens, J. A., Krams, M., and Bouloux, P. M. (1997). Mirror movements in X-linked Kallmann's syndrome. I. A neurophysiological study. *Brain* 120(Pt. 7), 1199–1216. doi: 10.1093/brain/120.7.1199

Mayston, M. J., Harrison, L. M., and Stephens, J. A. (1999). A neurophysiological study of mirror movements in adults and children. *Ann. Neurol.* 45, 583–594. doi: 10.1002/1531-8249(199905)45:5<583::aid-ana6>3.0.co;2-w

Méneret, A., Depienne, C., Riant, F., Trouillard, O., Bouteiller, D., Cincotta, M., et al. (2014a). Congenital mirror movements: mutational analysis of RAD51 and DCC in 26 cases. *Neurology* 82, 1999–2002. doi: 10.1212/wnl.0000000000000477

Méneret, A., Trouillard, O., Vidailhet, M., Depienne, C., and Roze, E. (2014b). Congenital mirror movements: no mutation in DNAL4 in 17 index cases. *J. Neurol.* 261, 2030–2031. doi: 10.1007/s00415-014-7505-6

Metz, G. A., and Whishaw, I. Q. (2002). Cortical and subcortical lesions impair skilled walking in the ladder rung walking test: a new task to evaluate fore- and hindlimb stepping, placing and co-ordination. *J. Neurosci. Methods* 115, 169–179. doi: 10.1016/s0165-0270(02)00012-2

Meyer, B. U., Roricht, S., Grafin Von Einsiedel, H., Kruggel, F., and Weindl, A. (1995). Inhibitory and excitatory interhemispheric transfers between motor cortical areas in normal humans and patients with abnormalities of the corpus callosum. *Brain* 118(Pt. 2), 429–440. doi: 10.1093/brain/118.2.429

Moran-Rivard, L., Kagawa, T., Saueressig, H., Gross, M. K., Burrill, J., and Goulding, M. (2001). Evx1 is a postmitotic determinant of v0 interneuron identity in the spinal cord. *Neuron* 29, 385–399. doi: 10.1016/s0896-6273(01)00213-6

Mulherkar, S., Liu, F., Chen, Q., Narayanan, A., Couvillon, A. D., Shine, H. D., et al. (2013). The small GTPase RhoA is required for proper locomotor circuit assembly. *PLoS One* 8:e67015. doi: 10.1371/journal.pone.0067015

Murase, N., Duque, J., Mazzocchio, R., and Cohen, L. G. (2004). Influence of interhemispheric interactions on motor function in chronic stroke. *Ann. Neurol.* 55, 400–409. doi: 10.1002/ana.10848

Nass, R. (1985). Mirror movement asymmetries in congenital hemiparesis: the inhibition hypothesis revisited. *Neurology* 35, 1059–1062. doi: 10.1212/wnl.35.7.1059

Nawabi, H., and Castellani, V. (2011). Axonal commissures in the central nervous system: how to cross the midline? *Cell. Mol. Life Sci.* 68, 2539–2553. doi: 10.1007/s00018-011-0691-9

Papadopoulou, M., Chairopoulos, K., Anagnostou, E., Kokotis, P., Zambelis, T., and Karandreas, N. (2010). Concurrent bilateral projection and activation of motor cortices in a patient with congenital mirror movements: a TMS study. *Clin. Neurol. Neurosurg.* 112, 824–828. doi: 10.1016/j.clineuro.2010.06.016

Peng, J., and Charron, F. (2013). Lateralization of motor control in the human nervous system: genetics of mirror movements. *Curr. Opin. Neurobiol.* 23, 109–118. doi: 10.1016/j.conb.2012.08.007

Perez, M. A., and Cohen, L. G. (2008). Mechanisms underlying functional changes in the primary motor cortex ipsilateral to an active hand. *J. Neurosci.* 28, 5631–5640. doi: 10.1523/jneurosci.0093-08.2008

Piallat, B., Chabardes, S., Torres, N., Fraix, V., Goetz, L., Seigneuret, E., et al. (2009). Gait is associated with an increase in tonic firing of the sub-cuneiform nucleus neurons. *Neuroscience* 158, 1201–1205. doi: 10.1016/j.neuroscience.2008.10.046

Pierani, A., Moran-Rivard, L., Sunshine, M. J., Littman, D. R., Goulding, M., and Jessell, T. M. (2001). Control of interneuron fate in the developing spinal cord by the progenitor homeodomain protein Dbx1. *Neuron* 29, 367–384. doi: 10.1016/s0896-6273(01)00212-4

Plotnik, M., Giladi, N., and Hausdorff, J. M. (2008). Bilateral coordination of walking and freezing of gait in Parkinson's disease. *Eur. J. Neurosci.* 27, 1999–2006. doi: 10.1111/j.1460-9568.2008.06167.x

Plotnik, M., and Hausdorff, J. M. (2008). The role of gait rhythmicity and bilateral coordination of stepping in the pathophysiology of freezing of gait in

Parkinson's disease. *Mov. Disord.* 23(Suppl. 2), S444–S450. doi: 10.1002/mds.21984

Quinlan, K. A., and Kiehn, O. (2007). Segmental, synaptic actions of commissural interneurons in the mouse spinal cord. *J. Neurosci.* 27, 6521–6530. doi: 10.1523/jneurosci.1618-07.2007

Rabe, N., Gezelius, H., Vallstedt, A., Memic, F., and Kullander, K. (2009). Netrin-1-dependent spinal interneuron subtypes are required for the formation of left-right alternating locomotor circuitry. *J. Neurosci.* 29, 15642–15649. doi: 10.1523/jneurosci.5096-09.2009

Rabe Bernhardt, N., Memic, F., Gezelius, H., Thiebes, A. L., Vallstedt, A., and Kullander, K. (2012). DCC mediated axon guidance of spinal interneurons is essential for normal locomotor central pattern generator function. *Dev. Biol.* 366, 279–289. doi: 10.1016/j.ydbio.2012.03.017

Reis, J., Swayne, O. B., Vandermeeren, Y., Camus, M., Dimyan, M. A., Harris-Love, M., et al. (2008). Contribution of transcranial magnetic stimulation to the understanding of cortical mechanisms involved in motor control. *J. Physiol.* 586, 325–351. doi: 10.1113/jphysiol.2007.144824

Restrepo, C. E., Lundfald, L., Szabó, G., Erdelyi, F., Zeilhofer, H. U., Glover, J. C., et al. (2009). Transmitter-phenotypes of commissural interneurons in the lumbar spinal cord of newborn mice. *J. Comp. Neurol.* 517, 177–192. doi: 10.1002/cne.22144

Rolf, B., Bastmeyer, M., Schachner, M., and Bartsch, U. (2002). Pathfinding errors of corticospinal axons in neural cell adhesion molecule-deficient mice. *J. Neurosci.* 22, 8357–8362.

Rosenzweig, E. S., Brock, J. H., Culbertson, M. D., Lu, P., Moseanko, R., Edgerton, V. R., et al. (2009). Extensive spinal decussation and bilateral termination of cervical corticospinal projections in rhesus monkeys. *J. Comp. Neurol.* 513, 151–163. doi: 10.1002/cne.21940

Runker, A. E., Little, G. E., Suto, F., Fujisawa, H., and Mitchell, K. J. (2008). Semaphorin-6A controls guidance of corticospinal tract axons at multiple choice points. *Neural Dev.* 3:34. doi: 10.1186/1749-8104-3-34

Schieber, M. H. (2007). Chapter 2 comparative anatomy and physiology of the corticospinal system. *Handb. Clin. Neurol.* 82, 15–37. doi: 10.1016/s0072-9752(07)80005-4

Sehm, B., Perez, M. A., Xu, B., Hidler, J., and Cohen, L. G. (2010). Functional neuroanatomy of mirroring during a unimanual force generation task. *Cereb. Cortex* 20, 34–45. doi: 10.1093/cercor/bhp075

Serafini, T., Kennedy, T. E., Galko, M. J., Mirzayan, C., Jessell, T. M., and Tessier-Lavigne, M. (1994). The netrins define a family of axon outgrowth-promoting proteins homologous to C. elegans UNC-6. *Cell* 78, 409–424. doi: 10.1016/0092-8674(94)90420-0

Serradj, N., and Jamon, M. (2009). The adaptation of limb kinematics to increasing walking speeds in freely moving mice 129/Sv and C57BL/6. *Behav. Brain Res.* 201, 59–65. doi: 10.1016/j.bbr.2009.01.030

Serradj, N., Paixao, S., Sobocki, T., Feinberg, M., Klein, R., Kullander, K., et al. (2014). EphA4-mediated ipsilateral corticospinal tract misprojections are necessary for bilateral voluntary movements but not bilateral stereotypic locomotion. *J. Neurosci.* 34, 5211–5221. doi: 10.1523/JNEUROSCI.4848-13.2014

Shibasaki, H., and Hallett, M. (2006). What is the Bereitschaftspotential? *Clin. Neurophysiol.* 117, 2341–2356. doi: 10.1016/j.clinph.2006.04.025

Shibasaki, H., and Nagae, K. (1984). Mirror movement: application of movement-related cortical potentials. *Ann. Neurol.* 15, 299–302. doi: 10.1002/ana.410150317

Shik, M. L., Severin, F. V., and Orlovskii, G. N. (1966). [Control of walking and running by means of electric stimulation of the midbrain]. *Biofizika* 11, 659–666.

Shik, M. L., Severin, F. V., and Orlovskii, G. N. (1967). [Structures of the brain stem responsible for evoked locomotion]. *Fiziol. Zh. SSSR Im. I M Sechenova* 53, 1125–1132.

Shu, T., Valentino, K. M., Seaman, C., Cooper, H. M., and Richards, L. J. (2000). Expression of the netrin-1 receptor, deleted in colorectal cancer (DCC), is largely confined to projecting neurons in the developing forebrain. *J. Comp. Neurol.* 416, 201–212. doi: 10.1002/(sici)1096-9861(20000110)416:2<201::aid-cne6>3.0.co;2-z

Smith, J. C., and Feldman, J. L. (1987). *In vitro* brainstem-spinal cord preparations for study of motor systems for mammalian respiration and locomotion. *J. Neurosci. Methods* 21, 321–333. doi: 10.1016/0165-0270(87)90126-9

Srour, M., Rivière, J. B., Pham, J. M., Dube, M. P., Girard, S., Morin, S., et al. (2010). Mutations in DCC cause congenital mirror movements. *Science* 328:592. doi: 10.1126/science.1186463

Staudt, M., Grodd, W., Gerloff, C., Erb, M., Stitz, J., and Krageloh-Mann, I. (2002). Two types of ipsilateral reorganization in congenital hemiparesis: a TMS and fMRI study. *Brain* 125, 2222–2237. doi: 10.1093/brain/awf227

Stokke, M. F., Nissen, U. V., Glover, J. C., and Kiehn, O. (2002). Projection patterns of commissural interneurons in the lumbar spinal cord of the neonatal rat. *J. Comp. Neurol.* 446, 349–359. doi: 10.1002/cne.10211

Takakusaki, K., Habaguchi, T., Ohtinata-Sugimoto, J., Saitoh, K., and Sakamoto, T. (2003). Basal ganglia efferents to the brainstem centers controlling postural muscle tone and locomotion: a new concept for understanding motor disorders in basal ganglia dysfunction. *Neuroscience* 119, 293–308. doi: 10.1016/s0306-4522(03)00095-2

Talpalar, A. E., Bouvier, J., Borgius, L., Fortin, G., Pierani, A., and Kiehn, O. (2013). Dual-mode operation of neuronal networks involved in left-right alternation. *Nature* 500, 85–88. doi: 10.1038/nature12286

Tennant, K. A., and Jones, T. A. (2009). Sensorimotor behavioral effects of endothelin-1 induced small cortical infarcts in C57BL/6 mice. *J. Neurosci. Methods* 181, 18–26. doi: 10.1016/j.jneumeth.2009.04.009

Vallstedt, A., and Kullander, K. (2013). Dorsally derived spinal interneurons in locomotor circuits. *Ann. N Y Acad. Sci.* 1279, 32–42. doi: 10.1111/j.1749-6632.2012.06801.x

Verstynen, T., Spencer, R., Stinear, C. M., Konkle, T., Diedrichsen, J., Byblow, W. D., et al. (2007). Ipsilateral corticospinal projections do not predict congenital mirror movements: a case report. *Neuropsychologia* 45, 844–852. doi: 10.1016/j.neuropsychologia.2006.08.019

Vulliemoz, S., Raineteau, O., and Jabaudon, D. (2005). Reaching beyond the midline: why are human brains cross wired? *Lancet Neurol.* 4, 87–99. doi: 10.1016/s1474-4422(05)00990-7

Wallén-Mackenzie, A., Gezelius, H., Thoby-Brisson, M., Nygård, A., Enjin, A., Fujiyama, F., et al. (2006). Vesicular glutamate transporter 2 is required for central respiratory rhythm generation but not for locomotor central pattern generation. *J. Neurosci.* 26, 12294–12307. doi: 10.3410/f.1052770.504685

Whishaw, I. Q. (2000). Loss of the innate cortical engram for action patterns used in skilled reaching and the development of behavioral compensation following motor cortex lesions in the rat. *Neuropharmacology* 39, 788–805. doi: 10.1016/s0028-3908(99)00259-2

Whishaw, I. Q., Pellis, S. M., Gorny, B., Kolb, B., and Tetzlaff, W. (1993). Proximal and distal impairments in rat forelimb use in reaching follow unilateral pyramidal tract lesions. *Behav. Brain Res.* 56, 59–76. doi: 10.1016/0166-4328(93)90022-i

Winn, P. (2008). Experimental studies of pedunculopontine functions: are they motor, sensory or integrative? *Parkinsonism Relat. Disord.* 14(Suppl. 2), S194–S198. doi: 10.1016/j.parkreldis.2008.04.030

Yokoyama, N., Romero, M. I., Cowan, C. A., Galvan, P., Helmbacher, F., Charnay, P., et al. (2001). Forward signaling mediated by ephrin-B3 prevents contralateral corticospinal axons from recrossing the spinal cord midline. *Neuron* 29, 85–97. doi: 10.1016/s0896-6273(01)00182-9

Zhang, Y., Narayan, S., Geiman, E., Lanuza, G. M., Velasquez, T., Shanks, B., et al. (2008). V3 spinal neurons establish a robust and balanced locomotor rhythm during walking. *Neuron* 60, 84–96. doi: 10.3410/f.1125790.582877

Zijdewind, I., Butler, J. E., Gandevia, S. C., and Taylor, J. L. (2006). The origin of activity in the biceps brachii muscle during voluntary contractions of the contralateral elbow flexor muscles. *Exp. Brain Res.* 175, 526–535. doi: 10.1007/s00221-006-0570-z

Conflict of Interest Statement: The authors declare that the research was conducted in the absence of any commercial or financial relationships that could be construed as a potential conflict of interest.

Copyright © 2015 Welniarz, Dusart, Gallea and Roze. This is an open-access article distributed under the terms of the Creative Commons Attribution License (CC BY). The use, distribution and reproduction in other forums is permitted, provided the original author(s) or licensor are credited and that the original publication in this journal is cited, in accordance with accepted academic practice. No use, distribution or reproduction is permitted which does not comply with these terms.

D. Problématique et objectifs de la thèse

Les études de patients atteints de MMC ont permis de mettre en évidence deux mécanismes principaux, non exclusifs, impliqués dans la génération des mouvements latéralisés : (i) une anomalie développementale du FCS aboutissant à la mise en place de projections bilatérales de chacun des hémisphères sur la moelle ; (ii) des défauts de communication inter-hémisphérique, responsables d'une activation bilatérale anormale des deux cortex moteurs lors de l'exécution d'un mouvement unimanuel. Ces observations soulignent l'importance de deux structures dont le développement normal semble nécessaire au contrôle de la latéralisation motrice : le FCS et le CC. Les connaissances que nous avons sur les MMC ont cependant des limites, et plusieurs questions restent en suspens :

1) Les deux gènes identifiés à ce jour, *DCC* et *RAD51*, jouent *a priori* des rôles très différents au cours du développement. Comment les mutations de *RAD51* et *DCC* aboutissent-elle au phénotype de MMC ? Quel est le rôle précis de RAD51 et DCC dans le développement du FCS et du CC, les deux principales structures impliquées dans la physiopathologie des MMC ? Les mécanismes sont-ils les mêmes dans les deux cas ?

2) Les formes de MMC dues aux mutations des gènes *RAD51*, DCC, ainsi que celles dont la cause génétique est encore inconnue, sont caractérisées par un même phénotype clinique. L'homogénéité clinique des MM est-elle le reflet de mécanismes communs aux différentes formes génétiques de MMC ?

3) Plusieurs éléments indiquent que les interactions inter-hémisphériques nécessaires à la latéralisation de l'activité corticale au cours de la génération de mouvements unimanuels pourraient être dysfonctionnelles dès la phase de préparation motrice. Quels sont les

mécanismes responsables de la latéralisation motrice au cours de la préparation du mouvement ? En quoi ces mécanismes sont-ils altérés chez les patients atteints de MMC ?

Afin de répondre à ces questions, nous avons combiné des expériences sur des modèles animaux et chez des patients atteints de MMC.

Chez la souris, nous avons étudié le rôle de DCC et RAD51 dans le développement du FCS et du CC, les deux principales structures identifiées dans la physiopathologie des MMC, ainsi que leur implication dans la latéralisation du contrôle moteur. Nous avons dans un premier temps étudié le patron d'expression spatio-temporel de RAD51 et complété celui de DCC dans le système nerveux central, puis nous avons ensuite étudié le phénotype anatomique et comportemental de différentes lignées de souris déficientes pour les gènes *Rad51* ou *Dcc*.

Chez l'humain, l'étude avait un double objectif : d'une part déterminer s'il existe des différences physiopathologiques entre les différentes formes génétiques de MMC ; d'autre part comprendre les mécanismes impliqués dans la latéralisation de l'activité des aires motrices corticales pendant la préparation du mouvement, ainsi que le rôle des aires motrices secondaires, et en particulier de l'aire motrice supplémentaire (AMS) dans cette fonction. Pour cela, nous avons utilisé une approche multimodale neurophysiologie/neuroimagerie utilisant la stimulation magnétique transcrânienne (SMT) et l'imagerie par résonnance magnétique (IRM) afin d'étudier l'activation et les interactions inter-hémisphériques de différentes aires motrices primaires et secondaires chez : (i) des patients atteints de MMC ; et (ii) des sujets contrôles appariés avant et après inhibition transitoire de l'AMS.

Grâce à cette double approche, nous avons pu aborder de façon transversale différentes questions nécessitant des modèles d'étude différents, tout en conservant une problématique unique : comprendre les mécanismes responsables de la latéralisation motrice.

Dans la suite de cette introduction, je présenterai donc l'état des connaissances actuelles concernant l'évolution, l'anatomie, le développement et les pathologies du CC et du FCS. Dans une dernière partie, je m'intéresserai aux données concernant la préparation du mouvement.

II. Evolution, anatomie, développement et pathologies du corps calleux et du faisceau corticospinal

Le CC et le FCS sont deux structures impliquées dans la physiopathologie des mouvements en miroir, et leur développement normal est nécessaire à la latéralisation du contrôle moteur. Dans cette partie, nous allons nous intéresser à l'évolution, l'anatomie, le développement et aux pathologies du CC et du FCS, en prêtant une attention particulière aux mécanismes concernant le croisement de la ligne médiane et à leur lien avec les mouvements en miroir.

A. Evolution, anatomie, développement et pathologies du corps calleux

1) Le corps calleux au sein de l'évolution

Le clade phylogénique des mammifères comprend trois groupes : les protothériens (ou monotrèmes), les métathériens et les euthériens (Figure 4), qui se différencient les uns des autres par leur mode de développement embryonnaire (Kielan-Jaworowska et al., 2005). Les monotrèmes sont des ovipares : ils pondent des œufs, mais allaitent néanmoins leurs petits. Les représentants actuels des monotrèmes sont les ornithorynques et les tachyglossidés. Les euthériens et métathériens sont vivipares (le développement de l'embryon se fait au sein de l'utérus), mais les euthériens possèdent un placenta, à la différence des métathériens. Les métathériens comprennent les marsupiaux actuels (ainsi que d'autres espèces disparues), tandis que les euthériens rassemblent l'ensemble des mammifères placentaires.

Le corps calleux est la principale commissure assurant la connexion des deux hémisphères cérébraux. Cette commissure est apparue chez les mammifères placentaires (Aboitiz and Montiel, 2003; Suarez et al., 2014b). Le corpus calleux est donc absent chez les marsupiaux et les monotrèmes. Chez ces espèces, la communication entre les deux

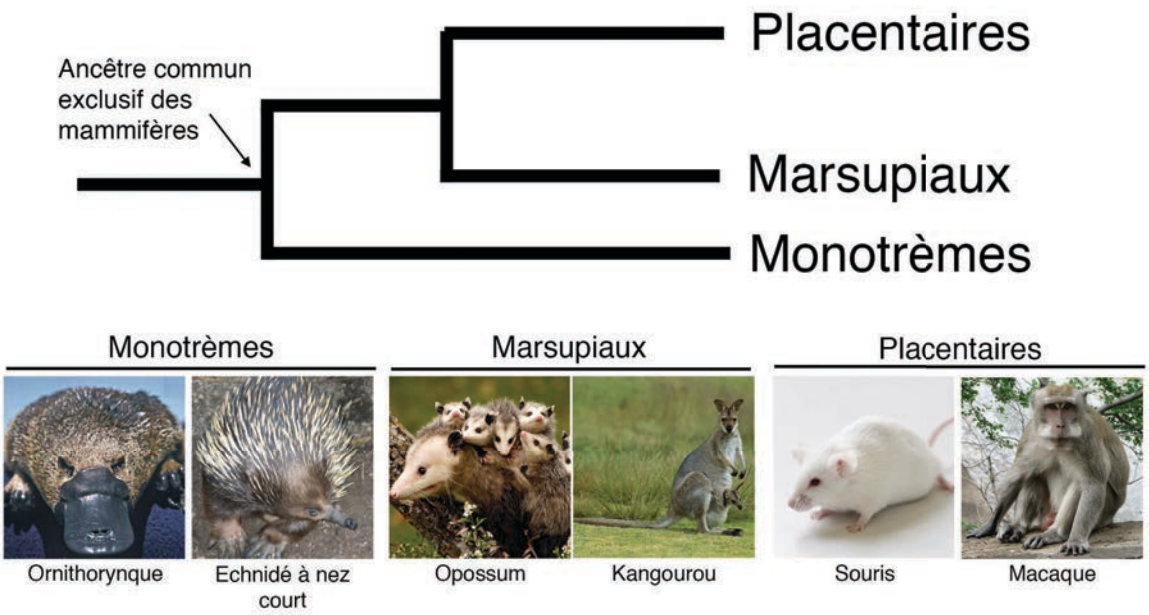

Figure 4. Phylogénie des mammifères. Les espèces de mammifères sont caractérisées par l'allaitement des jeunes. Cependant, en fonction des modes de reproduction et de développement, trois grands groupes peuvent être distingués au sein des mammifères. Les monotrèmes (ou protothériens) sont ovipares. Au contraire, les marsupiaux (métathériens) et mammifères placentaires (euthériens) sont vivipares. Chez les marsupiaux, le placenta, organe d'origine foeto-maternelle participant au développement de l'embryon, est absent.

hémisphères du cerveau est assurée par la commissure antérieure et la commissure hippocampique (Figure 5A, 5B). La commissure antérieure établit des connexions entre les paléocortex (cortex à trois couches dédié à l'olfaction) et néocortex (cortex à six couches) situés dans chaque hémisphère (Heath and Jones, 1971; Ashwell et al., 1996), tandis que la commissure hippocampique connecte les deux archicortex (cortex à trois couches comprenant l'hippocampe) (Smith, 1937). Ainsi, la commissure antérieure (située à l'avant du cerveau) assure la connexion de l'ensemble du néocortex, notamment des régions postérieures (comme le cortex occipital). Les fibres de ces régions doivent donc parcourir de grandes distances pour atteindre la commissure antérieure, puis pour rejoindre leur cible dans l'hémisphère contralatéral, rendant ainsi les délais de communication inter-hémisphériques relativement longs (Aboitiz and Montiel, 2003). Les axones commissuraux néocorticaux atteignent la commissure antérieure de différentes manières. Chez les monotrèmes et les marsupiaux non-diprotodontes (dont l'opossum), les fibres néocorticales rejoignent la commissure antérieure exclusivement via la capsule externe (Figure 5A) (Martin, 1967). Cette configuration a le désavantage de faire parcourir une grande distance aux fibres commissurales néocorticales pour atteindre la commissure antérieure (qui se situe en position ventrale). Chez les marsupiaux diprotodontes (koala, kangourou, possum), il existe une voie alternative traversant la capsule interne et appelée *fasciculus aberrans*, permettant aux fibres inter-hémisphériques de rejoindre la partie dorsale de la commissure antérieure, raccourcissant ainsi considérablement leur trajet (Figure 5B) (Ashwell et al., 1996).

Chez les euthériens, il existe trois grandes commissures assurant la communication entre les deux hémisphères du cerveau antérieur : à la commissure antérieure et la commissure hippocampique, s'ajoute le corpus calleux (Figure 5C, 5D). Ce dernier assure la communication entre régions homotypiques du néocortex : il a donc endossé le rôle qu'avait la commissure antérieure chez les marsupiaux et les monotrèmes

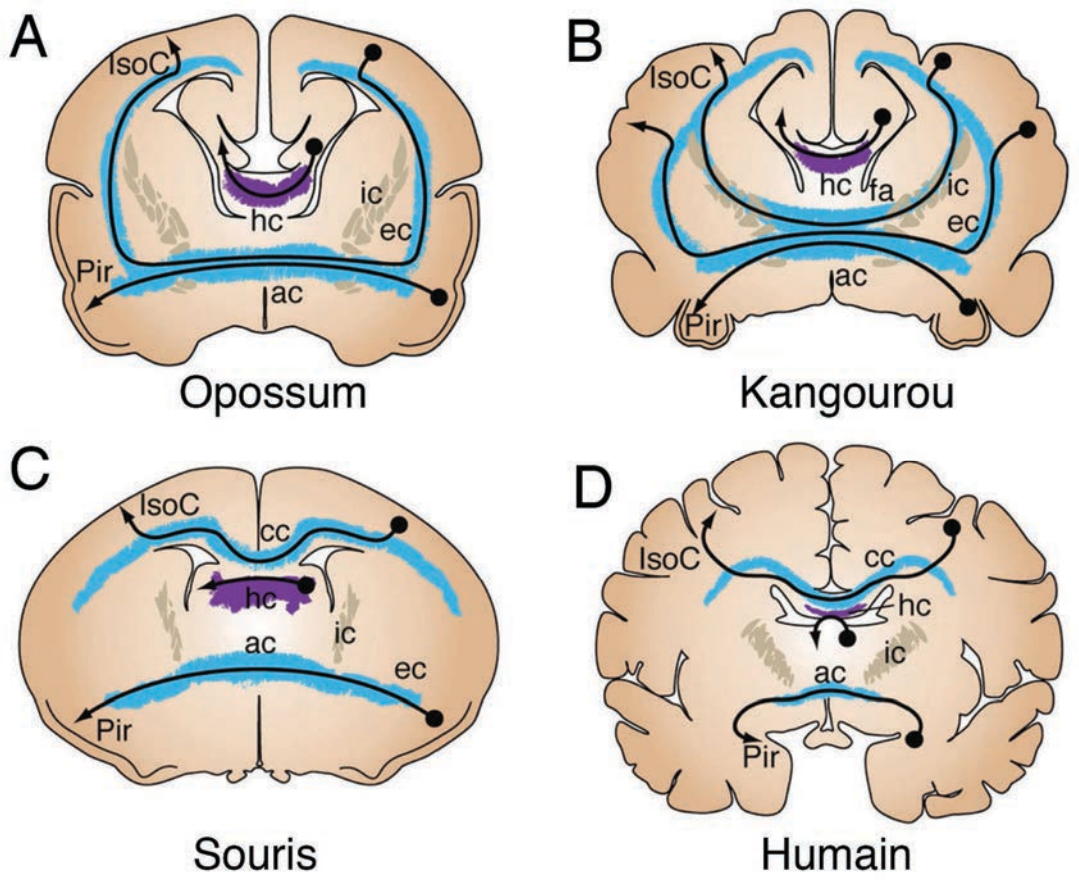

Figure 5. Anatomie comparée des commissures du cerveau antérieur chez les mammifères. (A, B) Chez les marsupiaux, le corps calleux étant absent, la communication entre les deux néocortex est assurée par la commissure antérieure. Tandis que chez les marsupiaux non-diprotodontes (A), les axones calleux provenant du néocortex rejoignent la commissure antérieure via la capsule externe, il existe chez les marsupiaux diprotodontes (B) un « raccourci » passant par la capsule interne, nommé le fasciculus aberrans. (C, D) Chez les mammifères placentaires (euthériens), le corpus calleux assure la communication entre les deux néocortex, tandis que le rôle de la commissure antérieure est limité à la connexion des deux paléocortex, ainsi que des régions homologues du néocortex temporal. IsoC : isocortex (néocortex) ; cc : corps calleux ; hc : commissure hippocampique ; ac : commissure antérieure ; ic : capsule interne ; ec : capsule externe ; fa : fasciculus aberrans ; Pir : cortex piriforme. Adapté de (Suarez et al, 2014b).

(Tomasch, 1954; Karol and Pandya, 1971; Yorke and Caviness, 1975; Hofer and Frahm, 2006). La commissure antérieure a en conséquence été « réduite » à la connexion des deux paléocortex, ainsi que des régions homologues du néocortex temporal (Jouandet and Gazzaniga, 1979; Jouandet, 1982; Jouandet et al., 1984). La commissure hippocampique assure quant à elle la mise en relation des deux hippocampes et établit aussi des connexions hétérotypiques entre l'hippocampe et le cortex entorhinal (Wyss et al., 1980; Demeter et al., 1985).

Il existe au sein des euthériens une corrélation négative entre la taille du paléocortex d'une part, et celle du néocortex et du corps calleux d'autre part. Cette observation suggère que l'expansion du néocortex au détriment du paléocortex pourrait être à l'origine du développement du corpus calleux chez les euthériens (Suarez et al., 2014b).

2) Anatomie et organisation du corps calleux

L'organisation des connexions calleuses présente de grandes similarités entre les différentes espèces de mammifères euthériens. Dans cette section, nous nous intéresserons plus particulièrement au cas des rongeurs, du chat, du singe et de l'humain.

Les corps cellulaires et terminaisons des neurones calleux ne sont pas répartis de façon uniforme au sein du néocortex. Les corps cellulaires des neurones calleux sont en majorité localisés dans les couches néocorticales superficielles (couches II/III, environ 80%), et en moindre proportion dans la couche V (environ 20%). De la même façon, les terminaisons des axones calleux dans l'hémisphère opposé sont principalement localisées dans les couches II/II et dans la couche V (Figure 6B) (Yorke and Caviness, 1975; Ivy and Killackey, 1981; Segraves and Rosenquist, 1982; Schwartz and Goldman-Rakic, 1984; Terashima et al., 1985; Houzel et al., 1994; Rouiller et al., 1994; Mizuno et al., 2007; Wang et al., 2007; Zhou et al., 2013; Suarez et al., 2014a).

A cette organisation laminaire, s'ajoute une organisation tangentielle (par rapport à la surface du cortex) spécifique. A l'âge adulte, les corps cellulaires et terminaisons des neurones calleux ne sont pas distribués de façon homogène, mais selon un motif discontinu, établissant ainsi des connexions spécifiques entre régions homologues (connexions homotypiques) ou non-homologues (connexions hétérotypiques) des deux hémisphères. Certaines zones corticales sont donc dénuées de neurones et de terminaisons calleuses à l'âge adulte. Prenons l'exemple des cortex sensoriels (somatosensoriel et visuel) : la densité des projections calleuses est particulièrement élevée au niveau de la frontière entre régions primaires et secondaires (frontière entre S1 et S2 pour le cortex somatosensoriel, frontière entre les aires 17 et 18 pour le cortex visuel) (Figure 6A). Une telle organisation a été décrite pour un grand nombre de régions corticales du rongeur, du chat et du singe, (Heimer et al., 1967; Karol and Pandya, 1971; Jones et al., 1975; Yorke and Caviness, 1975; Kunzle, 1976; Ivy and Killackey, 1981; Olavarria and Van Sluyters, 1985; Killackey and Chalupa, 1986; Houzel et al., 1994; Mizuno et al., 2007; Wang et al., 2007; Rochefort et al., 2009).

A ce double niveau d'organisation (laminaire et tangentiel), s'ajoute une organisation topographique du CC selon l'axe rostro-caudal. Les fibres calleuses provenant de régions néocorticales adjacentes sont regroupées au sein du CC, et la position de ces fibres selon l'axe rostro-caudal dépend de la localisation de leur territoire cortical d'origine. Le corps calleux peut être divisé en plusieurs régions selon des critères morphologiques grossiers. D'avant en arrière, on distingue le rostrum, le genou, le tronc, l'isthme et le splénium (Figure 6C). Le rostrum et le genou du corps calleux connectent les régions (pré)frontales. La partie antérieure du tronc du CC connecte les aires motrices primaires, secondaires et supplémentaires, tandis que la partie postérieure du tronc connecte les aires somatosensorielles primaires et secondaires ainsi que les aires pariétales postérieures. Enfin, la partie postérieure du CC (isthme et splénium) connecte les régions pariétales, temporales et occipitales. Une telle

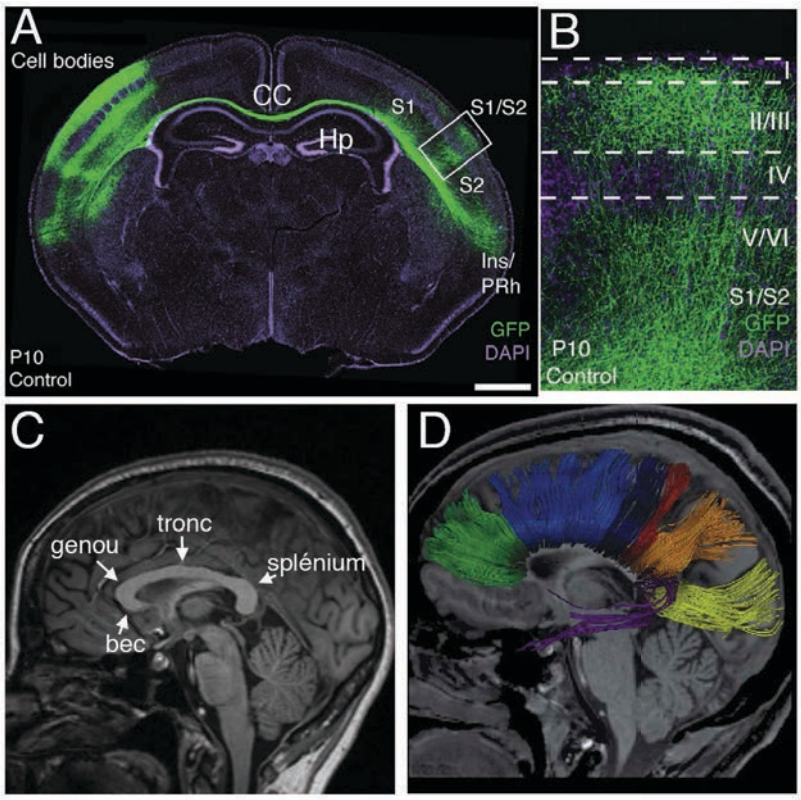

Figure 6. Organisation tangentielle, laminaire et topographique du corps calleux. (A, B) Coupes coronales d'un cerveau de souris à E10 après électroporation de la GFP à E15 dans le cortex somatosensoriel primaire (S1, cell bodies). (A) La distribution des terminaisons des neurones calleux marqués n'est pas uniforme au sein de l'hémisphère contralatéral : les connexions homotypiques sont concentrées au niveau de la frontière entre les cortex somatosensoriels primaires et secondaires (S1/S2). On observe aussi des projections hétérotypiques vers l'insula (Ins) et le cortex périrhinal (PRh). (B) Grossissement de la région délimitée par le rectangle dans (A). Au niveau de la région S1/S2, les terminaisons calleuses sont denses au niveau des couches superficielles (II/III) et profondes (V/VI), tandis que la couche IV est presque totalement dépourvue de terminaisons (Extrait de Suarez et al, 2014). (C) IRM anatomique en vue sagittale d'un sujet sain. Différentes régions du corps calleux sont identifiables sur des critères morphologiques : le rostrum, le genou, le tronc et le splénium (données personnelles). (D) Vue sagittale des fibres calleuses d'un sujet reconstruites par tractographie et superposées sur l'IRM anatomique. La position des fibres au sein du corps calleux dépend de leur territoire cortical d'origine (Extrait de Hofer and Frahm, 2006).

topographie a été décrite chez le rongeur (Yorke and Caviness, 1975; Olavarria and van Sluyters, 1986), le chat (Payne and Siwek, 1991; Matsunami et al., 1994), le singe (Pandya et al., 1971) et l'humain (Figure 6D) (de Lacoste et al., 1985; Hofer and Frahm, 2006). Il existe de plus une association étroite entre la composition histologique du CC et son organisation topographique chez les primates. En effet, les régions du CC connectant les aires préfrontales ainsi que les aires temporo-pariétales (qui sont des aires associatives supérieures) sont caractérisées par une forte densité d'axones de petit diamètre et faiblement myélinisés, à vitesse de conduction lente. Les régions du CC assurant la communication des cortex somato-moteurs primaires et secondaires ainsi que des cortex visuels primaires présentent une faible densité de fibres de diamètre important, fortement myélinisées, à vitesse de conduction rapide (Lamantia and Rakic, 1990b; Aboitiz et al., 1992; Aboitiz and Montiel, 2003). Ces éléments histologiques suggèrent qu'il existe des différences fonctionnelles dans l'intégration inter-hémisphérique d'informations de nature différente.

3) Développement comparé du corps calleux chez les euthériens

Les axones du CC croisent la ligne médiane avant la naissance, au 15e jour de développement embryonnaire (E15) chez la souris (Rash and Richards, 2001), autour de E38 chez le chat (Berbel and Innocenti, 1988), à E65 chez le singe rhésus (LaMantia and Rakic, 1990a) et autour de la 13e semaine de développement chez l'humain (Rakic and Yakovlev, 1968; Ren et al., 2006). Chez le rongeur comme l'humain, les premiers axones calleux à croiser la ligne médiane proviennent du cortex cingulaire, et serviront par la suite d'échafaudage pour guider les axones issus du néocortex (Koester and O'Leary, 1994; Rash and Richards, 2001). Chez les rongeurs, le chat et le singe, le nombre d'axones calleux augmente fortement au cours du développement embryonnaire, tandis qu'une réduction drastique est observée dans les premières semaines et premiers mois suivant la naissance

(O'Leary et al., 1981; Koppel and Innocenti, 1983; Berbel and Innocenti, 1988; LaMantia and Rakic, 1990a). Il semble que cette diminution du nombre d'axones calleux soit due à l'élimination de branches collatérales, et non pas à un processus de mort cellulaire (Ivy and Killackey, 1981; O'Leary et al., 1981; Innocenti et al., 1986; Chalupa and Killackey, 1989). Par ailleurs, de nombreuses études se sont intéressées au processus de maturation des projections calleuses, en particulier en ce qui concerne l'organisation laminaire, tangentielle et topographique de ces connexions. Une question importante se pose : quelle est la relation entre la période post-natale de diminution du nombre d'axones calleux et la maturation de ces connexions ?

Chez le rat et le chat, l'organisation tangentielle des neurones calleux est immature à la naissance. Les corps cellulaires et terminaisons des neurones calleux sont initialement distribués de façon continue au sein du néocortex. Il en résulte de nombreuses connexions calleuses exubérantes, provenant et innervant de territoires corticaux qui seront dénués de connexions à l'âge adulte (Figure 7) (Ivy et al., 1979; Innocenti and Caminiti, 1980; Innocenti, 1981; Ivy and Killackey, 1981; Olavarria and Van Sluyters, 1985; Elberger, 1994a; b; Ding and Elberger, 2001). L'apparition d'une organisation discontinue des connexions calleuses, en régions discrètes ou « patchs », ne se fait qu'au bout de deux semaines de développement chez le rongeur (Ivy et al., 1979; Ivy and Killackey, 1981; O'Leary et al., 1981; Olavarria and Van Sluyters, 1985; Ding and Elberger, 2001) et plusieurs mois chez le chat (Innocenti and Caminiti, 1980; Innocenti, 1981). La diminution importante du nombre d'axones calleux durant le développement post-natal reflète l'élimination des projections exubérantes chez le rongeur et le chat. La maturation des projections calleuses est fortement altérée dans des situations de privations sensorielles, et des projections exubérantes peuvent alors être maintenues à l'âge adulte. Ces expériences démontrent que la maturation post-natale des projections calleuses est dépendante de l'activité neuronale évoquée par

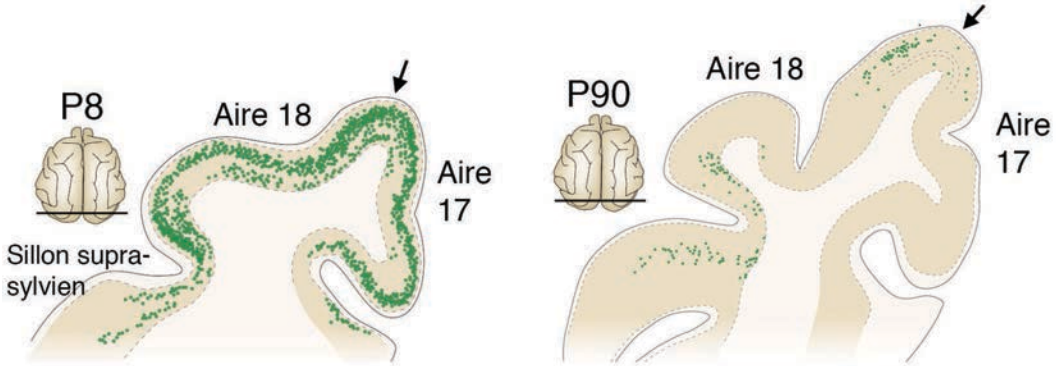

Figure 7. Maturation des connexions calleuses au cours du développement post-natal chez le chat. Schéma représentant la distribution des corps cellulaires des neurones calleux (points verts) au sein du cortex visuel après injection d'un traceur rétrograde dans l'hémisphère contralatéral à différents stades de développement. Dans la première semaine suivant la naissance, les corps cellulaires de neurones calleux sont distribués dans l'ensemble du cortex visuel. Au contraire, à trois mois, la plupart des corps cellulaires sont localisés au niveau de la frontière entre les aires 17 et 18 (indiquée par une flèche noire), ainsi qu'au niveau du sillon supra-sylvien. P8 : jour post-natal 8 (extrait de Innocenti and Price, 2005).

l'expérience sensorielle (Innocenti and Frost, 1979; Olavarria et al., 1987; Koralek and Killackey, 1990).

Concernant l'organisation laminaire, celle-ci est immature chez la rat à la naissance, les corps cellulaires des axones calleux étant initialement présents au niveaux des couches Va et VI. Durant les deux premières semaines de développement, le nombre de neurones situés dans les couches profondes diminue, tandis que celui des couches superficielles augmente (Olavarria and van Sluyters, 1986; Mizuno et al., 2007; Wang et al., 2007).

Au contraire de ce qui est observé chez le rongeur et le chat, l'organisation tangentielle et laminaire des connexions calleuses du singe est mature dès la naissance. La maturation des projections calleuses a lieu durant le dernier mois de développement embryonnaire, et repose sur une élimination de collatérales plutôt que sur un processus de mort cellulaire (Killackey and Chalupa, 1986; Chalupa and Killackey, 1989).

Chez le rat et le singe, il semble que l'organisation topographique du corps calleux soit acquise dès la naissance, avant la phase d'élimination des axones calleux (Olavarria and van Sluyters, 1986; LaMantia and Rakic, 1990a).

4) Génération des neurones calleux au cours du développement chez la souris

Les études génétiques réalisées sur les modèles murins ont permis de procéder à une véritable dissection des mécanismes moléculaires régulant la génération et le développement des neurones calleux. Nous commencerons dans un premier temps par décrire les mécanismes de la formation du néocortex (néocorticogenèse) chez la souris, avant de nous focaliser sur les spécificités de la génération des neurones du corps calleux. Pour une revue exhaustive de ces processus, voir (Molyneaux et al., 2007; Fame et al., 2011; Greig et al., 2013).

a) Diversité des neurones du néocortex

Le néocortex des mammifères est composé de deux grand types de neurones : les interneurones sont très majoritairement inhibiteurs, établissent des connexions locales et sont générés par des progéniteurs localisés dans le télencéphale ventral (pour revue, voir (Corbin and Butt, 2011)). Au contraire, les neurone dits « à projections » établissent des contacts avec des cibles distantes, sont glutamatergiques (excitateurs) et sont générés au sein de zones proliératives du télencéphale dorsal (Greig et al., 2013). Les différents types de neurones à projection du néocortex sont définis par un ensemble de propriétés morphologiques, hodologiques, électrophysiologiques, ainsi que par leur position laminaire au sein du néocortex. Selon ces critères, on peut distinguer plusieurs classes de neurones à projections (Figure 8) (pour revue, voir (Molyneaux et al., 2007; Greig et al., 2013)) :

- les neurones établissant des projections avec des cibles situées en dehors du néocortex sont localisés dans les couches profondes (V/VI) : on parle de projections corticofugales. Au sein de cette population, on distingue les neurones corticothalamiques situés dans la couche VI et les neurones à projections subcérébrales (neurones corticotectaux, corticopontiques et corticospinaux) situés dans la couche V.
- les neurones calleux établissent des connexions entre les deux hémisphères via le corps calleux. Ces neurones sont principalement localisés dans les couches superficielles (II/III), et dans une moindre proportion dans les couches profondes (V/VI).
- les neurones dits « associatifs » établissent des connexions entre différentes régions corticales au sein d'un même hémisphère, et ils sont présents dans l'ensemble des couches néocorticales.

Par la suite, nous nous intéresserons uniquement à la génération et à la spécification des neurones à projections, avant de nous focaliser sur le cas précis des neurones calleux.

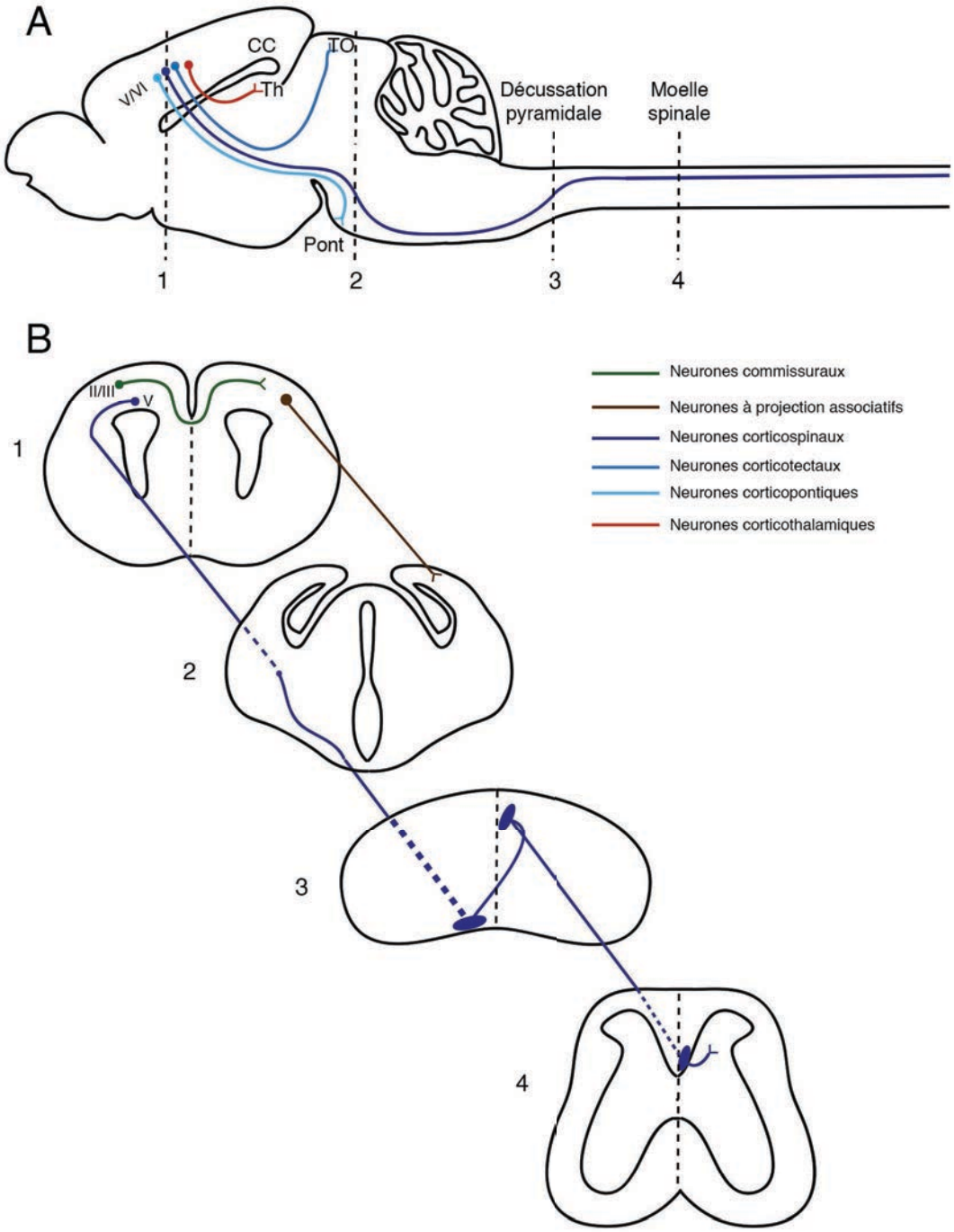

Figure 8. Les différents types de neurones à projection du néocortex. (A) Schéma avec vue sagittale du système nerveux central d'une souris adulte, représentant les différents types de neurones corticofugaux. (B) Schéma avec vues frontales du système nerveux central d'une souris adulte à différents niveaux selon l'axe rostro-caudal (indiqués en A), représentant les projections calleuses, associatives et corticospinales. Th : thalamus ; TO : tectum optique.

b) Progéniteurs néocorticaux des neurones à projections

Le mur dorso-latéral du télencéphale est initialement composé de cellules neuroépithéliales indifférenciées se divisant rapidement. Vers E10.5, ces progéniteurs donnent naissance à des cellules de la glie radiaire, formant ainsi la zone ventriculaire (ZV), lieu de divisions symétriques actives des progéniteurs néocorticaux (Haubensak et al., 2004; Noctor et al., 2004). Dans un deuxième temps (E12.5), les cellules de la glie radiaire donnent naissance à d'autres catégories de progéniteurs : les progéniteurs intermédiaires (Sessa et al., 2008) et la glie radiaire externe (Wang et al., 2011). Ces populations forment ensemble la zone sub-ventriculaire (ZSV) (Noctor et al., 2004; Noctor et al., 2007). Ces différentes catégories de progéniteurs sont caractérisées par leurs propriétés morphologiques ainsi que leur rythme de divisions. La glie radiaire s'étend sur toute l'épaisseur du cortex, et sert d'échafaudage aux neurones migrant au sein du cortex (Rakic, 1971). Les cellules de la glie radiaire peuvent adopter différents types de division. La plupart des divisions sont asymétriques, et aboutissent à la formation d'une nouvelle cellule de la glie radiaire ainsi qu'à une cellule fille de nature différente, qui peut être un neurone ou un progéniteur intermédiaire migrant alors vers la ZSV. Les divisions symétriques donnent naissance à deux nouvelles cellules de la glie radiaire (Noctor et al., 2001; Noctor et al., 2004). Les progéniteurs intermédiaires ont une morphologie multipolaire et ne sont pas ancrés à la surface apicale ou basale du cortex. Ces derniers ont principalement un rôle d'amplificateurs transitoires : ils prolifèrent peu et donnent le plus souvent naissance à deux neurones par division symétrique, contribuant ainsi à la formation de l'ensemble des couches corticales (Noctor et al., 2004; Sessa et al., 2008; Kowalczyk et al., 2009). Les cellules de la glie radiaire externe se divisent principalement de façon asymétrique, afin de se renouveler tout en produisant de nouveaux neurones (Wang et al., 2011). Pour un schéma bilan, voir (Figure 9).

c) Corticogenèse : génération séquentielle des différentes couches corticales

La pré-plaque se forme à E10.5 et donnera ensuite la zone marginale et la sous-plaque. Entre les deux, la plaque corticale donnera naissance aux couches corticales successives selon une architecture « à l'envers », les neurones nés les plus tard migrant au-delà de leurs prédécesseurs pour atteindre les couches corticales les plus superficielles (Figure 9). Les couches les plus profondes (VI et V) sont donc produites en premier, à partir de E12, puis suivent les couches superficielles (IV, III et II) à E14-E16 (Angevine and Sidman, 1961; Rakic, 1974; Raedler and Raedler, 1978). A cette ségrégation temporelle de la génération des couches profondes et superficielles, s'ajoute une ségrégation spatiale. Les neurones des couches profondes proviennent principalement de divisions asymétriques de cellules de la glie radiaire situées dans la ZV (Noctor et al., 2001). Au contraire, les couches superficielles sont issues de progéniteurs intermédiaires se divisant de façon symétrique dans la ZSV (Haubensak et al., 2004; Nieto et al., 2004; Noctor et al., 2004; Noctor et al., 2007).

Quels sont les mécanismes responsables de la formation séquentielle des différentes couches corticales ? Selon un premier modèle, l'ensemble des neurones néocorticaux dériverait d'une unique population dont les capacités mutlipotentes seraient de plus en plus restreintes au cours du temps. Cette hypothèse est notamment étayée par des expériences de transplantation. Les progéniteurs néocorticaux les plus précoces (E11.5) donnent majoritairement naissance à des neurones des couches profondes (V et VI), mais ils peuvent aussi former des neurones des couches les plus superficielles lorsqu'ils sont transplantés dans un embryon plus âgé. Inversement, un progéniteur tardif (des couches superficielles) transplanté dans un embryon plus jeune ne formera que des neurones des couches superficielles (McConnell, 1988; Frantz and McConnell, 1996). De plus, des progéniteurs cultivés *in vitro* donnent successivement naissance aux différentes populations de neurones néocorticaux, et ce au même rythme que leurs homologues *in vivo*. Autrement dit, ces cultures

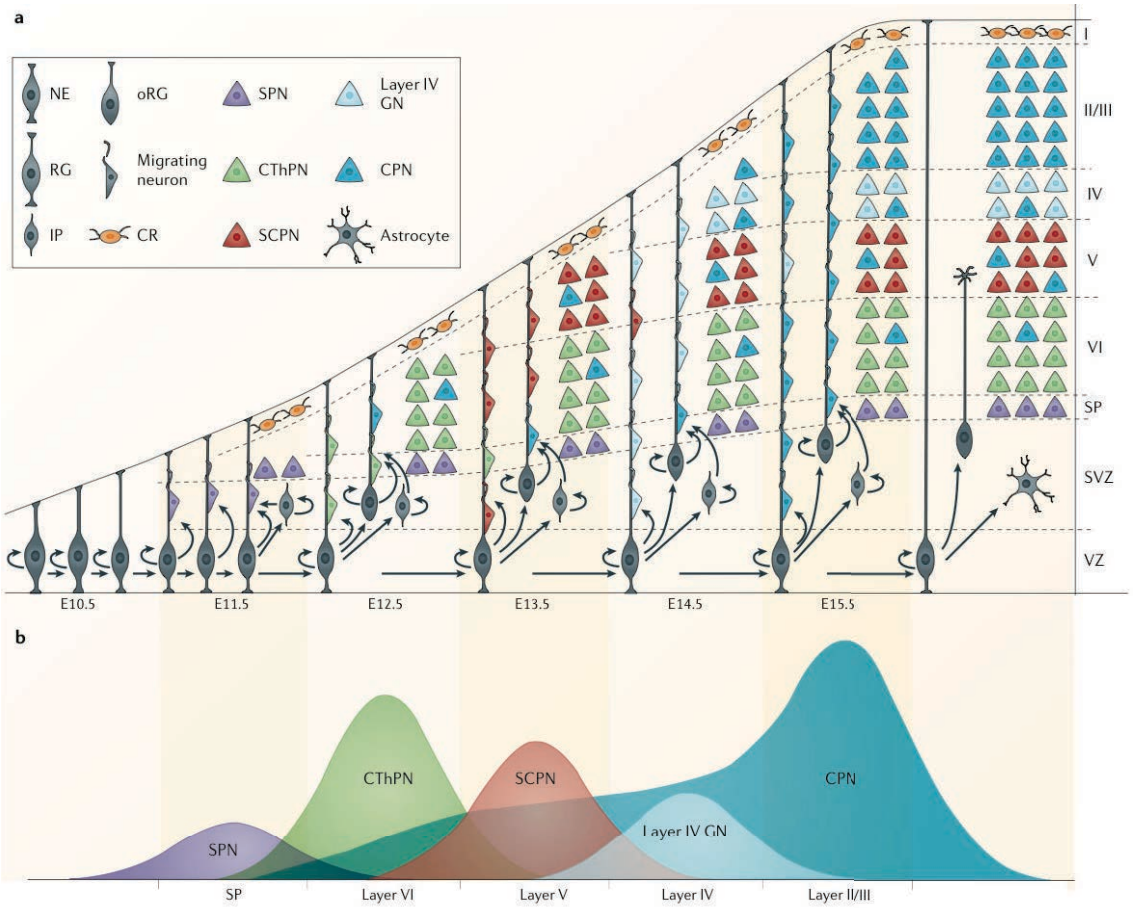

Figure 9. Génération séquentielle des différentes couches néocorticales. Différents types de progéniteurs contribuent à la génération séquentielle des six couches néocorticales selon un motif « à l'envers » (inside-out), les neurones nés les plus tard migrant au delà de leur prédécesseurs pour atteindre les couches corticales les plus superficielles. NE : neuroepithelial cell ; RG : radial glia ; IP : intermediate progenitor ; oRG : outer radial glia ; CR : Cajal-Retzius ; SPN : subplate neurons ; CThPN : corticothalamic projection neurons ; SCPN : subcerebral projections neurons ; GN : granular neurons ; CPN : callosal projection neurons. (Extrait de Greig et al, 2013).

in vitro reproduisent le développement et la génération séquentielle des différents types neuronaux des progéniteurs néocorticaux *in vivo,* ce qui soutient l'idée de l'existence d'une horloge intrinsèque (Shen et al., 2006).

Selon un deuxième modèle, il existerait des populations de progéniteurs distinctes, responsables de la génération des différents types de neurones néocorticaux. Les neurones des couches profondes seraient ainsi générés par des progéniteurs différents de ceux responsables de la formation des neurones des couches superficielles. Plusieurs observations permettent d'appuyer cette hypothèse. Certains facteurs de transcription, tels que FEZF2, sont exprimés dans les progéniteurs néocorticaux et la ZV et ZSV lors de la période de formation des couches néocorticales profondes (E11-E13), puis leur expression est maintenue dans les neurones de ces couches (Arlotta et al., 2005; Molyneaux et al., 2005). De façon similaire, les facteurs CUX1, CUX2 et SVET sont exprimés dans la ZSV durant la formation des couches superficielles, puis leur expression est maintenue dans les neurones post-mitotiques de ces même couches superficielles (Tarabykin et al., 2001; Nieto et al., 2004). Cependant, si certaines études ont démontré que les progéniteurs exprimant CUX2 étaient présents durant toute la phase de développement cortical, mais ne contribuaient qu'à la génération des couches superficielles (Franco et al., 2012; Gil-Sanz et al., 2015), d'autres soutiennent que ces progéniteurs sont pluripotents et participent à la formation de l'ensemble des couches (Eckler et al., 2015).

En conclusion, il existe aujourd'hui une multitude de modèles intermédiaires entre les deux extrêmes que nous avons présentés, et nous pouvons retenir que la détermination des progéniteurs néocorticaux dépend à la fois de facteurs extrinsèques et intrinsèques (Greig et al., 2013).

d) Spécification et développement des neurones calleux

Comme nous l'avons noté précédemment, il existe différentes populations de neurones calleux en fonction de leur position laminaire dans le néocortex. Les neurones calleux des couches profondes (V et VI) sont générés en même temps que celles-ci, entre E12 et E13.5, tandis que les neurones calleux des couches superficielles (qui représentent 80% des neurones calleux) sont générés entre E14.5 et 16.5 par les progéniteurs intermédiaires de la ZSV (Noctor et al., 2004; Noctor et al., 2007; Greig et al., 2013).

Au sein d'une population neuronale donnée, l'expression d'un programme génétique spécifique aboutit à l'acquisition d'un ensemble de caractères qui définissent l'identité de cette population. Les facteurs génétiques responsables de la spécification des neurones des couches superficielles ne sont pas tous connus. De nombreux facteurs sont exprimés dans la ZSV lors de la production des neurones des couches superficielles : parmi eux, SVET (Tarabykin et al., 2001) et CUX2 (Nieto et al., 2004; Gil-Sanz et al., 2015) ont la particularité d'être aussi exprimés dans les neurones post-mitotiques des couches superficielles. Ces deux facteurs pourraient donc jouer un rôle important dans la spécification des couches superficielles. CUX2 intervient directement dans le contrôle du rythme des divisions cellulaires au sein de la ZSV (Cubelos et al., 2008). BRN1 et BRN2 sont deux facteurs de transcription co-exprimés dans les couches néocorticales II-IV. Ils sont nécessaires à la migration cellulaire, à l'organisation laminaire du néocortex, ainsi qu'à la formation des couches superficielles (McEvilly et al., 2002; Sugitani et al., 2002; Dominguez et al., 2013).

SATB2 est l'un des principaux régulateurs de la spécification des neurones calleux. SATB2 est principalement exprimé dans les neurones des couches superficielles (Figure 10A, 10B). En l'absence de SATB2, le CC ne se forme pas (Figure 10C, 10D) : les neurones des couches superficielles expriment alors de façon ectopique CTIP2, un déterminant majeur de l'identité des neurones de la couche V (Arlotta et al., 2005), et développent des projections

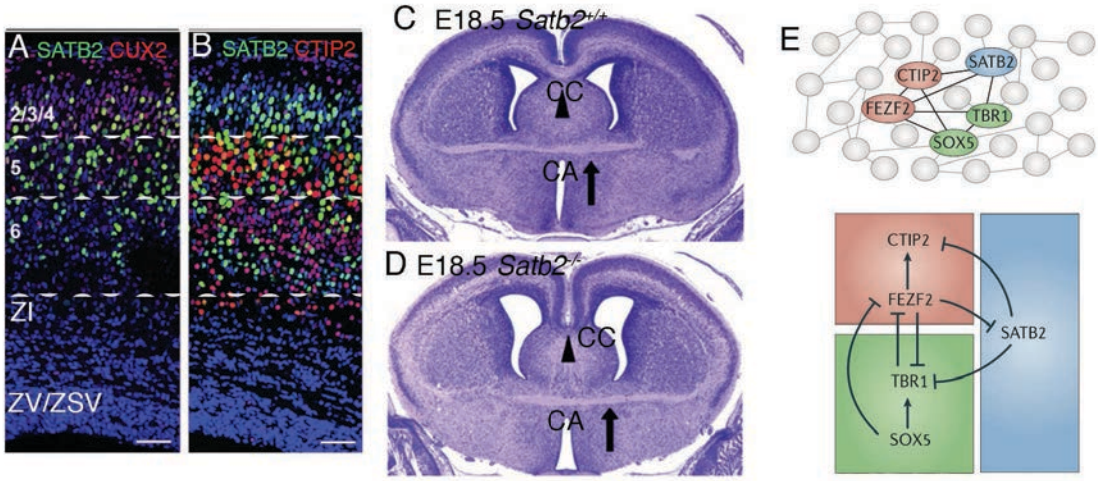

Figure 10. *Satb2* intervient dans la spécification des neurones calleux chez la souris. (A, B) Coupes coronales de neocortex de souris à E18.5 avec un immuno-marquage anti-SATB2, anti-CUX2 et anti-CTIP2. CUX2 est un marqueur des couches superficielles, tandis que CTIP2 est un marqueur de la couche V. On remarque que l'expression de SATB2 est relativement étendue à E18.5, ce dernier étant détecté dans les couches superficielles et dans les couches profondes. ZI : zone intermédiare ; ZV : zone ventriculaire ; SVZ : zone sub-ventriculaire (Extrait de Alcamo et al, 2008). (C, D) Coupes coronales de neocortex de souris *Satb2*$^{+/+}$ et *Satb2*$^{-/-}$ à E18.5 avec un marquage au crésyl violet. Le corps calleux est extrêmement réduit chez les mutants *Satb2*$^{-/-}$, tandis que la commissure antérieure est normale. CC : corps calleux ; CA : commissure antérieure (Extrait de Alcamo et al, 2008). (E) Schéma représentant le réseau d'interactions réciproques entre les différents facteurs de transcription impliqués dans la spécification des différentes couches néocorticales (Extrait de Greig et al, 2013).

vers des cibles subcérébrales (Alcamo et al., 2008; Britanova et al., 2008). La répression de l'expression de *Ctip2* est cruciale pour la formation du CC (Srivatsa et al., 2014). SATB2 et SKI forment un complexe se liant directement à des régions régulatrices du gène *Ctip2* afin d'inhiber son expression par remodèlement de la chromatine (Alcamo et al., 2008; Baranek et al., 2012). SATB2 et CTIP2 apparaissent donc comme deux facteurs antagonistes, mutuellement exclusifs, déterminant la spécification de deux populations néocorticales distinctes au cours du développement (Figure 10E). Pourtant, plusieurs études ont observé qu'une fraction de neurones des couches profondes co-expriment SATB2 et CTIP2 de façon transitoire au cours du développement embryonnaire, puis au cours du développement post-natal (Alcamo et al., 2008; Britanova et al., 2008; Leone et al., 2015; Harb et al., 2016). Cette co-expression transitoire au cours du développement précoce est nécessaire à la formation du FCS (Leone et al., 2015), tandis qu'à des stades plus tardifs elle est associée à la formation de deux populations distinctes de neurones calleux et de neurones cortico-pontiques (Harb et al., 2016). Enfin, au-delà de la spécification des neurones calleux, SATB2 est directement impliqué dans la régulation de l'expression de récepteurs de guidage axonal (Srivatsa et al., 2014).

5) Développement des structures nécessaires à la formation du corps calleux

a) Fusion des hémisphères au niveau de la ligne médiane du télencéphale

Au cours du développement précoce du système nerveux central, la partie rostrale du cerveau est constituée d'une vésicule unique appelée prosencéphale. Le prosencéphale forme ensuite le télencéphale et le diencéphale, processus marqué par le passage d'une structure à une vésicule (prosencéphale) à une structure à deux vésicules (télencéphale). Cette réorganisation du cerveau antérieur nécessite la fusion des deux hémisphères nouvellement formés au niveau du septum, formant ainsi la ligne médiane du télencéphale. Cette étape est

absolument critique, car elle fournira le substrat physique sur lequel les axones calleux (ainsi que ceux des autres commissures) se développeront par la suite (Donahoo and Richards, 2009).

Les mécanismes moléculaires régulant la fusion des deux hémisphères ne sont pas bien connus. En revanche, il existe deux types de pathologies développementales associées à des défauts de fusion des hémisphères : les holoprosencéphalies et la formation de kystes inter-hémisphériques (Donahoo and Richards, 2009; Edwards et al., 2014). L'holoprosencéphalie est une séparation anormale des deux hémisphères cérébraux au cours du développement, aboutissant à la formation d'une vésicule unique (Marcorelles and Laquerriere, 2010). En conséquence, l'ensemble des structures de la ligne médiane, dont le CC, est altéré. Au contraire, dans le cas de kystes inter-hémisphériques, la ligne médiane séparant les deux hémisphères est présente, mais elle est interrompue par une cavité. Selon les cas, il semble que la présence de ces kystes puisse être la cause ou la conséquence d'un problème de fusion des hémisphères au niveau de la ligne médiane (Utsunomiya et al., 2006).

Les lignées de souris ayant des anomalies de fusion des deux hémisphères présentent systématiquement des agénésies du CC, du fait de l'absence de substrat physique permettant aux axones de croiser la ligne médiane (Bronson and Lane, 1990; Demyanenko et al., 1999; Brouns et al., 2000; Wahlsten et al., 2006).

b) Formation de la plaque commissurale

La plaque commissurale est définie comme un plan oblique du cerveau au sein duquel les axones commissuraux des trois grandes commissures du télencéphale antérieur (corps calleux, commissure hippocampique, commissure antérieure) croisent la ligne médiane. Cette structure, initialement décrite chez l'humain, existe aussi chez la souris (Rakic and Yakovlev, 1968; Moldrich et al., 2010). De nombreux morphogènes sont nécessaires à la formation de la

plaque commissurale et à sa subdivision en différents territoires : BMP, WNT, SHH, FGF8 (pour revue, voir (Moldrich et al., 2010; Suarez et al., 2014b)). La spécification des différents domaines de la plaque commissurale est cruciale pour la formation des commissures du cerveau antérieur. En effet, ces différentes zones de la plaque commissurale, ainsi que leurs frontières, définissent les points de passage des axones commissuraux selon l'axe dorso-ventral. Des altérations de l'organisation de la plaque commissurale sont associées à des malformations du CC (Smith et al., 2006; Tole et al., 2006; Moldrich et al., 2010; Benadiba et al., 2012; Amaniti et al., 2013; Magnani et al., 2014).

6) Guidage des axones calleux au cours du développement

Pour une revue exhaustive, voir (Lindwall et al., 2007; Donahoo and Richards, 2009; Chedotal, 2011). Pour un schéma bilan, voir (Figure 11).

Les facteurs qui permettent aux axones calleux de franchir la ligne médiane sont de deux types. On peut distinguer d'un part les facteurs directs (ou cellulaire-autonomes) dont l'expression et le fonctionnement correct au sein des axones calleux sont nécessaires à leur développement. Il s'agit principalement des récepteurs de guidage axonal exprimés à la membrane des cônes de croissance des axones calleux. En conséquence, une altération de ces facteurs dans les axones calleux est suffisante pour affecter leur développement. D'autre part, les facteurs indirects (ou non cellulaires-autonomes) ne sont pas nécessaires au niveau des axones calleux. L'altération de ces facteurs dans les axones calleux n'a pas d'effet sur leur développement. Il s'agit d'éléments impliqués dans la fusion des deux hémisphères cérébraux, ou dans la mise en place de populations neuronales et gliales, présentes au niveau de la ligne médiane, que nous allons décrire dans le prochain paragraphe.

a) Développement des structures de la ligne médiane

Les axones formant le CC franchissent la ligne médiane à un emplacement bien spécifique au niveau de l'axe dorso-ventral du télencéphale, délimité par différentes structures gliales et neuronales. Trois grandes populations gliales, caractérisées par l'expression de la GFAP (Bignami and Dahl, 1974), ont ainsi été identifiées au niveau de la ligne médiane. Tandis que l'indusium griseum (IG), est situé en position dorsale par rapport au CC, le « glial wedge » (GW) et la « midline zipper glia » (MZG) sont eux localisés ventralement (Silver et al., 1982; Shu and Richards, 2001). Le « subcallosal sling » (SCS) est une structure neuronale située juste en dessous du CC (Shu et al., 2003b; Chedotal, 2011). Ces populations gliales et neuronales nécessaires à la formation du CC, initialement identifiées chez le rongeur, ont été retrouvées chez l'humain (Ren et al., 2006).

La MZG est située sous le CC, au niveau de la ligne médiane. Sur la base de sa position anatomique, il a été proposé que la MZG joue un rôle important dans la fusion des hémisphères cérébraux au niveau du septum lors du développement (Silver et al., 1982). Cette étape est fondamentale, car elle crée le substrat anatomique sur lequel les axones du CC se développeront ultérieurement. Le GW forme une barrière située en position ventro-latérale par rapport au CC. Il empêche les axones calleux de croître ventralement dans le septum grâce à la sécrétion de la molécule SLIT2, qui a un effet répulsif sur les axones calleux exprimant le récepteur ROBO1 (Shu and Richards, 2001; Bagri et al., 2002; Shu et al., 2003c; Andrews et al., 2006). L'IG est une structure gliale située en position dorso-médiale par rapport au CC, exprimant aussi SLIT2 (Shu et al., 2003c). Le GW et l'IG, situées de part et d'autre du CC, permettent ainsi de contrôler finement l'emplacement dorso-ventral du chemin emprunté par les axones calleux. Le SCS est une structure neuronale située immédiatement en-dessous du CC (Shu et al., 2003b), et des altérations morphologiques de cette structure ont été associées à une agénésie du CC, selon des mécanismes qui ne sont pas encore connus (Silver et al.,

1982). Enfin, des études ont récemment démontré l'importance de populations de neurones GABAergiques et glutamatergiques transitoires, disséminés au sein du CC, appelés neurones de signalisation (« guidepost neurons »), participant au développement des axones calleux via la sécrétion de facteurs de guidage à courte portée, notamment SEMA3C (Niquille et al., 2009; Niquille et al., 2013).

La malformation de ces structures de la ligne médiane est souvent associée à une agénésie (absence) ou dysgénésie (malformation) du CC, qui est alors une conséquence secondaire de l'altération des populations citées dans le paragraphe précédent. Le récepteur 1 au FGF (FGFR1) est impliqué dans le développement des trois populations gliales de la ligne médiane (IG, GW et MZP) (Smith et al., 2006; Tole et al., 2006). Chez les mutants FGFR1$^{-/-}$, l'absence de ces populations gliales est associée à une agénésie du CC. Cependant, les mutants hétérozygotes FGFR1$^{+/-}$ présentent aussi des anomalies de formation du CC, malgré le développement apparemment normal des populations gliales de la ligne médiane (Tole et al., 2006). Ceci suggère que FGFR1 pourrait être directement impliqué dans le guidage des axones calleux. La mutation des facteurs de transcription *Nfia* et *Nfib* est responsable de défauts de formation du GW, de l'IG, ainsi que du SCS, anomalies associées à une agénésie du CC (Shu et al., 2003a; Steele-Perkins et al., 2005; Piper et al., 2009b). Chez ces souris, les axones calleux croissent ventralement dans le septum, ce qui est la conséquence d'une diminution de la sécrétion de SLIT2 par le GW (Shu et al., 2003a; Piper et al., 2009b). En plus de ce rôle de guidage, les molécules SLIT interviennent aussi dans la mise en place de l'IG (Unni et al., 2012). BPM7 est aussi impliqué dans la formation du GW, de l'IG et du SCS. Son absence perturbe la formation de ces trois structures, et en conséquence les axones calleux ne franchissent pas la ligne médiane (Sánchez-Camacho et al., 2011). La mutation du facteur de transcription LHX2 induit une absence du GW, et en conséquence une agénésie calleuse (Chinn et al., 2015). Les mutants JSAP1 présentent des anomalies de la formation du

SCS, associées à une absence de CC (Ha et al., 2005). Nous avons évoqué précédemment l'importance du facteur FGF8 dans le processus de formation de la plaque commissurale, déterminant ainsi l'emplacement des futures commissures du télencéphale (Moldrich et al., 2010). Il a été récemment montré que RFX3 module l'expression de FGF8 par le biais de GLI3, permettant ainsi le développement normal des populations gliales et neuronales de la ligne médiane impliquées dans la formation du CC (Benadiba et al., 2012; Amaniti et al., 2013; Magnani et al., 2014).

L'ensemble de ces études ont permis : (i) de mieux comprendre les mécanismes moléculaires impliqués dans le formation des populations gliales et neuronales de la ligne médiane ; (ii) de démontrer l'importance de ces populations pour la formation du CC. Les défauts de formation du CC chez ces mutants sont en grande majorité la conséquence secondaire du développement anormal de populations cellulaires de la ligne médiane. Tandis que l'altération de la MZG est potentiellement associée à des défauts de la fusion des deux hémisphères, il semble que le GW, l'IG et les neurones de signalisation interviennent dans la formation du CC par le biais de la sécrétion de molécules de guidage (que nous aborderons dans le prochain paragraphe). Enfin, il semble que le rôle précis du SCS ne soit toujours pas élucidé. Il est aussi important de noter que parmi les gènes que nous avons évoqué, certains jouent un double rôle, à la fois dans la mise en place des populations de la ligne médiane (rôle indirect), et dans l'expression de récepteurs au niveau des axones commissuraux (rôle direct).

b) Molécules de guidage au niveau de la ligne médiane

Dans ce paragraphe, nous allons nous intéresser aux récepteurs exprimés à la membrane des axones calleux, et aux molécules sécrétées par diverses structures du système nerveux central qui guident les axones calleux au niveau de la ligne médiane (Figure 11).

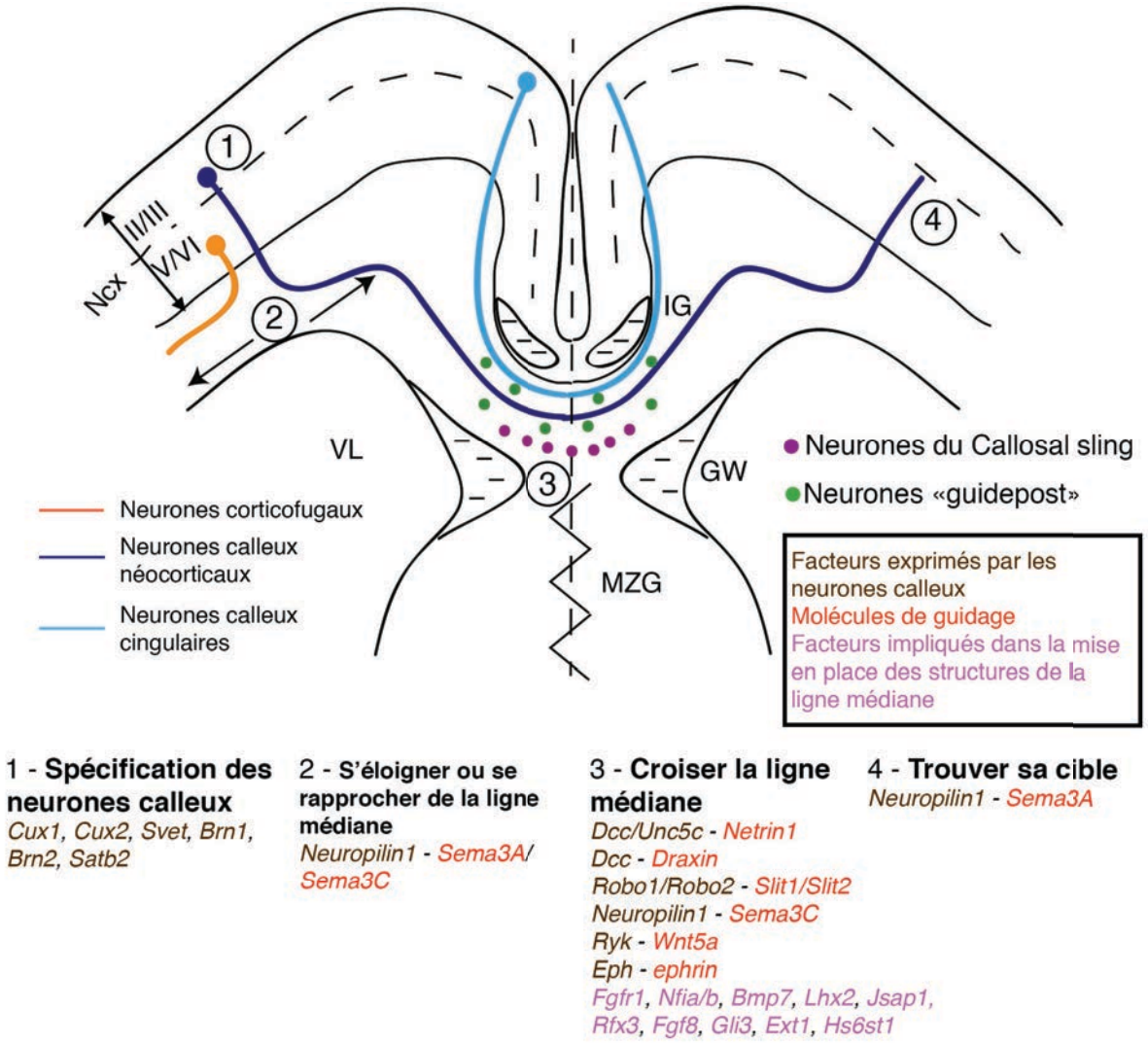

Figure 11. Molécules impliquées dans la spécification et le guidage des neurones calleux. Suite à la spécification des neurones calleux (1), ceux-ci quittent le néocortex et se dirigent vers la ligne médiane (2), se séparant alors des neurones corticofugaux qui se dirigent vers la capsule interne. Au niveau de la ligne médiane (3), de nombreuses molécules sécrétées par des structures gliales et neuronales guident les axones calleux vers l'hémisphère contralatéral. Une fois la ligne médiane franchie, d'autres facteurs moléculaires interviennent pour guider les axones calleux vers leur cible (4). Ncx : néocortex ; VL : ventricule latéral ; IG : indusium griseum ; GW : « glial wedge » ; MZG : « midline zipper glia ».

Les sémaphorines sont une famille de molécules de guidage qui jouent un rôle important dans le guidage des axones calleux au cours du développement. Elles agissent par le biais de leur récepteur NEUROPILIN1 (NRP1), exprimé par les axones des neurones pionniers du cortex cingulaire sous le contrôle de EMX1 (Ren et al., 2006; Piper et al., 2009b; Lim et al., 2015). Les axones calleux du cortex cingulaire sont sensibles à deux types de sémaphorines différentes : SEMA3A, exprimée selon un gradient décroissant latéro-médian, a un effet répulsif sur les axones exprimant NRP1, et les oriente ainsi en direction de la ligne médiane à leur sortie du néocortex (Zhao et al., 2011). Ces axones exprimant NRP1 sont au contraire attirés par SEMA3C, qui est sécrétée par les neurones de signalisation glutamatergiques situés à la ligne médiane (Gu et al., 2003; Niquille et al., 2009; Piper et al., 2009b). Le développement des axones pionniers du cortex cingulaire joue un rôle important, car ces derniers servent ensuite de guide aux axones du néocortex qui croisent la ligne médiane 24h après leur passage (Rash and Richards, 2001). C'est pourquoi l'altération du guidage des neurones cingulaires, qui représentent pourtant une population réduite par rapport à la totalité des neurones calleux, altère la formation de l'ensemble du CC (Niquille et al., 2009; Piper et al., 2009b).

SLIT1 et SLIT2 sont des molécules de guidage exprimées par les cellules de l'IG et du GW (Shu and Richards, 2001; Shu et al., 2003c), qui ont un effet répulsif sur les axones calleux exprimant ROBO1/ROBO2. Cette interaction permet dans un premier temps de positionner précisément les axones calleux selon l'axe dorso-ventral du télencéphale lorsqu'ils arrivent à la ligne médiane. Dans un deuxième temps, après le croisement, cela leur permet d'être repoussés en dehors de la ligne médiane (Shu et al., 2003c). L'absence de ROBO1/ROBO2 ou SLIT1/2 est responsable de dysgénésies du CC (Shu and Richards, 2001; Bagri et al., 2002; Shu et al., 2003c; Andrews et al., 2006; Lopez-Bendito et al., 2007).

La molécule de guidage WNT peut agir pas le biais d'une voie canonique qui fait intervenir le récepteur FRIZZLED3, tandis que la voie non canonique se fait via le récepteur RYK (Ciani and Salinas, 2005). Les mutants FRIZZLED3 présentent des altérations variables du CC (Wang et al., 2002). RYK joue un double rôle vis-à-vis des axones calleux. Avant le croisement, il permet la fasciculation des axones calleux. Après le croisement, il leur permet de quitter la ligne médiane via l'action répulsive de la molécule WNT5A sécrétée par l'IG et le GW (Keeble et al., 2006).

La mutation du récepteur Eph de classe A (EphA5) cause des dysgénésie calleuses qui ne semblent pas associées à des malformations des structures de la ligne médiane (Hu et al., 2003). Les ephrins de classe B et leurs récepteurs Eph sont exprimés dans le CC ainsi que dans les structures gliales de la ligne médiane. Des mutations isolées ou combinées des molécules de cette voie de signalisation sont responsables d'un spectre d'anomalies calleuses allant de l'hypoplasie à l'agénésie complète (Mendes et al., 2006; Robichaux et al., 2016). Cette absence de CC pourrait être due à des défauts de guidage directs, ainsi qu'à des anomalies de développement des cellules gliales de la ligne médiane (Mendes et al., 2006).

DRAXIN est une molécule de guidage répulsive, interagissant avec le récepteur DCC, exprimée par les cellules gliales entourant le CC, et dont l'absence cause des agénésies du CC (Islam et al., 2009; Ahmed et al., 2011).

Les mutants *Dcc*$^{-/-}$ et *Netrin1*$^{-/-}$ présentent tous deux une agénésie complète du CC (Serafini et al., 1994; Fazeli et al., 1997). De plus, DCC est exprimé dans les axones calleux lorsque ces derniers croisent la ligne médiane (Shu et al., 2000), tandis que NETRIN1 est exprimée à la ligne médiane du télencéphale dorsal (Serafini et al., 1994). Si l'importance du couple DCC/NETRIN1 dans la formation du CC est donc connue depuis longtemps, ce n'est que récemment que leurs fonctions précises ont été élucidées. NETRIN1 joue en fait deux rôles distincts vis-à-vis des axones pionniers du cortex cingulaire et du néocortex. NETRIN1

attire directement les axones cingulaire exprimant DCC. En revanche, NETRIN1 participe au guidage des axones néocorticaux en masquant l'interaction répulsive entre SLIT2 et ROBO1, par le biais d'une interaction entre ROBO1 et son récepteur DCC (Fothergill et al., 2014). Un autre récepteur de NETRIN1, UNC5C, est impliqué dans le guidage des axones calleux à la ligne médiane. Alors que la NETRIN a un effet attractif sur les axones exprimant DCC, elle a au contraire un effet répulsif sur les axones co-exprimant DCC et UNC5C (Hamelin et al., 1993; Colamarino and Tessier-Lavigne, 1995). Les facteurs de transcription SATB2 et CTIP2 inhibent respectivement les récepteurs DCC et UN5C. Les neurones calleux exprimant SATB2 présentent ainsi de forts niveaux de UNC5C et de faibles niveaux de DCC. Les neurones sub-cérébraux exprimant CTIP2 présentent un profil d'expression opposé. Ces deux profils d'expression pourraient déterminer des comportements distincts vis-à-vis d'une source de NETRIN1 située ventralement : cela permettrait d'attirer les axones sub-cérébraux, exprimant CTIP2 (et donc DCC), tandis que les axones des neurones exprimant SATB2 (et donc UNC5C) seraient repoussés, et se dirigeraient vers la ligne médiane (Srivatsa et al., 2014). Le phénotype des mutants *Satb2*$^{-/-}$ étaye cette hypothèse. En effet, chez ces mutants, les axones calleux ne sont pas bloqués à la ligne médiane, mais sont anormalement dirigés vers la capsule interne ou la commissure antérieure (Alcamo et al., 2008; Britanova et al., 2008). Ainsi, ce n'est pas juste le croisement de la ligne médiane qui est altéré chez les mutants *Satb2*$^{-/-}$, mais une étape plus précoce, qui détermine l'orientation des axones néocorticaux vers la ligne médiane ou vers des cibles subcérébrales.

c) Mécanismes cellule-autonomes et non cellule-autonomes impliqués dans le développement du CC

Il est admis que DCC et NETRIN1 jouent un rôle direct dans le guidage des axones calleux au niveau de la ligne médiane (Fothergill et al., 2014). Cependant, le phénotype des

mutants *Dcc*$^{-/-}$ et *Netrin1*$^{-/-}$ révèle la présence d'un kyste au niveau de la ligne médiane, à l'emplacement où les axones du CC devraient croiser la ligne médiane (voir Figure 2) (Hakanen and Salminen, 2015). Nous avons vu précédemment que de tels kystes pouvaient être dus à des défauts de fusion des deux hémisphères cérébraux. En accord avec cette hypothèse, il a été proposé que NETRIN1 contribue à la fusion des deux hémisphères au cours du développement en contrôlant l'élimination d'une population de cellules lepto-méningées située au niveau de la ligne médiane (Hakanen and Salminen, 2015). Ainsi, il se peut qu'en plus de leur rôle de guidage cellule-autonome, DCC et NETRIN1 soient aussi impliqué dans le processus de fusion inter-hémisphérique au niveau du septum. D'autres molécules, que nous avons citées précédemment, assurent un tel « double-jeu », contribuant à la formation du CC par des mécanismes à la fois cellule-autonomes et non cellule-autonomes. C'est le cas de *Nfib*, qui participe à la mise en place des structures gliales de la ligne médiane, mais qui régule aussi l'expression de NRP1 au niveau des axones calleux du cortex cingulaire (Piper et al., 2009a). De même, les molécules SLIT interviennent dans le guidage des axones calleux exprimant ROBO1, mais elles participent aussi au développement de l'IG (Unni et al., 2012). Enfin, même si cela n'a pas été démontré formellement, plusieurs éléments suggèrent que FGFR1 participe non seulement à la formation des populations gliales de la ligne médiane, mais qu'il ait aussi un rôle cellule-autonome dans le guidage des axones calleux (Tole et al., 2006).

d) Rôle de la microglie

La plupart des cellules de signalisation impliquées dans le guidage axonal sont des cellules gliales ou des neurones. Cependant, des études récentes ont mis en lumière le rôle d'une population dont l'implication dans le guidage axonal était jusqu'alors insoupçonnée : la microglie. Les cellules microgliales sont les « macrophages » du système nerveux central.

Au-delà de leur rôle dans le contrôle de l'homéostasie cérébrale et la lutte contre les agents infectieux, leur implication dans le développement du système nerveux central est de plus en plus étudiée (pour revue, voir (Squarzoni et al., 2015)). Le CC ne fait pas exception : la perturbation des populations microgliales au cours du développement engendre des défauts du fasciculation du CC (Pont-Lezica et al., 2014).

e) Rôle de la matrice extracellulaire

Plusieurs éléments indiquent un rôle des héparanes sulfates (HS) dans le développement du CC. Les HS sont des polysaccharides sulfatés qui peuvent être ajoutés de façon covalente à la surface cellulaire ou à des protéines de la matrice extracellulaire, les protéoglycanes. Ces derniers jouent un rôle fondamental dans le guidage axonal (pour revue, voir (Masu, 2015)). L'inhibition de la synthèse des HS par la suppression de l'enzyme EXT1 cause une agénésie complète du CC (Inatani et al., 2003). D'autres études se sont intéressées aux motifs de sulfatation des HS, et à leur rôle dans la formation du CC. La mutation d'enzymes responsables de la sulfatation des HS (les héparane sulfotransférases, telles que HS2ST ou HS6ST1) est responsable d'un positionnement anormal du GW et de l'IG au cours du développement, entraînant des malformations sévères du CC (Conway et al., 2011; Clegg et al., 2014).

f) L'établissement des connexions dans l'hémisphère contralatéral

Comme vu précédemment, la distribution des terminaisons des axones calleux n'est pas uniforme au sein du cortex. Les axones calleux établissent des connexions entre des régions des deux hémisphères selon un double spécificité, laminaire et tangentielle. Ainsi, une fois la ligne médiane franchie, encore faut-il que les axones calleux atteignent leur région cible dans l'hémisphère contralatéral.

Une étude récente a démontré que le site de projection des axones calleux dans l'hémisphère contralatéral est déterminé par leur position au sein du CC, et que cette organisation est régulée par une interaction entre NRP1 et SEMA3A (Zhou et al., 2013).

Des études récentes se sont intéressées au rôle de l'activité intrinsèque, spontanée, des neurones calleux au cours du développement. L'utilisation d'électroporations *in utero* permet de procéder à un marquage des neurones calleux tout en réduisant leur activité électrique spontanée ou leur transmission synaptique (Mizuno et al., 2007; Wang et al., 2007). La diminution de l'activité électrique spontanée des neurones calleux ou de leur cible aboutit à des défauts de guidage des axones au niveau de l'hémisphère contralatéral (Suarez et al., 2014a), ainsi qu'à des anomalies de croissance, d'arborisation et de distribution laminaire des terminaisons calleuses au sein du néocortex (Mizuno et al., 2007; Wang et al., 2007; Mizuno et al., 2010).

De nombreuses expériences de privation sensorielle ont démontré l'importance de l'activité neuronale évoquée par l'expérience sensorielle pour la maturation et le maintien de la double spécificité laminaire/tangentielle des connexions calleuses (Innocenti and Frost, 1979; 1980; Olavarria et al., 1987; Frost and Moy, 1989; Koralek and Killackey, 1990). Deux études récentes ont démontré que la symétrie des afférences sensorielles est nécessaire à l'établissement des projections calleuses au niveau de la frontière S1/S2 dans le cortex somatosensoriel de la souris (Huang et al., 2013; Suarez et al., 2014a). En l'absence de cette symétrie d'activité, aucune projection calleuse ne se développe à la frontière S1/S2. Ces expériences démontrent qu'en plus de son rôle connu dans la maturation des projections calleuses, l'activité évoquée par l'expérience sensorielle est aussi impliquée dans le guidage des axones calleux vers leur région cible dans l'hémisphère contralatéral (Suarez et al., 2014a).

L'ensemble de ces études démontre un rôle de l'activité neuronale, spontanée et évoquée, dans la formation du CC, que ce soit le guidage des axones calleux vers leur cible contralatérale (Huang et al., 2013; Suarez et al., 2014a), ou leur développement au sein du néocortex de la région cible (Mizuno et al., 2007; Wang et al., 2007; Mizuno et al., 2010). La façon dont l'activité neuronale intervient dans le développement et le guidage des axones calleux n'est pas encore claire. Cependant, différentes études ont fourni des pistes pour répondre à cette question, en révélant que l'activité neuronale spontanée peut moduler la réponse de cônes de croissance à des molécules de guidage (Hanson and Landmesser, 2004; Nicol et al., 2007; Mire et al., 2012).

7) Pathologies développementales du corps calleux chez l'humain

L'agénésie du corps calleux chez l'humain (AgCC) est une anomalie développementale ayant pour conséquence une absence totale (agénésie complète) ou partielle (agénésie partielle) du corps calleux, ou une réduction de sa taille (hypoplasie) (Figure 12). Le nombre d'anomalies génétiques et de syndromes cliniques complexes associés avec des AgCC est extrêmement important. En effet, il s'agit de la malformation du cerveau la plus courante, avec une incidence de 1 pour 4000 naissances (Paul et al., 2007; Edwards et al., 2014).

Les AgCC sont un ensemble d'anomalies développementales hétérogènes. Les AgCC dites « primaires » sont des atteintes isolées du CC, mais elles sont le plus souvent associées à d'autres anomalies développementales (Paul et al., 2007; Edwards et al., 2014). Les causes d'AgCC peuvent être génétiques ou environnementales, comme dans le cas du syndrome d'alcoolisation fœtal (Roebuck et al., 1998). Parmi les formes génétiques d'AgCC, de nombreuses formes semblent être sporadiques, rendant les études génétiques difficiles (Schell-Apacik et al., 2008). Parmi les 40% de formes génétiques identifiées, celles dues à des

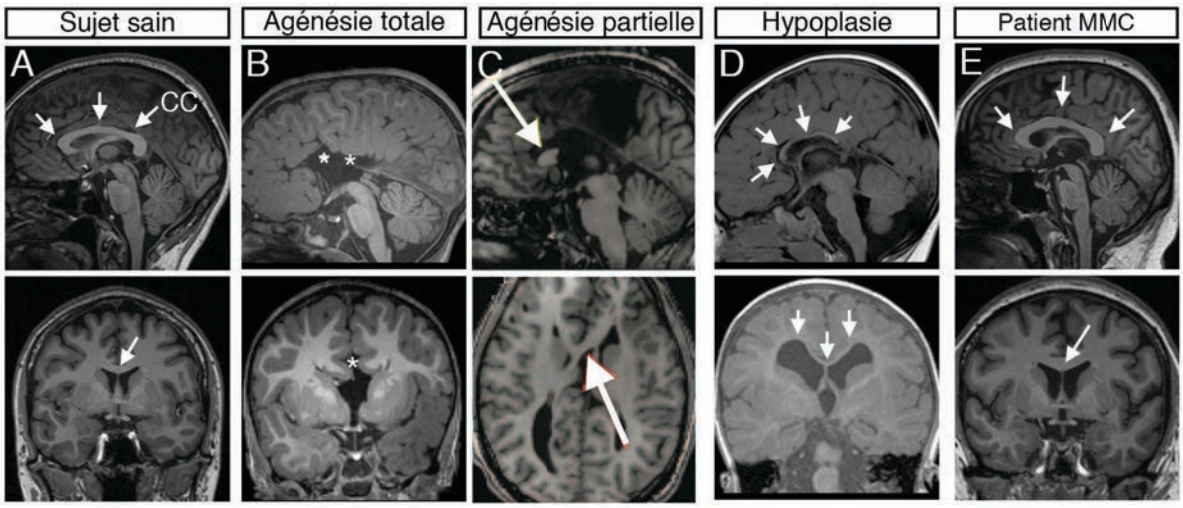

Figure 12. Différentes anomalies développementales du corps calleux chez l'humain. Vues sagittales et frontales (A, B, D, E) ou axiales (C) d'IRM anatomiques réalisées chez des sujets sains et des patients atteints d'anomalies développementales du CC. (A) Sujet sain (données personnelles). (B) Agénésie complète du CC. Les astérisques indiquent l'emplacement normal du CC (Extrait de Edwards et al, 2014). (C) Agénésie partielle du CC. Seuls le bec du CC est présent (Extrait de Wahl et al 2009). (D) Hypoplasie du CC. Toutes les parties du CC sont présentes, mais sa taille est fortement diminuée (Extrait de Edwards et al, 2014). (E) Patient atteint de MMC. L'anatomie du CC est normale (données personnelles). CC : corps calleux. Les flèches blanches indiquent l'emplacement du CC.

mutations monogéniques (environ 30%) ont grandement contribué à une meilleure compréhension des mécanismes moléculaires responsables de cette pathologie.

On peut classer les AgCC sur la base de l'étape développementale dont le dysfonctionnement mène à l'anomalie (Barkovich et al., 2012). On distingue ainsi les AgCC dues à des défauts : (i) de prolifération neuronale/gliale ; (ii) de spécification ou migration ; (iii) de spécification des structures de la ligne médiane ; (iv) de guidage ; (iv) d'évènements intervenant après la phase de guidage axonal. Pour une revue exhaustive des pathologies associées à des AgCC, voir (Edwards et al., 2014).

Tandis que les agénésies complètes du CC sont associées à une absence totale de connexions entre les deux hémisphères (Figure 12B), une partie des projections calleuses sont épargnées dans le cas des agénésies partielles (Figure 12C). Des connexions homotypiques sont maintenues, en fonction de la partie du CC qui est épargnée. De nombreux patients présentent des connexions hétérotypiques aberrantes : on parle de « fibres sigmoïdes », qui connectent des régions frontales antérieures avec des aires pariéto-occipitales de l'hémisphère opposé (Wahl et al., 2009).

Etant donné la grande diversité de la sévérité phénotypique des AgCC et de leurs causes génétiques, il n'est pas étonnant que le spectre d'anomalies comportementales correspondant puisse inclure des sujets asymptomatiques, ainsi que des patients souffrant de déficits comportementaux légers ou de graves problèmes neurologiques. De nombreuses études se sont initialement intéressées aux syndromes dits de « déconnexion », qui se manifestent par une absence de transfert d'information entre les deux hémisphères, ainsi qu'une absence d'intégration des informations sensori-motrices présentées indépendamment aux deux hémisphères (Bloom and Hynd, 2005). Une deuxième catégorie de troubles regroupe les anomalies cognitives, comportementales et psychiatriques. Dans le cas des AgCC primaires, les conséquences cognitives sont étonnamment réduites, et la plupart des

individus atteints présentent un QI dans la normale (Chiarello, 1980). En revanche, ces patients peuvent présenter des altérations des fonctions du langage, une forme d'inaptitude sociale, une diminution de la conscience de soi. Enfin, les AgCC peuvent aussi être associées à différentes maladies psychiatriques (Paul et al., 2007).

Il est étonnant de remarquer que si plusieurs éléments semblent indiquer une dysfonction du CC chez les patients atteints de MMC, les MM ne sont pas un symptôme couramment associé aux AgCC (Lepage et al., 2012). Des déficits de coordination bimanuelle ont été décrits chez des patients souffrant d'AgCC, mais leur capacité de réaliser des mouvements latéralisés semble intacte (Mueller et al., 2009). Des anomalies micro-structurelles du CC ont été décelées chez les patients atteints de MMC, mais il s'agissait d'altérations subtiles, ne modifiant pas la morphologie globale du CC (Figure 12E) (Gallea et al., 2013).

B. Revue de la littérature 2 : Le faisceau corticospinal, évolution, développement et pathologies humaines (soumis)

Le faisceau corticospinal est l'une des principales voies responsable de la motricité volontaire chez les mammifères. Des anomalies développementales du FCS ont été associées aux MM. En particulier, le guidage du FCS à la ligne médiane, au niveau de la décussation pyramidale puis dans la moelle, est un enjeu crucial pour assurer la latéralisation du contrôle moteur. Dans cette revue, nous nous sommes intéressés à l'évolution, au développement et aux pathologies du FCS, en portant une attention particulière à la décussation pyramidale.

The corticospinal tract: evolution, development, and human disorders

Corticospinal tract development and disorders

Quentin Welniarz[1,2], Isabelle Dusart[2], and Emmanuel Roze[1,3*].

[1] Sorbonne Universités, UPMC Univ Paris 06, INSERM U 1127, CNRS UMR 7225, Institut du Cerveau et de la Moelle épinière, F-75013, Paris, France

[2] Sorbonne Universités, UPMC Univ Paris 06, INSERM, CNRS, Institut de Biologie Paris Seine, Neuroscience Paris Seine, F-75005, Paris, France

[3] AP-HP, Hôpital de la Salpêtrière, Département des Maladies du Système Nerveux, Paris, France

Correspondence to: Emmanuel Roze

Département des maladies du système nerveux, Hôpital Pitié Salpêtrière,

47-83 boulevard de l'Hôpital, 75013 Paris

E-mail: flamand.roze.75012@gmail.com

Phone: +33142162748; Fax: +33142162474

ABSTRACT

The corticospinal tract (CST) plays a major role in cortical control of spinal cord activity. In particular, it is the principal motor pathway for voluntary movements. Here, we discuss: (i) the anatomic evolution and development of the CST across mammalian species, focusing on its role in motor functions; (ii) the molecular mechanisms regulating corticospinal tract formation and guidance during mouse development; and (iii) human disorders associated with abnormal CST development.

A comparison of CST anatomy and development across mammalian species first highlights important similarities. In particular, most CST axons cross the anatomical midline at the junction between the brainstem and spinal cord, forming the pyramidal decussation. Reorganization of the pattern of CST projections to the spinal cord during evolution led to improved motor skills. Studies of the molecular mechanisms involved in CST formation and guidance in mice have identified several factors that act synergistically to ensure proper formation of the CST at each step of development. Human CST developmental disorders can result in a reduction of the CST, or in guidance defects associated with abnormal CST anatomy. These latter disorders result in altered midline crossing at the pyramidal decussation or in the spinal cord, but spare the rest of the CST. Careful appraisal of clinical manifestations associated with CST malformations highlights the critical role of the CST in the lateralization of motor control.

Key words: pyramidal tract; axon guidance; mirror movements; development; movement disorders.

INTRODUCTION

The corticospinal tract (CST) is a complex system with multiple functions that share one characteristic, namely cortical control of spinal cord activity (Lemon and Griffiths, 2005; Lemon, 2008). These functions include the control of afferent inputs, spinal reflexes, and motor neuron activity (Lemon and Griffiths, 2005). The CST is of paramount importance in the motor system, as it mediates voluntary distal movements. The CST appeared in mammals, and is closely linked to the development of skilled voluntary movements through evolution (Heffner and Masterton, 1983; Davidoff, 1990; Vulliemoz et al., 2005; Schieber, 2007). The anatomy of the CST shows marked similarities across mammalian species. Importantly, most CST axons cross the anatomical midline at the junction between the brainstem and spinal cord, forming the pyramidal decussation. This is of critical importance for CST functions, as it means the left side of the brain controls the right side of the spinal cord, and *vice versa*.

This review examines current knowledge of CST anatomy and development in mammals, focusing on its role in motor functions. We then outline the molecular and genetic factors that govern the generation and development of the rodent CST. Finally, we discuss human CST developmental disorders.

OVERVIEW OF THE CORTICOSPINAL TRACT ACROSS EVOLUTION

Cortical areas contributing to the CST

The majority of CST axons originate from pyramidal cells located in the inferior part of cortical layer V in the primary motor and sensory cortex (M1 and S1), while other cortical regions make smaller contributions (Nudo and Masterton, 1990). In rodents, CST axons originate from motor, somatosensory, parietal, cingulate, visual and prefrontal regions (Miller, 1987; Akintunde and Buxton, 1992; Tennant et al., 2011; Kamiyama et al., 2015). In

cats, M1, S1, as well as the secondary sensorimotor cortices (S2), make major contributions to the CST (Armand and Kuypers, 1980). In monkeys, electrophysiological and histological studies have provided a precise description of the cortical territories that give rise to CST projections, and their relative contributions, as follows: M1 40%, supplementary motor area (SMA) 15%, S1 and S2 25%, cingulate cortex 10%, and insula 1% (Russell and Demyer, 1961; Biber et al., 1978; Macpherson et al., 1982; Toyoshima and Sakai, 1982; Dum and Strick, 1991; Luppino et al., 1991; Galea and Darian-Smith, 1994; Dum and Strick, 1996; Maier et al., 2002). In humans, intraoperative electrical stimulation of both the pre- and post-central gyri can elicit motor responses (Uematsu et al., 1992; Haseeb et al., 2007). A study of a patient with surgical ablation of the precentral gyrus suggested that this region accounts for approximately 60% of CST axons (Jane et al., 1967). The advent of non-invasive imaging technologies such as diffusion tensor imaging (DTI) has improved our understanding of CST anatomy in healthy subjects. The CST arises principally from M1 and S1, and also from the SMA and the ventral and dorsal premotor cortices (PMC) (Zilles et al., 1995; Newton et al., 2006; Kumar et al., 2009; Seo and Jang, 2013; Jang, 2014). DTI was recently used to quantify the contributions of different cortical areas to the CST: M1, S1, SMA and PMC were found to account for respectively 37%, 32%, 25% and 7% of CST axons (Seo and Jang, 2013). In all mammals, the CST arises from a large territory that extends far beyond the primary motor cortex. This supports the view that the CST is not solely involved in motor functions (Lemon and Griffiths, 2005).

CST trajectory from the cortex to the spinal cord

The trajectory of CST axons from the neocortex to the caudal medulla is conserved across mammals. After leaving the neocortex, CST axons form bundles and run through the internal capsule and cerebral peduncles before reaching the brainstem in a ventral position. CST axons

maintain their ventral position (forming the pyramids) until they reach the caudal part of the medulla. At the junction between the brainstem and spinal cord, the vast majority of CST axons cross the midline and pass from a ventral to a dorsal position, forming the pyramidal decussation, before continuing their trajectory in the contralateral spinal cord (Armand, 1982). There are some exceptions to this rule, however: the CST is uncrossed in hedgehogs for example (Nudo and Masterton, 1990). Likewise, in some species the decussation is not found at the level of the caudal medulla, being located instead in the pons in *Tachyglossus* (Goldby, 1939), in the high medulla in pangolins and chiroptera (Chang, 1944) and in the spinal cord in moles and *Procavia* (Linowiecki, 1914; Verhaart, 1967). In elephants and goats, the CST projects to both sides of the spinal cord (Verhaart, 1963; Haartsen and Verhaart, 1967).

The proportion of CST axons that cross the midline varies across species, ranging from 80% to 95% in rodents (Schreyer and Jones, 1982; Rouiller et al., 1991; Joosten et al., 1992), to 90% in cats (Armand and Kuypers, 1980), 85-90% in rhesus and macaque monkeys (Galea and Darian-Smith, 1994; Galea and Darian-Smith, 1995; Lacroix et al., 2004; Rosenzweig et al., 2009) and 75-90% in humans, with marked inter-individual differences (Davidoff, 1990; Nathan et al., 1990; Jang, 2014). CST axons crossing the midline in the spinal cord have been described in humans and monkeys (Nathan et al., 1990; Lacroix et al., 2004; Rosenzweig et al., 2009) and, to a lesser extent, in rodents (Rouiller et al., 1991).

The location of the CST in the spinal cord differs from one species to another. In rodents, monotremes and marsupials, the crossed CST is located in the most ventral part of the dorsal funiculus (Figure 1A) (Kuypers, 1981). The uncrossed CST runs in the ventral funiculus in rodents (Figure 1A) (Joosten et al., 1992; Uematsu et al., 1996; Brosamle and Schwab, 1997), and in the dorso-lateral funiculus in marsupials (Martin et al., 1970; Martin et al., 1972). In carnivores and primates (including cats, monkeys and humans), the crossed CST is located in the dorso-lateral funiculus of the spinal cord, contralateral to the hemisphere of origin (Figure

1B-C) (Kuypers, 1981). By contrast, the uncrossed CST can be found in the ventral and dorso-lateral funiculi of the ipsilateral spinal cord (Figure 1B-C) (Davidoff, 1990; Nathan et al., 1990; Galea and Darian-Smith, 1994; Lacroix et al., 2004; Vulliemoz et al., 2005; Rosenzweig et al., 2009; Oudega and Perez, 2012; Jang, 2014). Despite different sizes and locations in the spinal cord, the crossed and uncrossed CSTs originate from the same cortical regions (Galea and Darian-Smith, 1994; Brosamle and Schwab, 1997; Lacroix et al., 2004). The crossed CST is mainly involved in fine movements of the distal extremities, while the uncrossed CST targets motor neurons innervating the proximal or axial musculature (Brinkman and Kuypers, 1973; Davidoff, 1990; Nathan et al., 1990; Bawa et al., 2004; Vulliemoz et al., 2005).

CST termination pattern in the spinal cord

In the spinal cord, CST axons leave the white matter tract to enter the gray matter at cervical and lumbar enlargements, eventually transmitting motor commands to the fore and hind limbs. The CST termination pattern in the gray matter of the spinal cord switched from a dorsal to a ventral position during mammalian evolution. In rodents and cats, the crossed CST terminations are mainly located in the dorsal and intermediate horns of the contralateral spinal cord (Rexed's laminations I-VII), and the projection pattern of the uncrossed CST on the ipsilateral spinal cord is similar (Figure 1A, B) (Nyberg-Hansen and Brodal, 1963; Flindt-Egebak, 1977; Kuypers, 1982; Cheema et al., 1984; Brosamle and Schwab, 1997; Yang and Lemon, 2003). In monkeys and humans, crossed CST terminations are mostly found in the contralateral intermediate and ventral horns (Figure 1C, D) (Rexed's laminations V-VIII and IX) (Kuypers, 1982; Nathan et al., 1990; Bortoff and Strick, 1993; Armand et al., 1994; Galea and Darian-Smith, 1994; Dum and Strick, 1996; Armand et al., 1997; Lacroix et al., 2004; Rosenzweig et al., 2009; Morecraft et al., 2013). In monkeys, the uncrossed CST projects to

the intermediate and ventral zone of the ipsilateral spinal cord (laminae VII-VIII), but very few terminations are seen in lamina IX (Figure 1C) (Ralston and Ralston, 1985; Dum and Strick, 1996; Rosenzweig et al., 2009; Morecraft et al., 2013).

Consistent with these observations, direct corticospinal connections to motor neurons located in the ventral horn in the lamina IX (namely direct cortico-motoneuronal connections) are absent in non-primates such as cats (Illert et al., 1976), rats (Yang and Lemon, 2003; Alstermark et al., 2004) and mice (Alstermark and Ogawa, 2004), although it was recently shown that such direct connections might exist during a narrow developmental window in rats (Maeda et al., 2016). In cats, rats and mice, motor commands conveyed by the CST are eventually transmitted to forelimb motoneurons by segmental interneurons and propriospinal neurons (Lemon and Griffiths, 2005; Lemon, 2008). By contrast, direct cortico-motoneuronal connections are a specific feature of primates. In monkeys with strong cortico-motoneuronal connections, transmission of motor commands via the propriospinal system is reduced, and *vice versa* (Maier et al., 1998; Nakajima et al., 2000). In humans, anatomical (Kuypers, 1964) and electrophysiological data (Palmer and Ashby, 1992; Baldissera and Cavallari, 1993; de Noordhout et al., 1999) support the existence of direct cortico-motoneuronal connections. Direct cortico-motoneuronal connections have been described in distal muscles (de Noordhout et al., 1999), but appear to be very sparse in proximal muscles (Palmer and Ashby, 1992). The neuronal substrate of motor command transmission has thus evolved in mammals. Direct cortico-motoneuronal projections have gradually replaced the propriospinal system, resulting in more advanced hand function and manual dexterity (Heffner and Masterton, 1983; Bortoff and Strick, 1993; Maier et al., 1998; Nakajima et al., 2000; Lemon and Griffiths, 2005; Lemon, 2008).

The termination pattern of CST axons in the spinal gray matter depends on the cortical territory from which they originate, further stressing the different roles of this pathway. In

monkeys and cats, projections from the somatosensory cortex principally target the dorsal horn of the contralateral spinal cord and are thus likely to be involved in descending control of afferent inputs (Kuypers, 1981; Cheema et al., 1984; Armand et al., 1985; Ralston and Ralston, 1985; Martin, 1996). By contrast, CST axons originating from motor areas project mainly to the contralateral intermediate zone and, in monkeys, to the ventral horn (Cheema et al., 1984; Armand et al., 1994; Dum and Strick, 1996; Martin, 1996; Morecraft et al., 2013). In monkeys, several frontal regions project to the contralateral ventral horn, but projections from M1 are the most dense (Dum and Strick, 1996; Maier et al., 2002).

Comparative CST development across species: establishment of the mature pattern of CST projection to the spinal cord

Because the brains of different species develop and mature at different rates, care must be taken when comparing neurological development in mammals. Mammals can be divided into "precocial" and "altricial" species according to their degree of maturity and neurological development at birth. Neural altriciality/precocialty have been defined on the basis of two neonatal criteria: brain size (Sacher and Staffeldt, 1974) and brain myelination (Gibson, 1991). In this classification, rodents and cats are altricious, as their brains are relatively small and unmyelinated at birth. Old World monkeys, such as rhesus monkeys, are precocious: their brain is heavily myelinated and is already 65% of its adult size at birth. Humans are an intermediate case, the neonatal brain being moderately myelinated and only 25% of its adult size (Sacher and Staffeldt, 1974; Gibson, 1991). Thus, nervous system maturation takes place mostly before birth in Old World monkeys, but during postnatal development in humans and altricious species.

In mice, CST axons reach the brainstem at E17 (embryonic day 17) and the caudal medulla at E19. At post-natal day 0 (P0), CST axons cross the midline and enter the spinal cord, reaching

the lower cervical, thoracic and lumbar levels at P2, P5 and P9, respectively. Gray-matter innervation starts two days after CST axons arrive at the cervical enlargement (Gianino et al., 1999; Canty and Murphy, 2008). In cats, the CST enters the spinal cord around the 7th week of gestation, and has reached the lumbar spinal cord by birth (Alisky et al., 1992). In non-human primates such as macaques, the CST has reached all levels of the spinal cord at birth (after 21 weeks of gestation), although gray-matter innervation is not complete (Armand et al., 1994; Galea and Darian-Smith, 1995; Armand et al., 1997). In humans, CST axons reach the lower part of the cervical spinal cord by 24 weeks post-conception, and gray matter innervation begins a few weeks later (Eyre et al., 2000; Eyre, 2007).

At early developmental stages, the CST establishes large, non specific connections that are later refined. In rodents and macaques, the cortical territories giving rise to the CST are larger at birth than in adulthood. In rodents, layer-V neurons from the medial prefrontal cortex and visual cortex initially project to the spinal cord, and neurons originating from the motor cortex make aberrant collateral projections to the optic tectum (Figure 2A). These transient projections are later eliminated (Stanfield et al., 1982; Stanfield and O'Leary, 1985; Joosten and van Eden, 1989; Galea and Darian-Smith, 1995; Luo and O'Leary, 2005).

Studies of rodents and cats show that the CST first innervates the ventral, intermediate and dorsal spinal cord. This pattern is largely refined during post-natal development, with the elimination of CST projections to the ventral horn (Figure 2B) (Alisky et al., 1992; Curfs et al., 1994; Li and Martin, 2000; Canty and Murphy, 2008). In macaques, CST projections originating from M1 are distributed in the same regions of the spinal cord gray matter in newborns and adults, although their density increases markedly with age (Armand et al., 1994; Armand et al., 1997).

In humans, cats and rodents, the CST initially establishes strong bilateral projections to the spinal cord. This CST projection pattern is refined during early post-natal development,

resulting in the elimination of most ipsilateral projections (Figure 2B) (Alisky et al., 1992; Joosten et al., 1992; Muller et al., 1997; Eyre et al., 2000; Li and Martin, 2000; Eyre et al., 2001; Li and Martin, 2002). This refinement of ipsilateral projections is an activity-dependent process competing with crossed CST fibers originating from the contralateral motor cortex (Martin and Lee, 1999; Eyre et al., 2001; Eyre, 2003; Martin et al., 2004; Friel and Martin, 2007; Friel et al., 2014). By contrast, "transient" ipsilateral CST projections have not been observed during post-natal development in macaques (Armand et al., 1994; Armand et al., 1997).

Refinement of CST projections to spinal gray matter and elimination of transient ipsilateral projections during postnatal development appear to be specific to altricious species and humans. In monkeys, there is no evidence that such processes occur after birth, suggesting that the CST projection pattern to the spinal cord is established during embryonic development.

MOLECULAR MECHANISMS OF CST GENERATION AND GUIDANCE DURING DEVELOPMENT IN MOUSE

In the past decade, studies of mice with genetically induced CST alterations have advanced our understanding of the molecular underpinnings of corticospinal tract generation and development.

Generation and specification of CST neurons

Several classes of neocortical neurons can be distinguished on the basis of their morphology, neurotransmitter identity, electrophysiological properties and projection patterns. Each

population of neurons expresses a specific combination of genes, resulting in characteristics that define their identity (Molyneaux et al., 2007; Greig et al., 2013).

CST axons originate from the deep cortical layer V, along with other classes of subcerebral projection, including corticotectal and corticopontine neurons. In mice, cortical layer V neurons are generated on embryonic days 12-13 (E12-E13). Gene expression profiling of mouse CST neurons has identified key factors involved in CST specification and development, such as *Fezf2* (also named *Fezl*), *Ctip2 (*also named *Bcl11b)*, and *Sox5* (Arlotta et al., 2005; Molyneaux et al., 2015). *Fezf2* is crucial for the specification of layer-V neurons projecting to subcerebral targets. Loss of *Fezf2* results in a complete lack of CST neurons and in aberrant expansion of layer-VI corticothalamic neurons into the presumptive layer V (Chen et al., 2005; Molyneaux et al., 2005). *Fezf2* acts by regulating the expression of several genes (Lodato et al., 2014). In particular, *Fezf2* promotes the expression of *EphB1*, a gene involved in CST guidance in the ventral forebrain. Mutations of CTIP2, a transcription factor functioning downstream of FEZF2, lead to defective guidance of CST axons in the brainstem, preventing them from reaching their targets in the spinal cord (Arlotta et al., 2005). In mouse double mutants for *Ldb1* and *Ldb2* (Ldb adaptor proteins, LIM domain-binding proteins), two genes involved in the differentiation of CST neurons, CST axons fail to extend past the pyramidal decussation (Leone et al., 2016). The ERK/MAPK pathway was recently identified as a key factor in CST development. Mutations of this pathway result in delayed CST growth, followed by abnormal apoptosis of layer-V neurons during the first postnatal week (Xing et al., 2016).

Tbr1 is expressed in layer-VI corticothalamic neurons, and represses the specification into subcerebral projections neurons by directly binding *Fezf2* regulatory sequences (Bedogni et al., 2010; Han et al., 2011; McKenna et al., 2011). Generation of layer-VI corticothalamic neurons and layer-V corticospinal neurons is sequential and tightly regulated. *Sox5* and

Couptf1 are both involved in this process. In *Sox5* and *Couptf1* mutant mice, CST axons aberrantly terminate in the brainstem (Lai et al., 2008; Tomassy et al., 2010; Shim et al., 2012). BHLHB5 is a transcription factor that acts as a post-mitotic regulator of sensory-motor area identity. The CST is severely reduced in size and fails to reach the spinal cord in BHLHB5 mutants (Joshi et al., 2008). A recent study demonstrated that the transcription factor SIP1 is also critical for CST formation by regulating the axon growth rate (Srivatsa et al., 2015).

SATB2 is mostly expressed in superficial-layer neurons during development. It plays a critical role in the formation of the corpus callosum, as it inhibits a deep-layer differentiation program by binding *Ctip2* regulatory regions and thereby preventing its expression (Alcamo et al., 2008; Britanova et al., 2008; Baranek et al., 2012). SATB2 and CTIP2 were thus thought to be mutually exclusive, but recent studies indicate that a fraction of layer-V neurons transiently express SATB2 during embryonic development, and that this expression is required for CST formation (Leone et al., 2015).

Guidance of CST axons during development

CST guidance from cortex to brainstem

Following birth and the specification of CST neurons in cortical layer V, their axons have to travel a great distance from the neocortex to the contralateral spinal cord. Several molecules are known to ensure proper guidance of CST axons at specific choice points along this path (Figure 3).

Initially, corticofugal projections (which include both corticothalamic and corticospinal projections) grow out of the cortex and make a lateral turn, away from the midline, thus diverging from callosal projections. This first step involves SEMA3A and SEMA3C (Bagnard et al., 1998; Ruediger et al., 2013), as well as NETRIN-1, which acts as an attractive cue to

guide CST axons toward the ganglionic eminence (Metin et al., 1997; Srivatsa et al., 2014). After they have passed the pallial/subpallial boundary, CST axons make a medial turn to enter the internal capsule. In *Pax6* mutant mice, corticofugal projections overshoot the internal capsule and grow into the ventral telencephalon in an aberrant lateral position due to forebrain patterning defects (Jones et al., 2002). CST guidance into the internal capsule involves the receptors ROBO1/ROBO2 and their ligand SLIT1/SLIT2. In mice lacking both ROBO receptors or both SLITs, the internal capsule is ventrally displaced and large bundles of fibers aberrantly cross the midline in the ventral telencephalon (Bagri et al., 2002; Lopez-Bendito et al., 2007). CELSR3 and FRIZZLED3 are two planar cell polarity proteins, deletion of which leads to a complete lack of the internal capsule and, thus, to a greatly reduced CST (Wang et al., 2002; Tissir et al., 2005). Interestingly, specific deletion of CELSR3 and FRIZZLED3 in the ventral telencephalon reproduces most of the CST defects observed in complete mutants (Zhou et al., 2008; Hua et al., 2014). CELSR3 deletion in the neocortex also alters the formation of the internal capsule, showing that CELSR3 influences CST development through cell-autonomous and non cell-autonomous mechanisms (Zhou et al., 2008). CST axons fail to enter the diencephalon in *Nkx-2* mutant mice, which show defective ventral telencephalon patterning (Marin et al., 2002).

CST midline crossing at the pyramidal decussation

After entering the brainstem, CST axons navigate in a ventro-medial position to the caudal medulla, where they reach the pyramidal decussation. At this level, various molecules are required to ensure corticospinal tract midline crossing. DCC is a receptor that mediates the chemoattractive activity of its ligand NETRIN-1 for commissural axons (Keino-Masu et al., 1996). NETRIN-1 is secreted by floor plate cells and other midline structures in the CNS. The CST fails to cross the midline in DCC^{kanga} mice expressing a truncated DCC protein, and the

pyramidal decussation is reduced in *Netrin-1* mutants (Finger et al., 2002). UNC5H3, another NETRIN-1 receptor, is also involved in CST midline crossing. In *Unc5h3* mutants, the CST spreads laterally, rostral to the level of the pyramidal decussation. In consequence, a significant proportion of CST axons fail to cross the midline and instead remain in a ventral position in the ipsilateral spinal cord (Finger et al., 2002). This is reminiscent of observations in *Sema6A* and *PlexinA3/PlexinA4* mutants. Sema6A is expressed in the inferior olive (IO), a structure located in the caudal brainstem adjacent to the pyramidal decussation. A role of IO neurons in CST guidance has been proposed, through SEMA6A expression (Faulkner et al., 2008; Runker et al., 2008). L1 and NCAM are two neural cell adhesion molecules involved in axon fasciculation and guidance. In *L1* and *NCAM* mutants, the CST trajectory is normal from the cortex to the caudal brainstem, but a substantial number of axons fail to cross the midline at the pyramidal decussation and instead project ipsilaterally (Cohen et al., 1998; Rolf et al., 2002).

The number of molecules known to be associated with CST midline crossing is growing, but we do not yet know the exact molecular scenario that induces CST axons to cross (or not to cross) the midline at the pyramidal decussation. A small but significant fraction of CST axons (around 10% in mice) do not cross the midline at the pyramidal decussation and instead project to the ipsilateral spinal cord. The mechanisms underlying the formation of this uncrossed CST are completely unknown, but crossed and uncrossed CST axons are likely to express distinct receptors, resulting in separate trajectories when they encounter guidance molecules at the midline. A similar situation is encountered in the visual system of binocular species: retinal ganglion cells (RCGs) originating from the retina diverge at the optic chiasm, forming crossed and uncrossed projections (Petros et al., 2008). In mice, uncrossed RCGs originate from the ventro-temporal retina. They express the receptor EPHB2, which leads to midline avoidance upon interaction with its ligand EPHRIN-B1 (Petros et al., 2008). It has

been possible to unravel the mechanisms responsible for RCG divergence at the optic chiasm, because crossed and uncrossed RCGs originate from distinct territories in the retina. This specific organization of RCGs highlights differential expression of guidance receptors by crossed and uncrossed projections (Petros et al., 2008; Kuwajima et al., 2012). By contrast, crossed and uncrossed CST axons originate from the same cortical regions, making it difficult to isolate one population from the other and thus to detect different receptor expression profiles.

CST guidance in the spinal cord

In the spinal cord of wild type mice, EPHA4-expressing CST axons are repelled by EPHRIN-B3 secreted at the midline, preventing them from re-crossing the midline at the spinal level. By contrast, in EPHA4 and EPHRINB3 knockout mice, the pyramidal decussation is normal but CST axons re-cross the midline in the spinal cord (Dottori et al., 1998; Coonan et al., 2001; Kullander et al., 2001; Yokoyama et al., 2001). Growth of CST axons in the spinal cord involves several factors, such as *Wnt* and its receptor *Ryk* (Liu et al., 2005) and *Igf-1* (Ozdinler and Macklis, 2006), while *EphA4* controls gray-matter innervation. In *EphA4*$^{-/-}$ mice, the CST termination pattern in the spinal gray matter fails to refine, and CST terminations remain in the ventral and intermediate horn instead of innervating the dorsal horn (Dottori et al., 1998). In addition, hindlimb CST axons prematurely enter the spinal gray matter at the cervical level, resulting in fewer CST projections to the lumbar spinal cord (Dottori et al., 1998; Canty et al., 2006).

DEVELOPMENTAL DISORDERS OF THE CST IN HUMANS

Developmental disorders of the CST can be divided into two categories: (i) CST hypoplasia or aplasia; and (ii) guidance defects resulting in an abnormal CST anatomy (Table 1). All known guidance disorders result in altered midline crossing at the level of the pyramidal decussation or in the spinal cord, while sparing the rest of the CST.

Human disorders associated with a reduced CST

CST malformations are usually associated with diffuse brain malformation. In this case, the CST may be completely absent or hypoplastic, despite a normal anatomical location (Table 1). Post-mortem analysis of patients with anencephaly (Chow et al., 1985; ten Donkelaar et al., 2004), congenital aqueduct stenosis (Chow et al., 1985) and microcephaly (Chow et al., 1985; ten Donkelaar et al., 1999; ten Donkelaar et al., 2004) have revealed complete CST aplasia. Lissencephaly is a disorder of neuronal migration resulting in a complete lack of gyration. Histological studies have revealed that this condition is commonly associated with a hypoplastic CST, and a case of abnormal decussation has been reported (Roessmann and Hori, 1985). Walker-Warburg syndrome and the related disorder Fukuyama-type muscular dystrophy are due to migration defects leading to cerebro-ocular dysplasia and muscle atrophy. The CST is severely reduced in these two conditions (Miller et al., 1991; Kimura et al., 1993). Holoprosencephaly is a failure of the brain hemispheres to separate during development. Seven genes have so far been linked to this disorder. Some belong to the SHH signaling pathway, which is crucial for the development of ventral midline structures (Wallis and Muenke, 2000; Dyment et al., 2013). Histological and DTI studies suggest that the CST may be hypoplastic or absent, depending on the severity of the disease, but that the pyramidal decussation is normal when the CST is present (Kinsman, 2004; ten Donkelaar et al., 2004; Marcorelles and Laquerriere, 2010). Mutations of the human neural cell recognition molecule L1 cell adhesion molecule (L1CAM) result in a spectrum of X-linked disorders, including X-

linked hydrocephalus, MASA (mental retardation, adducted thumbs, spastic paraparesis, agenesis of the corpus callosum), X-linked agenesis of the corpus callosum, and spastic paraplegia type 1 (Dobson et al., 2001). In these patients, histological and electrophysiological/radiological investigations revealed CST hypoplasia but normal pyramidal decussation (Chow et al., 1985; Graf et al., 2000; Dobson et al., 2001). By contrast, mice lacking L1CAM have both a reduced CST and abnormal pyramidal decussation, due to guidance defects at the midline (Dahme et al., 1997; Cohen et al., 1998).

Human disorders associated with abnormal CST guidance at the midline

In normal subjects, most CST projections are contralateral: crossed fibers are more numerous than uncrossed fibers. Human disorders associated with an abnormal CST trajectory specifically involve defective midline crossing at the pyramidal decussation or in the spinal cord, while leaving the rest of the CST unaffected (Table 1; Figure 4). In consequence, CST projections to the spinal cord can be either bilateral, with each motor cortex projecting to both sides of the spinal cord via crossed and uncrossed fibers (Figure 4B, C); or strictly ipsilateral, with each motor cortex projecting to the ipsilateral spinal cord via uncrossed fibers (Figure 4D). Congenital mirror movements (CMM), X-linked Kallmann syndrome (KS) and Klippel-Feil syndrome are three disorders associated with abnormal pyramidal decussation resulting in bilateral CST projections to the spinal cord. These patients have mirror movements (MM), that is to say involuntary symmetrical movements of one hand that mirror voluntary movements of the other hand. By contrast, MM have not been described in patients with strictly ipsilateral CST projections to the spinal cord. This suggests that lateralization of CST projections to the spinal cord may be necessary to produce asymmetric hand movements.

Abnormal pyramidal decussation resulting in bilateral CST projections to the spinal cord

Congenital mirror movement disorder (CMM) is a rare genetic (autosomal dominant) disorder in which mirror movements are the only clinical abnormality. The two main culprit genes are *DCC* (deleted in colorectal cancer) and *RAD51* (Srour et al., 2010; Depienne et al., 2011; Depienne et al., 2012; Meneret et al., 2014). Syndromic forms of MM are accompanied by other symptoms. Mirror movements have been described in patients with Kallmann syndrome (KS), a disorder associating hypogonadotrophic hypogonadism and anosmia; MM in this setting are mostly associated with mutations of *KAL1*, the gene responsible for the X-linked form of KS (Quinton et al., 1996; Royal et al., 2002; Dode and Hardelin, 2010). Klippel-Feil syndrome is characterized by fusion of the cervical vertebrae (Bauman, 1932), leading to short neck, impaired cervical mobility, a low posterior hairline and, in many cases, mirror movements (Bauman, 1932; Baird et al., 1967; Royal et al., 2002). Three genes have been linked to Klippel-Feil syndrome, namely *GDF3*, *GDF6* and *MEOX1* (Tassabehji et al., 2008; Mohamed et al., 2013).

In patients with CMM and in patients with MM associated with X-linked KS or with Klippel-Feil syndrome, unilateral stimulation of the primary motor cortex hand area at rest by means of transcranial magnetic stimulation (TMS) elicits bilateral hand muscle responses with identical latencies, whereas in healthy volunteers the muscle response is strictly contralateral to the stimulated hemisphere (Farmer et al., 1990; Cincotta et al., 1994; Mayston et al., 1997; Cincotta et al., 2003; Cincotta et al., 2003; Bawa et al., 2004; Farmer et al., 2004; Gallea et al., 2013) (Figure 4A-C). This reveals the existence of fast-conducting corticospinal projections from the hand area of one primary motor cortex to both sides of the spinal cord, and suggests an anatomical-functional link between abnormal CST trajectories and the inability to produce purely unimanual movements. These bilateral corticospinal projections to the spinal cord could be due to: (i) abnormal pyramidal decussation, resulting in an aberrant uncrossed ipsilateral CST (Figure 4B); or (ii) aberrant branching of CST axons in the spinal

cord (Figure 4C). Abnormal pyramidal decussation rather than aberrant CST branching in the spinal cord is responsible for mirror movements in CMM and KS (Figure 4B). Diffusion tensor imaging, used to study the precise anatomy of the pyramidal decussation in *RAD51*-CMM patients, confirmed abnormal CST decussation (Gallea et al., 2013). The *RAD51* expression pattern in the developing mouse central nervous system (Depienne et al., 2012), and the known role of DCC in mouse CST guidance at the midline (Finger et al., 2002), further suggest that abnormal axonal guidance at the pyramidal decussation, rather than impaired CST maturation, is responsible for the bilateral CST projections in CMM patients. In X-linked KS, MRI findings support the existence of an abnormal uncrossed CST (Krams et al., 1999; Koenigkam-Santos et al., 2008; Koenigkam-Santos et al., 2010). An aberrant uncrossed CST has also been reported in male subjects with trisomy 18 (Miyata et al., 2014), but their motor phenotype is poorly documented. By contrast, autopsy of a patient with Klippel-Feil syndrome and mirror movements showed that the pyramidal decussation was completely absent (Gunderson and Solitare, 1968), suggesting that uncrossed CST axons might branch bilaterally in the spinal cord (Figure 4C). This abnormal bilateral branching of the CST might seek to compensate for the absence of the pyramidal decussation.

Mirror movements have also been reported occasionally in patients with Joubert, Möbius and Gorlin syndromes, three disorders likely associated with abnormal pyramidal decussation, at least in some cases. Joubert syndrome is a heterogeneous entity characterized by malformations of the cerebellar vermis and brainstem. Clinical features of Joubert syndrome can include early-onset hypotonia progressing to ataxia, developmental delay sometimes associated with autistic behaviors, oculomotor apraxia, respiratory dysfunction, and variable involvement of multiple organs (mainly the retina, kidney, liver and skeleton) (Romani et al., 2013). Mirror movements are occasionally part of the clinical picture. This disorder has been linked to mutations of numerous genes (see Table 1). Möbius syndrome consists of congenital

facial palsy with impaired ocular abduction likely related to brainstem malformation. The genetic and/or non genetic factors underlying this disorder are unclear (Verzijl et al., 2003). A recent article described three patients with Möbius syndrome and mirror movements (Webb et al., 2014). Gorlin syndrome is an autosomal dominant disorder characterized by multiple basal cell carcinomas, jaw keratocysts and skeletal malformations (Gorlin and Goltz, 1960). One case of Gorlin syndrome associated with MM has been reported (Sag et al., 2016). The occurrence of MM suggests the existence of bilateral CST projections to the spinal cord in these three syndromes, although direct electrophysiological evidence is lacking. Post-mortem histological analysis revealed a near-complete absence of the pyramidal decussation in several patients with Joubert syndrome (Friede and Boltshauser, 1978; Yachnis and Rorke, 1999; ten Donkelaar et al., 2000), and its complete absence in patients with Möbius syndrome (ten Donkelaar et al., 1999; Verzijl et al., 2005). DTI findings have confirmed that CST fibers fail to cross the midline in some patients with Joubert syndrome and in one patient with Gorlin syndrome (Poretti et al., 2007; Sag et al., 2016).

Absent pyramidal decussation resulting in ipsilateral CST projections to the spinal cord

Post-mortem studies of patients with Apert's syndrome (Maksem and Roessmann, 1979; Cohen and Kreiborg, 1990; ten Donkelaar et al., 2004; Raybaud and Di Rocco, 2007), Dandy-Walker syndrome (Lagger, 1979; Janzer and Friede, 1982) and encephalocele (Verhaart and Kramer, 1952) have revealed a complete lack of pyramidal decussation. Apert's syndrome is an autosomal dominant craniosynostosis associated with defects of the fibroblast growth factor receptor 2 (FGFR2) (Raybaud and Di Rocco, 2007), a protein known to interact with L1CAM (Colombo and Meldolesi, 2015). Dandy-Walker syndrome is characterized by partial or complete agenesis of the cerebellar vermis, enlargement of the posterior fossa, and cystic dilation of the fourth ventricle. *FOXC1*, *ZIC1* and *ZIC4* mutations cause Dandy-Walker

syndrome, potentially by interfering with SHH signaling pathways (Dyment et al., 2013). In patients with horizontal-gaze palsy with progressive scoliosis (HGPPS), a disorder linked to ROBO3 mutations, electrophysiological and DTI studies show that the CST fails to cross the midline and instead projects ipsilaterally onto the spinal cord (Figure 4D) (Jen et al., 2004; Bosley et al., 2005; Amoiridis et al., 2006; Sicotte et al., 2006; Haller et al., 2008). Interestingly, ROBO3 is known to ensure proper midline crossing of several axonal populations in the mouse central nervous system. It is strongly expressed in the commissures of the mouse hindbrain and spinal cord, and most commissural axons in these regions fail to cross the midline in *Robo3*$^{-/-}$ mutant mice (Long et al., 2004; Marillat et al., 2004; Sabatier et al., 2004; Tamada et al., 2008; Renier et al., 2010). *Robo3*$^{-/-}$ knockout mice die within 24 hours after birth, while the CST is known to cross the midline and enter the spinal cord around P0. The anatomy of the CST has not therefore been studied in these mice.

In *RAD51*-CMM, *KAL1*-KS and Klippel-Feil syndrome, three disorders associated with mirror movements, the pyramidal decussation is abnormal and CST axons originating from one side of the motor cortex project to both sides of the spinal cord. By contrast, mirror movements have not been described in patients with HGPPS, in whom the absence of the pyramidal decussation results in each cortex projecting to the ipsilateral spinal cord. Joubert syndrome, Möbius syndrome, Gorlin syndrome, Apert's syndrome, Dandy-Walker syndrome and encephalocele are associated with abnormal pyramidal decussation, but further electrophysiological studies are needed to determine whether CST projections to the spinal cord are bilateral or strictly ipsilateral in these patients. Together, these findings suggest that mirror movements are due to bilateral spinal cord projections arising from a single hemisphere cortex rather than to abnormal decussation of the CST *per se*.

CONCLUSION

Comparisons of mammalian species have helped to understand the evolution of the corticospinal tract. The anatomy of the CST from the cortex to the caudal brainstem is largely similar across species, whereas its organization within the spinal cord shows striking differences. The majority of CST axons cross the midline at the junction between the brainstem and spinal cord in almost all mammals, whereas the CST projection pattern to the spinal cord has undergone major reorganization through evolution, resulting in finer hand motor function. Cross-species comparisons of the developmental steps leading to the establishment of the CST projection pattern to the spinal cord have revealed the critical role of postnatal development in altricious species and humans, whereas CST maturation in monkeys seems to occur mainly during embryonic life.

Human CST developmental disorders involve either a general reduction or abnormal guidance of the CST. Abnormal CST guidance results in altered midline crossing at the pyramidal decussation or in the spinal cord, but apparently spares the rostral part of the CST. This underlines the importance and sensitivity of this choice point during CST development. Recent insights from studies of genetically modified mice have refined our knowledge of the molecular scenario that controls CST midline crossing at the decussation, by identifying several factors that must act synergistically to ensure proper CST guidance at the midline.

Careful appraisal of clinical manifestations associated with CST malformations highlights the critical role of the CST in the lateralization of motor control. In humans, aberrant bilateral CST projections to the spinal cord result in an inability to produce purely unimanual or asymmetric hand movements. However, mirror movements have not been described in patients who lack the pyramidal decussation and who have strictly ipsilateral CST projections to the spinal cord. A recent study of conditional-knockout EPHA4 mice demonstrated that

bilateral CST projections to the spinal cord result in abnormal symmetric voluntary movements, possibly providing a good murine model of mirror movements (Friel et al., 2014; Serradj et al., 2014). Together, these observations suggest that proper lateralization of CST projections to the spinal cord is the main determinant of our ability to produce asymmetric hand movements.

REFERENCES

Akintunde A, Buxton DF. 1992. Differential sites of origin and collateralization of corticospinal neurons in the rat: a multiple fluorescent retrograde tracer study. Brain Res 575:86-92.

Alcamo EA, Chirivella L, Dautzenberg M, Dobreva G, Farinas I, Grosschedl R, McConnell SK. 2008. Satb2 regulates callosal projection neuron identity in the developing cerebral cortex. Neuron 57:364-377.

Alisky JM, Swink TD, Tolbert DL. 1992. The postnatal spatial and temporal development of corticospinal projections in cats. Experimental brain research 88:265-276.

Alstermark B, Ogawa J. 2004. In vivo recordings of bulbospinal excitation in adult mouse forelimb motoneurons. J Neurophysiol 92:1958-1962.

Alstermark B, Ogawa J, Isa T. 2004. Lack of monosynaptic corticomotoneuronal EPSPs in rats: disynaptic EPSPs mediated via reticulospinal neurons and polysynaptic EPSPs via segmental interneurons. J Neurophysiol 91:1832-1839.

Amoiridis G, Tzagournissakis M, Christodoulou P, Karampekios S, Latsoudis H, Panou T, Simos P, Plaitakis A. 2006. Patients with horizontal gaze palsy and progressive scoliosis due to ROBO3 E319K mutation have both uncrossed and crossed central nervous system pathways and perform normally on neuropsychological testing. J Neurol Neurosurg Psychiatry 77:1047-1053.

Arlotta P, Molyneaux BJ, Chen J, Inoue J, Kominami R, Macklis JD. 2005. Neuronal subtype-specific genes that control corticospinal motor neuron development in vivo. Neuron 45:207-221.

Armand J. 1982. The origin, course and terminations of corticospinal fibers in various mammals. Prog Brain Res 57:329-360.

Armand J, Edgley SA, Lemon RN, Olivier E. 1994. Protracted postnatal development of corticospinal projections from the primary motor cortex to hand motoneurones in the macaque monkey. Exp Brain Res 101:178-182.

Armand J, Holstege G, Kuypers HG. 1985. Differential corticospinal projections in the cat. An autoradiographic tracing study. Brain Res 343:351-355.

Armand J, Kuypers HG. 1980. Cells of origin of crossed and uncrossed corticospinal fibers in the cat: a quantitative horseradish peroxidase study. Exp Brain Res 40:23-34.

Armand J, Olivier E, Edgley SA, Lemon RN. 1997. Postnatal development of corticospinal projections from motor cortex to the cervical enlargement in the macaque monkey. J Neurosci 17:251-266.

Bagnard D, Lohrum M, Uziel D, Puschel AW, Bolz J. 1998. Semaphorins act as attractive and repulsive guidance signals during the development of cortical projections. Development 125:5043-5053.

Bagri A, Marin O, Plump AS, Mak J, Pleasure SJ, Rubenstein JL, Tessier-Lavigne M. 2002. Slit proteins prevent midline crossing and determine the dorsoventral position of major axonal pathways in the mammalian forebrain. Neuron 33:233-248.

Baird PA, Robinson GC, Buckler WS. 1967. Klippel-Feil syndrome. A study of mirror movement detected by electromyography. Am J Dis Child 113:546-551.

Baldissera F, Cavallari P. 1993. Short-latency subliminal effects of transcranial magnetic stimulation on forearm motoneurones. Exp Brain Res 96:513-518.

Baranek C, Dittrich M, Parthasarathy S, Bonnon CG, Britanova O, Lanshakov D, Boukhtouche F, Sommer JE, Colmenares C, Tarabykin V, Atanasoski S. 2012. Protooncogene Ski cooperates with the chromatin-remodeling factor Satb2 in specifying callosal neurons. Proc Natl Acad Sci U S A 109:3546-3551.

Bauman GI. 1932. Absence of the cervical spine. Journal of the American Medical Association 98:129-132.

Bawa P, Hamm JD, Dhillon P, Gross PA. 2004. Bilateral responses of upper limb muscles to transcranial magnetic stimulation in human subjects. Exp Brain Res 158:385-390.

Bedogni F, Hodge RD, Elsen GE, Nelson BR, Daza RA, Beyer RP, Bammler TK, Rubenstein JL, Hevner RF. 2010. Tbr1 regulates regional and laminar identity of postmitotic neurons in developing neocortex. Proc Natl Acad Sci U S A 107:13129-13134.

Biber MP, Kneisley LW, LaVail JH. 1978. Cortical neurons projecting to the cervical and lumbar enlargements of the spinal cord in young and adult rhesus monkeys. Exp Neurol 59:492-508.

Bortoff GA, Strick PL. 1993. Corticospinal terminations in two new-world primates: further evidence that corticomotoneuronal connections provide part of the neural substrate for manual dexterity. J Neurosci 13:5105-5118.

Bosley TM, Salih MA, Jen JC, Lin DD, Oystreck D, Abu-Amero KK, MacDonald DB, al Zayed Z, al Dhalaan H, Kansu T, Stigsby B, Baloh RW. 2005. Neurologic features of horizontal gaze palsy and progressive scoliosis with mutations in ROBO3. Neurology 64:1196-1203.

Brinkman J, Kuypers HG. 1973. Cerebral control of contralateral and ipsilateral arm, hand and finger movements in the split-brain rhesus monkey. Brain 96:653-674.

Britanova O, de Juan Romero C, Cheung A, Kwan KY, Schwark M, Gyorgy A, Vogel T, Akopov S, Mitkovski M, Agoston D, Sestan N, Molnar Z, Tarabykin V. 2008. Satb2 is a postmitotic determinant for upper-layer neuron specification in the neocortex. Neuron 57:378-392.

Brosamle C, Schwab ME. 1997. Cells of origin, course, and termination patterns of the ventral, uncrossed component of the mature rat corticospinal tract. J Comp Neurol 386:293-303.

Canty AJ, Greferath U, Turnley AM, Murphy M. 2006. Eph tyrosine kinase receptor EphA4 is required for the topographic mapping of the corticospinal tract. Proc Natl Acad Sci U S A 103:15629-15634.

Canty AJ, Murphy M. 2008. Molecular mechanisms of axon guidance in the developing corticospinal tract. Prog Neurobiol 85:214-235.

Chang HT. 1944. High level decussation of the pyramids in the pangolin (Manis pentadactyla Dalmanni). Journal of Comparative Neurology 81:333-338.

Cheema SS, Rustioni A, Whitsel BL. 1984. Light and electron microscopic evidence for a direct corticospinal projection to superficial laminae of the dorsal horn in cats and monkeys. J Comp Neurol 225:276-290.

Chen B, Schaevitz LR, McConnell SK. 2005. Fezl regulates the differentiation and axon targeting of layer 5 subcortical projection neurons in cerebral cortex. Proc Natl Acad Sci U S A 102:17184-17189.

Chow CW, Halliday JL, Anderson RM, Danks DM, Fortune DW. 1985. Congenital absence of pyramids and its significance in genetic diseases. Acta Neuropathol 65:313-317.

Cincotta M, Borgheresi A, Balzini L, Vannucchi L, Zeloni G, Ragazzoni A, Benvenuti F, Zaccara G, Arnetoli G, Ziemann U. 2003. Separate ipsilateral and contralateral corticospinal projections in congenital mirror movements: Neurophysiological evidence and significance for motor rehabilitation. Mov Disord 18:1294-1300.

Cincotta M, Borgheresi A, Ragazzoni A, Vanni P, Balestrieri F, Benvenuti F, Zaccara G, Ziemann U. 2003. Motor control in mirror movements: studies with transcranial magnetic stimulation. Suppl Clin Neurophysiol 56:175-180.

Cincotta M, Ragazzoni A, de Scisciolo G, Pinto F, Maurri S, Barontini F. 1994. Abnormal projection of corticospinal tracts in a patient with congenital mirror movements. Neurophysiol Clin 24:427-434.

Cohen MM, Jr., Kreiborg S. 1990. The central nervous system in the Apert syndrome. Am J Med Genet 35:36-45.

Cohen NR, Taylor JS, Scott LB, Guillery RW, Soriano P, Furley AJ. 1998. Errors in corticospinal axon guidance in mice lacking the neural cell adhesion molecule L1. Curr Biol 8:26-33.

Colombo F, Meldolesi J. 2015. L1-CAM and N-CAM: From Adhesion Proteins to Pharmacological Targets. Trends Pharmacol Sci 36:769-781.

Coonan JR, Greferath U, Messenger J, Hartley L, Murphy M, Boyd AW, Dottori M, Galea MP, Bartlett PF. 2001. Development and reorganization of corticospinal projections in EphA4 deficient mice. J Comp Neurol 436:248-262.

Curfs MH, Gribnau AA, Dederen PJ. 1994. Selective elimination of transient corticospinal projections in the rat cervical spinal cord gray matter. Brain Res Dev Brain Res 78:182-190.

Dahme M, Bartsch U, Martini R, Anliker B, Schachner M, Mantei N. 1997. Disruption of the mouse L1 gene leads to malformations of the nervous system. Nat Genet 17:346-349.

Davidoff RA. 1990. The pyramidal tract. Neurology 40:332-339.

de Noordhout AM, Rapisarda G, Bogacz D, Gerard P, De Pasqua V, Pennisi G, Delwaide PJ. 1999. Corticomotoneuronal synaptic connections in normal man: an electrophysiological study. Brain 122 (Pt 7):1327-1340.

Depienne C, Bouteiller D, Meneret A, Billot S, Groppa S, Klebe S, Charbonnier-Beaupel F, Corvol JC, Saraiva JP, Brueggemann N, Bhatia K, Cincotta M, Brochard V, Flamand-Roze C, Carpentier W, Meunier S, Marie Y, Gaussen M, Stevanin G, Wehrle R, Vidailhet M, Klein C, Dusart I, Brice A, Roze E. 2012. RAD51 haploinsufficiency causes congenital mirror movements in humans. Am J Hum Genet 90:301-307.

Depienne C, Cincotta M, Billot S, Bouteiller D, Groppa S, Brochard V, Flamand C, Hubsch C, Meunier S, Giovannelli F, Klebe S, Corvol JC, Vidailhet M, Brice A, Roze E. 2011. A novel DCC mutation and genetic heterogeneity in congenital mirror movements. Neurology 76:260-264.

Dobson CB, Villagra F, Clowry GJ, Smith M, Kenwrick S, Donnai D, Miller S, Eyre JA. 2001. Abnormal corticospinal function but normal axonal guidance in human L1CAM mutations. Brain 124:2393-2406.

Dode C, Hardelin JP. 2010. Clinical genetics of Kallmann syndrome. Ann Endocrinol (Paris) 71:149-157.

Dottori M, Hartley L, Galea M, Paxinos G, Polizzotto M, Kilpatrick T, Bartlett PF, Murphy M, Kontgen F, Boyd AW. 1998. EphA4 (Sek1) receptor tyrosine kinase is required for the development of the corticospinal tract. Proc Natl Acad Sci U S A 95:13248-13253.

Dum RP, Strick PL. 1991. The origin of corticospinal projections from the premotor areas in the frontal lobe. J Neurosci 11:667-689.

Dum RP, Strick PL. 1996. Spinal cord terminations of the medial wall motor areas in macaque monkeys. J Neurosci 16:6513-6525.

Dyment DA, Sawyer SL, Chardon JW, Boycott KM. 2013. Recent advances in the genetic etiology of brain malformations. Curr Neurol Neurosci Rep 13:364.

Eyre JA. 2003. Development and plasticity of the corticospinal system in man. Neural Plast 10:93-106.

Eyre JA. 2007. Corticospinal tract development and its plasticity after perinatal injury. Neurosci Biobehav Rev 31:1136-1149.

Eyre JA, Miller S, Clowry GJ, Conway EA, Watts C. 2000. Functional corticospinal projections are established prenatally in the human foetus permitting involvement in the development of spinal motor centres. Brain 123 (Pt 1):51-64.

Eyre JA, Taylor JP, Villagra F, Smith M, Miller S. 2001. Evidence of activity-dependent withdrawal of corticospinal projections during human development. Neurology 57:1543-1554.

Farmer SF, Harrison LM, Mayston MJ, Parekh A, James LM, Stephens JA. 2004. Abnormal cortex-muscle interactions in subjects with X-linked Kallmann's syndrome and mirror movements. Brain 127:385-397.

Farmer SF, Ingram DA, Stephens JA. 1990. Mirror movements studied in a patient with Klippel-Feil syndrome. J Physiol 428:467-484.

Faulkner RL, Low LK, Liu XB, Coble J, Jones EG, Cheng HJ. 2008. Dorsal turning of motor corticospinal axons at the pyramidal decussation requires plexin signaling. Neural Dev 3:21.

Finger JH, Bronson RT, Harris B, Johnson K, Przyborski SA, Ackerman SL. 2002. The netrin 1 receptors Unc5h3 and Dcc are necessary at multiple choice points for the guidance of corticospinal tract axons. J Neurosci 22:10346-10356.

Flindt-Egebak P. 1977. Autoradiographical demonstration of the projections from the limb areas of the feline sensorimotor cortex to the spinal cord. Brain Res 135:153-156.

Friede RL, Boltshauser E. 1978. Uncommon syndromes of cerebellar vermis aplasia. I: Joubert syndrome. Dev Med Child Neurol 20:758-763.

Friel KM, Martin JH. 2007. Bilateral activity-dependent interactions in the developing corticospinal system. J Neurosci 27:11083-11090.

Friel KM, Williams PT, Serradj N, Chakrabarty S, Martin JH. 2014. Activity-Based Therapies for Repair of the Corticospinal System Injured during Development. Front Neurol 5:229.

Galea MP, Darian-Smith I. 1994. Multiple corticospinal neuron populations in the macaque monkey are specified by their unique cortical origins, spinal terminations, and connections. Cereb Cortex 4:166-194.

Galea MP, Darian-Smith I. 1995. Postnatal maturation of the direct corticospinal projections in the macaque monkey. Cereb Cortex 5:518-540.

Gallea C, Popa T, Hubsch C, Valabregue R, Brochard V, Kundu P, Schmitt B, Bardinet E, Bertasi E, Flamand-Roze C, Alexandre N, Delmaire C, Meneret A, Depienne C, Poupon C, Hertz-Pannier L, Cincotta M, Vidailhet M, Lehericy S, Meunier S, Roze E. 2013. RAD51 deficiency disrupts the corticospinal lateralization of motor control. Brain 136:3333-3346.

Gianino S, Stein SA, Li H, Lu X, Biesiada E, Ulas J, Xu XM. 1999. Postnatal growth of corticospinal axons in the spinal cord of developing mice. Brain Res Dev Brain Res 112:189-204.

Gibson KR. 1991. Myelination and behavioral development: A comparative perspective on questions of neoteny, altriciality and intelligence. Brain maturation and cognitive development: Comparative and cross-cultural perspectives:29-63.

Goldby F. 1939. An experimental investigation of the motor cortex and pyramidal tract of Echidna aculeata. Journal of anatomy 73:509.

Gorlin RJ, Goltz RW. 1960. Multiple nevoid basal-cell epithelioma, jaw cysts and bifid rib. A syndrome. N Engl J Med 262:908-912.

Graf WD, Born DE, Shaw DW, Thomas JR, Holloway LW, Michaelis RC. 2000. Diffusion-weighted magnetic resonance imaging in boys with neural cell adhesion molecule L1 mutations and congenital hydrocephalus. Ann Neurol 47:113-117.

Greig LC, Woodworth MB, Galazo MJ, Padmanabhan H, Macklis JD. 2013. Molecular logic of neocortical projection neuron specification, development and diversity. Nat Rev Neurosci 14:755-769.

Gunderson CH, Solitare GB. 1968. Mirror movements in patients with the Klippel-Feil syndrome. Neuropathologic observations. Arch Neurol 18:675-679.

Haartsen AB, Verhaart WJC. 1967. Cortical projections to brain stem and spinal cord in the goat by way of the pyramidal tract and the bundle of Bagley. Journal of Comparative Neurology 129:189-201.

Haller S, Wetzel SG, Lutschg J. 2008. Functional MRI, DTI and neurophysiology in horizontal gaze palsy with progressive scoliosis. Neuroradiology 50:453-459.

Han W, Kwan KY, Shim S, Lam MM, Shin Y, Xu X, Zhu Y, Li M, Sestan N. 2011. TBR1 directly represses Fezf2 to control the laminar origin and development of the corticospinal tract. Proc Natl Acad Sci U S A 108:3041-3046.

Haseeb A, Asano E, Juhasz C, Shah A, Sood S, Chugani HT. 2007. Young patients with focal seizures may have the primary motor area for the hand in the postcentral gyrus. Epilepsy Res 76:131-139.

Heffner RS, Masterton RB. 1983. The role of the corticospinal tract in the evolution of human digital dexterity. Brain Behav Evol 23:165-183.

Hua ZL, Jeon S, Caterina MJ, Nathans J. 2014. Frizzled3 is required for the development of multiple axon tracts in the mouse central nervous system. Proc Natl Acad Sci U S A 111:E3005-3014.

Illert M, Lundberg A, Tanaka R. 1976. Integration in descending motor pathways controlling the forelimb in the cat. 1. Pyramidal effects on motoneurones. Exp Brain Res 26:509-519.

Jane JA, Yashon D, DeMyer W, Bucy PC. 1967. The contribution of the precentral gyrus to the pyramidal tract of man. J Neurosurg 26:244-248.

Jang SH. 2014. The corticospinal tract from the viewpoint of brain rehabilitation. J Rehabil Med 46:193-199.

Janzer RC, Friede RL. 1982. Dandy-Walker syndrome with atresia of the fourth ventricle and multiple rhombencephalic malformations. Acta Neuropathol 58:81-86.

Jen JC, Chan WM, Bosley TM, Wan J, Carr JR, Rub U, Shattuck D, Salamon G, Kudo LC, Ou J, Lin DD, Salih MA, Kansu T, Al Dhalaan H, Al Zayed Z, MacDonald DB, Stigsby B, Plaitakis A, Dretakis EK, Gottlob I, Pieh C, Traboulsi EI, Wang Q, Wang L, Andrews C, Yamada K, Demer JL, Karim S, Alger JR, Geschwind DH, Deller T, Sicotte NL, Nelson SF, Baloh RW, Engle EC. 2004. Mutations in a human ROBO gene disrupt hindbrain axon pathway crossing and morphogenesis. Science 304:1509-1513.

Jones L, Lopez-Bendito G, Gruss P, Stoykova A, Molnar Z. 2002. Pax6 is required for the normal development of the forebrain axonal connections. Development 129:5041-5052.

Joosten EA, Schuitman RL, Vermelis ME, Dederen PJ. 1992. Postnatal development of the ipsilateral corticospinal component in rat spinal cord: a light and electron microscopic anterograde HRP study. J Comp Neurol 326:133-146.

Joosten EA, van Eden CG. 1989. An anterograde tracer study on the development of corticospinal projections from the medial prefrontal cortex in the rat. Brain Res Dev Brain Res 45:313-319.

Joshi PS, Molyneaux BJ, Feng L, Xie X, Macklis JD, Gan L. 2008. Bhlhb5 regulates the postmitotic acquisition of area identities in layers II-V of the developing neocortex. Neuron 60:258-272.

Kamiyama T, Kameda H, Murabe N, Fukuda S, Yoshioka N, Mizukami H, Ozawa K, Sakurai M. 2015. Corticospinal tract development and spinal cord innervation differ between cervical and lumbar targets. J Neurosci 35:1181-1191.

Keino-Masu K, Masu M, Hinck L, Leonardo ED, Chan SS, Culotti JG, Tessier-Lavigne M. 1996. Deleted in Colorectal Cancer (DCC) encodes a netrin receptor. Cell 87:175-185.

Kimura S, Sasaki Y, Kobayashi T, Ohtsuki N, Tanaka Y, Hara M, Miyake S, Yamada M, Iwamoto H, Misugi N. 1993. Fukuyama-type congenital muscular dystrophy and the Walker-Warburg syndrome. Brain Dev 15:182-191.

Kinsman SL. 2004. White matter imaging in holoprosencephaly in children. Curr Opin Neurol 17:115-119.

Koenigkam-Santos M, de Castro M, Versiani BR, Diniz PR, Santos AC. 2010. Kallmann syndrome and mirror movements: White matter quantitative evaluation with magnetic resonance imaging. J Neurol Sci 292:40-44.

Koenigkam-Santos M, Santos AC, Borduqui T, Versiani BR, Hallak JE, Crippa JA, Castro M. 2008. Whole-brain voxel-based morphometry in Kallmann syndrome associated with mirror movements. AJNR Am J Neuroradiol 29:1799-1804.

Krams M, Quinton R, Ashburner J, Friston KJ, Frackowiak RS, Bouloux PM, Passingham RE. 1999. Kallmann's syndrome: mirror movements associated with bilateral corticospinal tract hypertrophy. Neurology 52:816-822.

Kullander K, Mather NK, Diella F, Dottori M, Boyd AW, Klein R. 2001. Kinase-dependent and kinase-independent functions of EphA4 receptors in major axon tract formation in vivo. Neuron 29:73-84.

Kumar A, Juhasz C, Asano E, Sundaram SK, Makki MI, Chugani DC, Chugani HT. 2009. Diffusion tensor imaging study of the cortical origin and course of the corticospinal tract in healthy children. AJNR Am J Neuroradiol 30:1963-1970.

Kuwajima T, Yoshida Y, Takegahara N, Petros TJ, Kumanogoh A, Jessell TM, Sakurai T, Mason C. 2012. Optic chiasm presentation of Semaphorin6D in the context of Plexin-A1 and Nr-CAM promotes retinal axon midline crossing. Neuron 74:676-690.

Kuypers H. 1981. Anatomy of the descending pathways. Comprehensive Physiology.

Kuypers HG. 1964. The Descending Pathways to the Spinal Cord, Their Anatomy and Function. Prog Brain Res 11:178-202.

Kuypers HG. 1982. A new look at the organization of the motor system. Prog Brain Res 57:381-403.

Lacroix S, Havton LA, McKay H, Yang H, Brant A, Roberts J, Tuszynski MH. 2004. Bilateral corticospinal projections arise from each motor cortex in the macaque monkey: a quantitative study. J Comp Neurol 473:147-161.

Lagger RL. 1979. Failure of pyramidal tract decussation in the Dandy-Walker syndrome. Report of two cases. J Neurosurg 50:382-387.

Lai T, Jabaudon D, Molyneaux BJ, Azim E, Arlotta P, Menezes JR, Macklis JD. 2008. SOX5 controls the sequential generation of distinct corticofugal neuron subtypes. Neuron 57:232-247.

Lemon RN. 2008. Descending pathways in motor control. Annu Rev Neurosci 31:195-218.

Lemon RN, Griffiths J. 2005. Comparing the function of the corticospinal system in different species: organizational differences for motor specialization? Muscle Nerve 32:261-279.

Leone DP, Heavner WE, Ferenczi EA, Dobreva G, Huguenard JR, Grosschedl R, McConnell SK. 2015. Satb2 Regulates the Differentiation of Both Callosal and Subcerebral Projection Neurons in the Developing Cerebral Cortex. Cereb Cortex 25:3406-3419.

Leone DP, Panagiotakos G, Heavner WE, Joshi P, Zhao Y, Westphal H, McConnell SK. 2016. Compensatory Actions of Ldb Adaptor Proteins During Corticospinal Motor Neuron Differentiation. Cereb Cortex.

Li Q, Martin JH. 2000. Postnatal development of differential projections from the caudal and rostral motor cortex subregions. Exp Brain Res 134:187-198.

Li Q, Martin JH. 2002. Postnatal development of connectional specificity of corticospinal terminals in the cat. J Comp Neurol 447:57-71.

Linowiecki A. 1914. The comparative anatomy of the pyramidal tract. Journal of Comparative Neurology 24:509-530.

Liu Y, Shi J, Lu CC, Wang ZB, Lyuksyutova AI, Song XJ, Zou Y. 2005. Ryk-mediated Wnt repulsion regulates posterior-directed growth of corticospinal tract. Nat Neurosci 8:1151-1159.

Lodato S, Molyneaux BJ, Zuccaro E, Goff LA, Chen HH, Yuan W, Meleski A, Takahashi E, Mahony S, Rinn JL, Gifford DK, Arlotta P. 2014. Gene co-regulation by Fezf2 selects neurotransmitter identity and connectivity of corticospinal neurons. Nat Neurosci 17:1046-1054.

Long H, Sabatier C, Ma L, Plump A, Yuan W, Ornitz DM, Tamada A, Murakami F, Goodman CS, Tessier-Lavigne M. 2004. Conserved roles for Slit and Robo proteins in midline commissural axon guidance. Neuron 42:213-223.

Lopez-Bendito G, Flames N, Ma L, Fouquet C, Di Meglio T, Chedotal A, Tessier-Lavigne M, Marin O. 2007. Robo1 and Robo2 cooperate to control the guidance of major axonal tracts in the mammalian forebrain. J Neurosci 27:3395-3407.

Luo L, O'Leary DD. 2005. Axon retraction and degeneration in development and disease. Annu Rev Neurosci 28:127-156.

Luppino G, Matelli M, Camarda RM, Gallese V, Rizzolatti G. 1991. Multiple representations of body movements in mesial area 6 and the adjacent cingulate cortex: an intracortical microstimulation study in the macaque monkey. J Comp Neurol 311:463-482.

Macpherson J, Wiesendanger M, Marangoz C, Miles TS. 1982. Corticospinal neurones of the supplementary motor area of monkeys. A single unit study. Exp Brain Res 48:81-88.

Maeda H, Fukuda S, Kameda H, Murabe N, Isoo N, Mizukami H, Ozawa K, Sakurai M. 2016. Corticospinal axons make direct synaptic connections with spinal motoneurons innervating forearm muscles early during postnatal development in the rat. J Physiol 594:189-205.

Maier MA, Armand J, Kirkwood PA, Yang HW, Davis JN, Lemon RN. 2002. Differences in the corticospinal projection from primary motor cortex and supplementary motor area to macaque upper limb motoneurons: an anatomical and electrophysiological study. Cereb Cortex 12:281-296.

Maier MA, Illert M, Kirkwood PA, Nielsen J, Lemon RN. 1998. Does a C3-C4 propriospinal system transmit corticospinal excitation in the primate? An investigation in the macaque monkey. J Physiol 511 (Pt 1):191-212.

Maksem JA, Roessmann U. 1979. Apert's syndrome with central nervous system anomalies. Acta Neuropathol 48:59-61.

Marcorelles P, Laquerriere A. 2010. Neuropathology of holoprosencephaly. Am J Med Genet C Semin Med Genet 154C:109-119.

Marillat V, Sabatier C, Failli V, Matsunaga E, Sotelo C, Tessier-Lavigne M, Chedotal A. 2004. The slit receptor Rig-1/Robo3 controls midline crossing by hindbrain precerebellar neurons and axons. Neuron 43:69-79.

Marin O, Baker J, Puelles L, Rubenstein JL. 2002. Patterning of the basal telencephalon and hypothalamus is essential for guidance of cortical projections. Development 129:761-773.

Martin G, Megirian D, Conner J. 1972. The origin, course and termination of the corticospinal tracts of the Tasmanian potoroo (Potorous apicalis). Journal of anatomy 111:263.
Martin GF, Megirian D, Roebuck A. 1970. The corticospinal tract of the marsupial phalanger (Trichosurus vulpecula). Journal of Comparative Neurology 139:245-257.
Martin JH. 1996. Differential spinal projections from the forelimb areas of the rostral and caudal subregions of primary motor cortex in the cat. Exp Brain Res 108:191-205.
Martin JH, Choy M, Pullman S, Meng Z. 2004. Corticospinal system development depends on motor experience. J Neurosci 24:2122-2132.
Martin JH, Lee SJ. 1999. Activity-dependent competition between developing corticospinal terminations. Neuroreport 10:2277-2282.
Mayston MJ, Harrison LM, Quinton R, Stephens JA, Krams M, Bouloux PM. 1997. Mirror movements in X-linked Kallmann's syndrome. I. A neurophysiological study. Brain 120 (Pt 7):1199-1216.
McKenna WL, Betancourt J, Larkin KA, Abrams B, Guo C, Rubenstein JL, Chen B. 2011. Tbr1 and Fezf2 regulate alternate corticofugal neuronal identities during neocortical development. J Neurosci 31:549-564.
Meneret A, Depienne C, Riant F, Trouillard O, Bouteiller D, Cincotta M, Bitoun P, Wickert J, Lagroua I, Westenberger A, Borgheresi A, Doummar D, Romano M, Rossi S, Defebvre L, De Meirleir L, Espay AJ, Fiori S, Klebe S, Quelin C, Rudnik-Schoneborn S, Plessis G, Dale RC, Sklower Brooks S, Dziezyc K, Pollak P, Golmard JL, Vidailhet M, Brice A, Roze E. 2014. Congenital mirror movements: mutational analysis of RAD51 and DCC in 26 cases. Neurology 82:1999-2002.
Metin C, Deleglise D, Serafini T, Kennedy TE, Tessier-Lavigne M. 1997. A role for netrin-1 in the guidance of cortical efferents. Development 124:5063-5074.
Miller G, Ladda RL, Towfighi J. 1991. Cerebro-ocular dysplasia--muscular dystrophy (Walker Warburg) syndrome. Findings in 20-week-old fetus. Acta Neuropathol 82:234-238.
Miller MW. 1987. The origin of corticospinal projection neurons in rat. Exp Brain Res 67:339-351.
Miyata H, Miyata M, Ohama E. 2014. Pyramidal tract abnormalities in the human fetus and infant with trisomy 18 syndrome. Neuropathology 34:219-226.
Mohamed JY, Faqeih E, Alsiddiky A, Alshammari MJ, Ibrahim NA, Alkuraya FS. 2013. Mutations in MEOX1, encoding mesenchyme homeobox 1, cause Klippel-Feil anomaly. Am J Hum Genet 92:157-161.
Molyneaux BJ, Arlotta P, Hirata T, Hibi M, Macklis JD. 2005. Fezl is required for the birth and specification of corticospinal motor neurons. Neuron 47:817-831.
Molyneaux BJ, Arlotta P, Menezes JR, Macklis JD. 2007. Neuronal subtype specification in the cerebral cortex. Nat Rev Neurosci 8:427-437.
Molyneaux BJ, Goff LA, Brettler AC, Chen HH, Brown JR, Hrvatin S, Rinn JL, Arlotta P. 2015. DeCoN: genome-wide analysis of in vivo transcriptional dynamics during pyramidal neuron fate selection in neocortex. Neuron 85:275-288.
Morecraft RJ, Ge J, Stilwell-Morecraft KS, McNeal DW, Pizzimenti MA, Darling WG. 2013. Terminal distribution of the corticospinal projection from the hand/arm region of the primary motor cortex to the cervical enlargement in rhesus monkey. J Comp Neurol 521:4205-4235.
Muller K, Kass-Iliyya F, Reitz M. 1997. Ontogeny of ipsilateral corticospinal projections: a developmental study with transcranial magnetic stimulation. Ann Neurol 42:705-711.
Nakajima K, Maier MA, Kirkwood PA, Lemon RN. 2000. Striking differences in transmission of corticospinal excitation to upper limb motoneurons in two primate species. J Neurophysiol 84:698-709.

Nathan PW, Smith MC, Deacon P. 1990. The corticospinal tracts in man. Course and location of fibres at different segmental levels. Brain 113 (Pt 2):303-324.
Newton JM, Ward NS, Parker GJ, Deichmann R, Alexander DC, Friston KJ, Frackowiak RS. 2006. Non-invasive mapping of corticofugal fibres from multiple motor areas--relevance to stroke recovery. Brain 129:1844-1858.
Nudo RJ, Masterton RB. 1990. Descending pathways to the spinal cord, III: Sites of origin of the corticospinal tract. J Comp Neurol 296:559-583.
Nyberg-Hansen R, Brodal A. 1963. Sites of termination of corticospinal fibers in the cat. An experimental study with silver impregnation methods. J Comp Neurol 120:369-391.
Oudega M, Perez MA. 2012. Corticospinal reorganization after spinal cord injury. J Physiol 590:3647-3663.
Ozdinler PH, Macklis JD. 2006. IGF-I specifically enhances axon outgrowth of corticospinal motor neurons. Nat Neurosci 9:1371-1381.
Palmer E, Ashby P. 1992. Corticospinal projections to upper limb motoneurones in humans. J Physiol 448:397-412.
Petros TJ, Rebsam A, Mason CA. 2008. Retinal axon growth at the optic chiasm: to cross or not to cross. Annu Rev Neurosci 31:295-315.
Poretti A, Boltshauser E, Loenneker T, Valente EM, Brancati F, Il'yasov K, Huisman TA. 2007. Diffusion tensor imaging in Joubert syndrome. AJNR Am J Neuroradiol 28:1929-1933.
Quinton R, Duke VM, de Zoysa PA, Platts AD, Valentine A, Kendall B, Pickman S, Kirk JM, Besser GM, Jacobs HS, Bouloux PM. 1996. The neuroradiology of Kallmann's syndrome: a genotypic and phenotypic analysis. J Clin Endocrinol Metab 81:3010-3017.
Ralston DD, Ralston HJ, 3rd. 1985. The terminations of corticospinal tract axons in the macaque monkey. J Comp Neurol 242:325-337.
Raybaud C, Di Rocco C. 2007. Brain malformation in syndromic craniosynostoses, a primary disorder of white matter: a review. Childs Nerv Syst 23:1379-1388.
Renier N, Schonewille M, Giraudet F, Badura A, Tessier-Lavigne M, Avan P, De Zeeuw CI, Chedotal A. 2010. Genetic dissection of the function of hindbrain axonal commissures. PLoS Biol 8:e1000325.
Roessmann U, Hori A. 1985. Agyria (lissencephaly) with anomalous pyramidal crossing. Case report and review of literature. J Neurol Sci 69:357-364.
Rolf B, Bastmeyer M, Schachner M, Bartsch U. 2002. Pathfinding errors of corticospinal axons in neural cell adhesion molecule-deficient mice. J Neurosci 22:8357-8362.
Romani M, Micalizzi A, Valente EM. 2013. Joubert syndrome: congenital cerebellar ataxia with the molar tooth. Lancet Neurol 12:894-905.
Rosenzweig ES, Brock JH, Culbertson MD, Lu P, Moseanko R, Edgerton VR, Havton LA, Tuszynski MH. 2009. Extensive spinal decussation and bilateral termination of cervical corticospinal projections in rhesus monkeys. J Comp Neurol 513:151-163.
Rouiller EM, Liang FY, Moret V, Wiesendanger M. 1991. Trajectory of redirected corticospinal axons after unilateral lesion of the sensorimotor cortex in neonatal rat; a phaseolus vulgaris-leucoagglutinin (PHA-L) tracing study. Exp Neurol 114:53-65.
Royal SA, Tubbs RS, D'Antonio MG, Rauzzino MJ, Oakes WJ. 2002. Investigations into the association between cervicomedullary neuroschisis and mirror movements in patients with Klippel-Feil syndrome. AJNR Am J Neuroradiol 23:724-729.
Ruediger T, Zimmer G, Barchmann S, Castellani V, Bagnard D, Bolz J. 2013. Integration of opposing semaphorin guidance cues in cortical axons. Cereb Cortex 23:604-614.
Runker AE, Little GE, Suto F, Fujisawa H, Mitchell KJ. 2008. Semaphorin-6A controls guidance of corticospinal tract axons at multiple choice points. Neural Dev 3:34.

Russell JR, Demyer W. 1961. The quantitative corticoid origin of pyramidal axons of Macaca rhesus. With some remarks on the slow rate of axolysis. Neurology 11:96-108.
Sabatier C, Plump AS, Le M, Brose K, Tamada A, Murakami F, Lee EY, Tessier-Lavigne M. 2004. The divergent Robo family protein rig-1/Robo3 is a negative regulator of slit responsiveness required for midline crossing by commissural axons. Cell 117:157-169.
Sacher GA, Staffeldt EF. 1974. Relation of gestation time to brain weight for placental mammals: implications for the theory of vertebrate growth. American Naturalist:593-615.
Sag E, Gocmen R, Yildiz FG, Ozturk Z, Temucin C, Teksam O, Utine E. 2016. Congenital Mirror Movements in Gorlin Syndrome: A Case Report With DTI and Functional MRI Features. Pediatrics 137:1-5.
Schieber MH. 2007. Chapter 2 Comparative anatomy and physiology of the corticospinal system. Handb Clin Neurol 82:15-37.
Schreyer DJ, Jones EG. 1982. Growth and target finding by axons of the corticospinal tract in prenatal and postnatal rats. Neuroscience 7:1837-1853.
Seo JP, Jang SH. 2013. Different characteristics of the corticospinal tract according to the cerebral origin: DTI study. AJNR Am J Neuroradiol 34:1359-1363.
Serradj N, Paixao S, Sobocki T, Feinberg M, Klein R, Kullander K, Martin JH. 2014. EphA4-mediated ipsilateral corticospinal tract misprojections are necessary for bilateral voluntary movements but not bilateral stereotypic locomotion. J Neurosci 34:5211-5221.
Shim S, Kwan KY, Li M, Lefebvre V, Sestan N. 2012. Cis-regulatory control of corticospinal system development and evolution. Nature 486:74-79.
Sicotte NL, Salamon G, Shattuck DW, Hageman N, Rub U, Salamon N, Drain AE, Demer JL, Engle EC, Alger JR, Baloh RW, Deller T, Jen JC. 2006. Diffusion tensor MRI shows abnormal brainstem crossing fibers associated with ROBO3 mutations. Neurology 67:519-521.
Srivatsa S, Parthasarathy S, Britanova O, Bormuth I, Donahoo AL, Ackerman SL, Richards LJ, Tarabykin V. 2014. Unc5C and DCC act downstream of Ctip2 and Satb2 and contribute to corpus callosum formation. Nat Commun 5:3708.
Srivatsa S, Parthasarathy S, Molnar Z, Tarabykin V. 2015. Sip1 downstream Effector ninein controls neocortical axonal growth, ipsilateral branching, and microtubule growth and stability. Neuron 85:998-1012.
Srour M, Riviere JB, Pham JM, Dube MP, Girard S, Morin S, Dion PA, Asselin G, Rochefort D, Hince P, Diab S, Sharafaddinzadeh N, Chouinard S, Theoret H, Charron F, Rouleau GA. 2010. Mutations in DCC cause congenital mirror movements. Science 328:592.
Stanfield BB, O'Leary DD. 1985. The transient corticospinal projection from the occipital cortex during the postnatal development of the rat. J Comp Neurol 238:236-248.
Stanfield BB, O'Leary DD, Fricks C. 1982. Selective collateral elimination in early postnatal development restricts cortical distribution of rat pyramidal tract neurones. Nature 298:371-373.
Tamada A, Kumada T, Zhu Y, Matsumoto T, Hatanaka Y, Muguruma K, Chen Z, Tanabe Y, Torigoe M, Yamauchi K, Oyama H, Nishida K, Murakami F. 2008. Crucial roles of Robo proteins in midline crossing of cerebellofugal axons and lack of their up-regulation after midline crossing. Neural Dev 3:29.
Tassabehji M, Fang ZM, Hilton EN, McGaughran J, Zhao Z, de Bock CE, Howard E, Malass M, Donnai D, Diwan A, Manson FD, Murrell D, Clarke RA. 2008. Mutations in

GDF6 are associated with vertebral segmentation defects in Klippel-Feil syndrome. Hum Mutat 29:1017-1027.
ten Donkelaar HJ, Hoevenaars F, Wesseling P. 2000. A case of Joubert's syndrome with extensive cerebral malformations. Clin Neuropathol 19:85-93.
ten Donkelaar HJ, Lammens M, Wesseling P, Hori A, Keyser A, Rotteveel J. 2004. Development and malformations of the human pyramidal tract. J Neurol 251:1429-1442.
ten Donkelaar HJ, Wesseling P, Semmekrot BA, Liem KD, Tuerlings J, Cruysberg JR, de Wit PE. 1999. Severe, non X-linked congenital microcephaly with absence of the pyramidal tracts in two siblings. Acta Neuropathol 98:203-211.
Tennant KA, Adkins DL, Donlan NA, Asay AL, Thomas N, Kleim JA, Jones TA. 2011. The organization of the forelimb representation of the C57BL/6 mouse motor cortex as defined by intracortical microstimulation and cytoarchitecture. Cereb Cortex 21:865-876.
Tissir F, Bar I, Jossin Y, De Backer O, Goffinet AM. 2005. Protocadherin Celsr3 is crucial in axonal tract development. Nat Neurosci 8:451-457.
Tomassy GS, De Leonibus E, Jabaudon D, Lodato S, Alfano C, Mele A, Macklis JD, Studer M. 2010. Area-specific temporal control of corticospinal motor neuron differentiation by COUP-TFI. Proc Natl Acad Sci U S A 107:3576-3581.
Toyoshima K, Sakai H. 1982. Exact cortical extent of the origin of the corticospinal tract (CST) and the quantitative contribution to the CST in different cytoarchitectonic areas. A study with horseradish peroxidase in the monkey. J Hirnforsch 23:257-269.
Uematsu J, Ono K, Yamano T, Shimada M. 1996. Development of corticospinal tract fibers and their plasticity I: quantitative analysis of the developing corticospinal tract in mice. Brain Dev 18:29-34.
Uematsu S, Lesser R, Fisher RS, Gordon B, Hara K, Krauss GL, Vining EP, Webber RW. 1992. Motor and sensory cortex in humans: topography studied with chronic subdural stimulation. Neurosurgery 31:59-71; discussion 71-52.
Verhaart W. 1967. The non-crossing of the pyramidal tract in procavia capensis (storr) and other instances of absence of the pyramidal crossing. Journal of Comparative Neurology 131:387-392.
Verhaart WJ. 1963. Pyramidal Tract in the Cord of the Elephant. J Comp Neurol 121:45-49.
Verhaart WJ, Kramer W. 1952. The uncrossed pyramidal tract. Acta Psychiatr Neurol Scand 27:181-200.
Verzijl HT, van der Zwaag B, Cruysberg JR, Padberg GW. 2003. Mobius syndrome redefined: a syndrome of rhombencephalic maldevelopment. Neurology 61:327-333.
Verzijl HT, van der Zwaag B, Lammens M, ten Donkelaar HJ, Padberg GW. 2005. The neuropathology of hereditary congenital facial palsy vs Mobius syndrome. Neurology 64:649-653.
Vulliemoz S, Raineteau O, Jabaudon D. 2005. Reaching beyond the midline: why are human brains cross wired? Lancet Neurol 4:87-99.
Wallis D, Muenke M. 2000. Mutations in holoprosencephaly. Hum Mutat 16:99-108.
Wang Y, Thekdi N, Smallwood PM, Macke JP, Nathans J. 2002. Frizzled-3 is required for the development of major fiber tracts in the rostral CNS. J Neurosci 22:8563-8573.
Webb BD, Frempong T, Naidich TP, Gaspar H, Jabs EW, Rucker JC. 2014. Mirror movements identified in patients with moebius syndrome. Tremor Other Hyperkinet Mov (N Y) 4:256.
Xing L, Larsen RS, Bjorklund GR, Li X, Wu Y, Philpot BD, Snider WD, Newbern JM. 2016. Layer specific and general requirements for ERK/MAPK signaling in the developing neocortex. Elife 5.

Yachnis AT, Rorke LB. 1999. Neuropathology of Joubert syndrome. J Child Neurol 14:655-659; discussion 669-672.

Yang HW, Lemon RN. 2003. An electron microscopic examination of the corticospinal projection to the cervical spinal cord in the rat: lack of evidence for cortico-motoneuronal synapses. Exp Brain Res 149:458-469.

Yokoyama N, Romero MI, Cowan CA, Galvan P, Helmbacher F, Charnay P, Parada LF, Henkemeyer M. 2001. Forward signaling mediated by ephrin-B3 prevents contralateral corticospinal axons from recrossing the spinal cord midline. Neuron 29:85-97.

Zhou L, Bar I, Achouri Y, Campbell K, De Backer O, Hebert JM, Jones K, Kessaris N, de Rouvroit CL, O'Leary D, Richardson WD, Goffinet AM, Tissir F. 2008. Early forebrain wiring: genetic dissection using conditional Celsr3 mutant mice. Science 320:946-949.

Zilles K, Schlaug G, Matelli M, Luppino G, Schleicher A, Qu M, Dabringhaus A, Seitz R, Roland PE. 1995. Mapping of human and macaque sensorimotor areas by integrating architectonic, transmitter receptor, MRI and PET data. J Anat 187 (Pt 3):515-537.

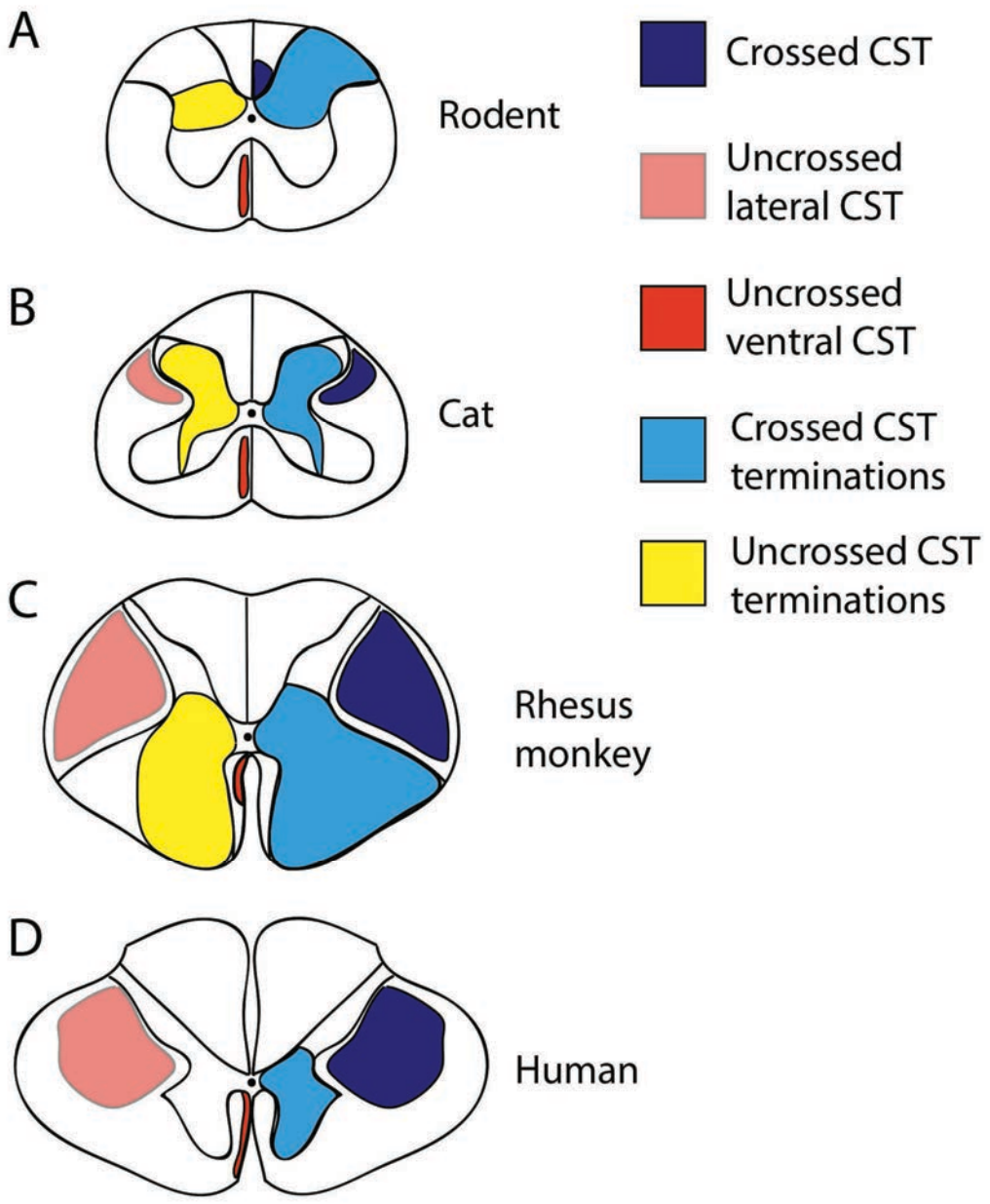

Figure 1. Evolution of CST projections to the spinal cord in mammals. The location of the CST and the terminations of CST projections in the spinal cord have gradually switched from dorsal to ventral through evolution. (A-D) Representation of the spinal cord at the cervical level in rodents, cats, monkeys and humans. In rodents (A), the crossed CST (dark blue) is located in the most ventral part of the dorsal funiculus, and the uncrossed CST (red) runs in the ventral funiculus. In cats (B), non-human primates (C) and humans (D), the crossed CST (dark blue) is located in the dorso-lateral funiculus of the spinal cord, contralateral to the hemisphere of origin, while the uncrossed CST is found in ventral (red) and dorso-lateral (pale red) funiculi of the ipsilateral spinal cord. In cats and rodents, the crossed CST terminations are mainly located in the intermediate and dorsal horns of the spinal cord (light blue), and the terminations of the uncrossed CST exhibit a similar pattern (yellow; A, B). By contrast, in non-human primates and humans, most crossed CST terminations are found in the intermediate and ventral horns (light blue), while uncrossed CST terminations are absent from the lateral motor nuclei in monkeys (yellow; C, D). CST = corticospinal tract.

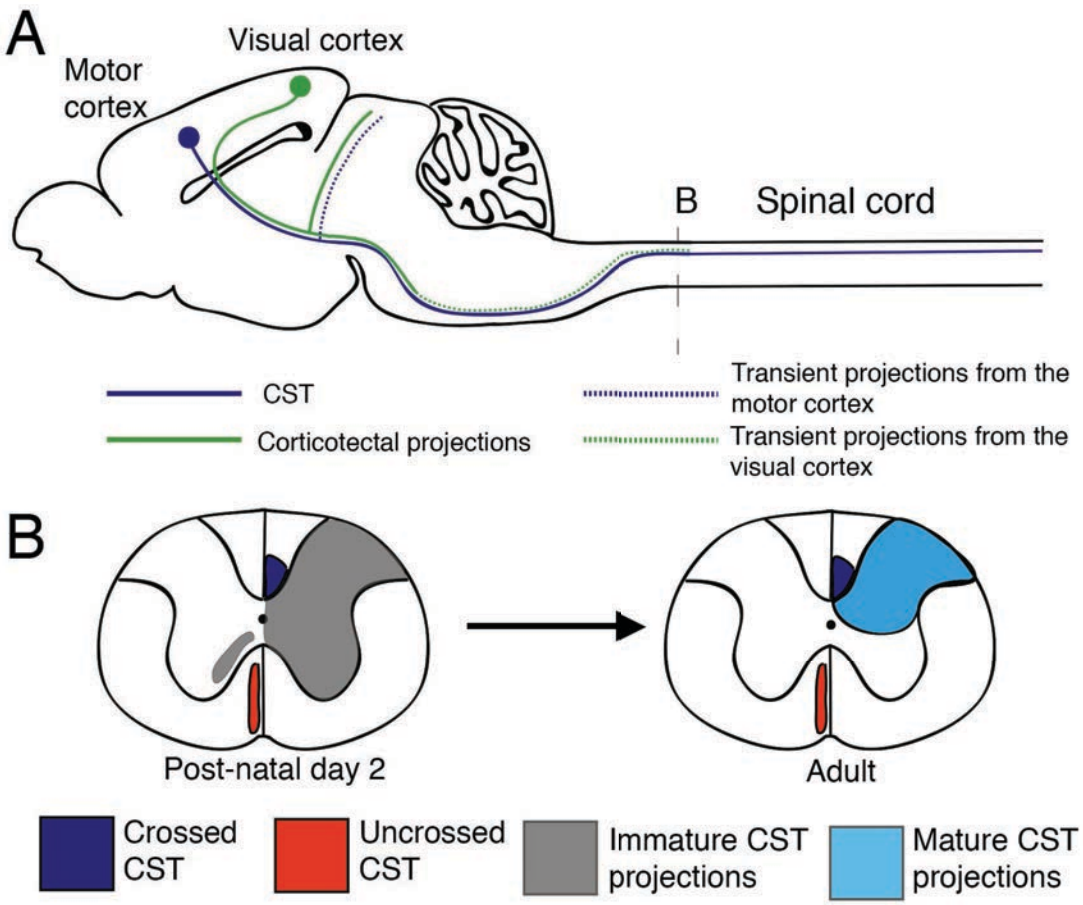

Figure 2. Post-natal maturation of the rodent corticospinal tract. (A) In newborn rodents, the cortical territory from which the CST originates is larger than in adulthood. In particular, neurons located in the visual cortex initially project to the spinal cord (green dashed line), and neurons located in the motor cortex extend collaterals into the optic tectum (dashed blue line). These aberrant projections are later eliminated. (B) In rodents, the CST initially innervates the ventral, intermediate and dorsal spinal cord, as well as the ipsilateral spinal cord (gray). This pattern is refined during post-natal development, resulting in restriction of the projections to the intermediate and dorsal horns of the contralateral spinal cord (blue). CST = corticospinal tract.

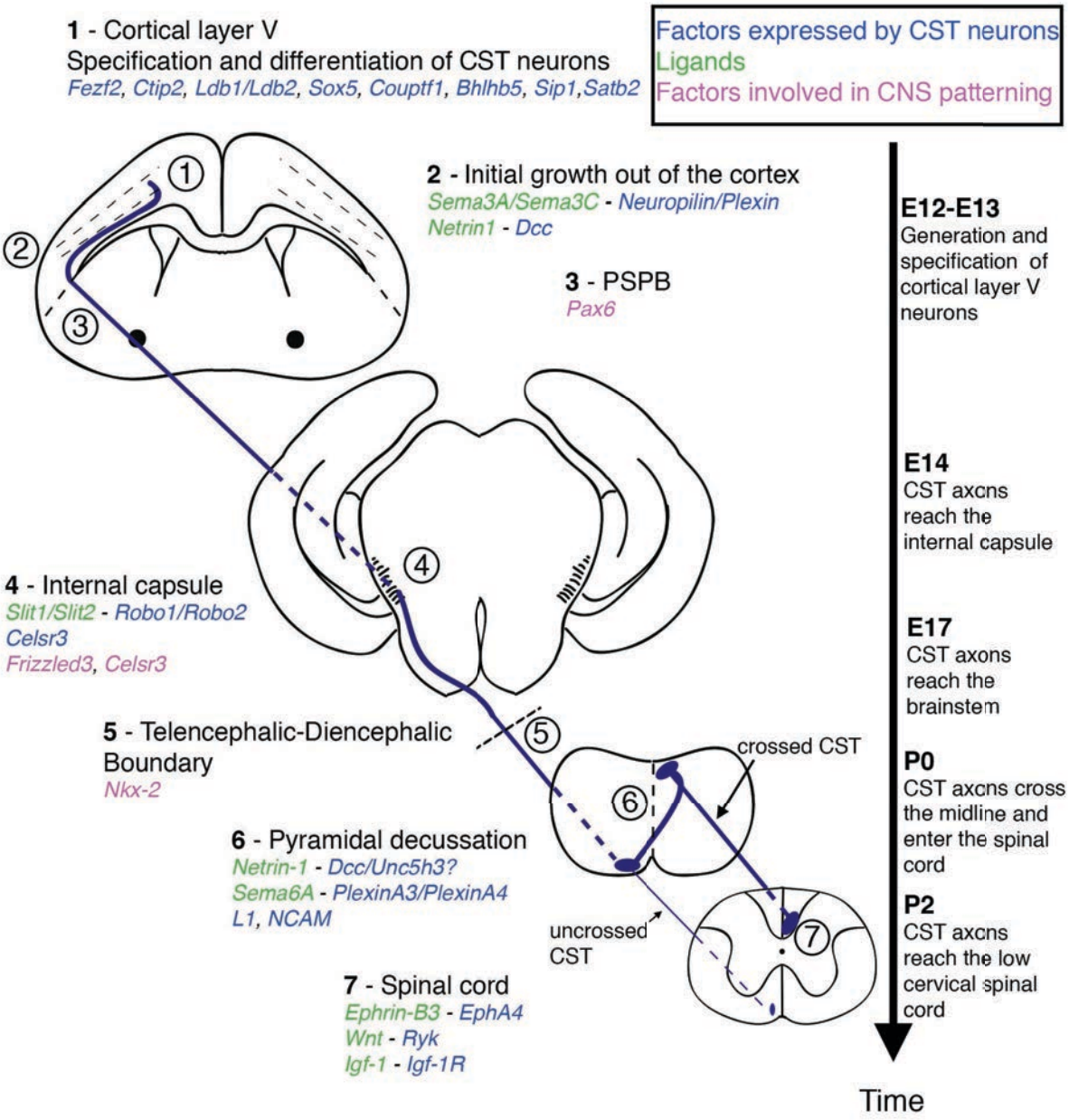

Figure 3. Mechanisms and time course of mouse CST development. The left side of the figure shows the trajectory of the mouse CST from the cortex to the spinal cord. The genes involved in CST development are indicated at the corresponding level. The right side of the figure indicates the time course of CST development. CNS = central nervous system; CST = corticospinal tract; PSPB = pallial/subpallial boundary.

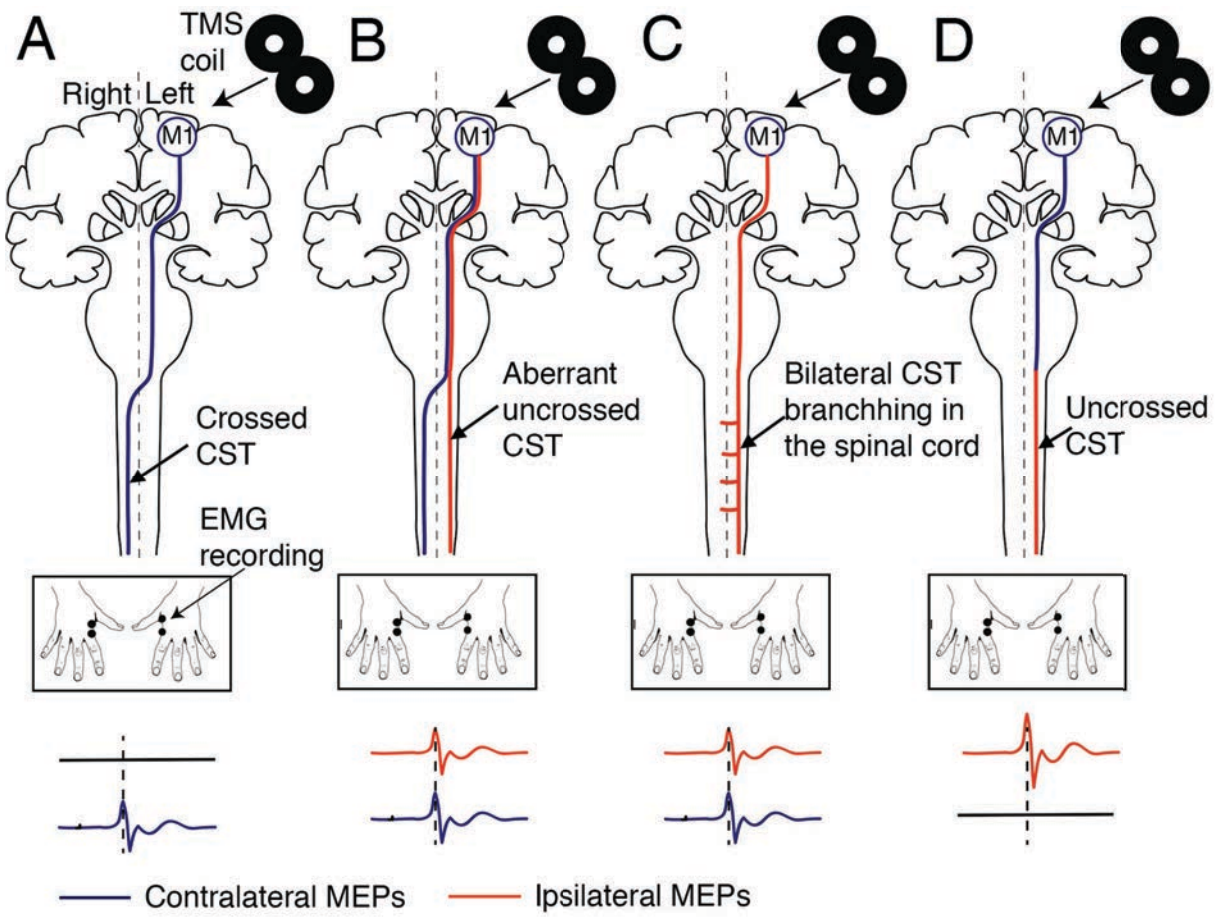

Figure 4. CST anatomy and lateralization of motor control. Schematic representation of transcranial magnetic stimulation (TMS) experiments. **(A**) In healthy humans, unilateral TMS of the hand area of one motor cortex elicits only contralateral MEPs (blue line), reflecting transmission of the motor command via the crossed CST (dark blue). In patients with mirror movements, abnormal decussation of the CST **(B)** or, possibly, abnormal branching of the uncrossed CST in the spinal cord **(C)**, leads to bilateral transmission of the motor command to the spinal cord, resulting in both contralateral and ipsilateral MEPs (red line). **(D)** Mirror movements have not been described in patients with horizontal gaze palsy with progressive scoliosis (HGPPS), in whom the absence of a pyramidal decussation results in each cortex projecting on the ipsilateral spinal cord. This suggests that mirror movements are related to the presence of bilateral spinal cord projections arising from a single primary motor cortex, rather than to abnormal decussation of the CST *per se*.

Dark blue: crossed corticospinal tract; Red: uncrossed corticospinal tract. CST = corticospinal tract; EMG = electromyographic M1 = primary motor cortex; MEP = motor evoked potential; TMS = transcranial magnetic stimulation.

C. Développement comparé du système nerveux central chez différents mammifères

Chez le rongeur, le chat de l'humain, les FCS et le CC subissent de profondes modifications au cours du développement post-natal, avant que ces systèmes n'atteignent leur état définitif. Cette maturation implique notamment l'élimination de projections exubérantes par des mécanismes dépendants de l'activité évoquée par l'expérience sensorielle, mais aussi de l'activité spontanée des neurones (Ivy et al., 1979; Innocenti and Caminiti, 1980; Innocenti, 1981; Ivy and Killackey, 1981; Olavarria and Van Sluyters, 1985; Olavarria et al., 1987; Koralek and Killackey, 1990; Alisky et al., 1992; Joosten et al., 1992; Elberger, 1994a; b; Muller et al., 1997; Eyre et al., 2000; Li and Martin, 2000; Ding and Elberger, 2001; Eyre et al., 2001; Li and Martin, 2002; Mizuno et al., 2007; Suarez et al., 2014a). En revanche, s'il existe bien une phase d'élimination des axones corticospinaux et calleux au cours du développement post-natal chez le singe (LaMantia and Rakic, 1990a; Galea and Darian-Smith, 1995), la spécificité et la topographie des connexions sont établies dès la naissance chez cette espèce (Killackey and Chalupa, 1986; Chalupa and Killackey, 1989) (Armand et al., 1997).

Il existe donc une différence fondamentale entre ces espèces concernant la période à laquelle a lieu la maturation de l'organisation des projections du FCS et du CC. Tandis que ce processus se déroule en grand partie après la naissance chez le rongeur et le chat et l'humain, l'organisation mature de ces faisceaux est présente à la naissance chez le singe, même si des modifications quantitatives auront lieu par la suite. Cette observation est à mettre en lien avec le mode de reproduction de ces différentes espèces. Les rongeurs et les chats sont qualifiés d'espèces nidicoles. Chaque portée est constituée d'un grand nombre de nouveaux nés dont l'autonomie motrice et le développement neurologique sont réduits à la naissance. Au contraire, les primates non-humains sont qualifiés d'espèce nidifuge : la femelle donne

naissance à un nombre réduit de petits, et si leur capacités motrices sont réduites à la naissance, le développement de leur système nerveux est très avancé. En particulier, les singes rhésus nouveaux nés présentent un cerveau presque entièrement myélinisé, dont la taille représente déjà 65% de ses proportions adultes (Sacher and Staffeldt, 1974; Gibson, 1991). Par plusieurs aspects, l'humain semble donc appartenir au groupe des espèces nidifuges, notamment par sa stratégie de reproduction. En revanche, d'un point de vue de la maturité du système nerveux à la naissance, il représente un cas intermédiaire : en effet, par comparaison aux singes, la myélinisation et le développement (en termes de taille) du cerveau humain sont réduits chez le nouveau né (Sacher and Staffeldt, 1974; Gibson, 1991). Les observations concernant la maturation du FCS chez l'humain et le singe vont dans ce sens. En effet, tandis que la topographie des projections corticospinales évolue durant les premières années de développement post-natal chez l'humain, notamment du fait d'une élimination de projections ipsilatérales exubérantes (Eyre et al., 2001), chez le singe nouveau né, la topographie des connexions corticospinales est déjà mature (Armand et al., 1994; Armand et al., 1997).

III. Latéralisation du contrôle moteur au cours de la préparation du mouvement

A. MM et préparation motrice

Nous avons vu précédemment qu'il existe deux mécanismes impliqués dans la physiopathologie des MM : (i) une anomalie développementale du FCS aboutissant à la mise en place de projections bilatérales de chacun des hémisphères sur la moelle ; (ii) des défauts d'interactions inter-hémisphériques, responsables d'une activation bilatérale anormale des deux cortex moteurs lors de l'exécution d'un mouvement unimanuel (Gallea et al., 2011; Welniarz et al., 2015).

Plusieurs éléments permettent de supposer que ces défauts de communication inter-hémisphérique pourraient être présents avant même le début du mouvement, durant la phase de préparation motrice. Premièrement, deux études utilisant des enregistrements électro-encéphalographiques (EEG) ont démontré l'existence d'activations bilatérales anormales d'aires motrices corticales lors de la préparation de mouvements unimanuels chez des patients présentant des MM (Figure 13A) (Shibasaki and Nagae, 1984; Cohen et al., 1991). Deuxièmement, des études menées dans le laboratoire ont démontré une activation et une connectivité fonctionnelle anormale de l'AMS lors de phases d'exécution motrice chez des patients atteints de MMC (Figure 13B, 13C) (Gallea et al., 2013). L'AMS est connue pour son rôle dans la coordination bimanuelle (Brinkman, 1984; Chan and Ross, 1988; Serrien et al., 2002; Steyvers et al., 2003; Ullen et al., 2003; Grefkes et al., 2008; Duque et al., 2010a) ainsi que pour son implication dans la préparation motrice (Brinkman and Porter, 1983; Deiber et al., 1996; Richter et al., 1997; Lee et al., 1999; Cunnington et al., 2002; Shibasaki and Hallett, 2006)

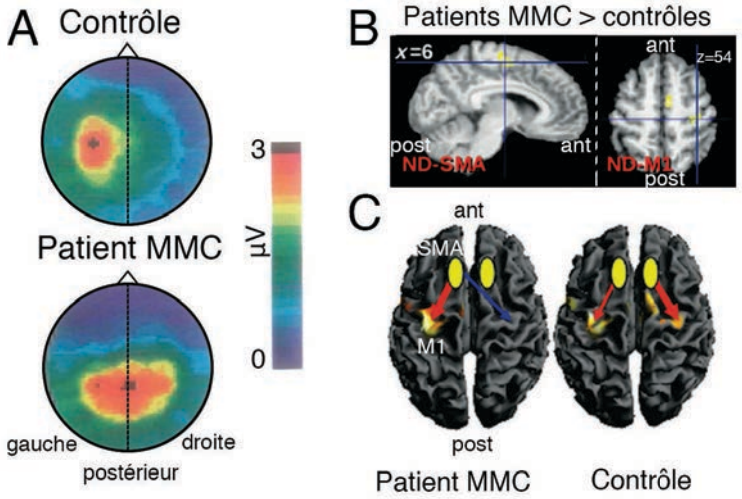

Figure 13. Préparation motrice anormale chez les patients MMC lors de mouvements unimanuels de la main droite (dominante). (A) Enregistrement EEG de l'activité électrique corticale précédant l'exécution d'un mouvement unimanuel de la main droite chez un sujet sain et chez un patient atteint de MMC. Chez le sujet sain, l'activité électrique corticale est latéralisée : seul l'hémisphère contralatéral au mouvement à venir (gauche) est activé. Au contraire, chez le patient, l'activité corticale liée à la préparation du mouvement est distribuée de façon bilatérale. Adapté de (Cohen et al, 1991). (B, C) Activation et connectivité fonctionnelle anormale de l'aire motrice supplémentaire (AMS) lors de l'exécution de mouvements unimanuels de la main droite. (B) Chez les patients, l'AMS gauche est anormalement activée lors de mouvements de la main droite. (C) Cette activation est associée à une augmentation anormale de la connectivité de la SMA gauche avec le M1 gauche. Adapté de (Gallea et al, 2013).

(pour revue, voir (Cunnington et al., 2005; Nachev et al., 2008; Gallea et al., 2011)). Cette activation anormale de l'AMS observée chez les patients atteints de MMC pourrait donc être le signe d'un dysfonctionnement de la préparation motrice.

Dans un premier temps, nous décrirons les mécanismes intervenant dans la latéralisation de l'activité corticale lors de l'exécution de mouvements unimanuels. Nous nous intéresserons ensuite aux mécanismes, moins connus, de la préparation de mouvements latéralisés, avant d'étudier plus en détail le cas d'une région prémotrice : l'AMS.

B. Exécution de mouvements latéralisés

1) L'exécution d'un mouvement unimanuel est associée à l'activation latéralisée du système moteur

Lors de l'exécution d'un mouvement unimanuel, on observe l'activation de nombreuses régions de l'hémisphère contralatéral au mouvement (aires motrices/prémotrices corticales, ganglions de la base, thalamus), ainsi que du cervelet ipsilatéral. En particulier, l'activation des aires motrices et prémotrices corticales contralatérales au mouvement reflète l'anatomie croisée du système corticospinal. Cette activation asymétrique, latéralisée, des aires motrices corticales est fondamentale : en restreignant l'activité du cerveau à un hémisphère, la commande motrice sera transmise à la partie opposée du corps uniquement, via le FCS.

Des méthodes d'imagerie telles que la tomographie par émission de positrons (TEP) et l'imagerie par résonnance magnétique fonctionnelle (IRMf), ont décrit une activation du cortex moteur primaire contralatéral au mouvement ($M1_c$) et une désactivation du M1 ipsilateral ($M1_i$) lors de l'exécution de mouvements unimanuels simples (Catalan et al., 1998; Nirkko et al., 2001; Hamzei et al., 2002; Newton et al., 2005; Buetefisch et al., 2014). La

SMT a aussi été utilisée pour mettre en évidence des asymétries d'activité corticale lors de la réalisation de mouvements latéralisés. La stimulation par SMT de l'aire de la main au niveau de M1 engendre des potentiels évoqués moteurs (PEM) dans la main opposée à l'hémisphère stimulé, dont l'amplitude représente l'état d'excitabilité de la voie corticospinale. Pour ce type de protocole, on parle de SMT simple-pulse (Figure 14). Pendant l'exécution d'un mouvement unimanuel, on observe une augmentation de l'excitabilité du $M1_c$ par rapport au repos. Cette excitabilité est modulée par différents paramètres : l'intensité de la force déployée, la complexité du mouvement, l'utilisation de la main dominante ou non-dominante (Flament et al., 1993; Brouwer et al., 2001; Hasegawa et al., 2001; Newton et al., 2005). Au contraire, l'excitabilité du $M1_i$ est diminuée lors de l'exécution de mouvements unimanuels (Liepert et al., 2001; Sohn et al., 2003).

De nombreuses études ont par ailleurs décrit une implication du $M1_i$ dans l'exécution de mouvements unimanuels, ce qui peut sembler, à première vue, contradictoire avec ce qui vient d'être énoncé. Cette implication peut se traduire de différentes façons : par une activation du $M1_i$ mesurée en IRMf (Cramer et al., 1999; Koeneke et al., 2004; Newton et al., 2005; Verstynen et al., 2005; Horenstein et al., 2009; Diedrichsen et al., 2013; Buetefisch et al., 2014; Tzourio-Mazoyer et al., 2015) ; par une augmentation de l'excitabilité du $M1_i$ mesurée par SMT (Muellbacher et al., 2000; Ziemann and Hallett, 2001; Liang et al., 2008; Perez and Cohen, 2008) ; par une diminution des performances comportementales suite à l'inhibition transitoire du $M1_i$ (Chen et al., 1997a; Chen et al., 1997b). Le recrutement du $M1_i$ lors de l'exécution de mouvements unimanuels dépend de nombreux paramètres de la tâche effectuée, tels que sa difficulté, la précision qu'elle requiert, l'utilisation de la main dominante ou non-dominante. Les mécanismes responsables de cette activité du $M1_i$ lors de l'exécution de mouvements unimanuels, ainsi que son rôle fonctionnel, ne sont pas bien connus. L'augmentation de la résolution spatiale des méthodes d'imagerie a cependant permis

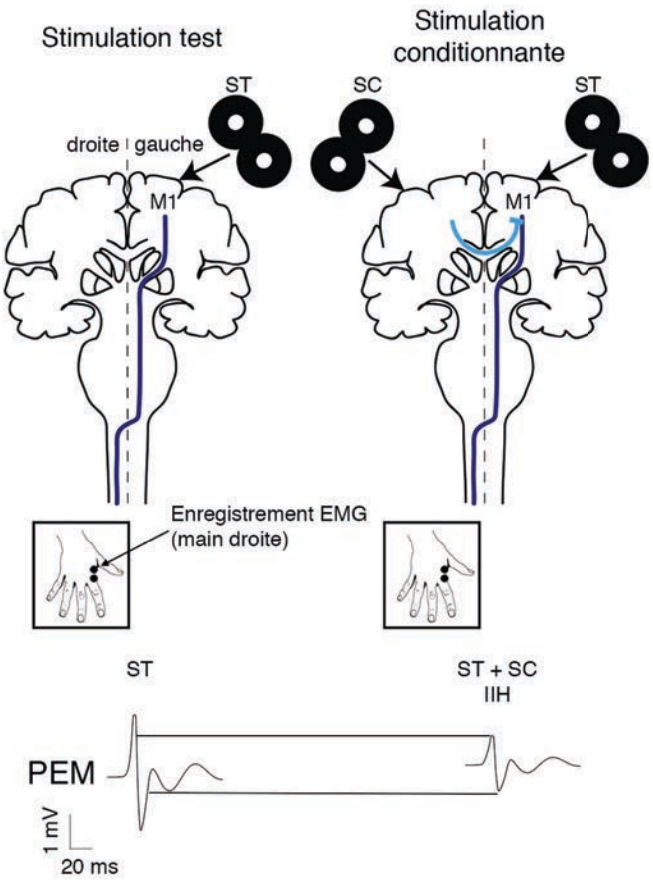

Figure 14. Le principe de la stimulation double-pulse : l'inhibition inter-hémisphérique. Une stimulation test (ST) délivrée seule au niveau de la représentation de la main du M1 de l'hémisphère gauche engendre un potentiel évoqué moteur (PEM) au niveau de la main droite. L'amplitude du PEM représente l'excitabilité du M1 stimulé. Lorsque la ST est précédée de quelques millisecondes par une stimulation dite « conditionnante » (SC) délivrée au niveau du M1 de l'hémisphère opposé (droit), l'amplitude du PEM engendré par la ST est diminuée. Cette modulation de l'amplitude du PEM traduit une inhibition du M1 gauche par le M1 droit : on parle d'inhibition inter-hémisphérique (IIH). Cette IIH est due à des fibres transcalleuses glutamatergiques (recrutée par la SC) activant des interneurones inhibiteurs au niveau de l'hémisphère gauche, diminuant ainsi son excitabilité.

d'apporter de nouveaux éléments de réponse. Plusieurs études ont démontré qu'il existe différentes zones présentant des profils d'activité distincts au sein du $M1_i$ lors de la réalisation d'un mouvement unimanuel complexe. Tandis qu'une activation est décelée au niveau de régions antérieures du $M1_i$, à la frontière avec le cortex prémoteur (PM), la région de l'aire de la main (qui est activée lors de la réalisation d'un mouvement contralatéral) est désactivée (Cramer et al., 1999; Verstynen et al., 2005; Horenstein et al., 2009). Une étude récente, utilisant une séquence motrice simple, s'est intéressée aux modulations de l'activité du $M1_i$ lors de mouvements unimanuels ou bimanuels (Diedrichsen et al., 2013). Lors de la réalisation de mouvements unimanuels, la région du $M1_i$ dont l'activité est modulée correspond à l'aire de la main, et se superpose à la région qui est activée lors d'un mouvement de la main contralatérale. Au contraire, lors de la réalisation de mouvements bimanuels, les régions recrutées sont situées en avant (à la frontière M1/PM) et en arrière (au niveau de S1) du $M1_i$, et semblent recouper partiellement les régions activées lors de la réalisation de mouvements unimanuels complexes. Les deux types d'activations observés au niveau du $M1_i$ lors de la réalisation d'un mouvement unimanuel représenteraient donc deux processus distincts. Le recrutement de régions du $M1_i$ situées en dehors de l'aire de la main (notamment au niveau de la frontière M1/PM) lors de l'exécution de mouvements unimanuels complexes serait le reflet de l'existence d'un réseau moteur bilatéral, qui serait aussi recruté lors de l'exécution de mouvements bimanuels : ces régions ne seraient donc pas recrutées de façon latéralisée lors de l'exécution de mouvements unimanuels. Au contraire, l'activité de la région de la main est fortement latéralisée, et serait liée à celle de la région homologue dans le cortex opposé : il s'agirait de la résultante d'une transmission passive d'activité depuis le cortex opposé ($M1_c$), et de sa modulation. A partir de maintenant, nous nous intéresserons uniquement à ce dernier processus, car c'est celui-ci qui est impliqué dans la physiopathologie des mouvements en miroir.

2) *Interactions inter-hémisphériques et latéralisation de l'activité corticale lors de la réalisation d'un mouvement unimanuel.*

L'exécution d'un mouvement unimanuel requiert des interactions complexes entre les aires motrices et prémotrices corticales des deux hémisphères, afin d'assurer l'activation latéralisée des régions responsables du mouvement (Beaule et al., 2012).

Les interactions entre différentes aires corticales peuvent être testées par le biais de la SMT dite double-site (ou double-pulse : voir Figure 14). Nous avons dit précédemment que l'amplitude des PEMs résultant de la stimulation du cortex moteur était une mesure indirecte de l'excitabilité de la voie corticospinale. Lorsque cette stimulation du cortex moteur (appelée stimulation test ou ST) est précédée par une stimulation dite « conditionnante » (SC) portée sur la même région ou une autre région corticale, la variation de l'amplitude du PEM (par rapport à la situation où la ST est délivrée seule) nous renseigne sur une modification de l'état d'excitabilité de la voie corticospinale (Chen, 2004; Reis et al., 2008). Une augmentation de l'amplitude du PEM après la SC traduira une facilitation, et on parlera d'inhibition dans le cas inverse.

Grâce à la SMT, on peut donc étudier les interactions entre différentes régions corticales, notamment entre les deux M1. Chaque M1 exerce une inhibition sur son homologue situé dans l'hémisphère opposé : on parle d'inhibition inter-hémisphérique (IIH, voir Figure 14) (Ferbert et al., 1992; Chen, 2004; Reis et al., 2008). Au repos, cette IIH est symétrique, c'est-à-dire qu'elle n'est pas différente de gauche à droite ou de droite à gauche, que le sujet soit droitier ou gaucher (Figure 15A) (Salerno and Georgesco, 1996; De Gennaro et al., 2004; Davidson and Tremblay, 2013). Au contraire, l'IIH est fortement asymétrique au cours de la réalisation d'un mouvement unimanuel (Figure 15B). L'IIH dirigée vers le $M1_i$ (IIH_i) est maintenue lors de l'exécution d'un mouvement unimanuel, tandis que l'IIH ciblant

le $M1_c$ (IIH_c) est levée et se transforme en facilitation (Murase et al., 2004; Duque et al., 2007; Perez and Cohen, 2008; Giovannelli et al., 2009; Kroeger et al., 2010; Hinder et al., 2012). Des études de connectivité fonctionnelle réalisées en IRMf vont dans le même sens : elles ont permis de montrer que de nombreuses connexions ciblant le $M1_c$ deviennent facilitatrices, tandis que celles dirigées vers le $M1_i$ deviennent inhibitrices, lors de la réalisation de mouvements unimanuels (Figure 15B) (Grefkes et al., 2008). Il existe de plus une corrélation entre l'IIH_i (mesurée par SMT) d'une part, et l'activation du $M1_i$ (mesurée en IRMf) ainsi que la quantité d'activité miroir physiologique de la main au repos d'autre part. Plus l'IIH_i est faible, plus l'activation du $M1_i$ est forte (Talelli et al., 2008; Gallea et al., 2013) et plus l'activité miroir de la main au repos est forte (Arányi and Rösler, 2002; Hubers et al., 2008). De façon cohérente, l'augmentation de l'intensité du mouvement volontaire (qui est corrélée positivement à l'activité miroir de la main au repos (Mayston et al., 1999)) est associée à une diminution de l'IIH_i (Perez and Cohen, 2008). L'ensemble de ces éléments démontre le rôle fonctionnel de l'IIH dans la modulation de l'activité des deux M1 lors de la réalisation de mouvements unimanuels.

D'autres aires corticales sont impliquées dans la modulation de l'activité du cortex moteur au cours de l'exécution de mouvements unimanuels. En effet, l'inhibition transitoire du cortex prémoteur dorsal contralatéral au mouvement (PMd_c) est responsable d'une augmentation de l'excitabilité du $M1_i$ ainsi que d'une augmentation de l'activité miroir de la main au repos (Cincotta et al., 2004; Giovannelli et al., 2006).

L'ensemble de ces données suggère que lors de la réalisation d'un mouvement unimanuel, l'activité des deux M1 est modulée de façon asymétrique par différentes aires motrices et prémotrices corticales. Ces interactions inter-hémisphériques aboutissent à une activation latéralisée des aires motrices corticales, et sont donc probablement cruciales pour la

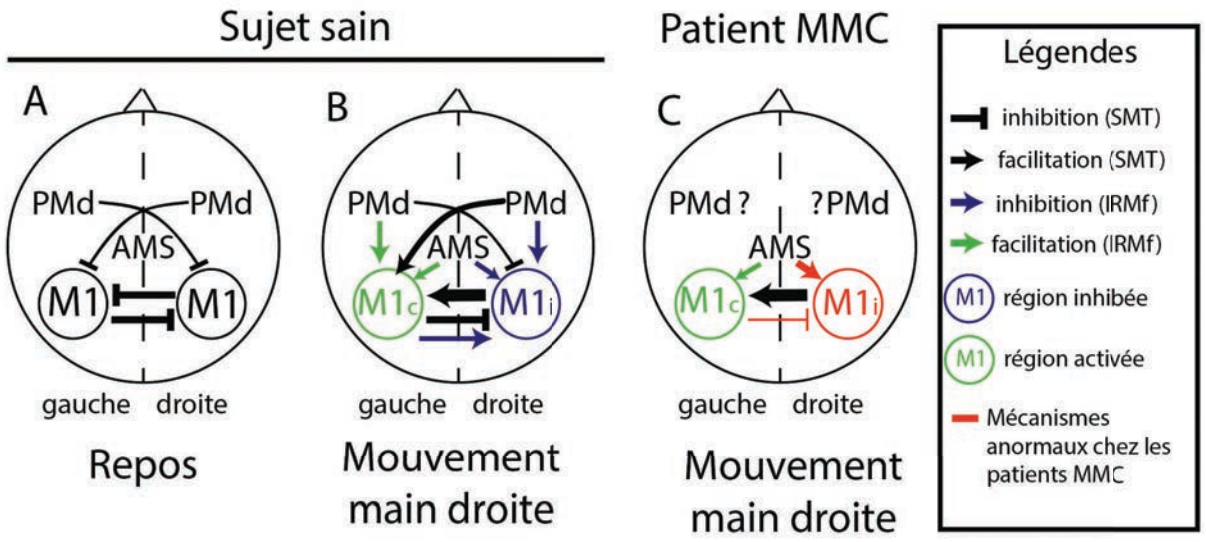

Figure 15. Modulation de l'excitabilité des cortex moteurs primaires lors de la réalisation de mouvements unimanuels chez des sujets sains et chez des patients atteints de MMC. Représentations des interactions entre différentes régions motrices et prémotrices, mesurées par SMT et en connectivité fonctionnelle (IRMf). (A) Interactions inter-hémisphériques chez un sujet sain au repos. L'inhibition entre les deux M1 et entre chacun des PMd et le M1 contralatéral est équilibrée. (B) Interactions inter-hémisphériques chez un sujet sain lors de l'exécution d'un mouvement de la main droite. Les inhibitions provenant du M1 droit (ipsilatéral au mouvement, M1i) et du PMd droit ciblant le M1 gauche (contralatéral au mouvement, M1c) sont levées, tandis que celles ciblant le M1i sont maintenues. (C) Interactions inter-hémisphériques chez un patient atteint de MMC lors de l'exécution d'un mouvement de la main droite. Deux mécanismes au moins contribuent à l'activation anormale du M1i lors d'un mouvement unimanuel: (1) l'inhibition inter-hémisphérique ciblant le M1i est anormalement faible ; (2) l'AMS active anormalement le M1i. Les interactions avec le PMd n'ont pas été étudiées chez les patients MMC. M1 : cortex moteur primaire ; AMS : aire motrice supplémentaire ; PMd : cortex prémoteur dorsal.

réalisation de mouvements strictement unimanuels sans activité miroir (Duque et al., 2007; Hubers et al., 2008; Giovannelli et al., 2009). Cette hypothèse est corroborée par plusieurs études ayant décrit une activation anormale du $M1_i$ lors de l'exécution de mouvements unimanuels chez des patients atteints de MM (Shibasaki and Nagae, 1984; Cohen et al., 1991; Mayer et al., 1995; Krams et al., 1997; Leinsinger et al., 1997; Gallea et al., 2013). De plus, une étude réalisée au sein du laboratoire a démontré que cette activation anormale du $M1_i$ est associée à une diminution de l'IIH_i et à une modification de la connectivité entre l'AMS et le $M1_i$ chez des patients *RAD51*-MMC (Figure 15C) (Gallea et al., 2013). Le corps calleux, qui est le substrat physique de ces interactions inter-hémisphériques, joue donc un rôle central dans la latéralisation motrice.

C. Préparation de mouvements latéralisés

1) La préparation d'un mouvement unimanuel est associée à une activation latéralisée du système moteur

Chez l'humain, de nombreuses études utilisant des enregistrements EEG ont permis de mettre en évidence un recrutement séquentiel et asymétrique de différentes aires motrices et prémotrices corticales lors de la préparation de mouvements unimanuels (pour revue, voir (Shibasaki and Hallett, 2006; Colebatch, 2007)). Lors de la préparation d'un mouvement, les enregistrements EEG permettent de déceler une activité électrique corticale commençant deux secondes avant le début du mouvement (on parle de potentiels de pré-mouvement), dont on peut discerner différentes composantes. La composante précoce de cette activité est nommée potentiel de préparation (*Bereitschaftspotential*). Ce potentiel qui débute 2s avant le mouvement est distribué de façon symétrique par rapport aux deux hémisphères : son amplitude est maximale à la ligne médiane, au niveau de la jonction fronto-pariétale, et ce

quel que soit le type de mouvement préparé (unimanuel droit ou gauche ou bimanuel). Il est généralement admis qu'il est généré par l'activité de l'AMS. Lors de la préparation d'un mouvement unimanuel, l'activité électrique corticale se latéralise au fur et à mesure de la phase de préparation, et 400 ms avant le début du mouvement, les composantes tardives du potentiel de pré-mouvement sont localisées au niveau du cortex précentral contralatéral au mouvement qui va être effectué (Figure 13A) (Shibasaki and Hallett, 2006). Ces observations provenant d'études EEG sont corroborées par des données d'IRMf, décrivant une activation de plusieurs aires motrices et prémotrices corticales (en particulier de M1 et de l'AMS) au sein de l'hémisphère contralatéral au mouvement préparé (Deiber et al., 1996; Richter et al., 1997; Lee et al., 1999; Zang et al., 2003).

Des études de SMT simple-pulse ont aussi permis de mettre en évidence une asymétrie d'excitabilité des deux cortex moteurs pendant la préparation de mouvements latéralisés. L'un des paradigmes le plus utilisé lors de ces études est celui des tâches à réponse différée. Un premier signal (que nous nommerons signal de consigne) indique au sujet la main avec laquelle il va devoir exécuter le mouvement. Après un délai, un deuxième signal (que nous nommerons signal d'exécution) informe le sujet qu'il doit réaliser le mouvement préparé. Ce type de paradigme permet d'étudier la modulation de l'excitabilité des M1 au cours de deux phases distinctes. Entre la présentation du signal de consigne et celle du signal d'exécution, le sujet prépare un mouvement précis, tout en restant immobile : nous désignerons cette période comme étant la phase de préparation. Entre le signal d'exécution et le début du mouvement, nous parlerons au contraire de phase de pré-mouvement. Cette dernière est encore considérée comme une phase de préparation, car elle a lieu avant le début de l'activité musculaire. Il est important de les distinguer, car les mécanismes mis en jeux au cours de ces deux phases sont différents.

Lors de la phase de pré-mouvement précédant un mouvement unimanuel, la modification de l'excitabilité de M1 débute 100 ms avant le début l'activité musculaire : on observe alors une augmentation de l'excitabilité du $M1_c$ juste avant le début du mouvement, tandis que le $M1_i$ est inhibé (Chen and Hallett, 1999; Leocani et al., 2000; Duque et al., 2005b; Koch et al., 2006; Duque et al., 2010b). Lors de la phase de préparation (avant le signal d'exécution) d'un mouvement unimanuel de la main gauche chez des sujets droitiers, de nombreuses études ont rapporté une inhibition du $M1_i$ et du $M1_c$ (Duque and Ivry, 2009; Duque et al., 2010b; Bestmann and Duque, 2015; Klein et al., 2016; Wilhelm et al., 2016). Cette inhibition précoce reflète deux processus différents (Bestmann and Duque, 2015). L'inhibition dite de « résolution de conflit » permet d'éviter un mouvement de la main n'ayant pas été sélectionnée. Au contraire, le « contrôle d'impulsion » permet d'éviter une exécution trop précoce du mouvement sélectionné (cependant, cette inhibition se joue probablement au niveau spinal). Ainsi, lors de la préparation de mouvements de la main non-dominante, il semble qu'il n'y ait pas d'asymétrie d'excitabilité corticale entre les deux M1. Une étude récente s'est intéressée à l'excitabilité de M1 lors de la préparation de mouvements unimanuels (droit ou gauche) chez des sujets droitiers (Wilhelm et al., 2016). Lors de la préparation de mouvements de la main non-dominante (gauche), l'excitabilité des deux M1 était en effet diminuée, de façon similaire à ce qui avait été décrit dans les études précédentes. Au contraire, la préparation d'un mouvement de la main droite était associée à une inhibition du $M1_i$, mais pas du $M1_c$. Il semble donc que la préparation de mouvements unimanuels de la main dominante soit associée à une asymétrie d'excitabilité des cortex moteurs.

L'ensemble de ces résultats suggère qu'il existe une asymétrie d'activité corticale entre les deux hémisphères lors de préparation de mouvements latéralisés. En particulier, les expériences d'EEG révèlent une latéralisation progressive de l'activité corticale durant la

phase de préparation, ce qui permet de supposer l'existence de mécanismes actifs nécessaires à ce processus.

2) *Interactions inter-hémisphériques et latéralisation de l'activité corticale lors de la préparation d'un mouvement unimanuel.*

Tout comme pour l'exécution de mouvements unimanuels, plusieurs éléments indiquent que les interactions inter-hémisphériques jouent un rôle central dans la latéralisation de l'activité corticale au cours de la préparation motrice. Lors de la phase de pré-mouvement précédant un mouvement unimanuel de la main dominante, l'IIH_c est modulée de façon dynamique : elle diminue progressivement, avant de se transformer en facilitation peu avant le début du mouvement, tandis que l'IIH_i reste constante tout au long de ce processus (Figure 16) (Murase et al., 2004; Duque et al., 2005a; Duque et al., 2007; Liuzzi et al., 2010).

L'activité du cortex moteur n'est pas modulée uniquement par son homologue de l'hémisphère opposé, mais aussi par d'autres régions prémotrices, telles que le PMd. Lors de la préparation d'un mouvement unimanuel, les interactions entre PMd et M1 sont modulées de façon similaire à ce qui a été décrit entre les deux M1. Le PMd ipsilateral (PMd_i) exerce une facilitation sur le $M1_c$, tandis qu'inversement, l'influence du PMd_c sur le $M1_i$ n'est pas modulée (Figure 16) (Koch et al., 2006; O'Shea et al., 2007; Kroeger et al., 2010; Liuzzi et al., 2010). Il est intéressant de remarquer que lors de la phase de pré-mouvement, la modulation des interactions inter-hémisphériques se fait selon une séquence temporelle organisée. La modulation de l'interaction PMd-M1 a lieu avant celle de l'interaction M1-M1, ce qui suggère l'existence d'une organisation hiérarchique des interactions inter-hémisphériques (Liuzzi et al., 2010). Encore une fois, le CC joue un rôle central dans ces interactions inter-hémisphériques, en tant que structure permettant la mise en relation des deux hémisphères.

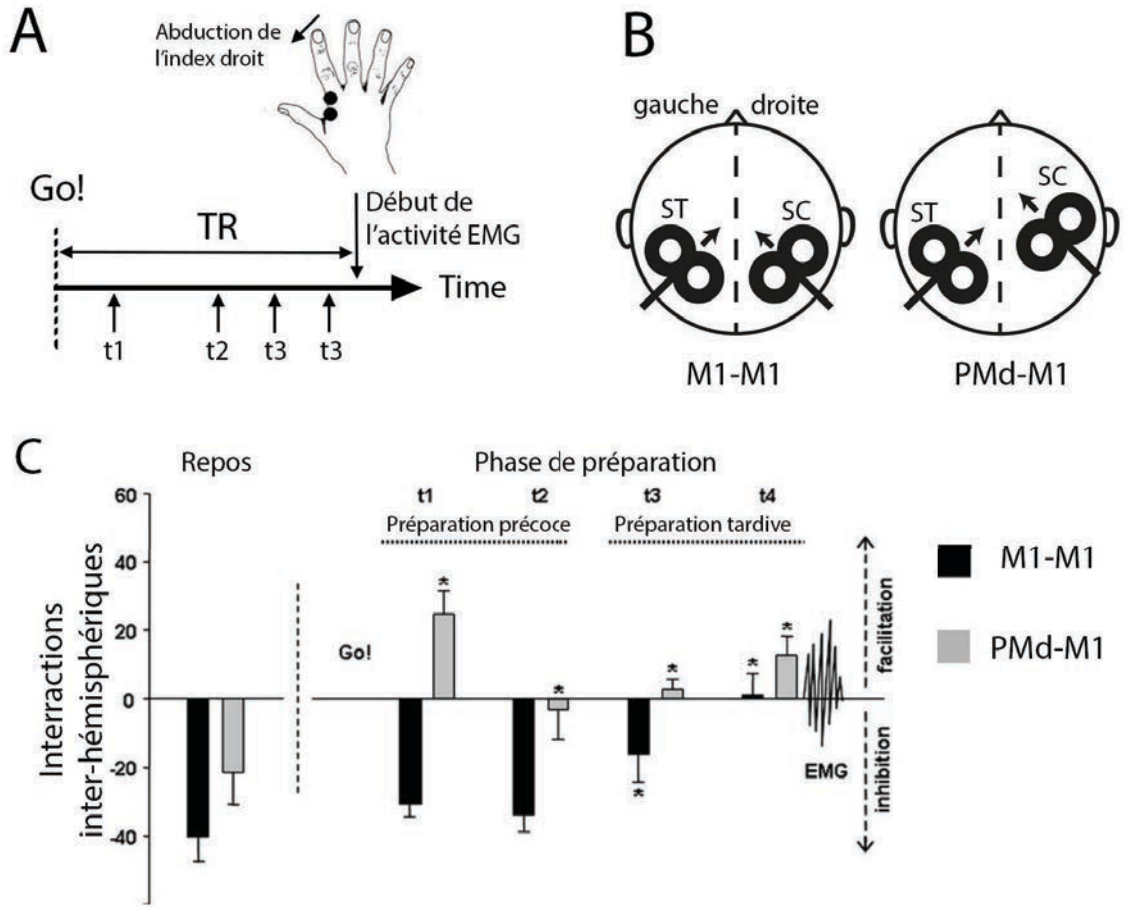

Figure 16. Interactions inter-hémisphériques entre PMd et M1 et entre les deux M1 au cours de la préparation d'un mouvement unimanuel. (A-B) Schéma représentant le paradigme expérimental utilisé. Il s'agit d'une tâche à réaction simple. Dès que le signal « Go » apparaît à l'écran, le sujet doit exécuter une abduction de l'index droit le plus rapidement possible. L'intervalle entre la consigne (Go) et le début de l'activité musculaire enregistrée par EMG est appelé temps de réaction (TR). L'interaction inter-hémisphérique entre le PMd droit (PMdi) et le M1 gauche (M1c) ou entre le M1 droit (M1i) et le M1c est mesurée par TMS double-pulse à différents moments de la phase de pré-mouvement (t1, t2, t3, t4). (C) Modulation de l'excitabilité du M1c. Au repos, le PMd droit et le M1 droit inhibent le M1 gauche. Au cours de la phase de pré-mouvement, cette inhibition se transforme en facilitation, avec une dynamique temporelle différente. La modulation des interactions entre le PMdi et le M1c est plus précoce que celle entre les deux M1. ST : stimulation test ; SC : stimulation conditionnante ; TR : temps de réaction ; EMG : électromyogramme ; M1 : cortex moteur primaire ; PMd : cortex prémoteur dorsal. Adapté de (Liuzzi et al, 2010).

D. Le rôle de l'AMS dans la préparation des mouvements latéralisés

Nous avons dans un premier temps insisté sur l'importance des interactions inter-hémisphériques, et donc du CC, pour la latéralisation de l'activité corticale au cours de la préparation et de l'exécution de mouvements latéralisés. Nous allons maintenant nous concentrer sur le rôle d'une région prémotrice, l'AMS, et nous allons montrer en quoi son rôle est fondamental pour la préparation des mouvements latéralisés.

1) Anatomie et localisation de l'AMS

L'AMS est localisée dans le gyrus précentral, en avant de M1, à l'intérieur de la scissure inter-hémisphérique. L'AMS peut être divisée en deux régions sur des critères anatomiques et fonctionnels (Figure 17A) (pour revue, voir (Picard and Strick, 1996; Vorobiev et al., 1998; Nachev et al., 2008)). Chez le singe, la partie postérieure (se situant en arrière de la ligne verticale passant par la commissure antérieure ou VCA), nommée AMS propre, possède des projections vers la moelle épinière (Figure 17C), ainsi que des connexions réciproques avec les aires motrices et prémotrices (M1, cortex cingulaire, AMS) dans les deux hémisphères. En particulier, il existe des projections transcalleuses denses entre les deux AMS propres ainsi qu'entre l'AMS propre et le M1 opposé. Au contraire, la partie antérieure, nommée pré-AMS, a peu de connexions avec M1, ne projette pas sur la moelle, et présente surtout des connexions réciproques avec les aires pré-frontales (Luppino et al., 1991; Luppino et al., 1993; Rouiller et al., 1994; Dum and Strick, 1996; Liu et al., 2002).

2) L'AMS est impliquée dans la préparation des mouvements

De nombreuses études soulignent l'importance de l'AMS lors de la phase de préparation du mouvement. Des enregistrements de neurones réalisés chez le singe ont révélé

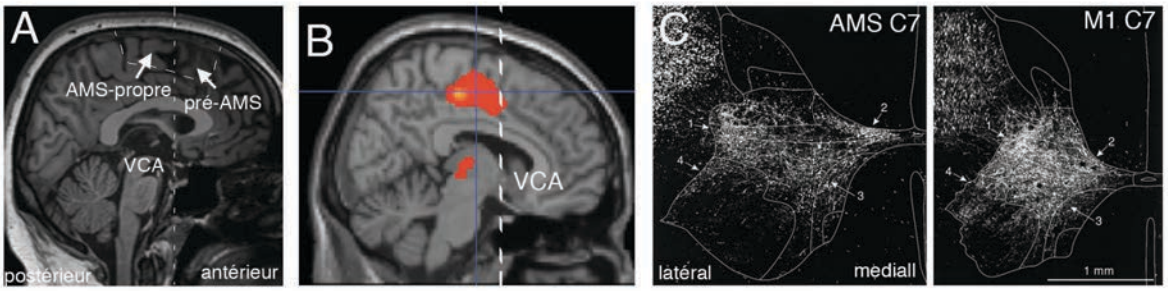

Figure 17. Organisation anatomique et rôle fonctionnel de l'AMS. (A) IRM en vue sagittale d'un sujet sain montrant la localisation anatomique de l'AMS, en position médiane, au sein de la scissure inter-hémisphérique. Deux sous-régions peuvent être définies en fonction de leur position par rapport à la VCA (ligne verticale passant par la commissure antérieure). En avant, il s'agit de la pré-AMS, et en arrière de l'AMS-propre (données personnelles). (B) IRMf en vue sagittale montrant l'activation de l'AMS lors de la préparation d'un mouvement unimanuel (données personnelles). (C) Coupe coronale de moelle de singe (au niveau cervical) montrant les projections de l'AMS propre et de M1. L'AMS projette principalement sur la zone intermédiaire de la matière grise (Dum and Strick, 1996).

une activation des neurones de l'AMS avant le début du mouvement (Alexander and Crutcher, 1990; Matsuzaka et al., 1992; Picard and Strick, 1996; Tanji and Mushiake, 1996). Comme nous l'avons dit précédemment, les enregistrements EEG réalisés chez des sujets sains montrent que le potentiel de pré-mouvement précoce (ou *Bereitschaftspotential*) est lié à l'activité de l'AMS (Shibasaki and Hallett, 2006). Par ailleurs, différentes études d'imagerie ont rapporté de façon consistante une activation de l'AMS lors de la préparation motrice (Figure 17B) (Deiber et al., 1996; Richter et al., 1997; Lee et al., 1999; Zang et al., 2003). L'AMS est impliquée dans certains aspects spécifiques de la préparation motrice. Son activation est plus importante lors de la réalisation de mouvements initiés librement, lors de la réalisation de séquences complexes, au cours de phases d'apprentissage ou encore lorsque nous devons modifier notre plan moteur (pour revue, voir (Tanji, 1996; Nachev et al., 2008)).

3) L'AMS est impliquée dans la production de mouvements bimanuels

L'AMS est particulièrement activée au cours de tâches bimanuelles asymétriques, chez le primate non-humain aussi bien que chez l'humain (Uhl et al., 1996; Sadato et al., 1997; Kermadi et al., 1998; Stephan et al., 1999; Toyokura et al., 1999; Immisch et al., 2001; Donchin et al., 2002; Ullen et al., 2003; Duque et al., 2010a). L'étude de cas de lésions réelles ou virtuelles de l'AMS a grandement contribué à une meilleure compréhension du rôle de cette aire dans le processus de production de mouvements bimanuels. A la suite de lésions de l'AMS réalisées chez le singe, les animaux éprouvent des difficultés à réaliser des mouvements bimanuels asymétriques, et auront tendance à produire des mouvements symétriques à la place (Brinkman, 1984). Des observations comparables ont été faites dans le cas de patients souffrant de lésions de l'AMS suite à des accidents vasculaires ou à des ablations chirurgicales. Chez ces patients, des altérations de la capacité à produire des mouvements bimanuels ont été décrites (Laplane et al., 1977; Chan and Ross, 1988; Stephan

et al., 1999). Dans un cas notamment, la tentative de réalisation de mouvements bimanuels asymétriques entraînait l'apparition de MM (Chan and Ross, 1988). L'inhibition transitoire et réversible de l'AMS par SMT altère spécifiquement la coordination de mouvements bimanuels asymétriques (Serrien et al., 2002; Steyvers et al., 2003), tandis que son excitation améliore les performances comportementales (Carter et al., 2015).

Les mécanismes par lesquels l'AMS influence la coordination bimanuelle ne sont pas bien connus. Cependant, sur la base de l'existence de connexions cortico-corticales et inter-hémisphériques entre l'AMS et le M1 dans les deux hémisphères (Luppino et al., 1993; Rouiller et al., 1994; Liu et al., 2002), on peut supposer que l'AMS intervient dans la modulation des interactions inter-hémisphériques entre les deux M1. Plusieurs observations soutiennent cette hypothèse. Tout d'abord, l'altération de la capacité à réaliser des mouvements bimanuels asymétriques à la suite d'une lésion latéralisée de l'AMS chez le singe est corrigée par une section du corps calleux (Brinkman, 1984). Ainsi, l'abolition des connexions entre l'AMS lésée d'une part et le M1 et l'AMS situés dans l'hémisphère contralatéral d'autre part semble restaurer une certaine indépendance des deux hémisphères. De plus, l'inhibition transitoire de l'AMS a pour conséquence de modifier le couplage fonctionnel entre les deux M1 (Serrien et al., 2002). Les résultats d'une étude plus récente ont montré une corrélation entre l'activation des deux AMS au cours de mouvements unimanuels et la taille du CC, et corroborent cette hypothèse (Stańák et al., 2003).

Nous pouvons conclure de l'ensemble de ces études que : (i) le rôle de l'AMS dans la préparation du mouvement et dans la réalisation de mouvements bimanuels asymétriques fait de cette aire une bonne candidate pour le contrôle de la préparation des mouvements latéralisés ; (ii) différents arguments anatomiques et fonctionnels suggèrent que l'AMS

pourrait moduler les interactions entre les deux hémisphères via des connexions directes (cortico-corticales et inter-hémisphériques) avec les deux M1.

RESULTATS

I. Article 1 : Le rôle de DCC dans le guidage du faisceau corticospinal n'est pas cellule-autonome (soumis)

Des mutations du gène *DCC* ont été identifiées chez des patients atteints de MMC, une pathologie associée à des anomalies anatomiques du FCS (Srour et al., 2010; Depienne et al., 2011). Cependant, il existe très peu de données concernant les patients *DCC*, et l'anatomie du FCS n'a pas été étudiée en détail chez ces derniers. Au contraire, le rôle de DCC dans le développement du FCS est bien connu chez la souris. Le FCS n'a pas été étudié chez les mutants $Dcc^{-/-}$ car ces derniers meurent à la naissance (Fazeli et al., 1997), c'est-à-dire au moment où le FCS croise la ligne médiane et entre dans la moelle chez la souris. En revanche, les mutants Dcc^{kanga} ont une mutation viable de *Dcc* aboutissant à la production d'une protéine tronquée. Ces derniers présentent des défauts majeurs de l'anatomie du FCS au niveau de la décussation pyramidale (Finger et al., 2002). Cependant, il semble que DCC ne soit pas exprimé dans le FCS chez la souris (Shu et al., 2000; Finger et al., 2002), ce qui soulève la question du rôle de cette protéine dans le guidage du FCS.

En premier lieu, nous avons étudié l'anatomie du FCS chez six patients atteints de MMC présentant des mutations du gène *DCC*. Chez ces patients, la stimulation du cortex moteur primaire par SMT engendrait des réponses musculaires au niveau de la main ipsilatérale qui étaient totalement absentes chez les sujets sains (ces derniers présentant des réponses strictement contralatérales). Ces résultats démontrent l'existence de projections corticospinales anormales depuis le cortex moteur vers la moelle ipsilatérale chez les patients *DCC*. Afin de déterminer plus précisément la cause de ces anomalies électrophysiologiques, nous avons étudié l'anatomie du FCS chez deux de ces patients avec des techniques de tractographie. Cette analyse a révélé que la décussation pyramidale des patients était anormale. En effet, le ratio entre le nombre de fibres corticospinales non-croisées et croisées était beaucoup plus important chez les patients que chez les sujets sains. Ces résultats

démontrent que DCC est impliqué dans le développement du FCS et dans la formation de la décussation pyramidale non seulement chez la souris, mais aussi chez l'humain.

Dans un second temps, nous avons étudié le rôle de DCC dans le guidage du FCS à la ligne médiane chez la souris. Nous avons précisé le patron d'expression de DCC au cours du développement de la souris : en particulier, nous n'avons pas pu détecter DCC au sein du FCS lorsque ce dernier croise la ligne médiane à P0. Nous avons ensuite étudié l'anatomie de la décussation pyramidale chez plusieurs lignées de souris ayant des mutations de *Dcc*. En particulier, nous avons comparé les souris Dcc^{kanga} avec des souris présentant une délétion totale de *Dcc* dans le télencéphale dorsal (souris $Emx1::cre\ ;Dcc^{lox/lox}$), et donc dans le FCS. Nous avons montré que contrairement aux souris Dcc^{kanga}, l'anatomie de la décussation pyramidale n'était pas altérée chez les souris $Emx1::cre\ ;Dcc^{lox/lox}$. Ces résultats démontrent que le rôle de DCC dans le guidage des axones corticospinaux à la ligne médiane n'est pas cellule-autonome. Nous supposons donc que le guidage du FCS fait intervenir d'autres structures, situées à proximité de la décussation pyramidale, qui sont altérées chez les mutants Dcc^{kanga}, mais pas chez les souris $Emx1::cre\ ;Dcc^{lox/lox}$. Nous avons observé une association entre l'absence de décussation du FCS et des anomalies anatomiques de l'olive inférieure (OI) chez les souris Dcc^{kanga}, ce qui corrobore notre hypothèse. Enfin, l'analyse du comportement moteur de ces différentes lignées de souris nous a permis de clarifier le rôle du FCS dans la génération de mouvements volontaires asymétriques avec les membres antérieurs.

Non cell-autonomous role of DCC in corticospinal tract guidance at the midline

Quentin Welniarz,[1,2] Marie-Pierre Morel,[2] Oriane Pourchet,[1,2] Cécile Gallea,[1] Jean-Charles Lamy,[1] Massimo Cincotta,[3] Mohamed Doulazmi,[4] Morgane Belle,[5] Aurélie Méneret,[1,7] Oriane Trouillard,[1] Marta Ruiz,[1] Vanessa Brochard,[6] Sabine Meunier,[1] Alain Trembleau,[2] Marie Vidailhet,[1,7] Alain Chédotal,[5] Isabelle Dusart,[2*] and Emmanuel Roze[1,7*]

[1] Sorbonne Universités, UPMC Univ Paris 06, INSERM U 1127, CNRS UMR 7225, Institut du Cerveau et de la Moelle épinière, F-75013, Paris, France

[2] Sorbonne Universités, UPMC Univ Paris 06, INSERM, CNRS, Institut de Biologie Paris Seine, Neuroscience Paris Seine, F-75005, Paris, France

[3] Unità Operativa di Neurologia-Firenze, Azienda USL Toscana Centro, Ospedale San Giovanni di Dio, 50143 Firenze, Italy

[4] Sorbonne Universités, UPMC Univ Paris 06, INSERM, CNRS, Institut de Biologie Paris Seine, Adaptation Biologique et vieillissement, F-75005, Paris, France

[5] Sorbonne Universités, UPMC Univ Paris 06, INSERM, CNRS, Institut de la Vision, F-75012, Paris, France

[6] Centre d'Investigation Clinique 14-22, INSERM/AP-HP, Paris, France

[7] Département de Neurologie, AP-HP, Hôpital Pitié Salpêtrière, Paris, France

[*] *Equal contributions*

Correspondance to: Emmanuel Roze

Département des maladies du système nerveux, hôpital Pitié Salpêtrière,

47-83 boulevard de l'Hôpital, 75013 Paris

E-mail: emmanuel.flamand-roze@psl.aphp.fr

Phone: +33142162748; Fax: +33142162474

Running title: DCC and corticospinal tract guidance

Abstract

The corticospinal tract is the principal motor pathway for voluntary movements. Most corticospinal tract axons cross the anatomic midline at the junction between the brainstem and the spinal cord, thus forming the pyramidal decussation. DCC, a NETRIN-1 receptor, ensures proper guidance of commissural axons at the midline. Humans with heterozygous *DCC* mutations have congenital mirror movements, a disorder associated with malformations of the pyramidal decussation, at least in some cases. The corticospinal tract fails to cross the midline in Kanga mice expressing a truncated DCC protein, but how DCC influences corticospinal tract midline crossing is not known.

Here, by investigating the anatomy of the corticospinal tract with multimodal approaches, we demonstrate that patients with congenital mirror movements due to *DCC* mutations have abnormal pyramidal decussation resulting in ipsilateral corticospinal tract projections to the spinal cord. Thus, *DCC* mutations result in abnormal corticospinal tract midline crossing in both humans and mice. In addition, we show that DCC is not detected in the normal mouse corticospinal tract, and that specific deletion of DCC in the neocortex of *Emx1::cre;Dcc*$^{lox/lox}$ mice does not affect the pyramidal decussation, demonstrating that the role of DCC in corticospinal tract axons guidance at the midline is non cell-autonomous. Altogether, our data unravel a new level of complexity in the role of DCC in corticospinal tract guidance at the midline.

Keywords: brain development, neuroanatomy, motor control, movement disorders, clinical neurophysiology

Abbreviations: CC = corpus callosum; CMM = congenital mirror movements; CST = corticospinal tract; FDI = first dorsal interosseous; IO = inferior olivary; M1 = primary motor

cortex; MAO = medial accessory olive; MEP = motor evoked potential; TMS = trans-cranial magnetic stimulation; DTI = diffusion tensor imaging

Introduction

The corticospinal tract (CST) is the principal motor pathway for voluntary movements (Heffner and Masterton, 1983; Davidoff, 1990; Vulliemoz *et al.*, 2005). Most CST axons cross the midline at the junction between the brainstem and spinal cord, known as the pyramidal decussation. To cross the midline, central nervous system (CNS) axons are guided by molecular cues whose expression, together with that of their receptors, is tightly controlled in time and space during development (Chedotal, 2011; Nawabi and Castellani, 2011). DCC (Deleted in colorectal cancer) is a receptor that mediates the chemoattractive activity of NETRIN-1, thereby modulating the crossing of CNS commissural axons (Keino-Masu *et al.*, 1996). In *Dcc*$^{-/-}$ knockout mice, midline crossing by commissural axons is altered at the level of the corpus callosum (CC), anterior commissure, hippocampal commissure (Fazeli *et al.*, 1997; Finger *et al.*, 2002; Fothergill *et al.*, 2014), habenulo-interpeduncular system (Belle *et al.*, 2014), inferior olive (Marcos *et al.*, 2009), and spinal cord (Fazeli *et al.*, 1997; Rabe Bernhardt *et al.*, 2012). The role of DCC in the development of the CST has not been investigated in *Dcc*$^{-/-}$ knockout mice since they die within 24 hours after birth, when the CST crosses the midline and enter the spinal cord. The study of *Dcc*^{kanga} mice provided evidence supporting a role of DCC in the development of the mouse CST. *Dcc*^{kanga} mice carry a spontaneous and viable *Dcc* mutation that removes the exon encoding the P3 intracellular domain (Finger *et al.*, 2002). These mice are characterized by a striking ‘‘kangaroo-like’’ hopping gait, and replicate most of the commissural defects observed in *Dcc*$^{-/-}$ mutants. At the level of the pyramidal decussation, the CST of Kanga mutants does not cross the midline but forms two bundles that remain in the ventral ipsilateral spinal cord (Finger *et al.*, 2002).

Many commissural neurons throughout the central nervous system express DCC (Keino-Masu *et al.*, 1996; Shu *et al.*, 2000). These commissural populations fail to cross the midline in *Dcc* mutants (Fazeli *et al.*, 1997; Finger *et al.*, 2002; Rabe Bernhardt *et al.*, 2012; Fothergill *et al.*,

2014), suggesting a cell-autonomous role for this receptor. However, DCC has not been detected in brainstem CST axons during normal development (Shu *et al.*, 2000; Finger *et al.*, 2002), raising questions as to the mechanism by which DCC influences CST midline crossing.

In human, heterozygous mutations in DCC have been identified in families with autosomal-dominant congenital mirror movements (CMM) (Srour *et al.*, 2010; Depienne *et al.*, 2011; Meneret *et al.*, 2014). CMM is associated with malformations of the pyramidal decussation, at least in some cases (Gallea *et al.*, 2013; Welniarz *et al.*, 2015). Two CMM patients with initially unknown genetic status were found to carry a *DCC* mutation, years after publication of their neurophysiological data. In these two patients, unilateral transcranial magnetic stimulation (TMS) of the primary motor cortex elicited bilateral motor responses, suggesting the existence of bilateral CST projections to the spinal cord (Cincotta *et al.*, 1994; Cincotta *et al.*, 2003; Borgheresi *et al.*, 2010). However, further neurophysiological and neuroimaging data are needed to validate these results and to clarify to what extent the pyramidal decussation is morphologically and functionally abnormal in *DCC*-CMM patients.

The aim of the present paper was to unravel the role of DCC in CST midline crossing in both human and mice. First, we used an optimized multimodal approach to characterize in details the abnormalities of the CST in a group of six *DCC*-CMM patients. Second, we investigated whether the role of DCC in CST midline crossing is cell-autonomous in mice by analyzing various *Dcc* deficient mouse mutants, including a line with a conditional deletion of DCC restricted to the neocortex. Last, we investigated the motor consequences of abnormal pyramidal decussation in mice.

Material and methods

Subjects

Six right-handed CMM patients with documented mutations in the *DCC* gene (Depienne *et al.*, 2011; Meneret *et al.*, 2014) were matched for age, gender and handedness with six healthy volunteers The severity of mirror movements was evaluated with the Woods and Teuber rating scale (Woods and Teuber, 1978). All the participants gave their written informed consent and the protocol was approved by the CPP Ile-de-France 6 (2013-A00616-39). Patients gave their written informed consent for videos appearing in the publication.

Electrophysiological experiments

EMG signals were recorded bilaterally from the first dorsal interosseous (FDI) muscles (Gallea *et al.*, 2013). Motor evoked potentials (MEPs) induced by single monophasic pulses delivered with a figure-of-eight coil connected to a Magstim 200 (Magstim, Dyfed, UK) were recorded from electromyographic signals. Coil positioning for the stimulation of the FDI muscles in M1 and measurements of the resting motor threshold were previously described (Gallea *et al.*, 2013). Between 30 and 60 MEPs evoked by calibrated stimulation (1.3x the resting motor threshold) of the dominant hemisphere were recorded bilaterally in the FDI muscles to compare the frequency, latency and amplitude of the normal contralateral MEPs with those of any mirror MEPs recorded in the hand ipsilateral to the stimulation site.

Magnetic resonance imaging

MRI was performed with a Siemens 3 T MAGNETOM Verio with a 32-channel head coil.

The MRI protocol included anatomical three-dimensional (3D) T1-weighted MPRAGE images (TR = 2.3 s; TE = 4.18 ms; flip angle = 9°; TI = 900 ms; voxel size = 1 × 1 × 1 mm^3; 176 slices) and spin-echo echo-planar diffusion tensor imaging (TR = 10 s, TE = 87 ms, voxel size = 2 × 2 × 2 mm^3, 60 slices, 60 gradient encoded directions with a b value of 1500 s/mm^2, 11 non diffusion-weighted volumes).

Tractography analysis

Tractography analysis was performed in two patients (#1 and 6).

Diffusion images were preprocessed as previously described with MRtrix software (http://www.brain.org.au/software/mrtrix/) (Gallea *et al.*, 2013). Raw diffusion-weighted data were corrected for motion and geometric distortions secondary to eddy currents by using a registration technique based on the geometric model of distortions (Mangin *et al.*, 2002). The fiber orientation distribution function (ODF) was estimated by using the constrained spherical deconvolution (CSD) method in MRtrix. The sufficient angular resolution allowed high-order fiber orientation estimation algorithms. The ODF information obtained from CSD was used, with a suitable fiber-tracking algorithm, to infer the connectivity of crossing fibers. We used a probabilistic streamlines algorithm with the entire ODF as a probability density function (ODF threshold = 0.1; step size = 0.2 mm as 1/10 of the voxel size; radius of curvature = 1 mm; up-sampling of DWI data to 1 mm). In the native individual space, we performed seed-to-target analysis in regions of interest defined along the CST (Gallea *et al.*, 2013). These regions included the anterior bundle of the CST in the upper part of the brainstem, the lower part of the brainstem, and the lateral horn of the spinal cord (see Figure 2A). We used a probabilistic tractography algorithm: the number of fibers connecting a seed voxel to a target voxel was calculated by sampling one million draws for each fiber connecting the seed to the target. The CST tracts (the normally crossed CST and the abnormally uncrossed CST) were

reconstructed for each subject. We analyzed the proportion of crossed versus uncrossed portions of the CST by using a laterality coefficient (NF Crossed - NF Uncrossed)/(NF Crossed + NF Uncrossed), where NF is the number of fibers. Ratios closer to 1 indicate greater crossed than uncrossed CST, whereas ratios closer to -1 indicate greater uncrossed than crossed CST.

Animals and genotyping

Dcc (Fazeli *et al.*, 1997), Dcc^{kanga} (Finger *et al.*, 2002) and Dcc^{lox} (Krimpenfort *et al.*, 2012) mice, as well as the *Emx1::cre* (Gorski *et al.*, 2002) and Tau^{GFP} (Hippenmeyer *et al.*, 2005) lines have previously been described and genotyped by PCR. Except for the Dcc^{kanga} line, all the mouse lines were maintained on a C57B/6J background. Dcc^{kanga} mice arose in a C.AKR-Tgn^{cog} research mouse colony at The Jackson Laboratory, and the Tgn^{cog} mutation has been segregated out of the line (Finger *et al.*, 2002). The day of the vaginal plug was E0, and the day of birth was P0. All animal procedures were approved by the Regional Animal Experimentation Ethics Committee C2EA-05 Charles Darwin (01558.01).

Immunohistochemistry

All the immunohistochemistry experiments were performed on at least 3 animals per age and per genotype. For light microscopy, P0-P2 mice were anesthetized on ice and adult mice were anesthetized with sodium pentobarbital (50 mg/kg i.p.). Embryos were fixed by immersion in 4% paraformaldehyde with 0.12 M phosphate buffer pH 7.4, and post-natal mice were perfused through the aorta with 0.12 M phosphate buffer, pH 7.4, containing 4% paraformaldehyde. Tissue preparation and immunostaining were carried out as described in (Repici *et al.*, 2012), using the following primary antibodies: goat anti-DCC (1/100; Santa

Cruz Biotechnology, Santa Cruz, California); rabbit anti-PKCγ (1/100, Santa Cruz); chicken GFP (1/500, Aveslab); mouse MBP (1/200, Chemicon, Millipore, Molsheim, France); rat L1 (1/400, Millipore) and mouse Calb1 (1/100; Swant, Bellinzona, Switzerland).

Tracing of the corticospinal tract

Surgery and sample collection. Adult male or female mice were anesthetized with a mixture of ketamine (146 mg/kg) and xylazine (7.4 mg/kg) and placed in a stereotaxic frame. Pressure injections of an anterograde tracer (biotinylated dextran amine, BDA, MW 10 000, SIGMA) targeting the left motor cortex were performed. Six 0.2-µl aliquots of 10% BDA solution in normal saline were injected (0.1 µl/min) with a 10-µl Hamilton microsyringes fitted with a removable needle (Hamilton, 7762-03) at the following coordinates, as determined in (Tennant *et al.*, 2011): i) A (anteriority: positive values are rostral to bregma, negative values are caudal to bregma) = 1, L (laterality to bregma) = 2, D (depth from the surface of the skull) = 1; ii) A = 1, L = 1, D = 1; iii) A = -0.25, L = 2, D = 1; iv) A = -0.25, L = 1, D = 1; v) A = -1, L = 2, D = 1; and vi) A = -1, L = 1, D = 1. At each injection point, the needle was left in place for 3 min before and after the injection to minimize leakage. After surgery, the wound was cleansed and the skin sutured. Fourteen days following BDA injections, the mice were deeply anesthetized and perfused as described for immunohistochemistry procedure.

Revelation of BDA labeling after cryostat sectioning. The brain and spinal cord were treated as described above for the immunohistochemistry procedure (Repici et al., 2012). Coronal sections 30 µm thick through the entire brain and spinal cord were cut on a cryostat. Sections were washed for 15 min in 0.1 M PBS pH 7.3 and incubated for one hour in PBSGT (PBS containing 0.25% Triton-X, 0.2% gelatin) and lysine (0.1 M). The sections were then incubated overnight in steptavidin-complex conjugated to horseradish peroxidase solution

(HRP, 1/400, Sigma) in PBSGT. The sections were washed 4 x 10 min in PBST, then incubated for 40 min in 1% DAB solution (3,3'-diaminobenzidine, Sigma-Aldrich) in 0.1 M Tris pH 7.6 containing 0.015% H_2O_2. The sections were washed 3 x 5 min in 0.1 M Tris in order to stop the reaction, then dehydrated before mounting in Eukitt (Sigma). Images were acquired with a DMR Leica microscope.

3DISCO clearing and light-sheet imaging. We used the 3DISCO clearing, 3D imaging and image processing procedures described in (Belle *et al.*, 2014).

Behavioral study of Dcc deficient mice

All the behavioral studies were performed blindly to the genotype. The tests were performed on male and female mice aged between 8 and 12 weeks. For the first three days, the mice were habituated to being handled by the experimenters in order to limit stress. Mice were then tested with a partial SHIRPA protocol (grasping, clasping and auditory tests were performed, and whisker state was evaluated) in order to rule out major neurological abnormalities.

The open field test was used to evaluate spontaneous activity and locomotion: mice were placed in the center of a 0.25-m^2 arena and allowed to explore freely for 5 minutes. During this time, they were tracked and recorded with a camera fixed above the arena, and the total walking distance was calculated with Topscan software.

The Ladder test apparatus (Locotronic) consists of a 124 cm x 8 cm corridor with a floor composed of 78 bars each 1 cm apart. The mice were made to cross the corridor, and the number of slips of the forelimbs, hindlimbs and tail was automatically detected by 158 infrared captors placed on the corridor walls (sampling frequency 1000 Hz). This test evaluates the precision and coordination of limb positioning.

Treadmill. Mice were placed on a transparent treadmill (14 cm x 6 cm) moving at 12 cm/s. After a short training session, the mice had to run for ten seconds, during which period the positioning of their paws was recorded by a camera fixed under the apparatus. The numbers of symmetric and asymmetric strides were counted after excluding frames in which the mouse was not running.

Rotarod. The accelerating Rotarod (BIOSEB) consists of a horizontal rod 3 cm in diameter, turning on its longitudinal axis. The training phase consisted of walking on the rod at a rotational speed varying from 4 to 40 rpm for one minute. The mice were then subjected to four trials in which the speed of rotation increased gradually from 4 rpm to 40 rpm over 5 min. Time spent on the rod was recorded and averaged for the 4 trials. The test was repeated three days in a row with the same procedure, except that the training session was performed only on the first day.

Grip test. Forepaw muscle strength was measured with a grip test. The mouse was held by the base of its tail and allowed to firmly grab the grid of the device with its forepaws. The mouse was then pulled gently backwards until it released its grip. The peak force (N) in each trial was considered as the grip strength. Four successive measurements were averaged. The same procedure was performed with forepaws and hindpaws at the same time.

Reaching exploratory behavior. When placed in a new environment, as a glass cylinder, mice engage in “reaching” exploratory behavior, in which they contact walls with their forepaws (Serradj *et al.*, 2014). This contact can be made with the two paws simultaneously (symmetric movement) or independently (asymmetric). Ten reaching movements were recorded with a video camera and then examined frame-by-frame to calculate the numbers of asymmetric and symmetric movements.

Statistical analysis

Data were analyzed with SPSS statistical software version 22.0 (Chicago, Illinois, USA). The normality of variable distributions and the homogeneity of variance across the groups were assessed with the Kolmogorov-Smirnov and Levene tests, respectively. Variables that failed any of these tests were analyzed with the nonparametric Mann–Whitney test. Variables that passed the normality test were analyzed with ANOVA followed by the Bonferroni *post hoc* test for multiple comparisons, or with Student's *t* test when comparing two groups. Paired data were analyzed by repeated-measures ANOVA with two factors, followed by the Bonferroni *post hoc* test for multiple comparisons. Categorical variables were compared using Pearson's χ^2 test or Fisher's exact test.

Results

Abnormal ipsilateral corticospinal projections in *DCC*-CMM patients

To determine whether DCC is involved in the formation of the pyramidal decussation in humans, we first studied six patients with typical congenital mirror movements due to *DCC* haploinsufficiency (Depienne *et al.*, 2011; Meneret *et al.*, 2014). In these patients, intentional movements of one hand are accompanied by involuntary mirror movements of the other hand (Supplementary movie 1). The patients had no additional clinical manifestations. We used single-pulse TMS to investigate how neural signals propagate along the CST (Table 1 and Fig. 1). In the healthy controls, stimulation of the cortical representation of hand muscles at rest elicited contralateral responses only (Fig. 1A). In contrast, in the six *DCC*-CMM patients, unilateral stimulation of the primary motor cortex at rest elicited ipsilateral responses, which were absent in all six controls. This suggested the existence of fast-conducting corticospinal projections from the hand area of the dominant primary motor cortex to motoneurons on the ipsilateral side of the spinal cord in the patients (Gallea *et al.*, 2013; Welniarz *et al.*, 2015). Ipsilateral MEPs were observed in 100% of the pulses in five *DCC*-CMM patients, and in 65% of the pulses in the remaining patient (Table 1).

The relative amplitude of the contralateral and ipsilateral MEPs was variable in the *DCC*-CMM patients. The amplitude of the ipsilateral MEPs was smaller than the normal contralateral MEPs in two of the six patients (Fig. 1B, Table 1) and larger in three of the six patients (Fig. 1C, Table 1), whereas only ipsilateral MEPs were observed in one patient (Fig. 1D, Table 1). This variability in the amplitude of ipsilateral and contralateral MEPs could reflect differences in the relative number of ipsilateral and contralateral CST projections to the spinal cord. In patients #1-5, who had bilateral MEPs, the difference in latency between ipsilateral and contralateral MEPs was less than 1 millisecond (Table 1), which is consistent

with the presence of direct corticospinal projections from the dominant hemisphere to the ipsilateral spinal cord. We then used diffusion tensor imaging (DTI) to investigate the CST projections in two patients and two controls (Fig. 2). The results suggested that the controls had more crossed CST fibers than uncrossed CST fibers, whereas the patients had more uncrossed CST fibers than crossed CST fibers (Fig. 2B, C). Together, these findings support the involvement of DCC in the development of the pyramidal decussation in humans, as previously observed in mice.

DCC expression in CST axons is not required for midline crossing

We then investigated whether the CST midline crossing defects of *Dcc*^{kanga} mice may result from a cell autonomous effect of DCC. CST axons were labeled at P0 using *Emx1::Cre* mice (in which cre recombinase is expressed in the neocortex from about E10 (Gorski *et al.*, 2002), including the neocortical layer V) crossed with Tau-lox-Stop-lox-mGFP-IRES-nls-lacZ mice (*Tau*^{GFP}), which express a membrane-tethered GFP in axons following Cre-mediated recombination (Hippenmeyer *et al.*, 2005). As previously described (Bareyre *et al.*, 2005), CST axons were GFP-positive in *Emx1::Cre;Tau*^{mGFP} mice (Fig. 3 and Supplementary Fig. 1). At P0, DCC was not detected in the CST of *Emx1::cre;Tau*^{GFP} mice, either in the brainstem (Fig. 3B, C) or at the pyramidal decussation (Fig. 3D), consistent with previous observations (Shu *et al.*, 2000; Finger *et al.*, 2002). As expected, DCC was detected in fasciculus retroflexus (Fig. 3B). The lack of DCC immunolabeling in the CST suggests that the role of DCC in CST development could be non cell-autonomous. However, it is possible that DCC expression in the CST is too low to be detected (Finger *et al.*, 2002).

To further address this issue, we selectively abolished *Dcc* expression in cortical neurons by using *Dcc* conditional knockout mice (Krimpenfort *et al.*, 2012) and the *Emx1::cre* mouse

line (Gorski *et al.*, 2002). We compared the CST anatomy of *Emx1::cre;Dcc*$^{lox/lox}$ *mice*, in which DCC is conditionally deleted in cortical neurons (Supplementary Fig.2), with various *Dcc* deficient mouse lines and their respective controls. *Dcc*^{kanga} is a spontaneous mutation that removes the exon encoding the P3 intracellular domain of DCC, and the CST fails to cross the midline in *Dcc*$^{kanga/kanga}$ mice (Finger *et al.*, 2002). As we were not able to generate *Dcc*$^{kanga/kanga}$ mice, *Dcc*$^{kanga/+}$ mice were crossed with *Dcc*$^{+/-}$ mice to obtain *Dcc*$^{kanga/-}$ mice, in which one allele bears a Kanga mutation and the other is deleted. *Dcc*$^{kanga/-}$ mice were compared to *Dcc*$^{kanga/+}$ mice. *Dcc*$^{+/-}$ mice with DCC haploinsufficiency were compared to *Dcc*$^{+/+}$ mice. We first verified that *Dcc*$^{kanga/-}$ (n = 3/3) and *Emx1::cre;Dcc*$^{lox/lox}$ (n = 3/3) adult mice lacked the CC (Supplementary Fig. 3) (Fazeli *et al.*, 1997; Finger *et al.*, 2002), demonstrating that DCC is lacking in the neocortex of *Emx1::cre;Dcc*$^{lox/lox}$ mice. The CST organization was investigated by PKCγ immunostaining and by unilateral BDA injection into the left motor cortex (Fig. 4 and Supplementary Fig. 4). In *Dcc*$^{+/+}$ control mice (n = 4/4), BDA-labeled CST axons crossed the midline at the pyramidal decussation (Fig. 4B, B'), then turned dorsally and continued their trajectory into the dorsal funiculus of the contralateral spinal cord (Fig. 4B-E, B'-E'). The anatomy of the CST at the pyramidal decussation was normal in *Dcc*$^{+/-}$ mice (n = 5/5; Supplementary Fig. 4 A-D, A'-D') and in *Dcc*$^{kanga/+}$ mice (data not shown, n = 4/4). As expected, *Dcc*$^{kanga/-}$ mice (n = 4/4) had major anomalies of the CST. Indeed, at the pyramidal decussation, CST axons completely failed to cross the midline, and three distinct fasciculi were observed within the ipsilateral spinal cord (Fig. 4F, F', G, G'): (i) a minor group of axons located in the ventral part of the dorsal funiculus (Fig. 4G, G', H, H'); (ii) a bundle in a ventro-medial position (Fig. 4I, I'); and (iii) a bundle in a ventro-lateral position (Fig. 4I, I'). These findings were reminiscent of what had been observed in *Dcc*$^{kanga/kanga}$ mice (Finger *et al.*, 2002), emphasizing the importance of DCC in CST guidance at the midline. To further study the CST of *Dcc*$^{kanga/-}$ mice, we combined unilateral CST

labeling with 3DISCO optical clearing and light-sheet microscopy of adult brains and spinal cords. In *Dcc*$^{kanga/+}$ mice (n = 1/1), the CST axons crossed the midline and turned dorsally at the decussation (Supplementary movie 2). No axons crossing the midline were detected in *Dcc*$^{kanga/-}$ mice (n = 1/1); the CST axons instead formed two bundles, one lateral and the other medial, that remained in the ventral ipsilateral spinal cord (Supplementary movie 3).

These results further support the role of DCC in CST axon guidance at the level of the pyramidal decussation. Interestingly, the pathway followed by CST axons was normal in *Emx1::cre;Dcc*$^{lox/lox}$ mice (n = 3/3), in which CST axons crossed the midline at the level of pyramidal decussation and continued their trajectory through the dorsal funiculus of the contralateral spinal cord (Fig. 4J-M, J'-M'). These results show that DCC deletion in the neocortex (and thus in the CST) is not sufficient to induce abnormal pyramidal decussation. The role of DCC in CST axon guidance at the midline is therefore non cell-autonomous.

Abnormal anatomy of the inferior olive associated with defective CST midline crossing of mice lacking functional DCC

In *Emx1::cre;Dcc*$^{lox/lox}$ mice, DCC deletion in CST neurons did not result in abnormal pyramidal decussation, contrary to *Dcc*$^{kanga/-}$ mice. CST guidance at the midline might thus involve other brainstem structures located in the vicinity of the decussation. The medial accessory olive (MAO) is the most caudal part of the inferior olivary (IO), and is located rostral to the decussation in wild type mice (Fig. 5A-F). It has been reported that IO neurons express DCC and that IO neuron migration is altered in *Dcc*$^{-/-}$ mutants (Bloch-Gallego *et al.*, 1991; Marcos *et al.*, 2009). We therefore investigated the anatomy of the inferior olivary and its position with respect to the CST in adult *Dcc*$^{kanga/-}$ mice. In the caudal MAO of control

mice (n = 4/4; Fig. 5A-F), the neurons were located in a lateral position and formed an elongated teardrop lining the pyramidal decussation, while in *Dcc*$^{kanga/-}$ mice (n = 5/5; Fig. 5G-L) they had an aberrant medial location. Together, these findings showed that the lack of CST axons crossing the midline in *Dcc*$^{kanga/-}$ mice is associated with an abnormal medial position of caudal IO neurons.

The study of *Dcc*$^{kanga/-}$ mice highlights the role of DCC in the generation of asymmetric movements

Dcc$^{kanga/kanga}$ mice present a hopping gait and some of them are ataxic (Finger *et al.*, 2002), but their motor phenotype has not been investigated in details. We therefore compared the performance of *Dcc*$^{kanga/-}$ mice with control mice (wildtype or *Dcc*$^{kanga/+}$) with various motor tests. Five of eleven *Dcc*$^{kanga/-}$ mice had major balance disorders: they were unable to stand on their limbs and therefore moved very little during the open-field test (ANOVA $F_{(2,25)} = 33.18$, $p < 0.001$, followed by the Bonferroni *post hoc* test; Fig. 6B). Because they were unable to perform most of the motor tests, they were excluded from further analysis. *Dcc*$^{kanga/-}$ mice were lighter than their littermate controls (ANOVA $F_{(2,20)} = 6.27$, $p = 0.008$, followed by the Bonferroni *post hoc* test, Fig. 6A), and therefore did not perform as well as the controls in the muscle strength test (Student's test, $p_{forelimbs} = 0.228$; $p_{hindlimbs} = 0.042$; Fig. 6C). *Dcc*$^{kanga/-}$ mice were undistinguishable from controls in the Rotarod test (repeated-measures ANOVA with two factors, $F_{(1,21)} = 0.71$, $p = 0.793$, followed by the Bonferroni *post hoc* test; Fig. 6D). On the treadmill test, *Dcc*$^{kanga/-}$ mice displayed a hopping gait, frequently moving both their forelimbs and hindlimbs simultaneously (Mann-Whitney test, $p_{forelimbs} < 0.0001$; $p_{hindlimbs} < 0.0001$; Fig. 6E, E2; Supplementary movie 4). In contrast, the control mice made alternating movements with their forelimbs and hindlimbs (Fig. 6E, E1; Supplementary movie 5). In the

ladder test, which evaluates the precision of limb positioning, *Dcc*$^{kanga/-}$ mice made more forelimb errors than controls (Freeman-Halton extension of Fisher's exact test, $p = 0.038$; Fig. 6F). The exploratory reaching test evaluates the lateralization of voluntary forelimb movements (Serradj *et al.*, 2014). When placed in a new walled environment, mice have a tendency to establish contacts on the walls with their forelimbs in an asymmetric (Fig. 6G, G1; Supplementary movie 6) or symmetric (Fig. 6G, G2; Supplementary movie 7) manner. In the reaching test, *Dcc*$^{kanga/-}$ mice made more symmetric movements of the forelimbs than the controls (Student's test, $p < 0.0001$; Fig. 6G). The motor phenotype of *Dcc*$^{kanga/-}$ mice underlines the importance of DCC in the generation of alternating movements during locomotion, and of voluntary asymmetric forelimb movements.

Discussion

We show that *DCC* mutations result in abnormal CST midline crossing at the level of the pyramidal decussation in both humans and mice. Selective suppression of DCC expression in the mouse neocortex did not affect the pyramidal decussation, demonstrating that the role of DCC in CST axon guidance at the midline is non cell-autonomous. CST guidance at the midline might thus involve other brainstem structures located in the vicinity of the decussation. In keeping with this hypothesis, we show that CST defects at the midline of $Dcc^{kanga/-}$ mice are associated with abnormal positioning of caudal olivary neurons. Behavioral analysis of *Dcc* deficient mouse lines revealed that lateralization of CST projections to the spinal cord is not the only factor involved in the generation of voluntary asymmetric forelimb movements.

DCC is involved in CST guidance at the midline of both humans and mice

Using a combination of TMS and DTI tractography, we obtained evidence that *DCC*-CMM patients have abnormal CST midline crossing at the level of the pyramidal decussation. Our TMS findings are consistent with those of previous TMS studies of two *DCC*-CMM patients (Cincotta *et al.*, 1994; Cincotta *et al.*, 2003; Borgheresi *et al.*, 2010). In all six of the *DCC*-CMM patients studied here, stimulation of the motor cortex hand representation elicited ipsilateral MEPs, whereas in healthy volunteers the MEPs are strictly contralateral to the stimulated hemisphere (Alagona *et al.*, 2001; Bawa *et al.*, 2004; Gallea *et al.*, 2011; Welniarz *et al.*, 2015). MEPs elicited by stimulation of the motor cortex with TMS result from the transmission of a neuronal signal from the cortex to the peripheral muscles via fast-conducting CST fibers and spinal motoneurons (Di Lazzaro *et al.*, 2008; Di Lazzaro and Ziemann, 2013; Bestmann and Krakauer, 2015). Direct connections of CST axons to motoneurons (direct cortico-motoneuronal connections) make a significant contribution to

MEPs in humans (Brouwer and Ashby, 1990; Mills, 1991; Palmer and Ashby, 1992; Petersen *et al.*, 2003). In our patients, the presence of ipsilateral MEPs with latencies similar to those of contralateral MEPs points strongly to the existence of direct connections of CST axons from one hemisphere to hand muscle motoneurons on both sides of the spinal cord. Moreover, these results are corroborated by DTI analysis of two of the *DCC*-CMM patients, in whom we found more uncrossed CST fibers than crossed CST fibers, contrary to the situation observed in control subjects. Our multimodal study strongly suggests that abnormal CST midline crossing, rather than aberrant CST branching in the spinal cord, is responsible for the abnormal ipsilateral MEPs observed in *DCC*-CMM patients. Our findings thus support the involvement of DCC in CST midline crossing at the level of the pyramidal decussation in humans.

In five of the six *DCC* patients, stimulation of the dominant hemisphere evoked ipsilateral responses in 100% of the pulses. In four of these patients, the amplitude of the ipsilateral MEPs was higher than that of the contralateral MEPs. In a previous study of seven *RAD51*-CMM patients, we found that the frequency of ipsilateral MEPs was always below 100% and that their amplitude was always smaller than that of normal contralateral MEPs (Gallea *et al.*, 2013). Another study showed that the relative amplitude of the ipsilateral and contralateral MEPs was variable across individuals in a group of thirteen patients with X-linked Kallmann syndrome, some of whom had greater ipsilateral MEPs than contralateral MEPs (Mayston *et al.*, 1997). The relative proportion of ipsilateral and contralateral CST projections is likely to be the main determinant of the relative amplitudes of contralateral and ipsilateral MEPs (Mayston *et al.*, 1997; Petersen *et al.*, 2003; Bestmann and Krakauer, 2015). In keeping with this hypothesis, *DCC*-CMM patients would have a majority of ipsilateral CST projections.

We found that the pyramidal decussation was completely absent in $Dcc^{kanga/-}$ mice, in keeping with descriptions of $Dcc^{kanga/kanga}$ mice (Finger *et al.*, 2002). The decussation is partial in

human *DCC*-CMM patients, while it is normal in *Dcc*$^{+/-}$ mice and completely absent in *Dcc*$^{kanga/-}$ mice. The organization of the CST is different in mice and humans. While 95% of CST axons cross the midline in rodents (Schreyer and Jones, 1982; Rouiller *et al.*, 1991; Joosten *et al.*, 1992), this proportion varies between 75% and 90% in humans with important inter-individual differences (Davidoff, 1990; Nathan *et al.*, 1990; Jang, 2014). CST axons crossing the midline at the level of the spinal cord have been described in humans and monkeys (Nathan *et al.*, 1990; Lacroix *et al.*, 2004; Rosenzweig *et al.*, 2009), but to a lesser extent in rodents (Rouiller *et al.*, 1991). Although there are species-related differences regarding the anatomy of the pyramidal decussation, our data suggest a role for DCC in CST guidance at the midline in both mice and humans.

The role of DCC in CST guidance at the midline is not cell-autonomous in mouse

In mice lacking a functional DCC, CST axons fail to cross the midline at the level of the pyramidal decussation. Yet, we showed that during normal development, DCC is not detected in CST axons at the level of the pyramidal decussation. Selective suppression of DCC in the mouse neocortex, and thus in the CST, did not alter CST midline crossing. These results demonstrate that the role of DCC in CST axon guidance at the midline is non cell-autonomous.

Other receptors involved in axon guidance have also been reported to have non cell-autonomous functions. In *Drosophila*, the DCC ortholog FRAZZLED1, a NETRIN-1 receptor, is required for the guidance of retinal cells and longitudinal axons in a non cell-autonomous manner, possibly by controlling NETRIN-1 distribution and presentation (Gong *et al.*, 1999; Hiramoto *et al.*, 2000). Likewise, a recent study showed that the WNT binding receptor FRIZZLED3 has a non cell-autonomous role in guiding medium spiny neurons in mice, possibly by positioning corridor guidepost cells (Morello *et al.*, 2015).

The DCC receptor has been described as a cell-autonomous regulator of axon guidance. Many commissural neurons throughout the central nervous system express DCC (Keino-Masu *et al.*, 1996; Shu *et al.*, 2000). These commissural populations fail to cross the midline in *Dcc* mutants (Fazeli *et al.*, 1997; Finger *et al.*, 2002; Rabe Bernhardt *et al.*, 2012; Fothergill *et al.*, 2014), suggesting a cell-autonomous role for this receptor in this setting. This is the case of the CC, which expresses DCC during development (Shu *et al.*, 2000) and which is lacking in *Dcc* mutant mice (Fazeli *et al.*, 1997; Fothergill *et al.*, 2014).

Our work shows for the first time that DCC controls CST midline crossing in a non cell-autonomous manner and suggests that normal guidance of the CST at the pyramidal decussation involves structures located in the vicinity of the pyramidal decussation, that might be absent or mis-located in *Dcc* mutants. The IO, which is located in the caudal brainstem adjacent to the pyramidal decussation, is a good candidate for this role. Positioning of IO neurons is completed before the CST reaches the pyramidal decussation at P0 (Bourrat and Sotelo, 1988; Bourrat and Sotelo, 1990). DCC is expressed in IO neurons (Bloch-Gallego *et al.*, 1991), and IO neurons migration is altered in $Dcc^{-/-}$ mutants (Marcos *et al.*, 2009). A role of IO neurons in CST guidance had been proposed, through SEMA6A expression (Faulkner *et al.*, 2008; Runker *et al.*, 2008). Here we show that the lack of CST axons crossing the midline in $Dcc^{kanga/-}$ mice is associated with an abnormal medial position of caudal IO neurons. For these reasons, we suspect that the abnormal IO formation observed in $Dcc^{kanga/-}$ mutants might eventually affect the guiding role of IO neurons for CST axons. Alternatively, the abnormal anatomy of the caudal IO observed in $Dcc^{kanga/-}$ mutants might be a consequence of CST defects.

Our data unravel a new level of complexity in the role of DCC in axon guidance at the midline. They also highlight that the formation of the pyramidal decussation depends upon prior set up of brainstem structures.

Motor behavior of *Dcc*$^{kanga/-}$ mice provides insights into the role of the CST in the production of asymmetric movements

Beside the description of the hopping gait and ataxia (Finger *et al.*, 2002), careful investigation of the motor behavior of *Dcc*$^{kanga/-}$ mice had not been performed. Here, we show that *Dcc*$^{kanga/-}$ mice have very specific motor impairments, as they are unable to generate alternating movements during stereotypic locomotion (hopping gait) or voluntary asymmetric forelimb movements (exploratory reaching behaviors). In *Dcc*$^{kanga/-}$ mice, DCC deficiency not only impacts CST and CC development but also affects other DCC-expressing cell populations, such as commissural spinal cord interneurons, that are critical for locomotion (Rabe Bernhardt *et al.*, 2012). Two recent studies used conditional knockout EPHA4 mice to dissect the neuronal circuits responsible for their hopping gait. In *Emx1::cre;EphA4*$^{flox/flox}$ mice, conditional EPHA4 deletion in the forebrain resulted in normal stereotypic locomotion despite bilateral CST projections to the spinal cord (Borgius *et al.*, 2014; Serradj *et al.*, 2014). In contrast, specific EPHA4 deletion in the spinal cord or in glutamatergic interneurons was sufficient to induce hopping locomotor activity (Borgius *et al.*, 2014). Together, these results show that stereotypic left-right alternation relies on spinal commissural circuits rather than on proper CST wiring.

Emx1::cre;EphA4$^{flox/flox}$ mice, which have bilateral CST projections to the spinal cord, exhibit symmetric voluntary movements in conditions in which asymmetric limb movements are normally produced (as in the exploratory reaching test), and might thus provide a good murine model of mirror movements (Borgius *et al.*, 2014; Friel *et al.*, 2014; Serradj *et al.*, 2014). *Dcc*$^{kanga/-}$ mice have a similar motor phenotype but, contrary to *Emx1::cre;EphA4*$^{flox/flox}$ mice, they have strictly ipsilateral CST projections to the spinal cord. This suggests that bilateral CST projection to the spinal cord is sufficient but not necessary to induce

symmetrical reaching behaviors. There is currently no mouse behavioral test specifically designed to assess the motor consequences of bilateral CST projections to the spinal cord. Human mirror movements are thought to result from CST projections to both the ipsilateral and contralateral spinal cord (Vulliemoz *et al.*, 2005; Gallea *et al.*, 2011; Peng and Charron, 2013; Welniarz *et al.*, 2015). Mirror movements have not been described in patients with horizontal gaze palsy with progressive scoliosis, despite their complete lack of CST decussation (Jen *et al.*, 2004; Bosley *et al.*, 2005; Amoiridis *et al.*, 2006; Haller *et al.*, 2008). This suggests that mirror movements are related to bilateral spinal cord projections arising from a single primary motor cortex rather than to abnormal decussation of the CST *per se*.

Acknowledgments

The authors thank the CENIR for MRI and TMS data acquisition; Magali Dumont and Marika Nosten for help in the design of the behavioral tests; David Godeffory for 3D imaging and 3DISCO image processing; Susan Ackerman (Jackson lab, Bar Harbor, USA) for providing *Dcc*^{kanga} mice and Anton Berns (Amsterdam, Netherlands) for providing the DCC^{lox} mice; and the ICM DNA and Cell Bank for DNA extraction and cell culture. The Development and Plasticity of Neural Networks team is affiliated with the Bio-Psy Laboratory of Excellence.

Funding

This work was supported by Fondation pour la Recherche sur le Cerveau (FRC, AO2010); INSERM (COSSEC); Merz-Pharma; IP-santé; Djillali Mehri and the French Government (IHU-A-ICM, “Investissement d’avenir” ANR-10-IAIHU-06 program).

References

Alagona G, Delvaux V, Gerard P, De Pasqua V, Pennisi G, Delwaide PJ, et al. Ipsilateral motor responses to focal transcranial magnetic stimulation in healthy subjects and acute-stroke patients. Stroke 2001; 32: 1304-9.

Amoiridis G, Tzagournissakis M, Christodoulou P, Karampekios S, Latsoudis H, Panou T, et al. Patients with horizontal gaze palsy and progressive scoliosis due to ROBO3 E319K mutation have both uncrossed and crossed central nervous system pathways and perform normally on neuropsychological testing. J Neurol Neurosurg Psychiatry 2006; 77: 1047-53.

Bareyre FM, Kerschensteiner M, Misgeld T, Sanes JR. Transgenic labeling of the corticospinal tract for monitoring axonal responses to spinal cord injury. Nat Med 2005; 11: 1355-60.

Bawa P, Hamm JD, Dhillon P, Gross PA. Bilateral responses of upper limb muscles to transcranial magnetic stimulation in human subjects. Exp Brain Res 2004; 158: 385-90.

Belle M, Godefroy D, Dominici C, Heitz-Marchaland C, Zelina P, Hellal F, et al. A simple method for 3D analysis of immunolabeled axonal tracts in a transparent nervous system. Cell Rep 2014; 9: 1191-201.

Bestmann S, Krakauer JW. The uses and interpretations of the motor-evoked potential for understanding behaviour. Exp Brain Res 2015; 233: 679-89.

Bloch-Gallego E, Huchet M, el M'Hamdi H, Xie FK, Tanaka H, Henderson CE. Survival in vitro of motoneurons identified or purified by novel antibody-based methods is selectively enhanced by muscle-derived factors. Development 1991; 111: 221-32.

Borgheresi A, Espay AJ, Giovannelli F, Vanni P, Zaccara G, Cincotta M. Congenital mirror movements in Parkinson's disease: clinical and neurophysiological observations. Mov Disord 2010; 25: 1520-3.

Borgius L, Nishimaru H, Caldeira V, Kunugise Y, Low P, Reig R, et al. Spinal glutamatergic neurons defined by EphA4 signaling are essential components of normal locomotor circuits. J Neurosci 2014; 34: 3841-53.

Bosley TM, Salih MA, Jen JC, Lin DD, Oystreck D, Abu-Amero KK, et al. Neurologic features of horizontal gaze palsy and progressive scoliosis with mutations in ROBO3. Neurology 2005; 64: 1196-203.

Bourrat F, Sotelo C. Migratory pathways and neuritic differentiation of inferior olivary neurons in the rat embryo. Axonal tracing study using the in vitro slab technique. Brain Res 1988; 467: 19-37.

Bourrat F, Sotelo C. Early development of the rat precerebellar system: migratory routes, selective aggregation and neuritic differentiation of the inferior olive and lateral reticular nucleus neurons. An overview. Arch Ital Biol 1990; 128: 151-70.

Brouwer B, Ashby P. Corticospinal projections to upper and lower limb spinal motoneurons in man. Electroencephalogr Clin Neurophysiol 1990; 76: 509-19.

Chedotal A. Further tales of the midline. Curr Opin Neurobiol 2011; 21: 68-75.

Cincotta M, Borgheresi A, Balzini L, Vannucchi L, Zeloni G, Ragazzoni A, et al. Separate ipsilateral and contralateral corticospinal projections in congenital mirror movements: Neurophysiological evidence and significance for motor rehabilitation. Mov Disord 2003; 18: 1294-300.

Cincotta M, Ragazzoni A, de Scisciolo G, Pinto F, Maurri S, Barontini F. Abnormal projection of corticospinal tracts in a patient with congenital mirror movements. Neurophysiol Clin 1994; 24: 427-34.

Davidoff RA. The pyramidal tract. Neurology 1990; 40: 332-9.

Depienne C, Cincotta M, Billot S, Bouteiller D, Groppa S, Brochard V, et al. A novel DCC mutation and genetic heterogeneity in congenital mirror movements. Neurology 2011; 76: 260-4.

Di Lazzaro V, Ziemann U. The contribution of transcranial magnetic stimulation in the functional evaluation of microcircuits in human motor cortex. Front Neural Circuits 2013; 7.

Di Lazzaro V, Ziemann U, Lemon RN. State of the art: Physiology of transcranial motor cortex stimulation. Brain Stimul 2008; 1: 345-62.

Faulkner RL, Low LK, Liu XB, Coble J, Jones EG, Cheng HJ. Dorsal turning of motor corticospinal axons at the pyramidal decussation requires plexin signaling. Neural Dev 2008; 3.

Fazeli A, Dickinson SL, Hermiston ML, Tighe RV, Steen RG, Small CG, et al. Phenotype of mice lacking functional Deleted in colorectal cancer (Dcc) gene. Nature 1997; 386: 796-804.

Finger JH, Bronson RT, Harris B, Johnson K, Przyborski SA, Ackerman SL. The netrin 1 receptors Unc5h3 and Dcc are necessary at multiple choice points for the guidance of corticospinal tract axons. J Neurosci 2002; 22: 10346-56.

Fothergill T, Donahoo AL, Douglass A, Zalucki O, Yuan J, Shu T, et al. Netrin-DCC Signaling Regulates Corpus Callosum Formation Through Attraction of Pioneering Axons and by Modulating Slit2-Mediated Repulsion. Cereb Cortex 2014; 24: 1138-51.

Friel KM, Williams PT, Serradj N, Chakrabarty S, Martin JH. Activity-Based Therapies for Repair of the Corticospinal System Injured during Development. Front Neurol 2014; 5.

Gallea C, Popa T, Billot S, Meneret A, Depienne C, Roze E. Congenital mirror movements: a clue to understanding bimanual motor control. J Neurol 2011; 258: 1911-9.

Gallea C, Popa T, Hubsch C, Valabregue R, Brochard V, Kundu P, et al. RAD51 deficiency disrupts the corticospinal lateralization of motor control. Brain 2013; 136: 3333-46.

Gong Q, Rangarajan R, Seeger M, Gaul U. The netrin receptor frazzled is required in the target for establishment of retinal projections in the Drosophila visual system. Development 1999; 126: 1451-6.

Gorski JA, Talley T, Qiu M, Puelles L, Rubenstein JL, Jones KR. Cortical excitatory neurons and glia, but not GABAergic neurons, are produced in the Emx1-expressing lineage. J Neurosci 2002; 22: 6309-14.

Haller S, Wetzel SG, Lutschg J. Functional MRI, DTI and neurophysiology in horizontal gaze palsy with progressive scoliosis. Neuroradiology 2008; 50: 453-9.

Heffner RS, Masterton RB. The role of the corticospinal tract in the evolution of human digital dexterity. Brain Behav Evol 1983; 23: 165-83.

Hippenmeyer S, Vrieseling E, Sigrist M, Portmann T, Laengle C, Ladle DR, et al. A developmental switch in the response of DRG neurons to ETS transcription factor signaling. PLoS Biol 2005; 3: e159.

Hiramoto M, Hiromi Y, Giniger E, Hotta Y. The Drosophila Netrin receptor Frazzled guides axons by controlling Netrin distribution. Nature 2000; 406: 886-9.

Jang SH. The corticospinal tract from the viewpoint of brain rehabilitation. J Rehabil Med 2014; 46: 193-9.

Jen JC, Chan WM, Bosley TM, Wan J, Carr JR, Rub U, et al. Mutations in a human ROBO gene disrupt hindbrain axon pathway crossing and morphogenesis. Science 2004; 304: 1509-13.

Joosten EA, Schuitman RL, Vermelis ME, Dederen PJ. Postnatal development of the ipsilateral corticospinal component in rat spinal cord: a light and electron microscopic anterograde HRP study. J Comp Neurol 1992; 326: 133-46.

Keino-Masu K, Masu M, Hinck L, Leonardo ED, Chan SS, Culotti JG, et al. Deleted in Colorectal Cancer (DCC) encodes a netrin receptor. Cell 1996; 87: 175-85.

Krimpenfort P, Song JY, Proost N, Zevenhoven J, Jonkers J, Berns A. Deleted in colorectal carcinoma suppresses metastasis in p53-deficient mammary tumours. Nature 2012; 482: 538-41.

Lacroix S, Havton LA, McKay H, Yang H, Brant A, Roberts J, et al. Bilateral corticospinal projections arise from each motor cortex in the macaque monkey: a quantitative study. J Comp Neurol 2004; 473: 147-61.

Mangin JF, Poupon C, Clark C, Le Bihan D, Bloch I. Distortion correction and robust tensor estimation for MR diffusion imaging. Med Image Anal 2002; 6: 191-8.

Marcos S, Backer S, Causeret F, Tessier-Lavigne M, Bloch-Gallego E. Differential roles of Netrin-1 and its receptor DCC in inferior olivary neuron migration. Mol Cell Neurosci 2009; 41: 429-39.

Mayston MJ, Harrison LM, Quinton R, Stephens JA, Krams M, Bouloux PM. Mirror movements in X-linked Kallmann's syndrome. I. A neurophysiological study. Brain 1997; 120 (Pt 7): 1199-216.

Meneret A, Depienne C, Riant F, Trouillard O, Bouteiller D, Cincotta M, et al. Congenital mirror movements: mutational analysis of RAD51 and DCC in 26 cases. Neurology 2014; 82: 1999-2002.

Mills KR. Magnetic brain stimulation: a tool to explore the action of the motor cortex on single human spinal motoneurones. Trends Neurosci 1991; 14: 401-5.

Morello F, Prasad AA, Rehberg K, Vieira de Sa R, Anton-Bolanos N, Leyva-Diaz E, et al. Frizzled3 Controls Axonal Polarity and Intermediate Target Entry during Striatal Pathway Development. J Neurosci 2015; 35: 14205-19.

Nathan PW, Smith MC, Deacon P. The corticospinal tracts in man. Course and location of fibres at different segmental levels. Brain 1990; 113: 303-24.

Nawabi H, Castellani V. Axonal commissures in the central nervous system: how to cross the midline? Cell Mol Life Sci 2011; 68: 2539-53.

Palmer E, Ashby P. Corticospinal projections to upper limb motoneurones in humans. J Physiol 1992; 448: 397-412.

Peng J, Charron F. Lateralization of motor control in the human nervous system: genetics of mirror movements. Curr Opin Neurobiol 2013; 23: 109-18.

Petersen NT, Pyndt HS, Nielsen JB. Investigating human motor control by transcranial magnetic stimulation. Exp Brain Res 2003; 152: 1-16.

Rabe Bernhardt N, Memic F, Gezelius H, Thiebes AL, Vallstedt A, Kullander K. DCC mediated axon guidance of spinal interneurons is essential for normal locomotor central pattern generator function. Dev Biol 2012; 366: 279-89.

Repici M, Chen X, Morel MP, Doulazmi M, Sclip A, Cannaya V, et al. Specific inhibition of the JNK pathway promotes locomotor recovery and neuroprotection after mouse spinal cord injury. Neurobiol Dis 2012; 46: 710-21.

Rosenzweig ES, Brock JH, Culbertson MD, Lu P, Moseanko R, Edgerton VR, et al. Extensive spinal decussation and bilateral termination of cervical corticospinal projections in rhesus monkeys. J Comp Neurol 2009; 513: 151-63.

Rouiller EM, Liang FY, Moret V, Wiesendanger M. Trajectory of redirected corticospinal axons after unilateral lesion of the sensorimotor cortex in neonatal rat; a phaseolus vulgaris-leucoagglutinin (PHA-L) tracing study. Exp Neurol 1991; 114: 53-65.

Runker AE, Little GE, Suto F, Fujisawa H, Mitchell KJ. Semaphorin-6A controls guidance of corticospinal tract axons at multiple choice points. Neural Dev 2008; 3.

Schreyer DJ, Jones EG. Growth and target finding by axons of the corticospinal tract in prenatal and postnatal rats. Neuroscience 1982; 7: 1837-53.

Serradj N, Paixao S, Sobocki T, Feinberg M, Klein R, Kullander K, et al. EphA4-mediated ipsilateral corticospinal tract misprojections are necessary for bilateral voluntary movements but not bilateral stereotypic locomotion. J Neurosci 2014; 34: 5211-21.

Shu T, Valentino KM, Seaman C, Cooper HM, Richards LJ. Expression of the netrin-1 receptor, deleted in colorectal cancer (DCC), is largely confined to projecting neurons in the developing forebrain. J Comp Neurol 2000; 416: 201-12.

Srour M, Riviere JB, Pham JM, Dube MP, Girard S, Morin S, et al. Mutations in DCC cause congenital mirror movements. Science 2010; 328: 592.

Tennant KA, Adkins DL, Donlan NA, Asay AL, Thomas N, Kleim JA, et al. The organization of the forelimb representation of the C57BL/6 mouse motor cortex as defined by intracortical microstimulation and cytoarchitecture. Cereb Cortex 2011; 21: 865-76.

Vulliemoz S, Raineteau O, Jabaudon D. Reaching beyond the midline: why are human brains cross wired? Lancet Neurol 2005; 4: 87-99.

Welniarz Q, Dusart I, Gallea C, Roze E. One hand clapping: lateralization of motor control. Frontiers in Neuroanatomy 2015; 9.

Woods BT, Teuber H-L. Mirror movements after childhood hemiparesis. Neurology 1978; 28: 1152-7.

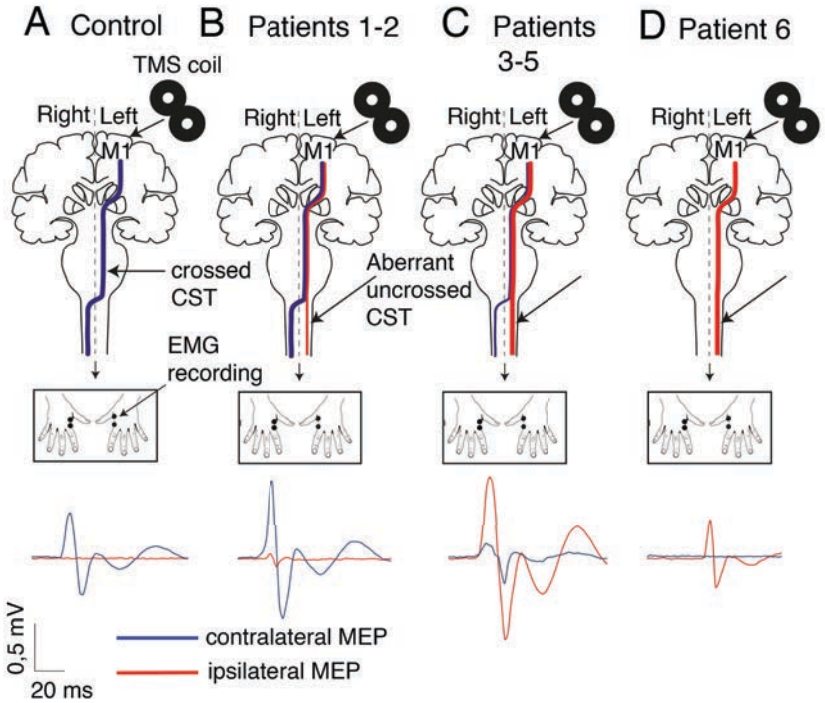

Figure 1. In healthy volunteers, unilateral stimulation of the hand area of the dominant primary motor cortex elicited only contralateral MEPs (A, blue line, right hand), whereas ipsilateral MEPs were observed in the DCC patients (B-D, red line, left hand). Depending on the patient, the ipsilateral MEPs were smaller (B) or larger (C) than the contralateral MEPs. In patient #6, stimulation of the dominant hemisphere elicited only ipsilateral MEPs (D).

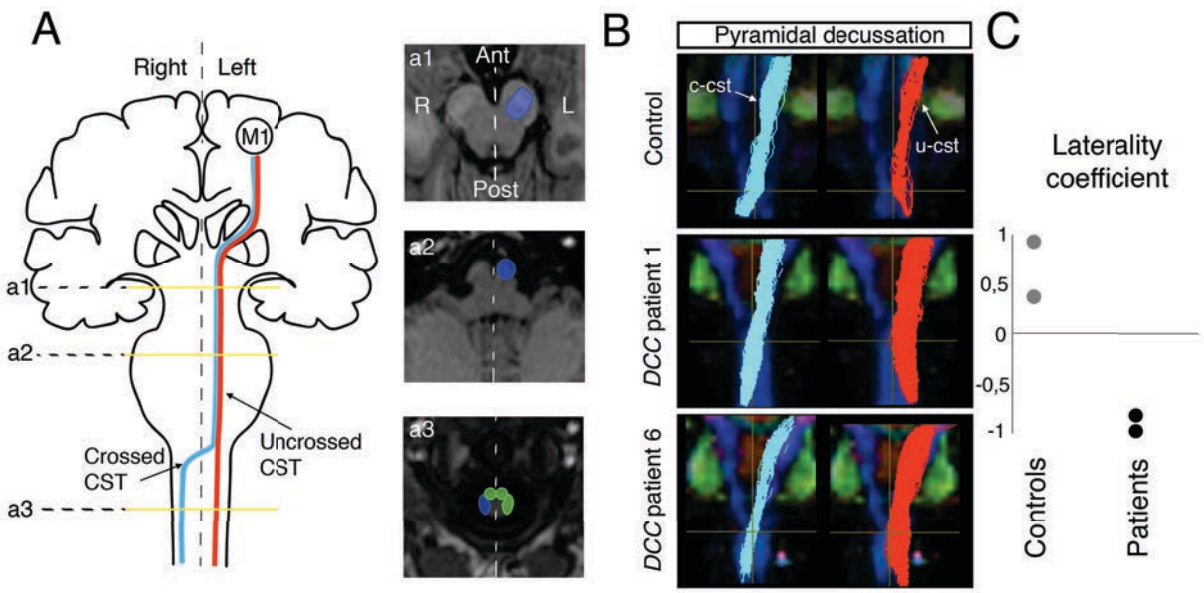

Figure 2. Tractography of the CST in *DCC*-CMM patients. (A) Left: color coding of the crossed (blue) and uncrossed (red) corticospinal tracts; Right: regions of interest (both in the diagram and superimposed on an axial slice of an anatomical image of a subject) used to reconstruct the fiber tracts (blue point) at the base of the pontine (a1), the anterior pyramid in the upper medulla (a2), and the crossed lateral funiculus of the upper cervical cord (a3). The crossed CST from the left M1 to the right upper cervical cord was reconstructed after excluding fibers reaching the right medial and left lateral and medial funiculi. (B) Tractography of the corticospinal tract superimposed on the individual fractional anisotropy color map of a control subject and two *DCC*-CMM patients. Individual coronal views at the level of the decussation are presented. Blue tracts represent the crossed CST, and red tracts the uncrossed CST. (C) The corticospinal tract laterality coefficient is expressed as (NF Crossed - NF Uncrossed)/(NF Crossed + NF Uncrossed), where NF is the number of fibers. The coefficient was positive for the two controls (indicating more fibers in the crossed corticospinal tract) and negative for the two *DCC*-CMM patients (indicating more fibers in the uncrossed corticospinal tract).

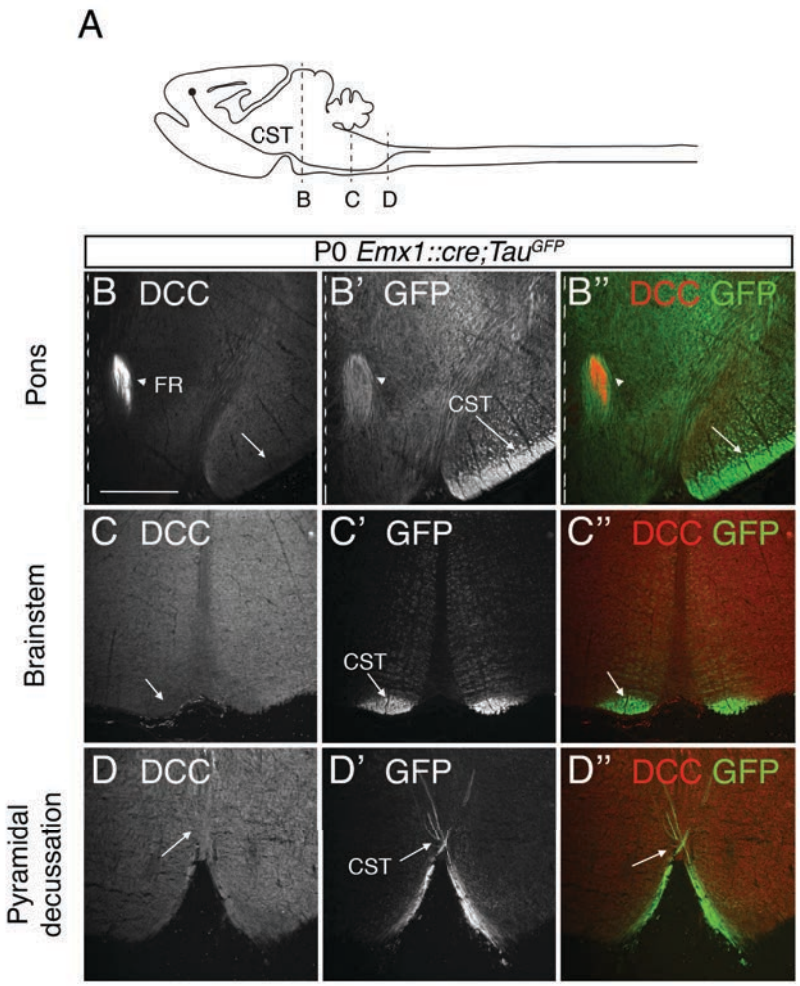

Figure 3. DCC is not detected in CST axons when they cross the midline. (A) Schematic representation of a P0 mouse sagittal section indicating the trajectory of the CST and the level of the coronal sections presented in this figure. Coronal sections of P0 *Emx1::cre;Tau*^{GFP} mice (n = 3) stained with anti-DCC (B-D), anti-GFP (B'-D'), and both labels (B"-D"). GFP staining was used as a marker of corticospinal tract axons. DCC was not detected at the CST in the pons (B), brainstem (C) or pyramidal decussation (D). DCC was expressed in the fasciculus retroflexus (FR, B), used as a positive control. Dashed lines indicate the midline. The scale bar represents 184 µm in B-D.

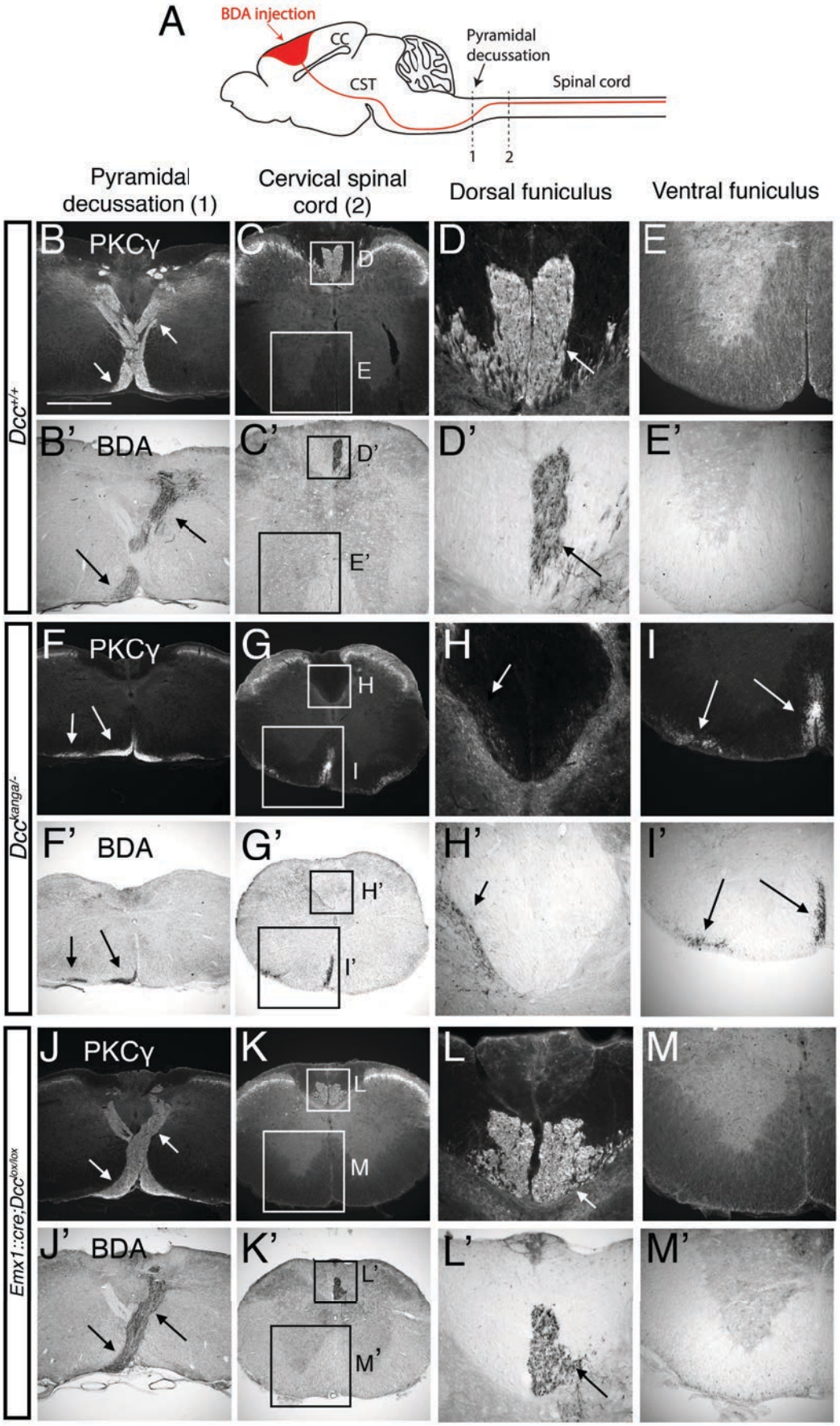
A
BDA injection
CC
CST
Pyramidal decussation
Spinal cord
1
2
Pyramidal decussation (1)
Cervical spinal cord (2)
Dorsal funiculus
Ventral funiculus
Dcc+/+
B PKCγ
C
D
E
B' BDA
C'
D'
E'
Dcckangal-
F PKCγ
G
H
I
F' BDA
G'
H'
I'
Emx1::cre;Dccflox/flox
J PKCγ
K
L
M
J' BDA
K'
L'
M'

Figure 4. Abrogation of neocortical DCC expression fails to reproduce the abnormal pyramidal decussation observed in *Dcc*$^{kanga/-}$ mice. (A) Schematic representation of an adult mouse sagittal section indicating the trajectory of the CST and the level of the coronal sections presented in this figure. Biotin dextran amine (BDA) was injected into the left motor cortex of *Dcc*$^{+/+}$ (n = 4; B-E, B'-E'), *Dcc*$^{kanga/-}$ (n = 4; F-I; F'-I') and *Emx1::cre;Dcc*$^{lox/lox}$ (n = 3; J-M, J'-M') mice to label the left-sided CST axons. The CST was visualized on coronal sections at the level of the pyramidal decussation and in the spinal cord, by immunostaining against the PKCγ (visualization of the two CSTs; B-M), or by revelation of the BDA tracer (visualization of the left-hand CST alone; B'-M'). The CST trajectory was similar in *Dcc*$^{+/+}$ (B-E) and *Emx1::cre;Dcc*$^{lox/lox}$ (J-M) mice. In *Dcc*$^{kanga/-}$ mice, the CST axons did not cross the midline at the pyramidal decussation (I) but spread in two bundles, one lateral and the other medial, that remained in the ventral ipsilateral spinal cord (F-I). The scale bar represents 336 µm in B, C, F, G, J, K; 168 µm in E, I, M; and 84 µm in D, H, L.

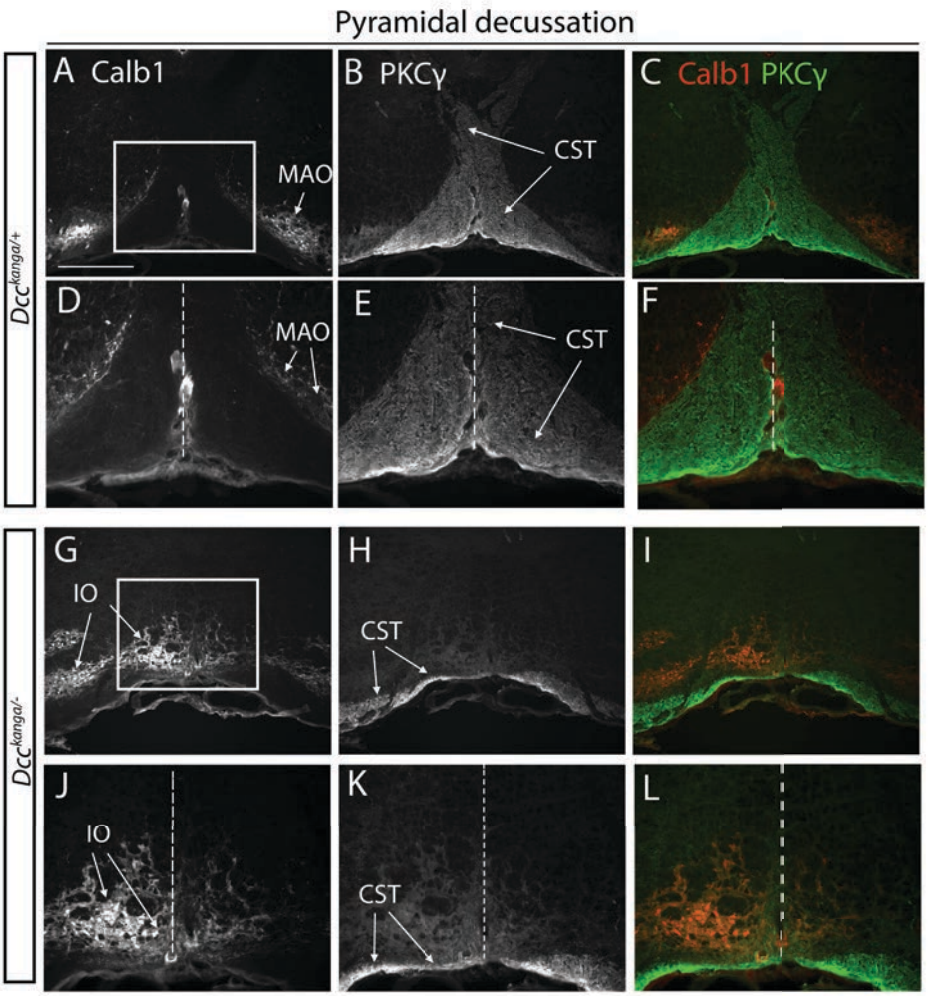

Figure 5. Absence of the pyramidal decussation and presence of inferior olivary neurons at the midline in mutants lacking functional DCC. The anatomy of the inferior olivary (IO) was investigated in adult *Dcc*$^{kanga/-}$ (n = 5) and *Dcc*$^{kanga/+}$ (n = 4) mice. IO neurons were immunostained for calbindin (Calb1). In adult *Dcc*$^{kanga/-}$ and *Dcc*$^{kanga/+}$ mice, the CST was visualized by PKCγ immunostaining. In controls, at the pyramidal decussation, the medial accessory olivary (MAO) neurons were located in a lateral position, while the CST axons turned medially and crossed the midline (A-F). At the most caudal part of the IO in *Dcc*$^{kanga/-}$ mice, the olivary neurons were located in a medial position (G-L). The dashed lines indicate the midline. The squares in A and G indicate the regions seen in D-F and J-L, respectively. The scale bar represents 168 µm in A-F and 84 µm in G-L.

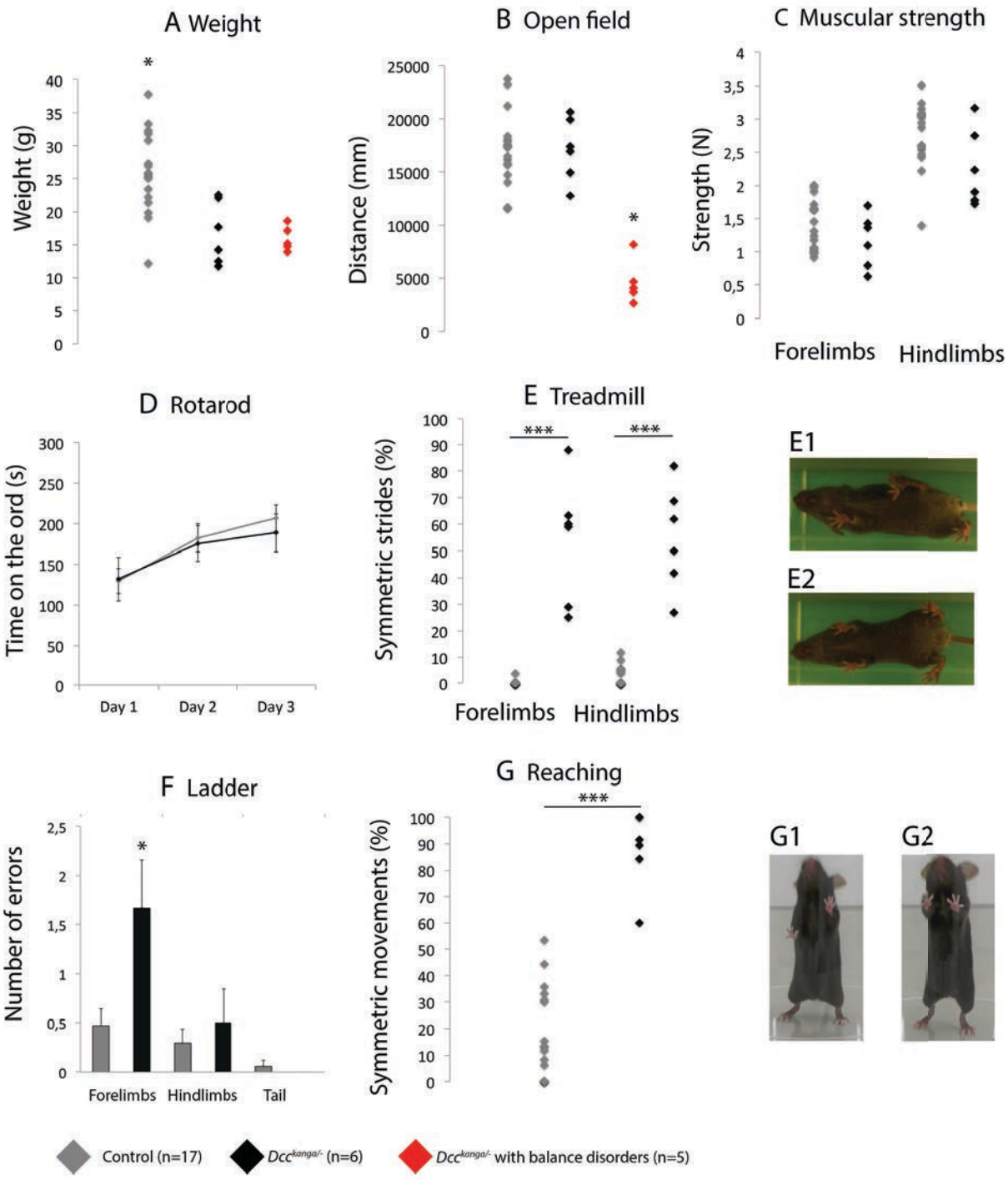

Figure 6. DCC is required for asymmetric movements. We used behavioral tests to investigate the motor phenotype of *Dcc*$^{kanga/-}$ mutant mice. *Dcc*$^{kanga/-}$ mice (n=11; black and red) were compared to *Dcc*$^{+/+}$ mice or *Dcc*$^{kanga/+}$ mice (that behave like wildtype mice, n=17; gray). Five of the 11 *Dcc*$^{kanga/-}$ mice displayed marked balance disorders (red): they were unable to stand on their limbs and thus moved very little in the open-field test (ANOVA $F_{(2,25)}$

= 33.18, $p < 0.001$, followed by the Bonferroni *post hoc* test; B). Because they were unable to perform most of the motor tests, they were excluded from further analysis. *Dcc*$^{kanga/-}$ mice were lighter than their littermate controls (ANOVA $F_{(2,20)} = 6.27$, $p = 0.008$, followed by the Bonferroni *post hoc* test; A) and were accordingly weaker in the muscle strength test (Student's test, $p_{forelimbs} = 0.228$; $p_{hindlimbs} = 0.042$; C). *Dcc*$^{kanga/-}$ mice were indistinguishable from controls in the Rotarod test (repeated-measures ANOVA with two factors. $F_{(1,21)} = 0.71$, $p = 0.793$, followed by the Bonferroni *post hoc* test; D). On the treadmill, *Dcc*$^{kanga/-}$ mice displayed a striking hopping gait, frequently moving both their forelimbs and their hindlimbs simultaneously (Mann-Whitney test, $p_{forelimbs} < 0.0001$; $p_{hindlimbs} < 0.0001$; E, E2). In contrast, control mice made alternating movements (E, E1) of their forelimbs and hindlimbs. In the ladder test, *Dcc*$^{kanga/-}$ mice made more forelimb errors than the controls (Freeman-Halton extension of Fisher's exact test, $p = 0.038$; F). When placed in a new walled environment, mice have a tendency to establish contacts on the walls with their forelimbs in an asymmetric (G1) or symmetric (G2) manner. In the reaching test, *Dcc*$^{kanga/-}$ mice made more symmetric forelimb movements than the controls (Student's test, $p < 0.0001$; G).

Table 1. Frequency, amplitude and latency of the ipsilateral MEPs in *DCC*-CMM patients

Subject	Gender/Age	MM WT score	Frequency of ipsilateral MEPs	Relative amplitude (MEPipsi/MEPcontra)	Latency of contralateral MEPs (ms)	Latency of ipsilateral MEPs (ms)
Patient 1	M/41	2	65%	4%	22,8	23,6
Patient 2	F/51	3	100%	47%	21,9	22,5
Patient 3	M/42	2	100%	392%	25,1	24,9
Patient 4	M/49	3	100%	322%	23,0	22,7
Patient 5	F/79	3	100%	409%	22,5	22,1
Patient 6	F/44	2	100%	ipsilateral MEPs only		20,7

The frequency of ipsilateral MEPs represents the percentage of trials in which unilateral stimulation of the dominant

hemishpere elicited ipsilateral muscular responses. MEP: motor evoked potentials; MM: mirror movements ;

WT: Woods and Teuber

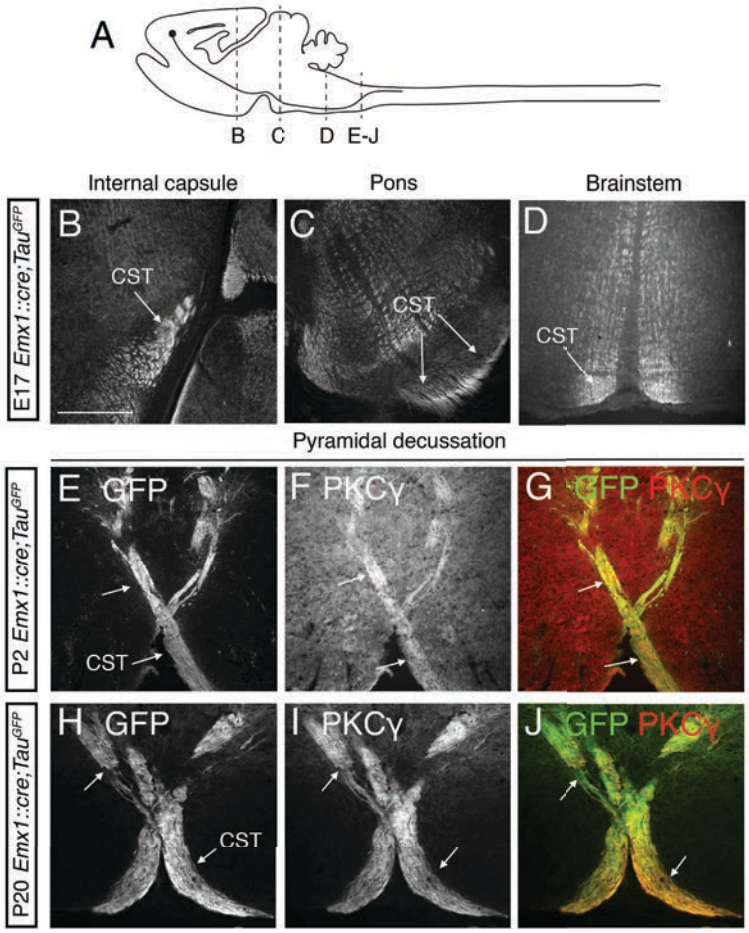

Supplementary Figure 1. EMX1 is expressed in CST neurons before they cross the midline. (A) Schematic representation of a mouse P2 sagittal section indicating the trajectory of the CST and the level of the coronal sections presented in this figure. Coronal sections of E17 (n = 3; B-D), P2 (n = 3; E-G) and P20 (n = 3; H-J) *Emx1::cre;Tau*^{GFP} mice stained with anti-GFP (B-M) and anti-PKCγ, a marker of the CST (E-J). At E17, GFP staining was detected along the entire trajectory of the CST axons: in the internal capsule (B); at the level of the pons, where the CST adopts a ventral position (C); and in the brainstem, in a ventral position (D). At P2 and P20, GFP staining co-located with PKCγ staining at the level of the pyramidal decussation (E-J). White arrows indicate CST axons. The scale bar represents 168 µm in B-J.

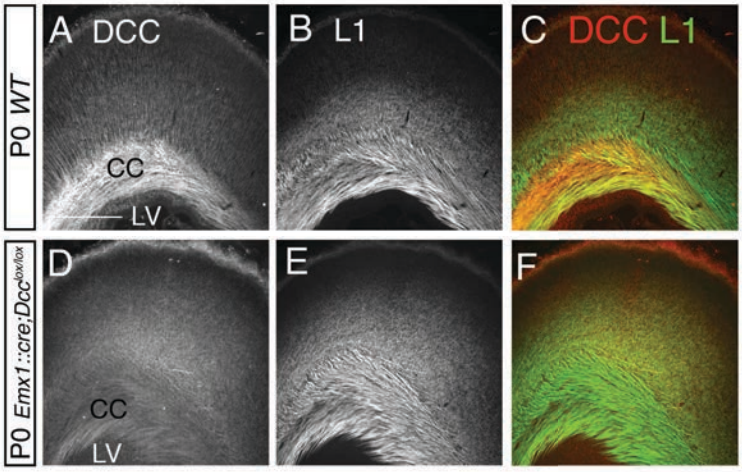

Supplementary Figure 2: DCC is expressed in the neocortex and CC of wild type mice but not in *Emx1::cre;Dcc*$^{lox/lox}$ mice. Coronal sections of P0 wild type mice (n = 3; A-C) and of P0 *Emx1::cre;Dcc*$^{lox/lox}$ mice (n = 3; D-F) stained with anti-DCC and anti-L1. At P0, DCC was detected in the neocortex and CC of wild type mice (A-C). However, it was not detected in the neocortex of *Emx1::cre;Dcc*$^{lox/lox}$ mice (D-F). The scale bar represents 168 µm in A-F. LV: lateral ventricule.

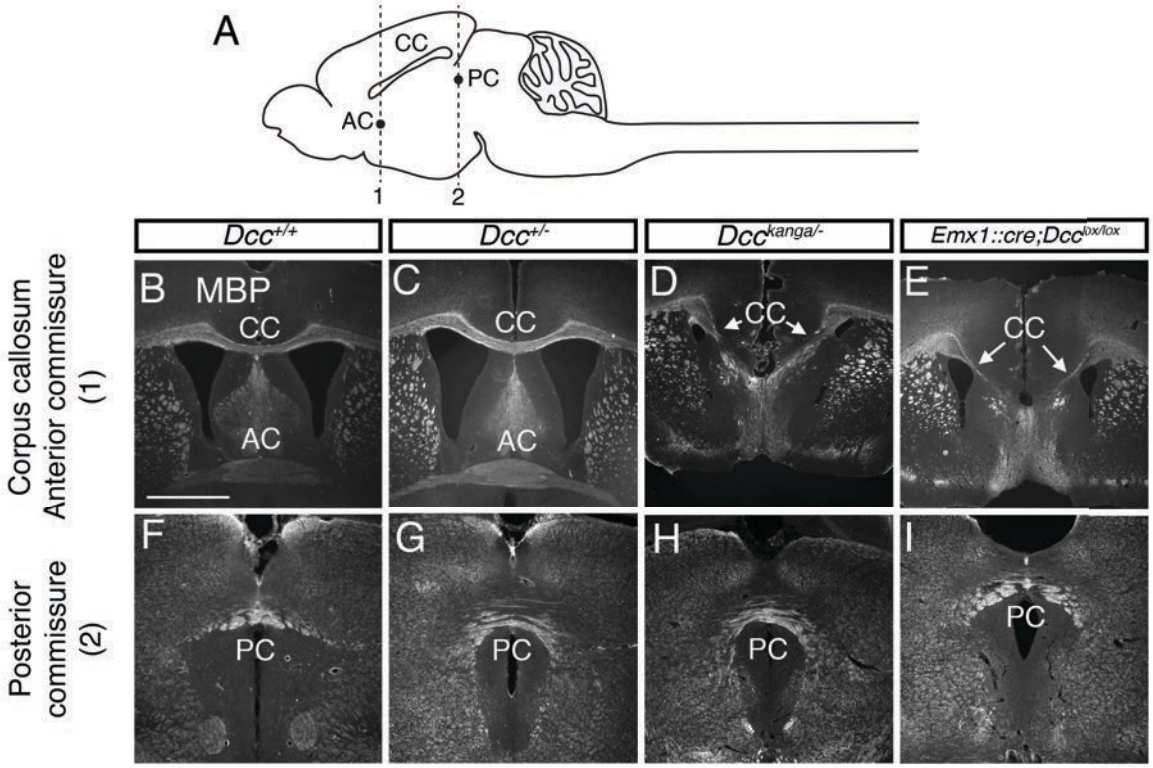

Supplementary Figure 3. Abrogation of neocortical DCC expression reproduces the lack of forebrain commissures observed in *Dcc*$^{kanga/-}$ mice. (A) Schematic representation of an adult mouse sagittal section indicating the level of the coronal sections presented in this figure. The corpus callosum (CC; B-E), anterior commissure (AC; B-E), and posterior commissure (PC; F-I) were revealed by myelin basic protein (MBP) immunostaining. The CC and AC were present in *Dcc*$^{+/-}$ mice (n = 4), as in *Dcc*$^{+/+}$ mice (n = 4; A-B). Note the absence of CC and AC in both *Dcc*$^{kanga/-}$ (n = 3; D) and *Emx1::cre;Dcc*$^{lox/lox}$ mice (n = 3; E). The posterior commissure was present in all *Dcc* mutants (F-I). The scale bar represents 672 µm in B-E and 336 µm in F-I.

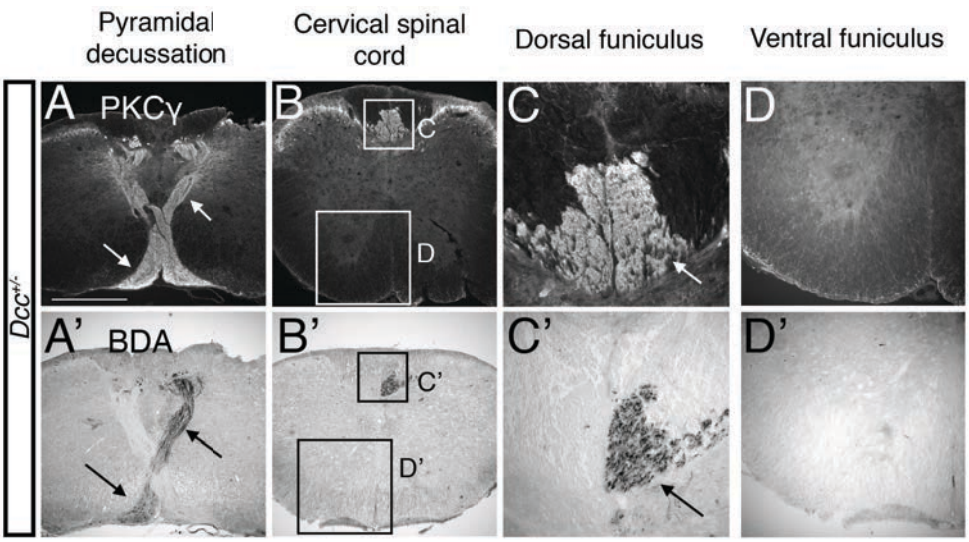

Supplementary Figure 4. The anatomy of the pyramidal decussation is normal in *Dcc*$^{+/-}$ mice. BDA was injected into the left motor cortex of adult *Dcc*$^{+/-}$ mice (n = 5) to label the left CST axons. The CST was visualized on coronal sections at the level of the pyramidal decussation and in the spinal cord by PKCγ immunostaining (visualization of the two CSTs; A-D), or by revelation of the BDA tracer (visualization of the left CST alone; A'-D'). The CST trajectory is normal in *Dcc*$^{+/-}$ mice: the CST axons cross the midline at the decussation (A, A'), turn dorsally and continue their trajectory in the dorsal funiculus of the contralateral spinal cord (B-D, B'-D'). The scale bar represents 336 µm in A, A', B, B'; and 168 µm in D, D'; 84 µm in C, C'.

II. Résultats complémentaires : Rôle de *Netrin-1* dans le guidage du FCS à la ligne médiane

NETRIN1, le ligand de DCC, est exprimé par de nombreuses structures au niveau de la ligne médiane du système nerveux central (Kennedy et al., 1994; Keino-Masu et al., 1996). L'effet chimio-attractif de NETRIN-1 permet aux axones commissuraux exprimant DCC de se diriger vers la ligne médiane puis de la franchir. Les mutants murins *Dcc*$^{-/-}$ et *Netrin1*$^{-/-}$ présentent des phénotypes similaires. En l'absence de *Netrin-1*, de nombreuses populations d'axones commissuraux exprimant DCC sont incapables de franchir la ligne médiane, notamment les commissures du cerveau antérieur ainsi que les axones commissuraux de la moelle (Serafini et al., 1996; Fazeli et al., 1997). Etant donné que les souris *Netrin1*$^{-/-}$ meurent à la naissance (Serafini et al., 1996), le rôle de cette molécule dans le développement du FCS n'a pas été étudié en détail. L'équipe d'Alain Chédotal a généré des mutants conditionnels présentant une délétion totale de *Netrin1* dans la plaque du plancher (floor plate) au niveau de la moelle et du tronc cérébral (souris *Shh::cre ;Netrin*$^{lox/lox}$). Cette lignée étant viable, nous avons analysé l'anatomie du FCS ainsi que le comportement moteur de ces mutants.

Nous avons procédé à des injections de BDA (biotinylated dextran amine) dans le cortex moteur gauche de souris adultes *Shh::cre;Netrin*$^{lox/lox}$ (n = 2), *Shh::cre;Netrin*$^{lox/-}$ (n = 2) et *Netrin*$^{lox/lox}$ (n = 3), comme décrit ci-dessus (Article 1 ; Figure 18A). Nous avons ensuite visualisé le FCS à différents niveaux du tronc cérébral et de la moelle. Dans la partie antérieure du tronc cérébral (avant l'OI), le FCS était similaire entre les mutants et les contrôles. En revanche, l'anatomie du FCS était anormale au niveau de l'OI chez les souris *Shh::cre;Netrin*$^{lox/lox}$. Tandis que chez les souris contrôle, le FCS est situé en position ventro-médiale, en dessous de l'olive (Figure 18C), nous avons observé que le FCS et l'olive étaient

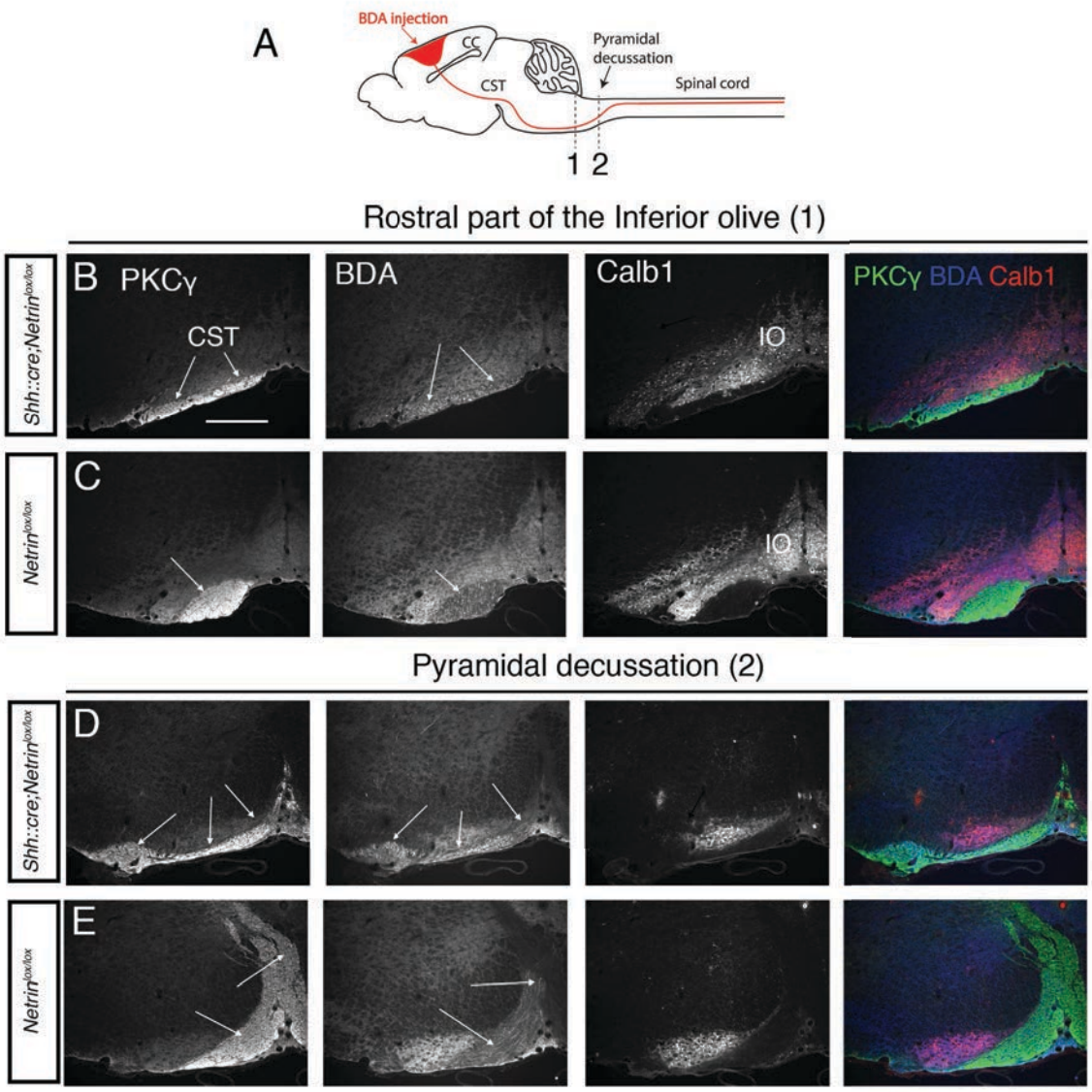

Figure 18. L'anatomie du FCS est anormale chez les souris Shh::cre;Netrin$^{lox/lox}$. (A) Représentation schématique d'une coupe sagittale de cerveau de souris adulte indiquant le niveau des coupes coronales présentées dans la figure. Nous avons injecté de la BDA dans le cortex moteur gauche de souris *Shh::cre ;Netrin$^{lox/lox}$*, *Shh::cre ;Netrin$^{lox/-}$* et *Netrin$^{lox/lox}$* afin de marquer les axones corticospinaux. Le FCS a été visualisé au niveau du tronc cérébral ou de la décussation par immuno-marquage anti-PKCγ ou par révélation de la BDA. Nous avons utilisé un immuno-marquage anti-Calb1 afin de marquer les neurones de l'olive inférieure (IO). La trajectoire du FCS était anormale chez les mutants *Shh::cre ;Netrin$^{lox/lox}$* et *Shh::cre ;Netrin$^{lox/-}$*. Au sein du tronc cérébral, chez les souris contrôles, le FCS était situé en position ventro-médiale, en dessous de l'olive (C), tandis que le FCS et l'olive s'étalaient anormalement en position latérale chez les mutants (comparer B et C). Au niveau de la décussation, une partie des axones corticospinaux croisait la ligne médiane, tandis que la majorité restait au sein de la moelle ipsilatérale, en position ventrale (comparer D et E). Les flèches blanches indiquent le FCS. CST : corticospinal tract; IO : inferior olive. La barre d'échelle représente 320 µm dans B-E.

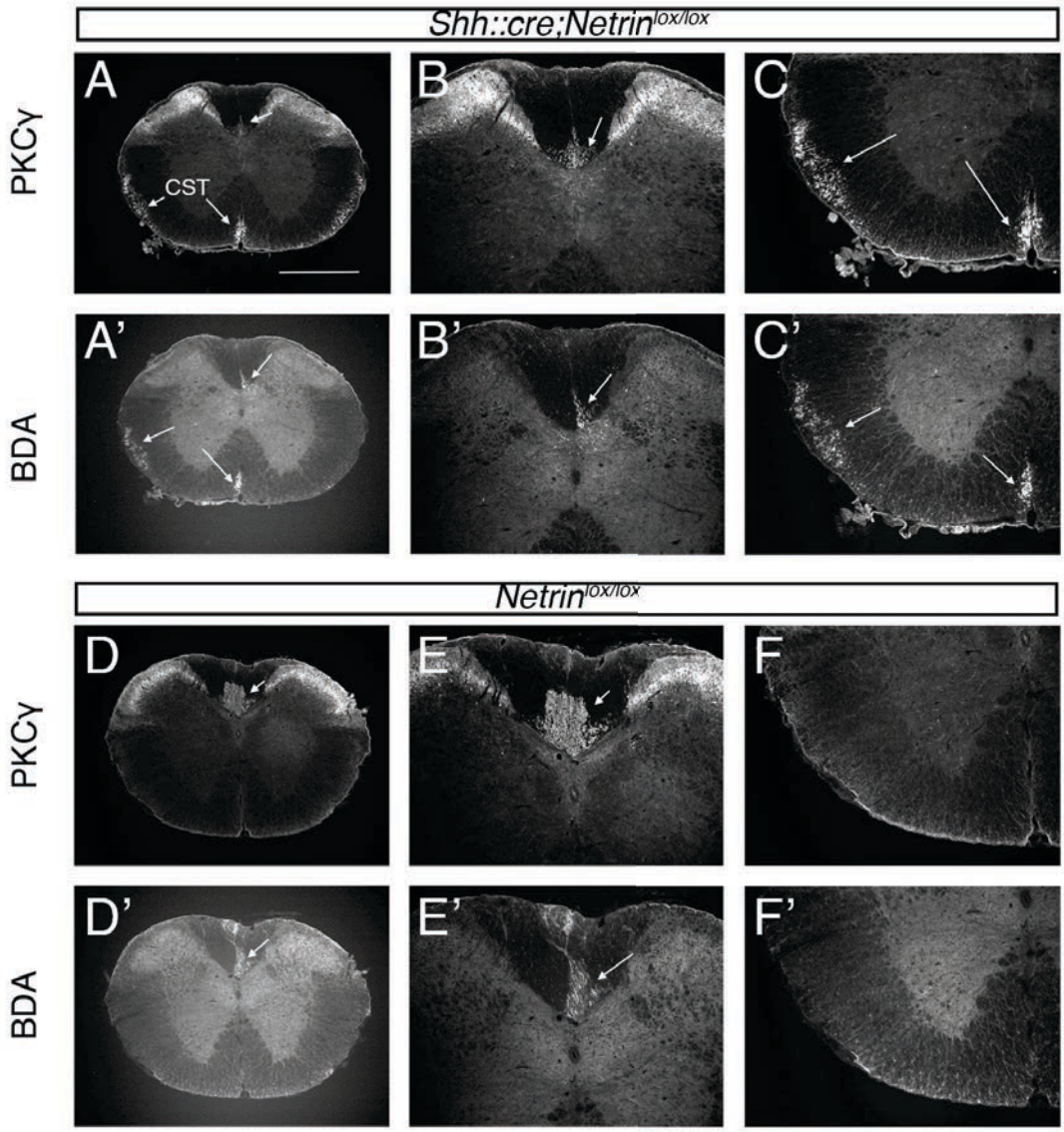

Figure 19. Organisation anormale du FCS dans la moelle chez les mutants Shh::cre;Netrin1$^{lox/lox}$ (suite de la figure 18). Au niveau de la moelle, trois composantes distinctes du FCS ont été identifiées chez les souris mutantes : (1) une partie des axones corticospinaux se trouvaient à son emplacement normal, dans le cordon dorsal de la moelle contralatérale à l'hémisphère d'origine (A, A', B, B') ; la majeure partie des axones n'avaient pas franchi la ligne médiane, et étaient restés au sein de la moelle ipsilatérale (2) en position ventrao-médiale, ou (3) en position ventro-latérale (A, A', C, C'). Au contraire, chez les contrôles, l'ensemble des axones corticospinaux se trouvait dans le cordon dorsal de la moelle contralatérale (D, D', E, E'), et aucune fibre n'a été observée au niveau du cordon ventral (F, F'). Les flèches blanches indiquent le faisceau corticospinal. L'échelle représente 640 µm dans A, D et 320 µm dans B, C, E, F.

anormalement étalés latéralement chez les mutants (Figure 18B). Au niveau de la décussation, une partie des axones corticospinaux parvenaient à franchir la ligne médiane, tandis que la majorité d'entre eux restait en position ventrale (comparer Figure 18D et 18E). En conséquence, l'organisation du FCS dans la moelle épinière des souris *Shh::cre;Netrin*$^{lox/lox}$ était complètement anormale, et trois composantes distinctes du FCS ont été identifiées : (i) une partie des axones corticospinaux se trouvait à son emplacement normal, dans le cordon dorsal de la moelle contralatérale à l'hémisphère d'origine (Figure 19A, A', B, B') ; la majeure partie des axones n'avait pas franchi la ligne médiane et était restée au sein de la moelle ipsilatérale (ii) en position ventro-médiale ; ou (iii) en position ventro-latérale (Figure 19 A, A', C, C'). Au contraire, chez les souris contrôles, l'ensemble des axones corticospinaux se trouvait dans le cordon dorsal de la moelle contralatérale (Figure 19 D, D', E, E'), et aucune fibre n'a été détectée au niveau du cordon ventral (Figure 19 F, F'). Nous avons observé les mêmes défauts chez les souris *Shh::cre;Netrin*$^{lox/-}$.

Nous avons ensuite analysé le phénotype moteur de souris *Shh::cre;Netrin*$^{lox/lox}$ (n = 10) et de contrôles *Netrin*$^{lox/lox}$ (n = 10) en utilisant les tests comportementaux décrits précédemment (Article 1). Il n'y avait pas de différence de poids entre les deux groupes (*t* test, p = 0.653, Figure 20A). La distance parcourue par les souris *Shh::cre;Netrin*$^{lox/lox}$ dans l'open-field était moins importante que celle parcourue par les contrôles (*t* test, p = 0.004, Figure 20B). Les performances des deux groupes étaient similaires pour le test de la force musculaire (*t* test, $p_{antérieur}$ = 0.271 ; $p_{postérieur}$ = 0.367, Figure 20C), du rotarod (2x2 ANOVA, F = 1.590, p = 0.223, Figure 20D), du treadmill (test de Mann-Whitney, $p_{antérieur}$ = 0.739, $p_{postérieur}$ = 0.315, Figure 20E) et de l'échelle de marche (2x2 ANOVA, F = 18, p = 0.395, Figure 20G). Nous avons ensuite utilisé des tests permettant d'évaluer de façon plus spécifique les conséquences de défauts anatomiques du FCS. Au cours de la locomotion libre,

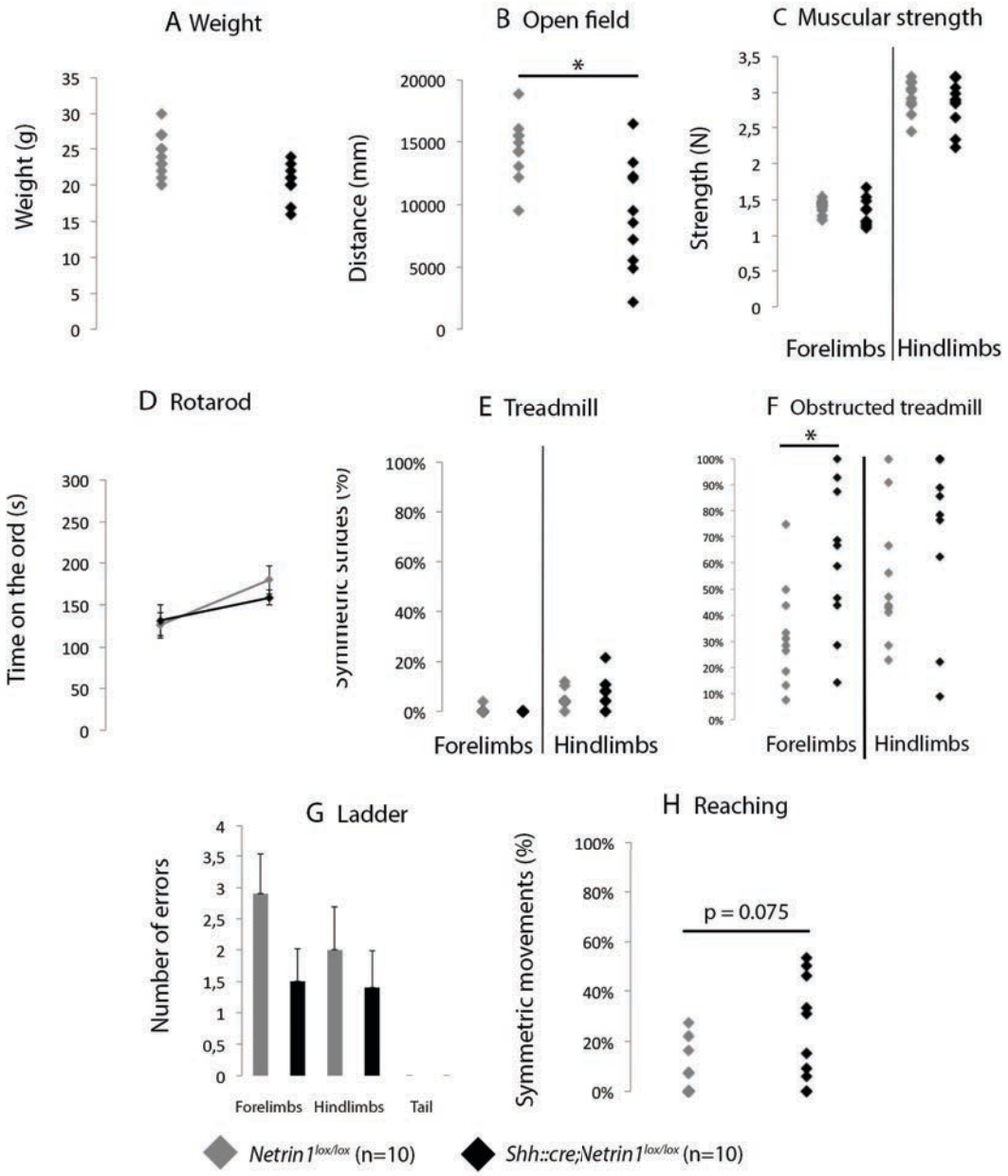

Figure 20. *Netrin-1* est impliquée dans la génération de mouvements asymétriques des membres antérieurs. Nous avons analysé le phénotype moteur de souris *Shh::cre ;Netrin*$^{lox/lox}$ et de contrôles *Netrin*$^{lox/lox}$. Il n'y avait pas de différence de poids entre les deux groupes (*t* test, p = 0.653, A). La distance parcourue dans l'open-field par les souris *Shh::cre;Netrin*$^{lox/lox}$ était moins importante que celle parcourue par les contrôles (*t* test, p = 0.004, B). Les performances des deux groupes étaient similaires pour le test de la force musculaire (*t* test, $p_{antérieur}$ = 0.271 ; $p_{postérieur}$ = 0.367, C), du rotarod (2x2 ANOVA, F = 1.590, p = 0.223, D), du treadmill (test de Mann-Whitney, $p_{antérieur}$ = 0.739, $p_{postérieur}$ = 0.315, E) et de l'échelle de marche (2x2 ANOVA, F = 18, p = 0.395, G). Les souris *Shh::cre ;Netrin*$^{lox/lox}$ produisaient des mouvements majoritairement symétriques avec les membres antérieurs au cours des tests du treadmill avec obstacles (test de Mann Whitney, $p_{antérieur}$ = 0.029, $p_{postérieur}$ = 0.19, F) et du « reaching » exploratoire (test de Mann Whitney, p = 0.075, H).

les circuits impliqués dans la génération des mouvements alternés des membres sont principalement spinaux. Au contraire, lors de phases de locomotion nécessitant de franchir des obstacles, un contrôle supra-spinal est mis en jeu et fait intervenir le FCS (Borgius et al., 2014; Serradj et al., 2014; Welniarz et al., 2015). Au cours de la locomotion avec obstacles, la proportion de mouvements symétriques produits avec les membres antérieurs était plus importante chez les souris *Shh::cre;Netrin*$^{lox/lox}$ que chez les contrôles (test de Mann Whitney, $p_{antérieur} = 0.029$, $p_{postérieur} = 0.19$, Figure 20F). Lorsque les souris sont placées dans un nouvel environnement, elles ont tendance à se redresser sur leurs membres postérieurs et à établir des contacts avec la paroi avec leurs membres antérieurs, de façon asymétrique ou symétrique (Serradj et al., 2014). Au cours de ce test du reaching exploratoire, les souris *Shh::cre;Netrin*$^{lox/lox}$ ont produit plus de mouvements symétriques que les souris contrôles (test de Mann Whitney, $p = 0.075$, Figure 20H).

Ces résultats soulignent l'importance du couple NETRIN1-DCC dans le développement du système moteur, et en particulier du FCS. Il est intéressant de remarquer que les mutants *Shh::cre;Netrin*$^{lox/lox}$, au même titre que les souris *Dcc*^{kanga}, présentent une association entre des défauts de guidage du FCS à la ligne médiane et des anomalies anatomiques de l'OI. Nous discuterons de façon plus approfondie ces résultats dans la partie II. B de la discussion.

III. Article 2 : Des mutations du gène *NETRIN1* sont responsables du syndrome des mouvements en miroir congénitaux (soumis)

Une partie du travail de l'équipe est concentrée sur les aspects génétiques des MMC, et notamment sur la recherche de nouveaux gènes responsables de cette pathologie. En effet, les mutations des gènes *RAD51*, *DCC* et *DNAL4* ne représentent que 35% des cas répertoriés (Meneret et al., 1993). Aurélie Méneret, en collaboration avec l'équipe de Liz Franz en Nouvelle-Zélande, a donc réalisé une analyse génétique par séquençage d'exomes de 25 patients atteints de MMC ne présentant aucune mutation dans *RAD51*, *DCC* ou *DNAL4*. Plus de 35000 variants génétiques ont été analysés chez chaque individu, et ces variants ont été classés en fonction de différents critères. Les variants les plus communs ou ceux n'étant pas situés dans des régions codantes ont été éliminés. Aurélie Méneret a ensuite suivi une approche dite de « gène candidat », c'est-à-dire qu'elle a pondéré les résultats de l'analyse d'exomes par la proximité des gènes identifiés avec *RAD51* ou *DCC*. En effet, si des mutations des gènes *RAD51* et *DCC* ont été identifiées chez des patients atteints, il est probable que d'autres mutations touchant les mêmes voies de signalisation puissent produire le même phénotype. Cette approche a mené à l'identification de mutations hétérozygotes du gène *NETRIN1*, le ligand de DCC, dans deux familles de patients atteints de MMC (une mutation faux-sens et une délétion d'acide aminé sans décalage du cadre de lecture) ainsi que dans un cas sporadique (mutation faux-sens).

L'équipe d'Alain Chédotal a ensuite procédé à des tests *in vitro* afin d'évaluer le caractère pathogène de ces mutations. Les trois formes mutées de *Netrin1* ont été introduites dans des plasmides et transfectées dans des cellules HEK. Les trois formes mutées de la protéine ont été détectées dans le lysat total des cellules, signifiant que la protéine mutée était bien produite. En revanche, aucune des trois formes mutées de la protéine n'a été détectée dans le surnageant des cellules, contrairement à la forme non mutée. Ces résultats suggèrent

que les trois mutations du gène *NETRIN1* identifiées chez les patients MMC aboutissent à la production d'une protéine qui n'est pas sécrétée en dehors de la cellule.

Nous avons reçu un patient MMC avec une mutation de *NETRIN1* dans le cadre de notre protocole, et j'ai procédé aux analyses électrophysiologiques et de neuroimagerie décrites dans l'article 1. L'IRM anatomique n'a révélé aucune anomalie majeure du système nerveux central. En particulier, le CC était présent et apparemment normal. La stimulation de l'aire de la main du M1 par SMT a engendré des réponses musculaires au niveau de la main ipsilatérale, réponses qui étaient totalement absentes chez les sujets sains (ces derniers présentant des réponses strictement contralatérales à l'hémisphère stimulé). Les mêmes expériences menées sur un patient néo-zélandais ont conduit à des résultats similaires. Cela démontre l'existence de projections corticospinales anormales depuis le cortex moteur vers la moelle ipsilatérale chez ces deux patients *NETRIN1*. Afin de déterminer plus précisément la cause de ces anomalies électrophysiologiques, nous avons étudié l'anatomie du FCS chez notre patient et chez un volontaire sain avec des techniques de tractographie. Cette analyse a révélé que chez le patient *NETRIN1*, la décussation pyramidale était anormale. En effet, le ratio entre le nombre de fibres corticospinales non-croisées et croisées était beaucoup plus important que chez le patient que chez le sujet sain. Ces résultats démontrent que NETRIN1 est impliquée dans le développement du FCS et la formation de la décussation pyramidale chez l'humain.

Mutations in the netrin-1 gene cause congenital mirror movements

A.Méneret,[1,2] E.A. Franz,[3] O. Trouillard,[1] T. Oliver,[4] Y. Zagar,[5] R.J.M. Gardner,[6] Q. Welniarz,[1,7] S.P. Robertson,[6] C. Gallea,[1] M. Srour,[8,9] C. Depienne,[1,10] C.L. Jasoni,[11] Caroline Dubacq,[7] F. Riant,[12,13] J.C. Lamy,[1] M.P. Morel,[7] M. Vidailhet,[1,2] I. Dusart,[7] G. Rouleau,[8,14,15] A. Brice,[1,10] A. Chédotal,[5] E. Roze,[1,2*] and D. Markie.[4*]

[1] Inserm U 1127, CNRS UMR 7225, Sorbonne Universités, UPMC Univ Paris 06 UMR S 1127, CIC-1422, Institut du Cerveau et de la Moelle épinière, ICM, F-75013, Paris, France

[2] AP-HP, Hôpital de la Pitié-Salpêtrière, Département de Neurologie, F-75013, Paris, France

[3] Department of Psychology and fMRI*otago*, University of Otago, Dunedin, New Zealand

[4] Pathology Department, Dunedin School of Medicine, University of Otago, Dunedin, New Zealand

[5] Sorbonne Universités, UPMC Univ Paris 06, INSERM, CNRS, Institut de la Vision, F-75012, Paris, France

[6] Department of Women's and Children's Health, Dunedin School of Medicine, University of Otago, Dunedin, New Zealand

[7] Sorbonne Universités, UPMC Univ Paris 06, INSERM, CNRS, Neuroscience Paris Seine, F-75005 Paris, France

[8] Department of Neurology and Neurosurgery, McGill University, Montreal, Quebec, H3A 2B4, Canada

[9] Department of Paediatrics, McGill University, Montreal, Quebec, H4A 3J1, Canada

[10] AP-HP, Hôpital de la Pitié-Salpêtrière, Fédération de Génétique, Département de Génétique et de Cytogénétique, Paris, France

[11] Department of Anatomy, Otago School of Medical Sciences, University of Otago, Dunedin, New Zealand

[12] AP-HP, Groupe hospitalier Lariboisière-Fernand Widal, Laboratoire de Génétique, Paris, France

[13] INSERM UMR_S740, Université Paris 7 Denis Diderot, Paris, France

[14] Montreal Neurological Institute, Montreal, Quebec, H3A 2B4, Canada

[15] Department of Human Genetics, McGill University, Montreal, Quebec, H3A 2B4, Canada

[*] These authors contributed equally to this work

Correspondence to Emmanuel Roze, Département de Neurologie, Groupe Hospitalier Pitié-Salpêtrière, 47-83 Boulevard de l'Hôpital, 75651 Paris cedex 13, France

E-mail: emmanuel.flamand-roze@aphp.fr

Phone: +33142162748; Fax: +33142162474

Summary paragraph

Netrin-1 is a secreted protein first identified 20 years ago as an axon guidance molecule regulating midline crossing in the central nervous system. It has since been shown to play critical roles in various tissues throughout development as well as in tumorigenesis and inflammation in adulthood. Despite extensive studies, no human disease has been directly associated with mutations in *NTN1*, the gene coding for netrin-1. Congenital mirror movements is a neurodevelopmental disorder characterized by involuntary movements of one hand that mirror intentional movements of the opposite hand. Here we show, in three unrelated families, that mutations in exon 7 of *NTN1* cause isolated congenital mirror movements through a defect in netrin-1 secretion. The pathophysiology likely involves haploinsufficiency and subsequent disruption of axon guidance with abnormal decussation of the corticospinal tracts. Given the numerous roles of netrin-1, the absence of manifestations other than mirror movements is unexpected.

Text

Netrins are a family of extracellular proteins regulating cell migration and survival during development and adulthood. The first member, netrin-1, was identified as a secreted protein mediating axon guidance in the spinal cord.[1] It is expressed at the midline of the developing central nervous system (CNS), where it acts as an attractive or repulsive cue for different populations of crossing/commissural axons.[2] In *netrin-1* knockout mice, many axons fail to cross the midline in the corpus callosum, the hippocampal and anterior commissures, the corticospinal tract (CST) and the spinal cord.[3-5] Netrin-1 binds to several transmembrane receptors including DCC (deleted in colorectal carcinoma)[6] and UNC5s, which respectively mediate attractive or repulsive axonal responses to netrin-1.

However, netrin-1 exerts a variety of functions beyond axon guidance and is involved in synaptogenesis, apoptosis, cell migration and angiogenesis.[7,8] There is also evidence

suggesting that netrin-1 influences remyelination and tumorigenesis.[9,10] Netrin-1 is a promising therapeutic target and/or biomarker in cancer, cardiovascular disease, neuroinflammation and kidney disease.[10-12] Variants in *UNC5C* have been linked to Alzheimer's disease and colorectal cancer,[13] while mutations in *DCC* have been shown to cause the rare disorder congenital mirror movements (CMM).[14] However, the 20th anniversary of the discovery of netrin-1 has passed without the identification of a single human disease caused by mutations in *NTN1*, the gene coding for netrin-1.

CMM is characterized by involuntary movements of one side of the body that accompany and mirror intentional movements on the opposite side (OMIM #157600).[15] CMM mostly involve the hands. Affected subjects are unable to perform pure unimanual movements and have difficulty with skills requiring dissociated movements of the two hands. It has been described as a familial disorder with autosomal dominant inheritance and incomplete penetrance, but simplex cases also exist. The pathophysiology of CMM is likely related to developmental abnormalities of the CST, which convey motor outputs from the motor cortex to the contralateral side of the body, and of the corpus callosum, which underlies communication between motor cortices. CMM usually involve abnormal decussation of the corticospinal tracts and altered interhemispheric inhibition with bilateral activation of the primary motor cortices during unimanual movements.[16,17] The known culprit genes are *DCC*, *RAD51*, which encodes a DNA repair protein, and possibly *DNAL4*, which encodes an axonemal dynein light chain.[14,18-20] However, only 35% of affected individuals or families carry a pathogenic variant in one of these genes.[15] We suspected that mutations in other axon guidance genes, particularly those interacting with DCC or belonging to the netrin-1/DCC pathway, might cause CMM. To explore this hypothesis, exome sequencing was conducted in 25 index cases of CMM (8 familial and 17 sporadic) without mutations in *DCC*, *RAD51* or *DNAL4*. Patient characteristics and genetic findings are summarized in Extended Data Table 1. More than

35000 variants were identified per individual. We initially filtered the data to remove variants that are too common to explain the low prevalence of the disorder [allele frequency greater than 0.1% in the ExAC database, comprising exome data of 60,706 unrelated individuals (Exome Aggregation Consortium, Cambridge, MA)], those unlikely to affect protein-coding genes (intronic and synonymous), and low confidence variant calls owing to poor coverage in our data (read depth less than 10x). Genes were then prioritized as candidates by known connection to *DCC* and *RAD51* function, by the number of unrelated individuals with variants, by functional prediction scores and by the rarity of variants in the ExAC database. Despite only two individuals carrying heterozygous variants, the most compelling candidate was the *NTN1* gene, coding for netrin-1, a known ligand for DCC. One missense variant (c.1801T>C/p.Cys601Arg) of *NTN1* segregated with CMM in all 3 affected members of a French family (Figure 1a), was predicted to be pathogenic by the Sift and Polyphen2 algorithms and was absent from the ExAC database. An in-frame deletion (c.1552_1554delCAT/p.Ile518del) of *NTN1* segregated with CMM in all 3 affected members of a family from the United Kingdom collected in New Zealand (Family C in Franz et al., 2015)[21] (Figure 1b) and was also absent from the ExAC database. Sequencing of the *NTN1* gene in 22 additional index cases (20 sporadic and 2 familial, all negative for *DCC* and *RAD51*) found another missense variant of *NTN1* (c.1802G>C/p.Cys601Ser) in a sporadic case (Figure 1c). This variant was also predicted to be pathogenic by Sift and Polyphen2 and was absent from the ExAC database. In addition, all 3 variants alter amino acids that are highly conserved among species (Extended Data Figure 1).

To assess the pathogenicity of the 3 variants, mutations (I518del, C601R, C601S) were introduced into mouse and human netrin-1 cDNAs fused to an alkaline phosphatase (AP) reporter. We showed that the mutated netrin1-AP proteins could be detected in HEK293 cell lysates, but that they were absent from the supernatant, contrary to the wild type (WT)

netrin1-AP constructs (Figure 2a-b). Similar results were obtained using untagged human netrin-1 and a netrin1^{C601R} variant (Figure 2c-b). These experiments show that all three *NTN1* mutations found in CMM patients likely prevent the secretion of netrin-1.

Clinically, the patients (including an 81 year old asymptomatic carrier) had normal eyesight, no oculomotor abnormalities, no cardiovascular or respiratory disease, no inflammatory disease and no cancer. Except for mirror movements, neurological examination was normal. Some of the patients had irritable bowel syndrome and/or peripheral vasoconstriction when exposed to cold. Brain MRI was normal, showing no corpus callosum hypoplasia or visible pontine abnormalities (Extended Data Figure 2). We used Tractography to investigate the projection of the CST in one patient and one control subject (Figure 3). Results suggested that a higher proportion of fibres was located in the crossed compared to the uncrossed CST in the control, whereas a higher proportion of fibres was located in the uncrossed CST in the patient (Figure 3b). We then used single pulse transcranial magnetic stimulation (TMS) to study the propagation of neural signals along the CST in two patients and two controls. We found that unilateral stimulation of the primary motor cortex frequently elicited bilateral motor evoked potentials (MEPs) in patients, compared to strictly unilateral MEPs, contralateral to the stimulation, in controls (Figure 4, Extended Data Table 2).

We have shown in two unrelated families and one sporadic case that heterozygous mutations in exon 7 of *NTN1* cause autosomal dominant CMM through a defect in netrin-1 secretion. Since netrin-1 is a diffusible extracellular cue, the pathophysiology probably involves haploinsufficiency. As a consequence, midline axon guidance was likely disrupted in the patients.

Despite the small number of patients, both tractography and TMS results converged to support the existence of an abnormal uncrossed CST in *NTN1* patients. This is consistent with findings in severe hypomorphic *NTN1* mutant mice that show much-reduced decussation of

the CST.[4] These mutants also exhibit corpus callosum agenesis,[5] absence of forebrain commissures and defects in spinal commissural axon projections.[3] *NTN1* hypomorphic mutants usually die shortly after birth. *DCC* knockout mice also display commissural axon guidance defects and are not viable.[22] Electrophysiological recordings in embryonic spinal cord preparations showed that neuronal circuits controlling locomotion are disorganized in *DCC* and *NTN1* mutants.[23] In addition, *DCC* mutants carrying the "kanga" mutation (which results in a deletion of the P3 domain in the cytoplasmic tail of DCC) have a hopping gait.[4] These mice also present with corpus callosum agenesis and defects in the decussation of the CST. This is consistent with the abnormalities found in CMM patients, involving both altered interhemispheric inhibition and abnormal decussation of the CST.[16,17]

Given the numerous roles of netrin-1 during development and beyond, the absence of manifestations other than mirror movements is quite surprising. Patients could be expected to have vision and hearing impairment,[24] oculomotor abnormalities,[25] hypogonadism,[26] cardiovascular diseases,[11] cancers[10] and inflammatory diseases.[12] Irritable bowel syndrome[27] and temperature regulation issues[8] have been observed in two patients, but might be unrelated because of their high prevalence in the general population. A possible explanation could be that the midline guidance function of netrin-1 is the most sensitive to gene dosage, with abnormalities occurring when only 50% of the protein is expressed, whereas alterations of other functions require greater deficits. The study of *NTN1* conditional knockout mice[8] might allow for a better understanding of the pathogenic underpinnings of CMM in *NTN1* patients.

The mechanism by which *NTN1* mutations alter netrin-1 secretion is unknown. Despite the fact that all 3 reported mutations alter the C-terminal part of the protein, this domain is not required for proper secretion.[28] The mutated proteins do not seem to be degraded either, as they are detectable in cell lysates. The mutations might induce alterations of the protein structure that interfere with the secretion process. The cysteine in position 601 seems to be of

particular importance, as it is mutated in 2 of our 3 families. The 6 conserved cysteines located in the NTR module form disulphide bonds that might be important for the structure of netrin-1.[29] Alternatively, the mutations might induce a reduced half-life of the secreted protein, preventing detection in the supernatant, or an abnormal relocation of the protein to other cell compartments. This hypothesis is consistent with reports of the existence of a nucleolus localization signal in the C-terminal part of netrin-1.[30] Further studies are needed to decipher the exact mechanisms by which *NTN1* mutations induce a defect in netrin-1 secretion. Since netrin-1 is considered as a potential therapeutic target for cancer and inflammatory diseases, identification of these mechanisms might open new therapeutic avenues.

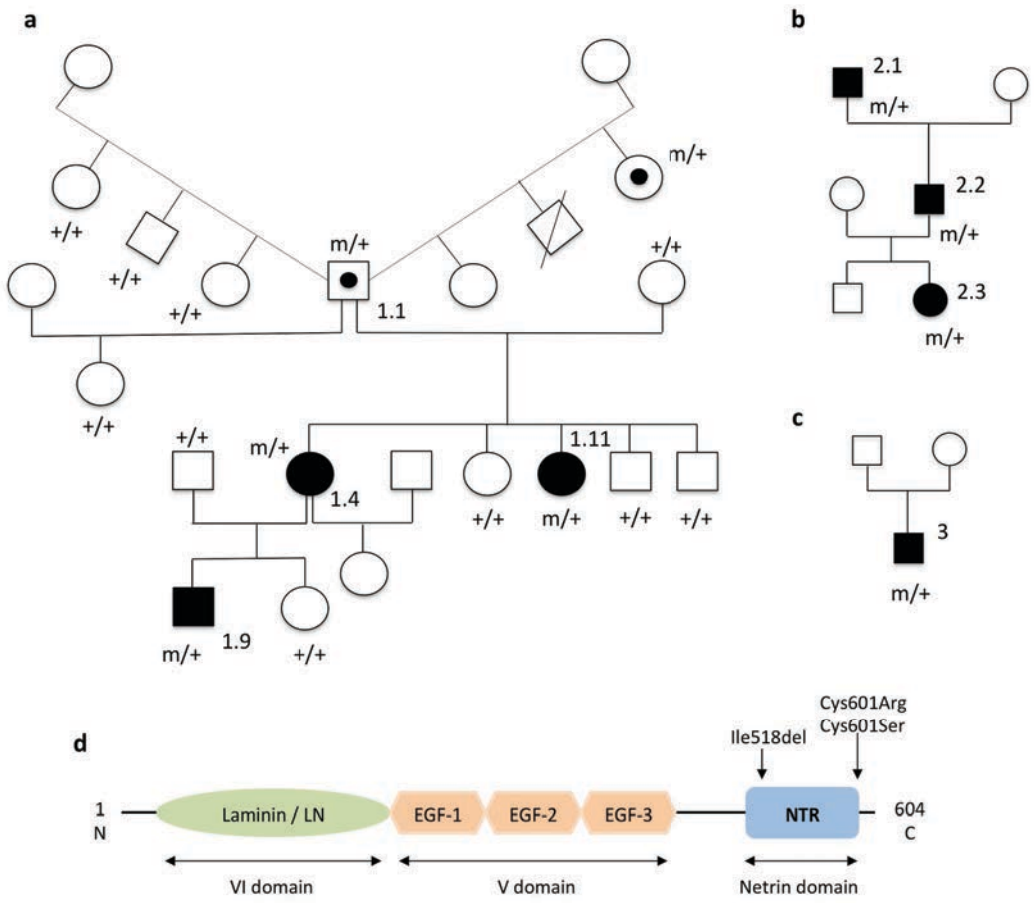

Figure 1. Pedigrees of the CMM families and distribution of the mutations in *NTN1*.

(a) Family 1 (from France) with a C601R mutation (the unusual family tree is due to the fact that individual 1.1 had children with 4 different women), (**b**) Family 2 (from the United Kingdom, collected in New Zealand, previously identified as family C in Franz et al., 2015) with a I518del mutation, (**c**) Canadian sporadic case with a C601S mutation.

(d) Schematic of the netrin-1 protein showing the laminin (LN) domain, the 3 Epidermal Growth Factor (EGF) – like domains and the Netrin (NTR) domain. Arrowheads show the location of the 3 mutations.

Filled symbols represent individuals with CMM, symbols with an embedded filled circle asymptomatic carriers, empty symbols unaffected individuals, squares are male and circles are female.

m: mutated allele, +: wild type allele.

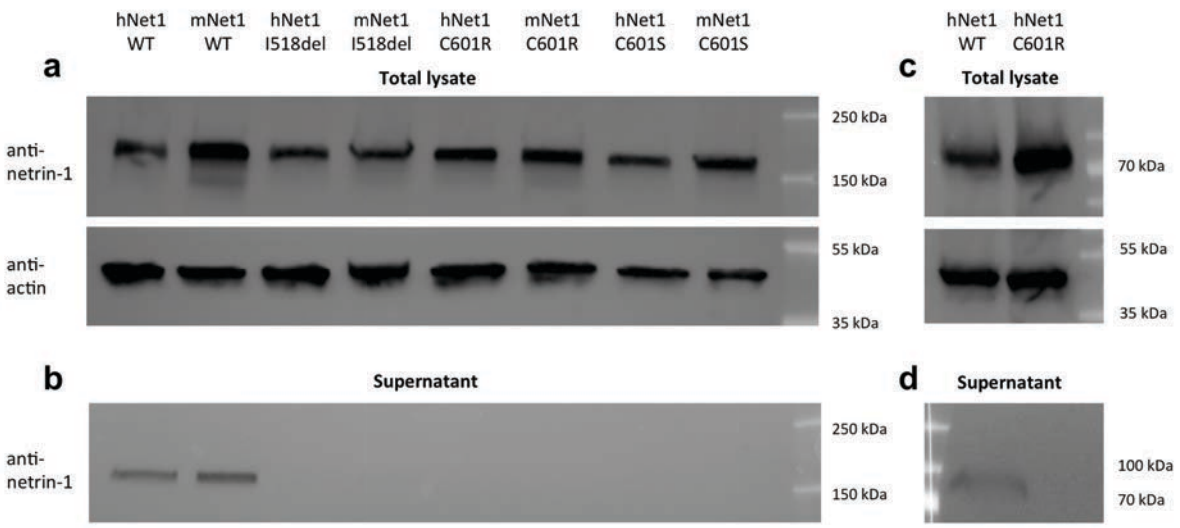

Figure 2. Expression of the WT and mutated netrin-1-AP and netrin-1 constructs.

HEK293 cells were transfected with mouse and human WT and mutated netrin1-AP **(a, b)** or human WT and mutated netrin-1 **(c, d)** plasmids and grown for 48 hours. Western blot showed the presence of the WT and mutated proteins in total lysates at the expected molecular weight **(a, c)** but the absence of the mutated proteins in the supernatant, contrary to WT **(b, d)**. Antibodies were anti-netrin-1 (a, b, c, d) and anti-actin (a, c).

AP: alkaline phosphatase, WT: wild type, h: human, m: mouse, Net1: netrin-1.

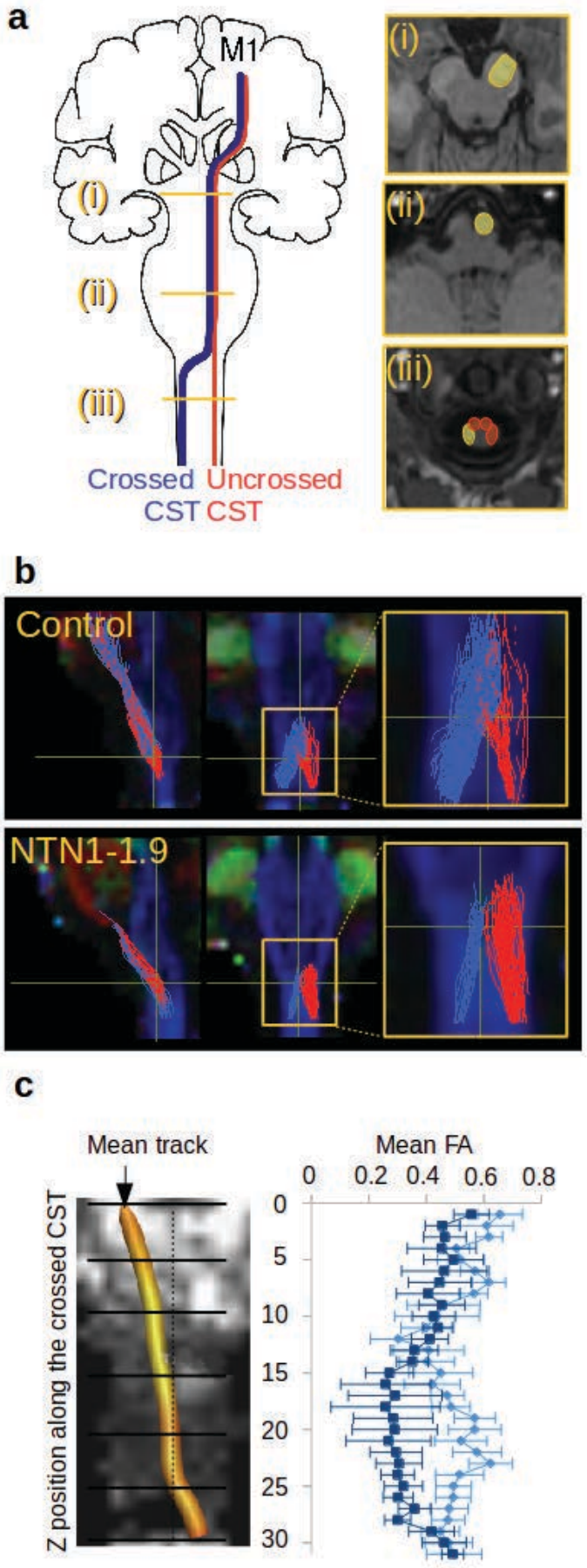
a
M1
(i)
(ii)
(iii)
Crossed CST
Uncrossed CST
b
Control
NTN1-1.9
c
Mean track
Mean FA
0
0.2
0.4
0.6
0.8
Z position along the crossed CST
0
5
10
15
20
25
30

Figure 3. Corticospinal tract analysis using tractography.

(a) Left: Diagram showing color coding of the crossed (blue) and uncrossed (red) corticospinal tracts; Right: Regions of interest (both in the diagram and superimposed on an axial slice of an anatomical image of a participant) used to reconstruct the fibre tracts at the base of the pontine (i), the anterior pyramid in the upper medulla (ii), and the crossed lateral (yellow) funiculus of the upper cervical cord (iii). For example, the crossed CST from the right M1 to the left upper cervical cord was reconstructed excluding fibres reaching the left medial and the right lateral and medial funiculus (red). **(b)** Tractography of the corticospinal tract superimposed on the individual fractional anisotropy colour map of a control subject (Control) and a *NTN1* patient (NTN1-1.9). Individual sagittal views superior to the decussation (left), their relative coronal views inferior to the decussation (middle) and a zoom of the tracts inferior to the decussation (right) are presented. Blue tracts represent the crossed CST, and red tracts represent the uncrossed CST. The corticospinal tract laterality coefficient was positive for the control (0.93, indicating more connections in the crossed corticospinal tract) and negative for the *NTN1* patient (-0.94, indicating more connections in the uncrossed corticospinal tract). **(c)** Mean fractional anisotropy (FA) along the crossed CST. The mean tract from the upper brainstem until the funiculus of the upper spinal cord is represented in yellow and is superimposed on the coronal view of the fractional anisotropy map of the control subject. Note that the z axis displays the anatomical correspondence between the coronal view (left) and the graph of the mean FA values (right), indicating that the pyramidal decussation occurs between $17<z<25$ when the mean track crosses the midline. Mean FA values increased in the NTN1-1.9 patient (light blue diamonds) compared to the control subject (dark blue squares) at the level of the pyramidal decussation. Error bars represent standard errors.

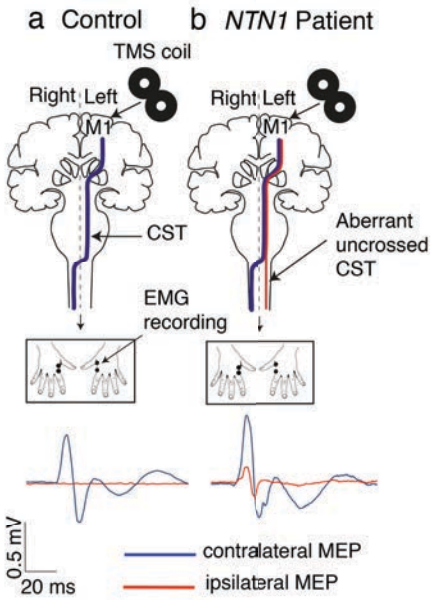

Figure 4. Analysis of neural signal propagation along the corticospinal tracts using single pulse transcranial magnetic stimulation.

(**a-b**) Schematic representation of the TMS experiments. In controls, unilateral stimulation of the hand area of the dominant primary motor cortex with TMS elicited contralateral MEPs only (a, blue line), whereas bilateral MEPs were observed in *NTN1* patients (b, red line).

Methods

Patient selection

International cases were collected over a period of 5 years in France and New Zealand. 25 index cases without mutation in either *DCC* or *RAD51* (rearrangements being excluded in 14 of them) were selected for exome sequencing. Each patient, as well as available family members, had a standardized neurologic assessment and DNA sampling. The severity of MM was scored with the Woods and Teuber scale. Familial history, MM location, associated disorders and reported functional disability were collected. Written informed consent was obtained from the patients (or the parents of minors) before genetic analyses. On the French side, the study was approved by the ethics committee of the Pitié-Salpêtrière Hospital, Paris. In New Zealand, all procedures were approved by the Health and Disability Ethics Committees, Multi-region Ethics Committee of New Zealand.

Exome sequencing

Concerning the exomes performed in France, genomic DNA was captured using Agilent in-solution enrichment methodology (SureSelect Human All Exon Kits Version 5, Agilent) with their biotinylated oligonucleotides probes library (Human All Exon v5 - 50 Mb, Agilent), followed by paired-end 75 bases massively parallel sequencing on Illumina HiSEQ 2000. Sequence capture, enrichment and elution were performed according to manufacturer's instruction and protocols (SureSelect, Agilent) without modification except for library preparation performed with NEBNext® Ultra kit (New England Biolabs®). For library preparation 600 ng of each genomic DNA were fragmented by sonication and purified to yield fragments of 150-200 bp. Paired-end adaptor oligonucleotides from the NEB kit were ligated on repaired, A tailed fragments then purified and enriched by 8 PCR cycles. 1200ng of these purified Libraries were then hybridized to the SureSelect oligo probe capture library for 72 hr. After hybridization, washing, and elution, the eluted fraction was PCR-amplified with 9

cycles, purified and quantified by QPCR to obtain sufficient DNA template for downstream applications. Each eluted-enriched DNA sample was then sequenced on an Illumina HiSEQ 2000 as paired-end 75b reads. Image analysis and base calling was performed using Illumina Real Time Analysis (RTA 2.1.3) with default parameters. The bioinfomatics analysis of sequencing data was based on the Illumina pipeline (CASAVA1.8.2). CASAVA performs alignment of a sequencing run to a reference genome (hg19), calls the SNPs based on the allele calls and read depth, and detects variants (SNPs &Indels). The alignment algorithm used was ELANDv2 (performs multiseed and gapped alignments). Only the positions included in the bait coordinates were conserved. Genetics variation annotation was realized from IntegraGen in-house pipeline. It consists on genes annotation (RefSeq), known polymorphisms (dbSNP 132, 1000Genome, EVS) followed by a mutation characterization (exonic, intronic, silent, nonsense….). For each position, the exomic frequencies (Homo & HTZ) are determined from all the exomes already sequenced at Integragen, and the exome results provided by 1000G, EVS and HapMap. Minimum average depth on the exome was around 50X. When coverage was below 50X for an exon and/or base pair in *NTN1* (which was the case for exon 6 and the first base pairs of exon 2 in most patients), the analysis was completed by Sanger sequencing.

Concerning the exomes performed in New Zealand, genomic DNA was collected and extracted from saliva samples using Oragene DNA kits (DNA Genotek Inc. Ontario, Canada). Exome sequencing was provided by Otogenetics Corporation (Norcross, GA, United States) using Agilent SureSelect Human All Exon V4 or Agilent SureSelect Human All Exon V5+UTR for capture and Illumina sequencing platforms for data generation (paired end, 100 cycles). Sequence alignment was undertaken with BWA mem using human genome assembly GRCh37 as the reference. Further processing was done with Picard tools and the Genome Analysis Toolkit following Broad Best Practice Guidelines (URL:

https://www.broadinstitute.org/gatk/) to produce called variants with HaplotypeCaller. Estimates for population allele frequencies of individual variants were obtained from the NHLBI GO Exome Sequencing Project (ESP6500) database (URL: http://evs.gs.washington.edu/EVS/), the 1000 Genomes Project (URL: http://www.1000genomes.org/) and the Exome Aggregation Consortium (URL: http://exac.broadinstitute.org/). The predicted effect of individual variants on gene function was identified through annotation with SnpEff (Cingolani *et al.* 2012).

The analysis was then conducted with Variant Studio (Illumina). Variants present at an allele frequency greater than 0.1% in the general population (ExAC data), synonymous variants and intronic variants that were not predicted to alter splicing were discarded. A total of 17 genes, with variants in at least 3 index cases or in 2 index cases but with a known function in axon guidance or known interaction with DCC or RAD51 were selected.

Sanger sequencing and QMPSF

The coding and flanking intronic regions of *NTN1* were amplified using primers available upon request. Forward and reverse sequencing reactions were performed with the Big Dye Terminator Cycle Sequencing Ready Reaction kit (PE Applied Biosystems, Foster City, CA), and the products were analyzed on an ABI 3730 automated sequencer (PE Applied Biosystems). Quantitative multiplex PCR of short fluorescent fragments analysis was performed for all exons of *NTN1* in 14 patients and results were analyzed using GeneMapper analysis software version 4.0 (Applied Biosystems).

Site-directed mutagenesis

To generate human and mouse netrin-1 Alkaline Phosphatase fusion proteins in C-terminal, human and mouse *NTN1* cDNAs were amplified by PCR and cloned in pAP-Tag-5 (GeneHunter, No.Q202) between Nhe1 and Bgl2 sites. Plasmids encoding human netrin-1 and mouse netrin-1 were provided by Dr Patrick Mehlen (Lyon, France). Mutations were

introduced by site-directed mutagenesis (Quikchange II Site-Directed Mutagenesis Kit, Agilent Technologies) with primers containing the mutations and verified by Sanger sequencing. Clones were then selected and purified (ZR Plasmid Miniprep™– Classic, Zymo Research and NucleBondXtra Midi/Maxi, Macherey-Nagel). We ensured that no other mutation was introduced by sequencing the entire cDNA of *NTN1*.

Western blot

HEK293 cells (cell line from human embryonic kidney, Ad5 DNA transformed; American Type Culture Collection) were transfected with mouse and human WT and mutated netrin1-AP plasmids using Lipofectamine2000 reagent and grown for 48 hours. The presence of the fusion protein in total lysates and in the supernatant at the expected molecular weight was confirmed by Western blot with anti-AP (1:1000;GenHunter) and anti-netrin-1 (1:500, MAB1109 RD Systems) antibodies. Actin (1:1000, C4-MAB1501 Millipore) was used as control. Briefly, samples were loaded on 4-15% mini-Protean TGX Tris-Glycine-buffer SDS-PAGE and transferred onto 0,2µm Trans-Blot Turbo nitrocellulose membrane (Biorad). Membranes were blocked for one hour at room temperature in 1xTBS (10mM Tris pH 8.0, 150 mM NaCl) supplemented with 5%(w/v) dried skim milk powder. Primary antibody incubation was carried out overnight at 4°C. Secondary HRP coupled antibodies were used: a donkey anti-Rat for detection of Netrin1, a goat anti-rabbit for AP and a goat anti-mouse for Actin, (Jackson ImmunoResearch, West Grove, PA). In between and after antibody incubations, membranes were extensively washed in TBS-T (TBS containing 2.5% Tween-20). Western blots were visualized using the enhanced chemiluminescence method (ECL prime Western Blotting detection reagent, Amersham).

To exclude an effect of the AP tag on netrin-1 secretion, we removed it from human WT and C601R-mutated netrin1-AP plasmids by BglII/XbaI digestion. We then conducted the same experiments as described above.

Magnetic resonance imaging

MRI data were acquired using a 3T scanner (Siemens, VERIO) with a 32-channel head coil. The MRI protocol included anatomical three-dimensional (3D) T1-weighted MPRAGE images (TR = 2.3 s; TE = 4.18 ms; flip angle = 9°; TI = 900 ms; voxel size = 1 × 1 × 1 mm^3; 176 slices), spin-echo echo-planar diffusion tensor imaging (TR = 10 s, TE = 87 ms, voxel size = 2 × 2 × 2 mm^3, 60 slices, 60 gradient encoded directions with a b-value of 1500 s/mm^2, 11 non-diffusion-weighted volumes).

Tractography analysis

References 31 to 39 are available in Extended Data.

Tractography analysis was performed in one patient (patient 1.9) and one control.

Diffusion images were pre-processed according to previous methods[31-33] and processed for probabilistic diffusion tractography with MRtrix (http://www.brain.org.au/software/mrtrix/). Raw diffusion-weighted data were corrected for motion and geometric distortions secondary to eddy currents using a registration technique based upon the geometric model of distortions.[34] The fibre orientation distribution function (ODF) was estimated using the constrained spherical deconvolution (CSD) method in MRtrix.[33,35] The sufficient angular resolution allowed high-order fibre orientation estimation algorithms.[35-37] The ODF information obtained from CSD was used with a suitable fibre-tracking algorithm to infer connectivity of crossing fibres. We used a probabilistic streamlines algorithm with the entire ODF as a probability density function (ODF threshold = 0.1; step size = 0.2 mm as 1/10 of the voxel size; radius of curvature = 1mm; up-sampling of DWI data to 1mm). In the native individual space, we performed a seed-to-target analysis from regions of interest defined along the CST (see Regions of interest section in Gallea et al., 2013).[16] These regions included the anterior bundle of the CST in the upper part of the brainstem, the lower part of the brainstem and the lateral horn of the spinal cord (see Figure 3a). We used a probabilistic

tractography algorithm: the number of fibres connecting a seed voxel to a target voxel was calculated by sampling one million draws for each fibre connecting the seed to the target. The CST tracts (the normally crossed CST and the abnormally uncrossed CST[a]) were reconstructed for each subject. After the tracts were reconstructed, two complementary measures were considered. First, the number of fibres reaching the target at the level of the lateral horn of the spinal cord (the crossed and the uncrossed CST separately) was calculated. We analysed the proportion of crossed compared to uncrossed portions of the CST using a laterality coefficient (NF Crossed - NF Uncrossed)/(NF Crossed + NF Uncrossed) (with NF = number of fibres, as in Vo et al., 2015).[38] Ratio values closer to 1 indicated greater Crossed than Uncrossed CST, whereas ratio values closer to -1 indicated greater Uncrossed than Crossed CST. Second, mean FA values were measured along the CST. Along track measures of FA were obtained based on B-spline resampling of the fibres and averaging the FA values for each individual fibre at the same location (elastic model with 30 points in space at analogous anatomical locations in each individual).[39] The upper location was defined at the ROI of the upper brainstem and the lower location was defined at the level of the ROI of the lateral horn of the spinal cord. Mean FA values were calculated at each point of the mean fibre along the Z axis to check for local difference at specific points of the tract.

Electrophysiological experiments

Electrophysiological experiments were conducted in two patients (patients 1.9 and 2.3).

EMG recordings. EMG signals were recorded bilaterally from the first dorsal interosseous muscle (FDI) (active electrode over the motor point and reference electrode on the metacarpophalangeal joint) with disposable surface Ag/AgCl electrodes placed 3 cm apart on the muscle belly.

Single-pulse TMS and corticospinal excitability. Motor evoked potentials (MEPs) induced by

[a] Note that the normally uncrossed CST passes through the anterior medial horn of the spinal cord.

single monophasic pulses delivered with a TMS device connected to a figure-of-eight coil (Magstim, UK) were recorded from electromyographic signals. TMS pulses were applied over the cortical representations (hot spot) of the first dorsal interosseus muscles in M1. The resting motor threshold was defined as the minimum stimulus intensity that resulted in MEPs of 50 µV in at least 5 out of 10 trials. Thirty to sixty MEPs evoked by a calibrated stimulation (1.2 - 1.3 x resting motor threshold) of the dominant and non-dominant hemisphere were recorded bilaterally in the first dorsal interosseus muscle to compare the frequency, latency and amplitude of the normal contralateral MEPs with those of potential mirror MEPs recorded in the hand ipsilateral to the stimulation site.

References

1 Kennedy, T. E., Serafini, T., de la Torre, J. R. & Tessier-Lavigne, M. Netrins are diffusible chemotropic factors for commissural axons in the embryonic spinal cord. *Cell* **78**, 425-435 (1994).

2 Chedotal, A. Further tales of the midline. *Current opinion in neurobiology* **21**, 68-75 (2011).

3 Serafini, T. *et al.* Netrin-1 is required for commissural axon guidance in the developing vertebrate nervous system. *Cell* **87**, 1001-1014 (1996).

4 Finger, J. H. *et al.* The netrin 1 receptors Unc5h3 and Dcc are necessary at multiple choice points for the guidance of corticospinal tract axons. *The Journal of neuroscience* **22**, 10346-10356 (2002).

5 Fothergill, T. *et al.* Netrin-DCC signaling regulates corpus callosum formation through attraction of pioneering axons and by modulating Slit2-mediated repulsion. *Cerebral cortex* **24**, 1138-1151 (2014).

6 Keino-Masu, K. *et al.* Deleted in Colorectal Cancer (DCC) encodes a netrin receptor. *Cell* **87**, 175-185 (1996).

7 Goldman, J. S. *et al.* Netrin-1 promotes excitatory synaptogenesis between cortical neurons by initiating synapse assembly. *The Journal of neuroscience* **33**, 17278-17289 (2013).

8 Brunet, I. *et al.* Netrin-1 controls sympathetic arterial innervation. *The Journal of clinical investigation* **124**, 3230-3240 (2014).

9 Tepavcevic, V. *et al.* Early netrin-1 expression impairs central nervous system remyelination. *Annals of neurology* **76**, 252-268 (2014).

10 Mehlen, P., Delloye-Bourgeois, C. & Chedotal, A. Novel roles for Slits and netrins: axon guidance cues as anticancer targets? *Nature reviews. Cancer* **11**, 188-197 (2011).

11 Bongo, J. B. & Peng, D. Q. The neuroimmune guidance cue netrin-1: a new therapeutic target in cardiovascular disease. *Journal of Cardiology* **63**, 95-98 (2014).

12 Ramesh, G. Role of Netrin-1 Beyond the Brain: From Biomarker of Tissue Injury to Therapy for Inflammatory Diseases. *Recent patents on biomarkers* **2**, 202-208 (2012).

13 Wetzel-Smith, M. K. *et al.* A rare mutation in UNC5C predisposes to late-onset Alzheimer's disease and increases neuronal cell death. *Nature Medicine* **20**, 1452-1457 (2014).

14 Srour, M. *et al.* Mutations in DCC cause congenital mirror movements. *Science* **328**, 592 (2010).

15 Meneret, A., Trouillard, O., Depienne, C. & Roze, E. in *GeneReviews(R)* (eds R. A. Pagon *et al.*) (1993).

16 Gallea, C. *et al.* RAD51 deficiency disrupts the corticospinal lateralization of motor control. *Brain* **136**, 3333-3346 (2013).

17 Gallea, C. *et al.* Congenital mirror movements: a clue to understanding bimanual motor control. *Journal of neurology* **258**, 1911-1919 (2011).

18 Depienne, C. *et al.* RAD51 haploinsufficiency causes congenital mirror movements in humans. *American journal of human genetics* **90**, 301-307 (2012).

19 Meneret, A. *et al.* Congenital mirror movements: mutational analysis of RAD51 and DCC in 26 cases. *Neurology* **82**, 1999-2002 (2014).

20 Ahmed, I. *et al.* Identification of a homozygous splice site mutation in the dynein axonemal light chain 4 gene on 22q13.1 in a large consanguineous family from Pakistan with congenital mirror movement disorder. *Human genetics* **133**, 1419-1429 (2014).

21 Franz, E. A. *et al.* Congenital mirror movements: phenotypes associated with DCC and RAD51 mutations. *Journal of the neurological sciences* **351**, 140-145 (2015).

22 Fazeli, A. *et al.* Phenotype of mice lacking functional Deleted in colorectal cancer (Dcc) gene. *Nature* **386**, 796-804 (1997).

23 Rabe Bernhardt, N. *et al.* DCC mediated axon guidance of spinal interneurons is essential for normal locomotor central pattern generator function. *Developmental biology* **366**, 279-289 (2012).

24 Gillespie, L. N., Marzella, P. L., Clark, G. M. & Crook, J. M. Netrin-1 as a guidance molecule in the postnatal rat cochlea. *Hearing Research* **199**, 117-123 (2005).

25 Burgess, R. W., Jucius, T. J. & Ackerman, S. L. Motor axon guidance of the mammalian trochlear and phrenic nerves: dependence on the netrin receptor Unc5c and modifier loci. *The Journal of neuroscience* **26**, 5756-5766 (2006).

26 Murakami, S., Ohki-Hamazaki, H., Watanabe, K., Ikenaka, K. & Ono, K. Netrin 1 provides a chemoattractive cue for the ventral migration of GnRH neurons in the chick forebrain. *The Journal of comparative neurology* **518**, 2019-2034 (2010).

27 Ratcliffe, E. M. *et al.* Netrin/DCC-mediated attraction of vagal sensory axons to the fetal mouse gut. *The Journal of comparative neurology* **498**, 567-580 (2006).

28 Kruger, R. P., Lee, J., Li, W. & Guan, K. L. Mapping netrin receptor binding reveals domains of Unc5 regulating its tyrosine phosphorylation. *The Journal of neuroscience* **24**, 10826-10834 (2004).

29 Banyai, L. & Patthy, L. The NTR module: domains of netrins, secreted frizzled related proteins, and type I procollagen C-proteinase enhancer protein are homologous with tissue inhibitors of metalloproteases. *Protein Science* **8**, 1636-1642 (1999).

30 Delloye-Bourgeois, C. *et al.* Nucleolar localization of a netrin-1 isoform enhances tumor cell proliferation. *Science Signaling* **5**, ra57 (2012).

Supplementary Information is linked to the online version of the paper at www.nature.com/nature.

Acknowledgments:

The authors would like to thank the patients for participating in this study, the DNA and cell bank of the ICM (in particular Christelle Dussert and Sylvie Forlani) for DNA extraction and the Exome Aggregation Consortium and the groups that provided exome variant data for comparison. The work undertaken in New Zealand was supported by a Royal Society of New Zealand Marsden Fund Grant.

Author Contributions:

AM, AC, ID, ER and DM drafted/revised the manuscript. ER and DM designed and supervised the study. AM, EAF, OT, TO, YZ, RJMG, QW, SPR, CG, CDe, MS, CLJ, CDu, FR, JCL, MPM, MV, ID, GR, AB acquired and analyzed/interpreted data.

Author Information:

Reprints and permissions information is available at www.nature.com/reprints.

The authors have no competing financial interests.

Correspondence and requests for materials should be addressed to ER (emmanuel.flamand-roze@aphp.fr).

IV. Article 3 : Etude du rôle de RAD51 dans le développement du système moteur (en préparation)

Le faisceau corticospinal et le corps calleux sont les deux principales structures impliquées à ce jour dans la physiopathologie des mouvements en miroir. Nous avons vu précédemment que les patients *DCC* et *NETRIN1* présentent des projections corticospinales bilatérales (ainsi qu'une diminution de l'IIH dans le cas des patients *DCC* ; Articles 1 et 2). Nous avons par ailleurs montré qu'en plus de son rôle connu dans le développement du CC, le couple NETRIN1-DCC est impliqué dans la formation de la décussation pyramidale chez la souris. *RAD51* est quant à lui connu pour son rôle de réparation de l'ADN, et le lien entre la fonction de RAD51 et les MMC n'est pas évident. En effet, les fonctions précises de RAD51 dans le développement du système nerveux central ne sont pas connues.

Nous avons donc étudié en détail le patron spatio-temporel d'expression de RAD51 au sein du système nerveux central. En plus d'être exprimée dans les zones prolifératives, en lien avec son rôle de réparation de l'ADN, RAD51 a aussi été détectée de façon transitoire au niveau du FCS. Ces résultats suggèrent que RAD51 pourrait être impliquée dans le développement de ce faisceau.

Nous avons ensuite étudié les conséquences de différentes mutations de *Rad51* aboutissant à des pertes de fonction chez la souris. En particulier, nous avons étudié des souris présentant une diminution de la quantité de protéine RAD51 produite (*Rad51*$^{+/-}$), et des souris ayant une suppression totale de RAD51 dans le télencéphale dorsal, et donc dans le FCS (*Emx1::cre;Rad51*$^{lox/lox}$). Les souris *Rad51*$^{+/-}$ présentaient des anomalies subtiles de l'anatomie du FCS au niveau de la décussation pyramidale associées à des défauts moteurs fins. Le comportement moteur des souris *Emx1::cre;Rad51*$^{lox/lox}$ était totalement normal et leur FCS ne présentait pas d'anomalies anatomiques (en termes de trajectoire). En revanche,

la taille du néocortex et du FCS était dramatiquement réduite chez ces mutants. Ces anomalies étaient associées à une augmentation de l'apoptose dans la zone proliférative du néocortex au cours de la génération des couches profondes. Ces résultats démontrent que RAD51 joue un rôle fondamental pour la prolifération des progéniteurs néocorticaux via son activité de réparation de l'ADN. Le patron d'expression de RAD51 dans le système nerveux central suggère que cette protéine pourrait assurer un rôle encore inconnu, distinct de celui de réparation de l'ADN.

Rad51, a gene associated with congenital mirror movements, is involved in the development of the mouse neocortex

Quentin Welniarz,[1,2] Marie-Pierre Morel,[2] Oriane Pourchet,[1,2] Mohamed Doulazmi,[3] Caroline Dubacq,[2] Aurélie Méneret,[1,5] Rosine Wehrlé,[2] Vidjeacoumary Cannaya,[2] Oriane Trouillard,[1] Marta Ruiz,[1] Teruhisa Tsuzuki,[4] Alain Trembleau,[2] Isabelle Dusart,[2*] and Emmanuel Roze[1,5*]

[1] Sorbonne Universités, UPMC Univ Paris 06, INSERM U 1127, CNRS UMR 7225, Institut du Cerveau et de la Moelle épinière, F-75013, Paris, France

[2] Sorbonne Universités, UPMC Univ Paris 06, INSERM, CNRS, Institut de Biologie Paris Seine, Neuroscience Paris Seine, F-75005, Paris, France

[3] Sorbonne Universités, UPMC Univ Paris 06, INSERM, CNRS, Institut de Biologie Paris Seine, Adaptation Biologique et vieillissement, F-75005, Paris, France

[4] Faculty of Medical Sciences, Kyushu University, 3-1-1 Higashi-ku, Maidashi, Fukuoka 812-8582, Japan

[5] Département de Neurologie, AP-HP, Hôpital Pitié Salpêtrière, Paris, France

[*] *Equal contributions*

Abstract

RAD51, a protein known for its role in DNA repair, has recently been linked to congenital mirror movements (CMM). CMM is a rare genetic disorder associated with altered interhemispheric connectivity at the level of the corpus callosum (CC) and abnormal bilateral projections of the corticospinal tract (CST). The two main culprit genes involved in CMM are *DCC* and *RAD51*. Whereas DCC plays a crucial role in CST and CC development in mice, the possible link between RAD51 and motor system development was unexpected.

Here, by investigating RAD51 spatio-temporal expression pattern in mouse central nervous system, we show that besides its expression in proliferative zone, RAD51 was transiently detected in the developing CST, suggesting a potential role in the development of this motor pathway. We did not detect RAD51 expression in the corpus callosum. Secondly, we studied the effects of RAD51 suppression on the CST anatomy and motor functions in various *Rad51* deficient model mice. *Rad51*$^{+/-}$ mice had subtle malformations of the CST associated with mild motor deficits. Complete deletion of RAD51 in the dorsal telencephalon in *Emx1::cre;Rad51*$^{lox/lox}$ mice resulted in normal CST trajectory and motor behavior. Nevertheless, *Emx1::cre;Rad51*$^{lox/lox}$ mice had a massive size reduction of the entire neocortex and CST, which was associated with high levels of apoptosis in neocortical proliferative zone during the generation of deep neocortical layers.

Introduction

RAD51 plays a critical role in maintaining genomic integrity as it mediates DNA double-strand break repair via homologous recombination (HR)(West, 2003; Li and Heyer, 2008; Park et al., 2008). RAD51 is required for the proliferation of progenitor cells during development, and the complete lack of RAD51 in mouse is lethal due to the accumulation of DNA damage (Lim and Hasty, 1996; Tsuzuki et al., 1996). Consistent with the known role of HR in genomic stability and tumor development, mutations in RAD51 partners involved in HR have been associated with increased risk of developing cancers. However, no *RAD51* mutations have been demonstrated to cause cancer predisposition (Lose et al., 2006; Moynahan and Jasin, 2010). Two missense mutations were recently found in patients showing atypical Fanconi anemia, lacking the bone marrow failure, acute myeloid leukemia and cancer phenotypes commonly associated with this disorder (Ameziane et al., 2015; Wang et al., 2015).

We recently identified *RAD51* mutations in patients with congenital mirror movements (CMM)(Depienne et al., 2012; Meneret et al., 2014). To this day, CMM is the only disorder associated with familial mutations of *RAD51* coding sequence (Depienne et al., 2012; Franz et al., 2015). Mirror movements are involuntary symmetrical movements of one side of the body that mirror voluntary movements of the other side (Bonnet et al., 2010). CMM is a rare genetic disorder transmitted in autosomal dominant manner, in which mirror movements are the only clinical abnormality. The mirror movements predominate in the distal upper limbs, leaving affected individuals unable to perform independent actions with the two hands or to perform purely unimanual movements. The two main culprit genes identified so far are *DCC* (deleted in colorectal cancer) and *RAD51*. Familial forms of CMM are associated with heterozygous mutations of *RAD51* or *DCC*, probably resulting in haploinsufficiency (Srour et al., 2010; Depienne et al., 2011; Meneret et al., 2014). Two main non exclusive mechanisms

may account for mirror movements: (i) abnormal interhemispheric communication, which normally relies on the corpus callosum (CC), resulting in bilateral activation of primary motor areas; and (ii) abnormal corticospinal tract (CST) midline crossing at the level of the pyramidal decussation, resulting in bilateral CST projections to the spinal cord (Gallea et al., 2011; Gallea et al., 2013; Welniarz et al., 2015). The role of DCC in the guidance of the mouse CC (Fazeli et al., 1997; Fothergill et al., 2013) and CST (Finger et al., 2002) axons at the midline is well known. By contrast, the involvement of *RAD51* in CMM unveiled a totally unexpected role of this gene in CNS development. *RAD51* is strongly expressed at early stage in the developing mouse brain within deep neocortical layers and at the level of the pyramid decussation at birth (Depienne et al., 2012). RAD51 might thus be involved in the development of the CST.

Our first aim was to precisely describe RAD51 spatio-temporal expression pattern in the mouse central nervous system. Secondly, we investigated the effects of RAD51 deletion on the CST anatomy and on motor functions. For this purpose, we studied the organization of the CST and the motor behavior in various *Rad51* deficient model mice, including a mouse line with a conditional deletion of RAD51 restricted to the neocortex.

Material and methods

Animals and genotyping

Rad51 (Tsuzuki et al., 1996) and *Emx1::cre* (Gorski et al., 2002) lines have previously been described and genotyped by PCR. All the mouse lines were maintained on a C57B/6J background. Swiss mice were used for the study of *Rad51* expression pattern. The day of the vaginal plug was E0, and the day of birth was P0. All animal procedures were approved by the Regional Animal Experimentation Ethics Committee C2EA-05 Charles Darwin (Project number 01558.01).

Generation of the Rad51^{lox} line

Rad51$^{los/lox}$ mouse line has been generated by the Clinique de la Souris (ICS, Strasbourg, France), from *Rad51* (MGI:97890/tm1a) ES generated by Eucomm. Briefly the exon 4 has been floxed.

Two pairs of primers were used for identifying *Rad51^{lox}* allele: Ef2-RAD51: 5'-gcacatgcttttctccaccgagcc-3'; and Er-RAD51 : 5'-gcagcatgtcttcacacctcacttc-3'.

Immunohistochemistry

All the immunohistochemistry experiments were performed on at least 3 animals per age and per genotype. For light microscopy, P0-P2 mice were anesthetized on ice and adult mice were anesthetized with sodium pentobarbital (50 mg/kg i.p.). Embryos were fixed by immersion in 4% paraformaldehyde with 0.12 M phosphate buffer pH 7.4, and post-natal mice were perfused through the aorta with 0.12 M phosphate buffer, pH 7.4, containing 4% paraformaldehyde. Tissue preparation and immunostaining were carried out as described in (Repici et al., 2012), using the following primary antibodies: goat anti-RAD51 (SC682, 1/50; Santa Cruz Biotechnology, Santa Cruz, California); rabbit anti-PKCgamma (1/100, Santa

Cruz); rat anti-CTIP2 (1/500, Abcam, Cambridge, UK); anti-TBR1 (1/500, Millipore, Molsheim, France), rabbit anti-CUX1 (1/200, Santa Cruz), rabbit anti-activated CASP3 (1/500, Pharmigen); mouse anti-Calb1 (1/100; Swant, Bellinzona, Switzerland); anti-PAX6 (1/500, Millipore). Images were acquired with a DMR Leica microscope.

In-situ hybridization

All the *in situ* hybridization experiments were performed on at least 3 animals per age and per genotype. The brain and spinal cord were treated as described above for the immunohistochemistry procedure (Repici et al., 2012). Coronal sections 20 µm thick through the entire brain and spinal cord were cut on a cryostat. Tissue sections were post-fixed for 10 min in 4%PFA, washed in PBS (pH7.4), treated with proteinase K (10 µg/ml; Invitrogen, CergyPontoise, France) for 3–5 min, post-fixed for 5 min in 4% PFA, washed in PBS, acetylated and washed in PBS 1% Triton X-100. Slides were incubated for 2 h at room temperature (RT) in hybridization buffer (50% formamide, 5 × SSC, 1 × Denhardt's, 250 µg/ml yeast tRNA and 500 µg/ml herring sperm, pH7.4). Then, tissue sections were hybridized overnight at 72 °C with riboprobes (full length of the mouse *Rad51* sequence) (1/200). Following hybridization, sections were rinsed for 30 min in 2× SSC at 72 °C, and blocked in 0.1 M Tris pH7.5, 0.15 M NaCl (B1) containing 10% normal goat serum (NGS) for 1 h at RT. After blocking, slides were incubated overnight at room temperature with anti-DIG antibody conjugated with the alkaline phosphatase (1/5000, Roche Diagnostics) in B1 containing 1% NGS. After further washes, the alkaline phosphatase activity was detected using nitrobluetetrazolium chloride (NBT) (337.5 µg/ml) and 5-bromo-4-chloro-3-indolyl phosphate (BCIP) (175 µg/ml; Roche Diagnostics). Sections were mounted in Mowiol (Calbiochem, VWR, Fontenay sous bois, France).

Tracing of the corticospinal tract

Adult male or female mice were anesthetized with a mixture of ketamine (146 mg/kg) and xylazine (7.4 mg/kg) and placed ina stereotaxic frame. Pressure injections of an anterograde tracer (biotinylated dextran amine, BDA, MW10000, SIGMA) targeting the left motor cortex were performed. Six 0.2-µl aliquots of 10% BDA solution in normal saline were injected (0.1 µl/min) with a 10-µl Hamilton microsyringes fitted with a removable needle (Hamilton, 7762-03)at the following coordinates, as determined in (Tennant et al., 2011): i) A (anteriority: positive values are rostral to bregma, negative values are caudal to bregma) = 1, L (laterality to bregma) = 2, D (depth from the surface of the skull) = 1; ii) A = 1, L = 1, D = 1; iii) A = -0.25, L = 2, D = 1; iv) A = -0.25, L = 1, D = 1; v) A = -1, L = 2, D = 1; and vi) A = -1, L = 1, D = 1. At each injection point, the needle was left in place for 3 min before and after the injection to minimize leakage. After surgery, the wound was cleansed and the skin sutured.

Fourteen days following BDA injections, the mice were deeply anesthetized and perfused as described for immunohistochemistry procedure. The brain and spinal cord were treated as described above for the immunohistochemistry procedure (Repici et al., 2012). Coronal sections 30 µm thick through the entire brain and spinal cord were cut on a cryostat. Sections were washed for 15 min in 0.1 M PBSpH 7.3and incubated for one hour in PBSGT (PBS containing 0.25% Triton-X, 0.2% gelatin) and lysine (0.1 M). The sections were then incubated overnight in steptavidin-complex conjugated to horseradish peroxidase solution (HRP, 1/400, Sigma) in PBSGT. The sections were washed 4 x 10 min in PBST, then incubated for 40 min in 1% DAB solution (3,3'-diaminobenzidine, Sigma-Aldrich) in 0.1M Tris pH 7.6 containing 0.015% H_2O_2. The sections were washed 3 x 5 min in 0.1M Tris in order to stop the reaction, then dehydrated before mounting in Eukitt (Sigma). Images were

acquired with a DMR Leica microscope.

Quantification of the number of CST axons. BDA-labeled axons of the corticospinal tract contralateral to the injection site were quantified in adult *WT* (*Rad51*$^{+/+}$*;* n = 6) and *Rad51*$^{+/-}$ (n = 6) mice from two independent experiments. The quantification of CST axons was performed at different levels of the brainstem and spinal cord: in a ventral position after the pons and before the pyramidal decussation, and in the dorsal funiculus after the pyramidal decussation and at the cervical enlargement in the spinal cord. Images were acquired with a DMR Leica microscope and the density of fibers of the CST was quantified using MetaVue software. At each level, three following sections were analyzed: for each section, the entire area occupied by the labeled CST was measured with a 20 objective. Labeled CST axons were acquired with a 63 oil immersion objective at three sampling sites (each of them covering a surface of 1 μm^2) per section selected pseudo-randomly, and outlined by MetaVue software to be quantified using a modified stereological method previously described (Rosenzweig et al., 2009). Measurements obtained from these three sampling sites in the three following sections were then averaged, and the total number of fibers per field was divided by the area of the sampled field to derive a mean fiber density per unit area value. This density value was eventually multiplied by the average surface of the CST to obtain an average of the total number of axons present in the CST at each level. For each mouse, in order to correct inter-experiment variability, the total number of axons obtained at each level of the CST path was normalized by the average number of axons of the experiment.

Measure of the CST cross-section surface. In adult *Emx1::cre;Rad51*$^{lox/lox}$ (n = 6) and control (*Rad51*$^{lox/lox}$; n = 5) mice, the surface of the CST labeled with the PKCγ was measured just before the pyramidal decussation and in the cervical spinal cord. At each level, three following sections were analyzed: for each section, the entire area occupied by the labeled CST was measured with a 20 objective using the MetaView software.

Behavioral study

All the behavioral studies were performed blindly to the genotype. The order of the tests, and the procedures, were identical across all the experiments in order to allow data pooling. The tests were performed on male and female mice aged between 8 and 12 weeks. For the first three days, the mice were habituated to being handled by the experimenters in order to limit stress. Mice were then tested with a partial SHIRPA protocol (grasping, clasping and auditory tests were performed, and whisker state was evaluated) in order to rule out major neurological abnormalities.

Open field. The open field test was used to evaluate spontaneous activity and locomotion: mice were placed in the center of a 0.25-m^2 arena and allowed to explore freely for 5 minutes. During this time, they were tracked and recorded with a camera fixed above the arena, and the total walking distance was calculated with Topscan software.

Ladder test. The ladder test apparatus (Locotronic) consists of a 124 cm x 8 cm corridor with a floor composed of 78 bars each 1 cm apart. The mice were made to cross the corridor, and the number of slips of the forelimbs, hindlimbs and tail was automatically detected by 158 infrared captors placed on the corridor walls (sampling frequency 1000 Hz). This test evaluates the precision and coordination of limb positioning.

Treadmill. Mice were placed on a transparent treadmill (14 cm x 6 cm) moving at 12 cm/s. After a short training session, the mice had to run for ten seconds, during which period the positioning of their paws was recorded by a camera fixed under the apparatus. To analyze the production of symmetric versus asymmetric movements during locomotion, the numbers of symmetric and asymmetric strides were counted after excluding frames in which the mouse

was not running.

Rotarod. The accelerating Rotarod (BIOSEB) consists of a horizontal rod 3 cm in diameter, turning on its longitudinal axis. Mice were placed on a 5-cm section of the rod, facing opposite the direction of rod rotation, such that the animal had to walk forward to avoid falling. The training phase consisted of walking on the rod at a rotational speed varying from 4 to 40 rpm for one minute. When a mouse managed to walk on the rotating rod, it was subjected to four trials in which the speed of rotation increased gradually from 4 rpm to 40 rpm over 5 min. The animal had to coordinate its walk with the speed of rotation. This test requires strength, balance and motor coordination. Time spent on the rod was recorded and averaged for the 4 trials. The test was repeated three days in a row with the same procedure, except that the training session was performed only on the first day.

Grip test. Forepaw muscle strength was measured with a grip test. The mouse was held by the base of its tail and allowed to firmly grab the grid of the device with its forepaws. The mouse was then pulled gently backwards until it released its grip. The peak force (N) in each trial was considered as the grip strength. Four successive measurements were averaged. The same procedure was performed with forepaws and hindpaws at the same time.

Reaching exploratory behavior. When placed in a new environment, mice engage in "reaching" exploratory behavior, in which they contact walls with their forepaws (Serradj et al., 2014). This contact can be made with the two paws simultaneously (symmetric movement) or independently (asymmetric). For this experiment, mice were placed in a glass cylinder. To promote movement toward the cylinder wall, a food pellet was suspended from the top of the cylinder. Ten reaching movements were recorded with a video camera and then examined frame-by-frame to calculate the numbers of asymmetric and symmetric movements.

Statistical analysis

Data were analyzed with SPSS statistical software version 22.0 (Chicago, Illinois, USA). The normality of variable distributions and the homogeneity of variance across the groups were assessed with the Kolmogorov-Smirnov and Levene tests, respectively. Variables that failed any of these tests were analyzed with the non parametric Mann–Whitney test. Variables that passed the normality test were analyzed with ANOVA followed by the Bonferroni *post hoc* test for multiple comparisons, or with Student's *t* test when comparing two groups. Paired data were analyzed by repeated-measures ANOVA with two factors, followed by the Bonferroni *post hoc* test for multiple comparisons. Categorical variables were compared using Pearson's χ^2 test or Fisher's exact test.

Results

Rad51 expression during central nervous system development

The identification of *RAD51* mutations in CMM patients suggests that it might play an unsuspected role during central nervous system development. Here, we studied in details RAD51 spatio-temporal expression pattern in the mouse central nervous system, with a particular focus on the CC and CST, the two structures that are involved in MM pathophysiology in *RAD51*-CMM patients (Gallea et al., 2013).

We first validated the specificity of the SC6862 RAD51 antibody by western blot and by the absence of immunostaining on *Rad51*$^{-/-}$ embryos (Supplementary Fig. 1). We then analyzed RAD51 expression in the CC and CST just after their axons have crossed the midline at E18 and P2, respectively (Gianino et al., 1999; Rash and Richards, 2001). At E18, RAD51 was not detected in the CC (Fig. 1B). In keeping with previous observations (Depienne et al., 2012), RAD51 was detected in the cytoplasm of the neocortical layers V/VI neurons at P2 (Fig. 1C). In the layer V, we found cells that co-expressed RAD51 and CTIP2, a marker of subcortical neurons including CST neurons (Arlotta et al., 2005)(Fig. 1D). RAD51 was also detected at the location of the CST in the brainstem (Fig. 1E) and at the pyramidal decussation (Fig. 1F), where it co-localized with the protein kinase C gamma (PKCγ), a known marker of the CST (Mori et al., 1990; Miki, 1996). We further studied the time course of RAD51 expression in the CST. In mouse, the CST axons reach the bottom of the cervical enlargement at P2, the seventh thoracic segment at P5 and the lumbar level of the spinal cord at P7 (Figure 2A). Gray matter innervation starts with a delay of two days after the CST axons have reached the cervical spinal cord (Gianino et al., 1999). In the spinal cord of P2 and P5 *WT* mice, RAD51 was detected along the entire length of the CST (Fig. 2B-G). Indeed, RAD51 and PKCγ

expressions were detected as the same levels of the spinal cord. For example at P5, they were expressed at the thoracic level (Fig. 2F, F') but not at the lumbar level (Fig. 2G, G'). At P7, when the CST axons reached the lumbar spinal cord, RAD51 was no longer detected in the CST at any levels (Fig. 2H-I). RAD51 is thus transiently expressed in the mouse CST when it crosses the midline and during gray matter innervation in the cervical spinal cord. RAD51 expression stops before the CST has reached the lumbar segments. This suggests that RAD51 might be involved in specific steps of CST development.

Consistent with previous observations, RAD51 protein and mRNA were expressed in regions characterized by intense proliferation of progenitor cells (Sharan et al., 1997; Ajioka et al., 2006): it was detected in the neocortical ventricular zone at E12 (Fig. 3A), and in the external grain layer of the cerebellum at P2 (Fig. 3B). Furthermore RAD51 protein and mRNA were both detected in the pontine nuclei (Fig. 3C) and in the inferior olivary (Fig. 3F), two structures located along the CST path.

Subtle morphological anomalies of the CST in Rad51$^{+/-}$ mice

We then assessed the effects of RAD51 haploinsufficiency on mouse motor system development. The CC was present and appeared normal in *Rad51*$^{+/-}$ mice (data not shown). We analyzed the anatomy of the CST in adult *Rad51*$^{+/-}$ (n = 6) and *Rad51*$^{+/+}$ (n = 6) mice by unilateral BDA injection into the left motor cortex (Fig. 4A). The global anatomy of the CST was preserved in *Rad51*$^{+/-}$ mice: BDA-labeled CST axons located in the ventral medulla (Fig. 4B) crossed the midline at the pyramidal decussation (Fig. 4C), then turned dorsally and continued their trajectory into the dorsal funiculus of the contralateral spinal cord (Fig. 4D-E). To look for subtle abnormalities, we then calculated the number of BDA-labeled CST axons at different levels of the hindbrain and spinal cord (Fig. 4A). The number of BDA-labeled

CST axons at the level of the pons and before the decussation was similar in *Rad51*$^{+/-}$ mice and in controls (Mann-Whitney test; p = 0.75; p = 0.52). This result points out that the quantity of BDA-labeled axons was similar in the two groups. After the decussation, the number of BDA-labeled axons was significantly reduced in *Rad51*$^{+/-}$ mice as compared to controls (Mann-Whitney test; p = 0.0163). It is noteworthy that in both groups, the number of BDA-labeled CST axons diminished as the CST progressed caudally. Indeed, numerous axons exit the tract to reach their targets in the brainstem and spinal cord. We calculated the axonal loss at different levels of the CST and we observed that it was significantly increased in *Rad51*$^{+/-}$ mice at the level of the pyramidal decussation (Mann-Whitney test; p = 0.039; Fig. 4F, G). This increased axonal loss at the pyramidal decussation was associated with an abnormal spreading of the CST (Fig. 4H-J). Altogether, our data show that *Rad51*$^{+/-}$ mice have subtle anomalies of the CST at the level of the pyramidal decussation.

Impaired motor behavior in Rad51$^{+/-}$ mice

We used behavioral tests to investigate the motor consequences of RAD51 haploinsufficiency. *Rad51*$^{+/-}$ mutant mice (n = 21) were compared to controls (*Rad51*$^{+/+}$; n = 17). There was no significant difference of weight between *Rad51*$^{+/-}$ and controls (Mann-Whitney test, p = 0.73; Fig. 5A). The performances of *Rad51*$^{+/-}$ mice were similar to that of the controls for the open-field (Mann-Whitney test, p = 0.99; Fig. 5B), the muscular strength (Mann-Whitney test, $p_{forelimbs}$ = 0.31; $p_{hindlimbs}$ = 0.74; Fig. 5C) and the ladder test (Mann-Whitney test, $p_{forelimbs}$ = 0.83; $p_{hindlimbs}$ = 0.61; p_{tail} = 0.78; Fig. 5D). The locomotion of *Rad51*$^{+/-}$ mice was normal; in particular, they made alternating movements with their forelimbs and hindlimbs. *Rad51*$^{+/-}$ mice fell off the Rotarod at significant shorter latencies than the controls (repeated-measures ANOVA with two factors. F = 13.2, p = 0.0004,

followed by followed by PLSD Fisher*post hoc* analysis; Fig. 5E). The exploratory reaching test evaluates the lateralization of voluntary forelimb movements (Serradj et al., 2014). When placed in a new walled environment, mice have a tendency to establish contacts on the walls with their forelimbs in an asymmetric or symmetric manner. In the reaching test, *Rad51*$^{+/-}$ mice made more symmetric forelimb movements than the controls (Mann-Whitney test, p = 0.014; Fig. 5F). The motor phenotype of *Rad51*$^{+/-}$ mice likely reflects difficulties in the generation of voluntary asymmetric forelimb movements. RAD51 may thus play a role in the proper set up of the motor circuits involved in this function.

Emx1::cre;Rad51$^{lox/lox}$ mice are viable and have no motor deficits

Rad51$^{-/-}$ mice die at E7 (Lim and Hasty, 1996; Tsuzuki et al., 1996), making it impossible to study the development of the motor system in these mice. We thus crossed *Rad51*$^{lox/lox}$ mice with *Emx1::cre* mice, in which cre recombinase is expressed in the dorsal telencephalon (neocortex, hippocampus and olfactory bulb) from E10 (Gorski et al., 2002). In particular, EMX1 is expressed in the neocortical progenitors that will form the CST neurons (Bareyre et al., 2005). The *Emx1::cre;Rad51*$^{lox/lox}$ mice are viable, fertile, and appear normal in the outer appearance. We studied the motor consequences of RAD51 deletion with the tests described previously. Strikingly, the motor behavior of *Emx1::cre;Rad51*$^{lox/lox}$ mice was undistinguishable from that of the *Rad51*$^{lox/lox}$ control mice (Supplementary Table 1).

Reduced neocortex in Emx1::cre;Rad51$^{lox/lox}$ mice

We then analyzed the gross brain anatomy of adult *Emx1::cre;Rad51*$^{lox/lox}$ mice. The cerebral cortex was dramatically reduced in size and weight in *Emx1::cre;Rad51*$^{lox/lox}$ mice as

compared to controls of the same age (Fig. 6A-C). In *Emx1::cre;Rad51*$^{lox/lox}$ mice, while the two cerebral hemispheres were correctly fused rostrally, they were completely separated caudally, revealing the underlying midbrain (Fig. 6A). By contrast, the olfactory bulbs, cerebellum and brainstem were similar between *Emx1::cre;Rad51*$^{lox/lox}$ mice and controls (Fig. 6A-C). Coronal sections of the brain of *Emx1::cre;Rad51*$^{lox/lox}$ mice revealed a reduction of the neocortex radial extension as compared to controls (Fig. 6D-I). Caudal to the hippocampus, the two hemispheres were not fused in *Emx1::cre;Rad51*$^{lox/lox}$ mice, and the CC was lacking (Fig. 6A, E). The hippocampus was smaller in *Emx1::cre;Rad51*$^{lox/lox}$ mice than in controls (Fig. 6E, G). We performed double immunostainings for CTIP2, which is predominantly expressed by early-born, deep-layer (V-VI) neurons (Arlotta et al., 2005), together with CUX1, which is predominantly expressed by later-born, upper-layer (III-II) neurons (Nieto et al., 2004). Although we did not performed quantification yet, we observed that CTIP2 neurons were found in the deep layers and CUX1 neurons in the upper layers in *Emx1::cre;Rad51*$^{lox/lox}$ as in control littermate (Fig. 6F and I), suggesting that the cortical layering is preserved in these mutants.

Reduced CST in Emx1::cre;Rad51$^{lox/lox}$ ***mice***

We analyzed the effect of a complete deletion of RAD51 in the neocortex on the organization of the CST. To that aim, we used unilateral BDA injection into the left motor cortex in *Emx1::cre;Rad51*$^{lox/lox}$ (n = 6) and *Rad51*$^{lox/lox}$ (n = 5) mice (Fig. 7A). The CST was then visualized on coronal sections at the level of the pyramidal decussation and in the spinal cord, by immunostaining against the PKCγ (visualization of the two CSTs), or by revelation of the BDA tracer (visualization of the left-hand CST alone). The CST trajectory was similar in *Emx1::cre;Rad51*$^{lox/lox}$ and *Rad51*$^{lox/lox}$ mice: the CST axons located in the ventral medulla

(Fig. 7B, B', F, F') crossed the midline at the decussation (Fig. 7C, C', G, G'), turned dorsally and continued their trajectory in the dorsal funiculus of the contralateral spinal cord (Fig. 7D-E, D'-E', H-I, H'-I'). Thus, complete deletion of RAD51 in the neocortex had not major effect on CST guidance and trajectory. However, measurement of the CST surface revealed that it was significant reduced in *Emx1::cre;Rad51*$^{lox/lox}$ mice as compared to controls in the medulla (Mann-Whitney test, p = 0.04; Fig. 7B, B', F, F', J) and in the spinal cord (Mann-Whitney test, p = 0.04; Fig. 7D-E, D'-E', H-I, H'-I', K). This observation is consistent with the decreased size of the neocortex in *Emx1::cre;Rad51*$^{lox/lox}$ mice (Fig. 6).

Increased apoptosis in the neocortical progenitors and neuronal layers at E13 but not E16 in Emx1::cre;Rad51$^{lox/lox}$ ***mice***

The lack of RAD51 is known to result in increased apoptosis, due to the accumulation of DNA double strand breaks (Lim and Hasty, 1996; Sonoda et al., 1998; Khanna and Jackson, 2001). Suppression of BRCA1, a crucial partner of RAD51 for HR (Welcsh et al., 2000; Thacker, 2005), leads to increased apoptosis of the neocortical progenitors during development (Pulvers and Huttner, 2009). We thus tested whether the reduction of the neocortical size in *Emx1::cre;Rad51*$^{lox/lox}$ mice could be associated with an increased apoptosis during the proliferation of the neocortical progenitors. We studied *Emx1::cre;Rad51*$^{lox/lox}$ and control mice at two distinct periods of the neocortical neurogenesis: at E13, during the generation of the deep-layer neurons (V-VI), and at E16, during the generation of upper-layer neurons (II-III)(Greig et al., 2013). We used an immunostaining against the activated caspase 3 to label apoptotic cells. At E13 and E16, we used CTIP2 staining as a neuronal marker, expressed in the post-mitotic neurons of the cortical plate, but not in the progenitors of the ventricular zone (VZ) and subventricular zone

(SVZ; Fig. 8) (Arlotta et al., 2005). Although the quantifications have not been performed yet, a massive number of activated caspase 3 positive cells were present in the neocortical progenitor's layers (VZ and SVZ), but also in the cortical plate of E13 *Emx1::cre;Rad51*$^{lox/lox}$ mice (Fig. 8 B-B', C-C'). By contrast, very few apoptotic cells were detected in *Rad51*$^{lox/lox}$ mice (Fig. 8 E-E', F-F'). At E16, the number of apoptotic cells appeared similar in the progenitor's layers of *Emx1::cre;Rad51*$^{lox/lox}$ and *Rad51*$^{lox/lox}$ mice (Fig. 8 G-L). However, there was an increased apoptosis in the marginal zone of *Emx1::cre;Rad51*$^{lox/lox}$ mice (Fig. 8 H-H', I-I').

Discussion

We show that RAD51 is transiently expressed in the CST when it crosses the midline and during gray matter innervation of the cervical spinal cord. RAD51 haploinsufficiency results in subtle alterations of the pyramidal decussation, associated with mild motor deficits that might reflect difficulties to generate asymmetric movements. Complete deletion of RAD51 in the dorsal telencephalon in *Emx1::cre;Rad51*$^{lox/lox}$ mice results in a normal trajectory of the CST from the cortex to the spinal cord with a normal motor phenotype. However, the size of the neocortex and CST is dramatically reduced in *Emx1::cre;Rad51*$^{lox/lox}$ mice, likely due to increased apoptosis during the proliferation of deep-layers neocortical progenitors.

RAD51 spatio-temporal expression pattern in the mouse central nervous system indicates a potential role in CST development

We analyzed the spatio-temporal expression pattern of RAD51 in the mouse developing central nervous system paying a particular attention to the CC and CST, two structures that have been involved in the pathophysiology of *RAD51*-CMM patients (Gallea et al., 2013). In keeping with previous observations (Depienne et al., 2012), RAD51 was detected in the

cytoplasm in different types of neurons, namely the cerebral cortex, olivary and pontic neurons. This suggests that RAD51 might have a role different from HR, which requires a nuclear location. Interestingly, we showed that RAD51 was transiently expressed in the CST, but not in the CC. RAD51 is expressed all along the CST until P5. This is the moment when the CST begins to innervate the gray matter of the cervical spinal cord, establishing the connections that will eventually convey the motor command to the forelimbs (Gianino et al., 1999; Canty and Murphy, 2008). By contrast, RAD51 was no longer expressed in the CST at P7, when it reaches the lumbar spinal cord, which is responsible for the motor control of the hindlimbs. The specific time course of RAD51 expression in the CST suggests that it might be involved in the formation of the pyramidal decussation and/or in the establishment of the neuronal circuits that ensure the transmission of the motor command to the forelimbs. This observation is of particular relevance, as mirror movements consistently involve the hands while the feet are rarely affected.

Consequences of RAD51 loss of function on the motor system

In CMM patients, two non exclusives mechanisms may account for the mirror movements: (i) abnormal interhemispheric communication, normally relying on the CC, resulting in bilateral motor cortices activation during the execution of intended unimanual movements; (ii) abnormal CST midline crossing at the level of the pyramidal decussation resulting in bilateral CST projections to the spinal cord (Gallea et al., 2013).

We investigated the consequences of RAD51 loss a function on the motor system in different mutant mouse line. *Rad51*$^{+/-}$ mice have a decreased quantity of RAD51 protein (Tsuzuki et al., 1996), thus reproducing the haploinsufficiency of the human patients. In these mice, we found subtle malformations of the pyramidal decussation, associated with mild motor deficits. It is worth noting that the *Rad51*$^{+/-}$ mice do no present bilateral CST projections to the spinal

cord, contrary to the human *RAD51*-CMM patients (Gallea et al., 2013). As *Rad51*$^{-/-}$ mice die at E7 (Lim and Hasty, 1996; Tsuzuki et al., 1996), we generated conditional mutant mice to study the effects of complete RAD51 suppression on motor system development. Surprisingly, complete suppression of RAD51 in the dorsal telencephalon in *Emx1::cre;Rad51*$^{lox/lox}$ mice resulted in normal motor behavior and CST trajectory, despite a massive size reduction of the entire neocortex and CST. The relative discrepancy of motor phenotype between the *Rad51*$^{+/-}$ and *Emx1::cre;Rad51*$^{lox/lox}$ mice might be due to the role of RAD51 in EMX1-negative neuronal populations (such as the cerebellum or inferior olive, which express RAD51 during development), or to compensatory mechanisms triggered by the reduction of the neocortex in *Emx1::cre;Rad51*$^{lox/lox}$ mice. In these later mice, the decreased size of the neocortex is associated with increased apoptosis during the proliferation of the deep-layers neocortical progenitors. This phenotype is reminiscent of what has been described in the *Emx1::cre;Brca1*$^{lox/lox}$ mutants (Pulvers and Huttner, 2009). In these two mutants, it is likely that defective HR leads to the accumulation of DNA damage in the neocortical progenitors, thereby triggering apoptosis via the p53 pathway (Lim and Hasty, 1996; Khanna and Jackson, 2001; Pulvers and Huttner, 2009).

How does RAD51 influence motor system development?

The mechanism by which RAD51 influences motor system development remains unknown. In particular, it is not known how *RAD51* loss of function alters CST and/or CC development in *RAD51*-CMM patients. Given the wide expression of RAD51 in progenitor cells during development, it is unlikely that increased apoptosis due to HR defects would result in such a subtle motor phenotype. Here, we further confirmed that increased apoptosis due to *RAD51* loss of function results in an overall reduction of the neocortex, but does not specifically alter CST guidance and trajectory. We reported cytosolic expression of RAD51, consistent with

previous findings (Sage et al., 2010; Depienne et al., 2012). This suggests that RAD51 might play a role unrelated to HR, which occurs within the nucleus. Similar dual function has been described for ATM, a protein involved in DNA repair. When located in the cytoplasm this protein is implicated in the modulation of synaptic function within the central nervous system (Li et al., 2009). So far, the cytoplasmic function of RAD51 is unknown. It has recently been shown that RAD51 binds to fidgetin-like 1 (FIGNL1), a protein expressed both at nuclear and cytoplasmic locations (Yang et al., 2005; Yuan and Chen, 2013). Fidgetins are microtubule-severing enzymes that have in a wide range of biological functions, including a role in axonal growth and neuronal morphogenesis (Sharp and Ross, 2012). RAD51 and FIGNL1 might cooperate to modulate the cytoskeleton dynamics, thereby influencing axonal growth, guidance or migration.

Is RAD51 loss of function responsible for MM?

RAD51 loss of function in mouse failed to reproduce the motor system anomalies observed in *RAD51*-CMM patients. In particular, complete removal of RAD51 in the mouse neocortex, and thus in the CST, did not alter CST midline crossing. Since we observed minor alterations of the CST in *Rad51*$^{+/-}$ mice, RAD51 could act at this level in a non-cell autonomous manner. However RAD51 expression pattern in the *wild type* mouse CST rather suggests a direct role of RAD51 on this structure.

The first heterozygous nonsense mutations identified in CMM families were predicted to result in haploinsufficiency (Depienne et al., 2012; Meneret et al., 2014; Franz et al., 2015), but this hypothesis has not been formerly tested. The identification of a point mutation (Franz et al., 2015) and of dominant negative point mutations of *RAD51* (Ameziane et al., 2015; Wang et al., 2015), as well as the lack of major CST alterations in *Rad51*$^{+/-}$ and

Emx1::cre;Rad51$^{lox/lox}$ mice raises the possibility that a dominant negative effect, rather than a loss of function, could be responsible for abnormal motor system development in *RAD51*-CMM patients.

References

Ajioka, I., Maeda, T., and Nakajima, K. (2006). Identification of ventricular-side-enriched molecules regulated in a stage-dependent manner during cerebral cortical development. *Eur J Neurosci* 23**,** 296-308.

Ameziane, N., May, P., Haitjema, A., Van De Vrugt, H.J., Van Rossum-Fikkert, S.E., Ristic, D., et al. (2015). A novel Fanconi anaemia subtype associated with a dominant-negative mutation in RAD51. *Nat Commun* 6**,** 8829.

Arlotta, P., Molyneaux, B.J., Chen, J., Inoue, J., Kominami, R., and Macklis, J.D. (2005). Neuronal subtype-specific genes that control corticospinal motor neuron development in vivo. *Neuron* 45**,** 207-221.

Bareyre, F.M., Kerschensteiner, M., Misgeld, T., and Sanes, J.R. (2005). Transgenic labeling of the corticospinal tract for monitoring axonal responses to spinal cord injury. *Nat Med* 11**,** 1355-1360.

Bonnet, C., Roubertie, A., Doummar, D., Bahi-Buisson, N., Cochen De Cock, V., and Roze, E. (2010). Developmental and benign movement disorders in childhood. *Mov Disord* 25**,** 1317-1334.

Canty, A.J., and Murphy, M. (2008). Molecular mechanisms of axon guidance in the developing corticospinal tract. *Prog Neurobiol* 85**,** 214-235.

Depienne, C., Bouteiller, D., Meneret, A., Billot, S., Groppa, S., Klebe, S., et al. (2012). RAD51 haploinsufficiency causes congenital mirror movements in humans. *Am J Hum Genet* 90**,** 301-307.

Depienne, C., Cincotta, M., Billot, S., Bouteiller, D., Groppa, S., Brochard, V., et al. (2011). A novel DCC mutation and genetic heterogeneity in congenital mirror movements. *Neurology* 76**,** 260-264.

Fazeli, A., Dickinson, S.L., Hermiston, M.L., Tighe, R.V., Steen, R.G., Small, C.G., et al. (1997). Phenotype of mice lacking functional Deleted in colorectal cancer (Dcc) gene. *Nature* 386**,** 796-804.

Finger, J.H., Bronson, R.T., Harris, B., Johnson, K., Przyborski, S.A., and Ackerman, S.L. (2002). The netrin 1 receptors Unc5h3 and Dcc are necessary at multiple choice points for the guidance of corticospinal tract axons. *J Neurosci* 22**,** 10346-10356.

Fothergill, T., Donahoo, A.L., Douglass, A., Zalucki, O., Yuan, J., Shu, T., et al. (2013). Netrin-DCC Signaling Regulates Corpus Callosum Formation Through Attraction of Pioneering Axons and by Modulating Slit2-Mediated Repulsion. *Cereb Cortex*.

Franz, E.A., Chiaroni-Clarke, R., Woodrow, S., Glendining, K.A., Jasoni, C.L., Robertson, S.P., et al. (2015). Congenital mirror movements: phenotypes associated with DCC and RAD51 mutations. *J Neurol Sci* 351**,** 140-145.

Gallea, C., Popa, T., Billot, S., Meneret, A., Depienne, C., and Roze, E. (2011). Congenital mirror movements: a clue to understanding bimanual motor control. *J Neurol* 258**,** 1911-1919.

Gallea, C., Popa, T., Hubsch, C., Valabregue, R., Brochard, V., Kundu, P., et al. (2013). RAD51 deficiency disrupts the corticospinal lateralization of motor control. *Brain* 136**,** 3333-3346.

Gianino, S., Stein, S.A., Li, H., Lu, X., Biesiada, E., Ulas, J., et al. (1999). Postnatal growth of corticospinal axons in the spinal cord of developing mice. *Brain Res Dev Brain Res* 112**,** 189-204.

Gorski, J.A., Talley, T., Qiu, M., Puelles, L., Rubenstein, J.L., and Jones, K.R. (2002). Cortical excitatory neurons and glia, but not GABAergic neurons, are produced in the Emx1-expressing lineage. *J Neurosci* 22**,** 6309-6314.

Greig, L.C., Woodworth, M.B., Galazo, M.J., Padmanabhan, H., and Macklis, J.D. (2013). Molecular logic of neocortical projection neuron specification, development and diversity. *Nat Rev Neurosci* 14**,** 755-769.

Hippenmeyer, S., Vrieseling, E., Sigrist, M., Portmann, T., Laengle, C., Ladle, D.R., et al. (2005). A developmental switch in the response of DRG neurons to ETS transcription factor signaling. *PLoS Biol* 3**,** e159.

Kato, M., Yano, K., Matsuo, F., Saito, H., Katagiri, T., Kurumizaka, H., et al. (2000). Identification of Rad51 alteration in patients with bilateral breast cancer. *J Hum Genet* 45**,** 133-137.

Khanna, K.K., and Jackson, S.P. (2001). DNA double-strand breaks: signaling, repair and the cancer connection. *Nat Genet* 27**,** 247-254.

Levy-Lahad, E., Lahad, A., Eisenberg, S., Dagan, E., Paperna, T., Kasinetz, L., et al. (2001). A single nucleotide polymorphism in the RAD51 gene modifies cancer risk in BRCA2 but not BRCA1 carriers. *Proc Natl Acad Sci U S A* 98**,** 3232-3236.

Li, J., Han, Y.R., Plummer, M.R., and Herrup, K. (2009). Cytoplasmic ATM in neurons modulates synaptic function. *Curr Biol* 19**,** 2091-2096.

Li, W., Liu, K.J., Song, J.S., Song, R., and Liu, Z.L. (2015). Association between RAD51 polymorphism and breast cancer susceptibility: a meta analysis. *Int J Clin Exp Med* 8**,** 2326-2333.

Li, X., and Heyer, W.D. (2008). Homologous recombination in DNA repair and DNA damage tolerance. *Cell Res* 18**,** 99-113.

Lim, D.S., and Hasty, P. (1996). A mutation in mouse rad51 results in an early embryonic lethal that is suppressed by a mutation in p53. *Mol Cell Biol* 16**,** 7133-7143.

Meneret, A., Depienne, C., Riant, F., Trouillard, O., Bouteiller, D., Cincotta, M., et al. (2014). Congenital mirror movements: mutational analysis of RAD51 and DCC in 26 cases. *Neurology* 82**,** 1999-2002.

Miki, A. (1996). Developmental expression of alpha-, beta- and gamma-subspecies of protein kinase C in the dorsal corticospinal tract in the rat spinal cord. *Neuroscience* 75**,** 939-948.

Mori, M., Kose, A., Tsujino, T., and Tanaka, C. (1990). Immunocytochemical localization of protein kinase C subspecies in the rat spinal cord: light and electron microscopic study. *J Comp Neurol* 299**,** 167-177.

Nieto, M., Monuki, E.S., Tang, H., Imitola, J., Haubst, N., Khoury, S.J., et al. (2004). Expression of Cux-1 and Cux-2 in the subventricular zone and upper layers II-IV of the cerebral cortex. *J Comp Neurol* 479**,** 168-180.

Park, J.Y., Yoo, H.W., Kim, B.R., Park, R., Choi, S.Y., and Kim, Y. (2008). Identification of a novel human Rad51 variant that promotes DNA strand exchange. *Nucleic Acids Res* 36**,** 3226-3234.

Pulvers, J.N., and Huttner, W.B. (2009). Brca1 is required for embryonic development of the mouse cerebral cortex to normal size by preventing apoptosis of early neural progenitors. *Development* 136**,** 1859-1868.

Rash, B.G., and Richards, L.J. (2001). A role for cingulate pioneering axons in the development of the corpus callosum. *J Comp Neurol* 434**,** 147-157.

Repici, M., Chen, X., Morel, M.P., Doulazmi, M., Sclip, A., Cannaya, V., et al. (2012). Specific inhibition of the JNK pathway promotes locomotor recovery and neuroprotection after mouse spinal cord injury. *Neurobiol Dis* 46**,** 710-721.

Rosenzweig, E.S., Brock, J.H., Culbertson, M.D., Lu, P., Moseanko, R., Edgerton, V.R., et al. (2009). Extensive spinal decussation and bilateral termination of cervical corticospinal projections in rhesus monkeys. *J Comp Neurol* 513**,** 151-163.

Sage, J.M., Gildemeister, O.S., and Knight, K.L. (2010). Discovery of a novel function for human Rad51: maintenance of the mitochondrial genome. *J Biol Chem* 285**,** 18984-18990.

Serradj, N., Paixao, S., Sobocki, T., Feinberg, M., Klein, R., Kullander, K., et al. (2014). EphA4-mediated ipsilateral corticospinal tract misprojections are necessary for bilateral voluntary movements but not bilateral stereotypic locomotion. *J Neurosci* 34**,** 5211-5221.

Sharan, S.K., Morimatsu, M., Albrecht, U., Lim, D.S., Regel, E., Dinh, C., et al. (1997). Embryonic lethality and radiation hypersensitivity mediated by Rad51 in mice lacking Brca2. *Nature* 386**,** 804-810.

Sharp, D.J., and Ross, J.L. (2012). Microtubule-severing enzymes at the cutting edge. *J Cell Sci* 125**,** 2561-2569.

Sonoda, E., Sasaki, M.S., Buerstedde, J.M., Bezzubova, O., Shinohara, A., Ogawa, H., et al. (1998). Rad51-deficient vertebrate cells accumulate chromosomal breaks prior to cell death. *EMBO J* 17**,** 598-608.

Srour, M., Riviere, J.B., Pham, J.M., Dube, M.P., Girard, S., Morin, S., et al. (2010). Mutations in DCC cause congenital mirror movements. *Science* 328**,** 592.

Tennant, K.A., Adkins, D.L., Donlan, N.A., Asay, A.L., Thomas, N., Kleim, J.A., et al. (2011). The organization of the forelimb representation of the C57BL/6 mouse motor cortex as defined by intracortical microstimulation and cytoarchitecture. *Cereb Cortex* 21**,** 865-876.

Thacker, J. (2005). The RAD51 gene family, genetic instability and cancer. *Cancer Lett* 219**,** 125-135.

Tsuzuki, T., Fujii, Y., Sakumi, K., Tominaga, Y., Nakao, K., Sekiguchi, M., et al. (1996). Targeted disruption of the Rad51 gene leads to lethality in embryonic mice. *Proc Natl Acad Sci U S A* 93**,** 6236-6240.

Wang, A.T., Kim, T., Wagner, J.E., Conti, B.A., Lach, F.P., Huang, A.L., et al. (2015). A Dominant Mutation in Human RAD51 Reveals Its Function in DNA Interstrand Crosslink Repair Independent of Homologous Recombination. *Mol Cell* 59**,** 478-490.

Welcsh, P.L., Owens, K.N., and King, M.C. (2000). Insights into the functions of BRCA1 and BRCA2. *Trends Genet* 16**,** 69-74.

Welniarz, Q., Dusart, I., Gallea, C., and Roze, E. (2015). One hand clapping: lateralization of motor control. *Frontiers in Neuroanatomy* 9.

West, S.C. (2003). Molecular views of recombination proteins and their control. *Nat Rev Mol Cell Biol* 4**,** 435-445.

Yang, Y., Mahaffey, C.L., Berube, N., Nystuen, A., and Frankel, W.N. (2005). Functional characterization of fidgetin, an AAA-family protein mutated in fidget mice. *Exp Cell Res* 304**,** 50-58.

Yuan, J., and Chen, J. (2013). FIGNL1-containing protein complex is required for efficient homologous recombination repair. *Proc Natl Acad Sci U S A* 110**,** 10640-10645.

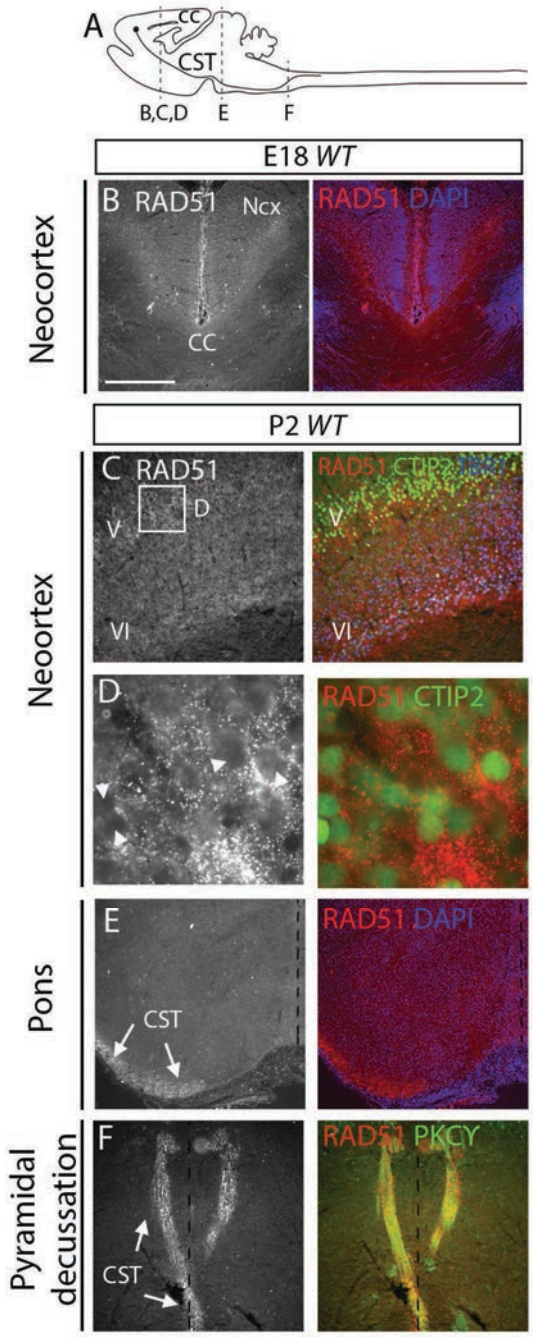

Figure 1. RAD51 is expressed in the mouse CST neurons during development. (A) Schematic representation of a P2 mouse sagittal section indicating the trajectory of the CST and the level of the coronal sections presented in this figure. Coronal sections of E18 and P2*WT* mice (n = 3 for each age) stained with anti-RAD51 and anti-CTIP2, anti-TBR1, anti-PKCγ or DAPI. (B) RAD51 was expressed in the neocortex but not in the CC at E18. (C-D) At P2, RAD51 was detected in neocortical layers V and VI, as shown by double staining with CTIP2 and TBR1, respectively. RAD51 was detected in the cytoplasm of CTIP2 positive cells. (E-F) RAD51 staining was detected along the trajectory of the CST axons: just rostral the pons, where the CST adopts a medial position (E), and at the level of the decussation, RAD51 staining co-located with PKCγ (F). White arrowheads in (D) indicate cells co-expressing RAD51 and CTIP2. White arrows indicate CST axons. The dashed lines indicate the midline. CC: corpus callosum; CST: corticospinal tract; LV: lateral ventricule; Ncx: neocortex. The scale bar represents 320 µm in A, E; 160 µm in B; 19 µm in C; 480 µm in D.

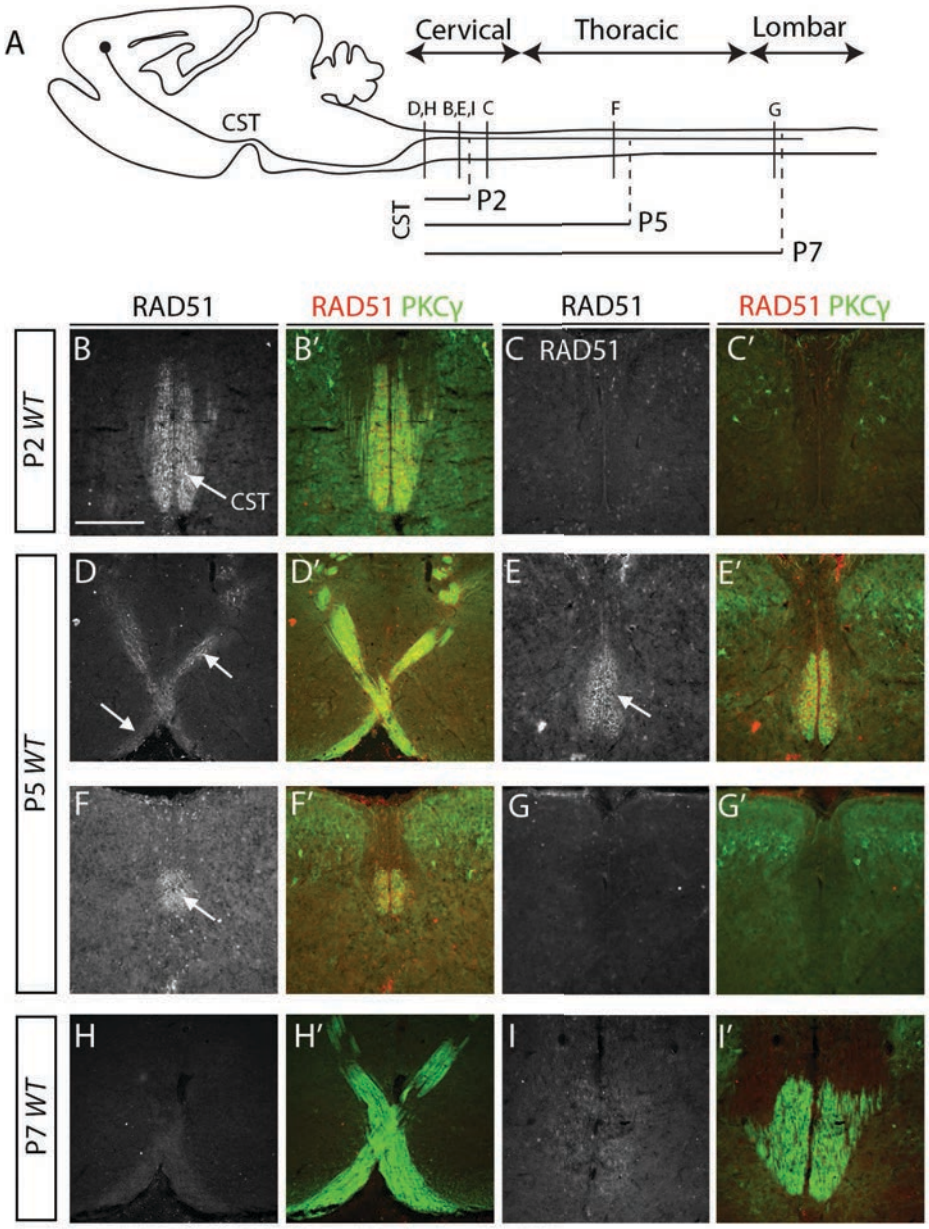

Figure 2. RAD51 is transiently expressed in the CST during development. (A) Schematic representation of a P2 mouse sagittal section indicating the trajectory of the CST, the level of the coronal sections presented in this figure and the temporal course of CST development in the spinal cord. (B-I, B'-I') Coronal sections of P2, P5 and P7 *WT* mice (n = 3 for each age) stained with anti-RAD51 and anti-PKCγ at the level of the pyramidal decussation (D, H) and in the cervical (B, C, E, I), thoracic (F) and lumbar (G) spinal cord. In the spinal cord of P2 and P5 mice, RAD51 was detected along the entire length of the CST, which has reached the cervical and thoracic levels, respectively. (H-I, H'-I') At P7, RAD51 was no longer detected in the CST. White arrows indicate CST axons. The scale bar represents 320 µm in D, H and 160 µm in B,C,E,F,G,I.

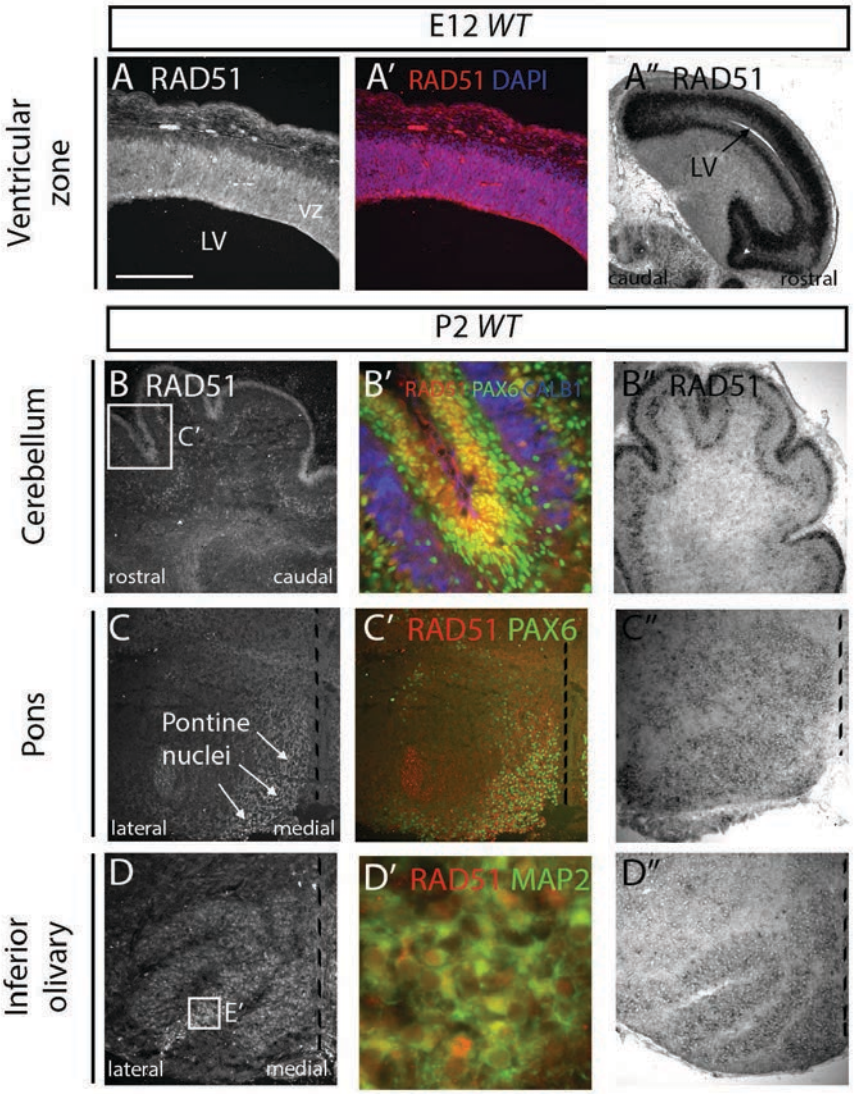

Figure 3. RAD51 expression throughout the central nervous system. (A-D, A'-D') Coronal (A-A'', B-B'') and sagittal (C-C'', D-D'') sections of E12 and P2 *WT* mice (n = 3) stained with anti-RAD51, anti-PAX6 (B', C'), anti-CALB1 (B'), anti-PKCγ (D'), anti-MAP2 (D') and DAPI (A'). (A''-D'') RAD51 in-situ hybridization in coronal and sagittal sections of E12 and P2 *WT* mice (n = 3). (A-A'', B-B'') At P2, RAD51 was detected in regions characterized by intense proliferation of progenitor cells: in the ventricular zone, and in the external granule cell layer of the cerebellum. (C-C'', D-D'') RAD51 was detected in the pontine nuclei, as well as in the inferior olive. ISH: in-situ hybridization; LV: lateral ventricule. The scale bar represents 160 µm in A, A'; 640 µm in A''; 320 µm in B, B''; 240 µm in C-C'', D, D''; 80 µm in B' and 30 µm in D'.

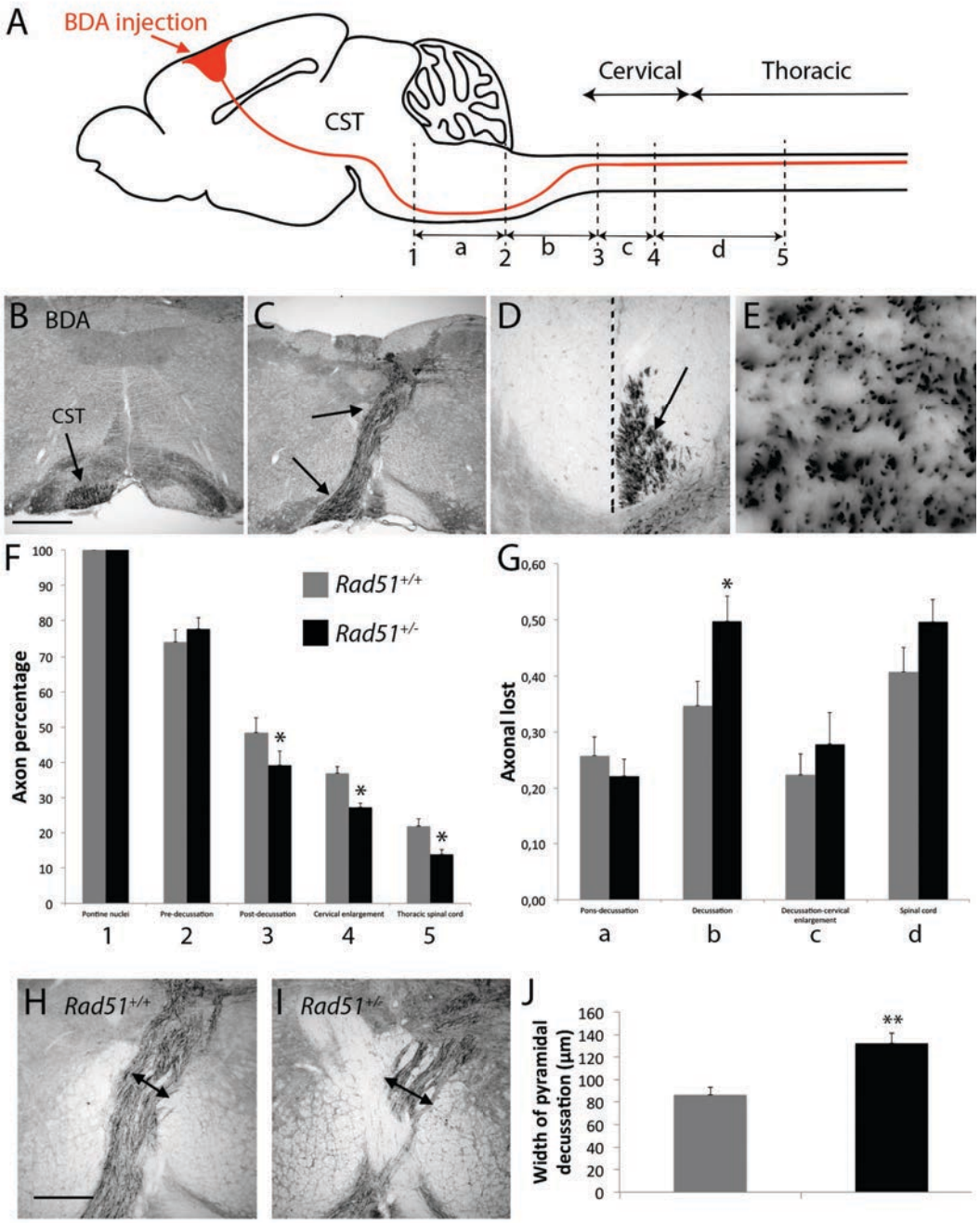

Figure 4. *Rad51*$^{+/-}$ mice have subtle anomalies of the CST. (A) Schematic representation of an adult mouse sagittal section indicating the trajectory of the CST and the level of the coronal sections presented in this figure. (B-E) Biotin dextran amine (BDA) was injected into the left motor cortex of *Rad51*$^{+/+}$ (n = 6) and *Rad51*$^{+/-}$ (n = 6) mice to label the left-sided CST axons. The CST trajectory was similar in *Rad51*$^{+/+}$ and *Rad51*$^{+/-}$ mice: CST axons crossed the midline at the level of pyramidal decussation and continued their trajectory through the dorsal funiculus of the contralateral spinal cord. (F, G) To further study the anatomy of the CST, the number of CST axons was quantified. The axonal lost at the level of the pyramidal decussation was more important in *Rad51*$^{+/-}$ mice compared to control (Mann-Whitney test, p = 0.039). (H-I) The width of the pyramidal decussation was more important in *Rad51*$^{+/-}$ mice compared to control (Mann-Whitney test, p = 0.004), indicating a disorganization of the CST. The scale bar represents 480 µm in B, C; 120 µm in D; 40 µm in E and 240 µm in H, I.

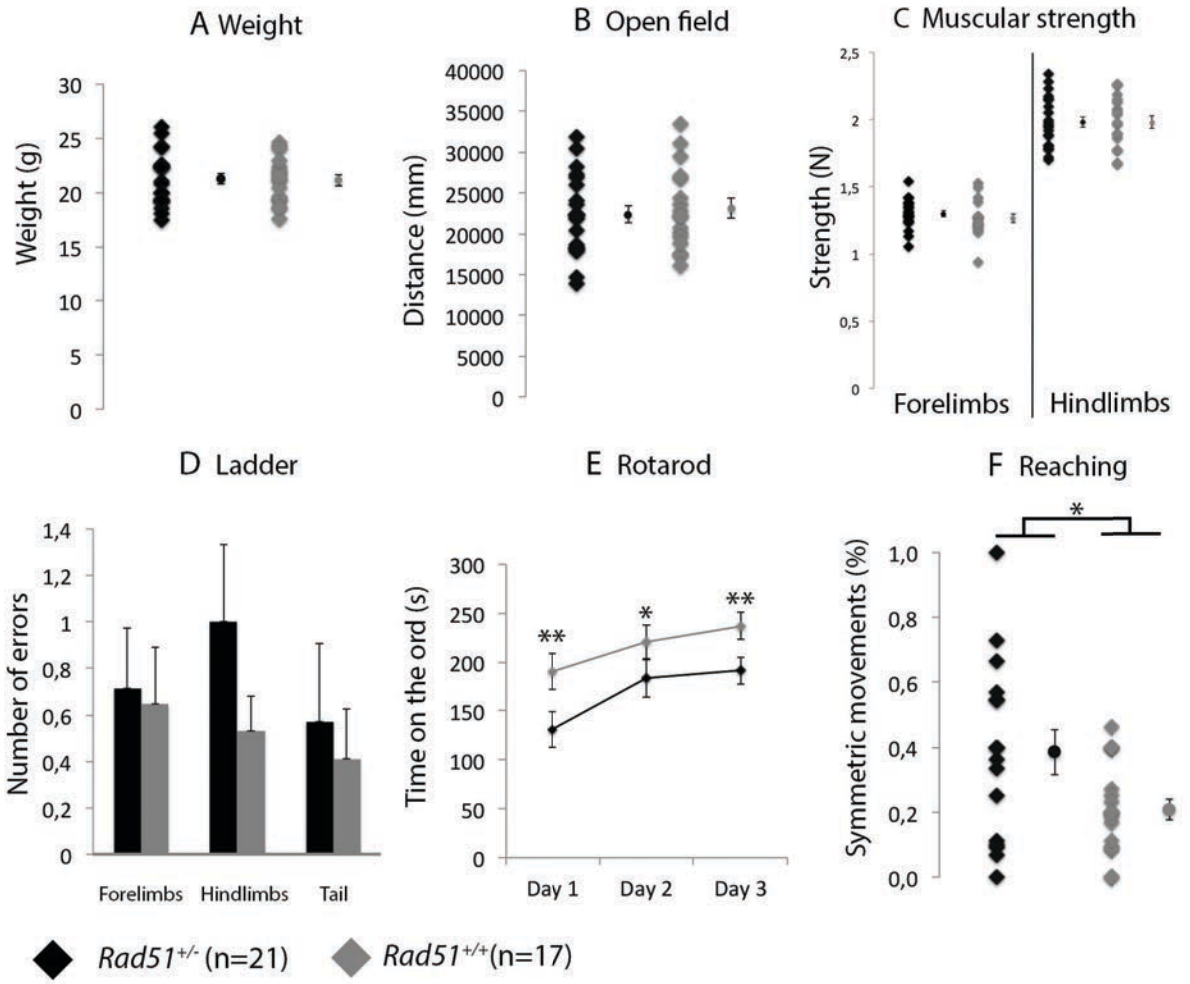

Figure 5. *Rad51*$^{+/-}$ mice have motor lateralization deficits. We used behavioral tests to investigate the motor phenotype of *Rad51*$^{+/-}$ mutant mice (n = 21) as compared to controls (*Rad51*$^{+/+}$; n = 17). There was no significant difference of weight between *Rad51*$^{+/-}$ and controls (Mann-Whitney test, p = 0.73; A). The performances of *Rad51*$^{+/-}$ mice were similar to that of the controls for the open-field (Mann-Whitney test, p = 0.99; B), the muscular strength (Mann-Whitney test, $p_{forelimbs}$ = 0.31; $p_{hindlimbs}$ = 0.74; C) and the ladder test (Mann-Whitney test, $p_{forelimbs}$ = 0.83; $p_{hindlimbs}$ = 0.61; p_{tail} = 0.78; D). *Rad51*$^{+/-}$ mice fell off the Rotarod at significant shorter latencies than controls (repeated-measures ANOVA with two factors. F = 13.2, p = 0.0004, followed by followed by PLSD Fisher*post hoc* analysis; E). When placed in a new walled environment, mice have a tendency to establish contacts on the walls with their forelimbs in an asymmetric or symmetric manner. In the reaching test, *Rad51*$^{+/-}$ mice made more symmetric forelimb movements than the controls (Mann-Whitney test, p = 0.014; F).

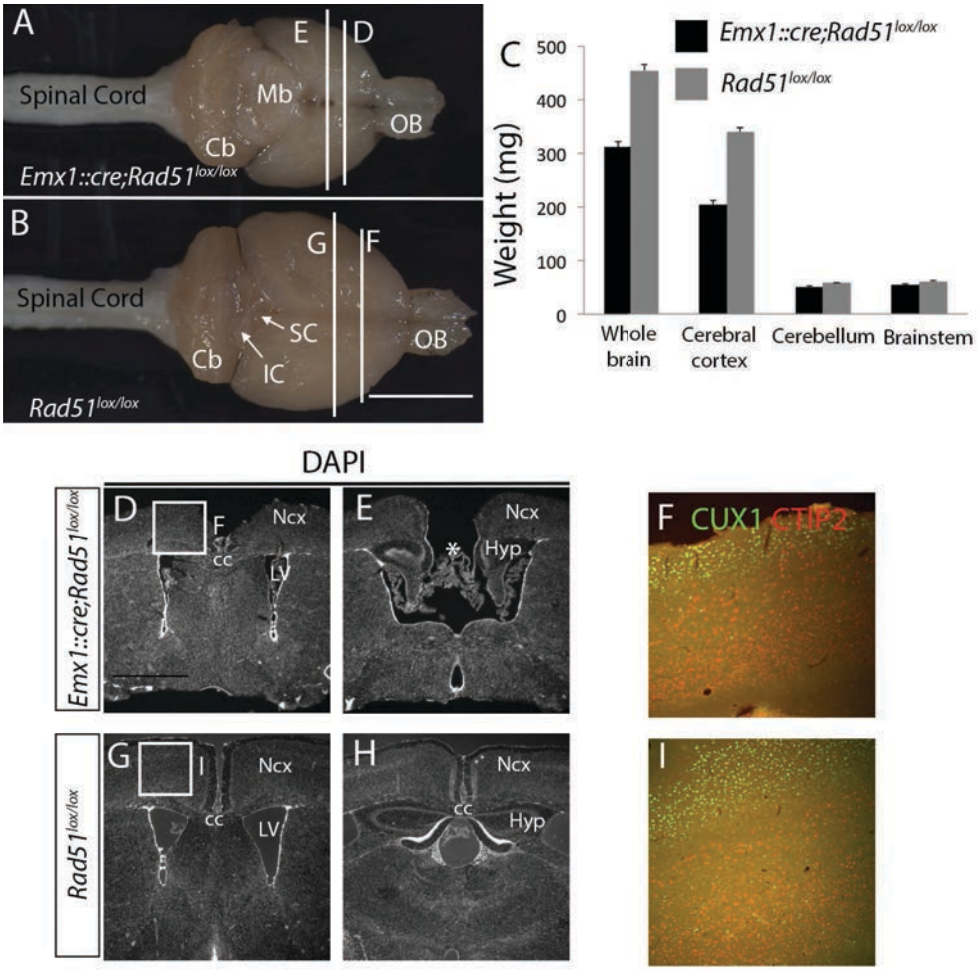

Figure 6. *Emx1::cre;Rad51*$^{lox/lox}$ mice have a reduced neocortex. (A, B) Brains of adult *Emx1::cre;Rad51*$^{lox/lox}$ mice and controls (*Rad51*$^{lox/lox}$). The size of the cerebral cortex was dramatically reduced in *Emx1::cre;Rad51*$^{lox/lox}$ mice, revealing the underlying midbrain. By contrast, the size of the olfactory bulb, cerebellum and spinal cord appeared normal. (C) The weight of the entire brain and cerebral cortex of *Emx1::cre;Rad51*$^{lox/lox}$ mice (n = 3) was reduced compared to that of controls (n = 3), while the weight of the cerebellum and brainstem appeared similar. (D-I) Coronal sections of adult *Emx1::cre;Rad51*$^{lox/lox}$ (n = 3) and *Rad51*$^{lox/lox}$ (n = 3) mice stained with DAPI (D, E, G, H), anti-CTIP2 and anti-CUX1 (F, I). The level of the sections is indicated in (A) and (B). (D, G) Note the reduction of the neocortex radial extension in *Emx1::cre;Rad51*$^{lox/lox}$mice as compared to controls. (E, H) At the level of the hippocampus, the two hemispheres were separated in *Emx1::cre;Rad51*$^{lox/lox}$ mice (*), and the corpus callosum was lacking. The hippocampus also appearedreduced in *Emx1::cre;Rad51*$^{lox/lox}$ mice. (F, I) Immunostainings with anti-CTIP2 and anti-CUX1, which are markers of the deep and superficial neocortical layers respectively, suggest that the cortical layering is preserved in *Emx1::cre;Rad51*$^{lox/lox}$ mice. OB: olfactory bulb; Cb: cerebellum; Mb: midbrain; IC: inferior colliculus; SC: superior colliculus; CC: corpus callosum; Hp: hippocampus; Ncx: neocortex; LV: lateral ventricule. The scale bar represents 0.5 cm in A, B; 1280 µm in D, E, G, H and 320 µm in H, I.

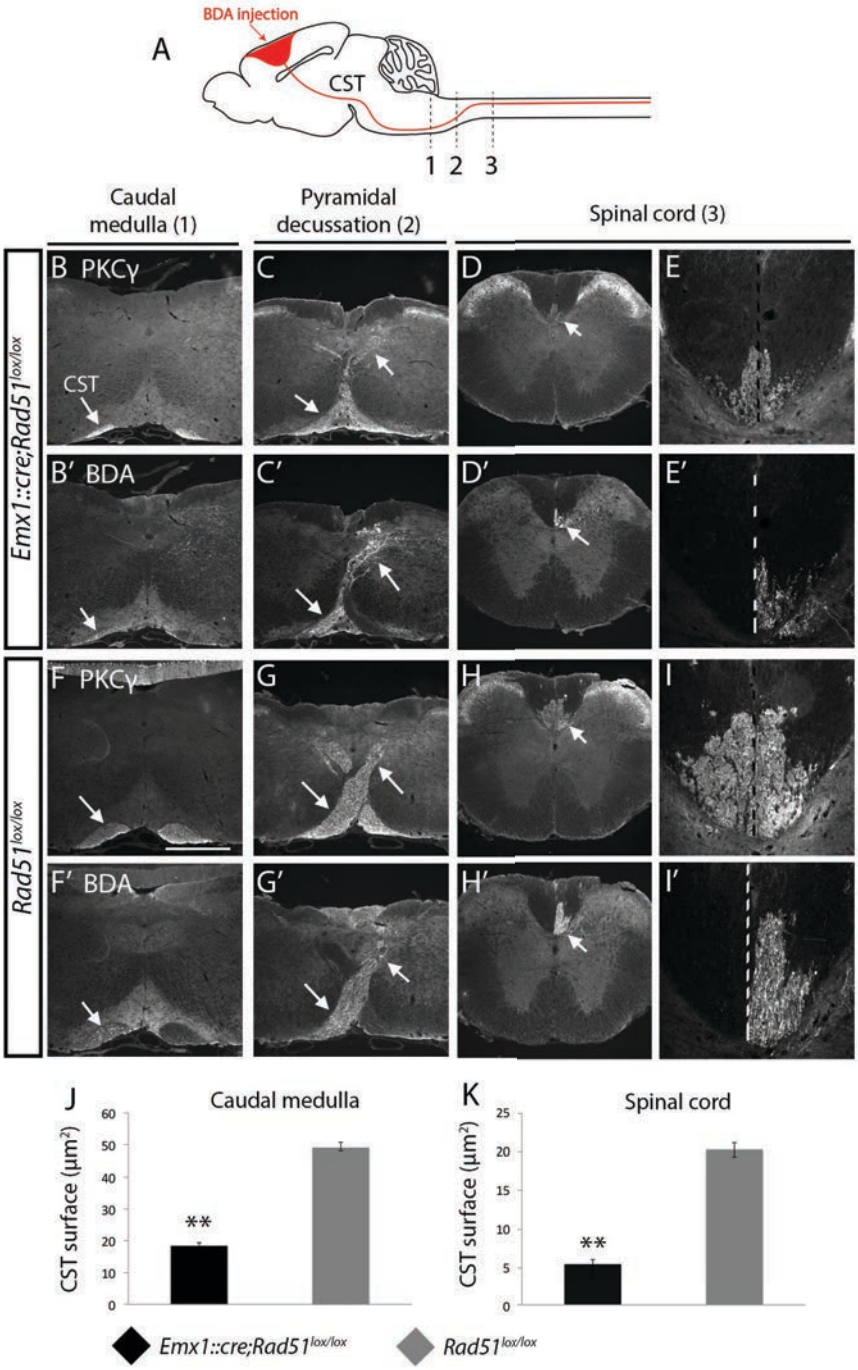

Figure 7. The size of the CST is reduced in *Emx1::cre;Rad51*$^{lox/lox}$ mice. (A) Schematic representation of an adult mouse sagittal section indicating the trajectory of the CST and the level of the coronal sections presented in this figure. Biotin dextran amine (BDA) was injected into the left motor cortex of adult *Emx1::cre;Rad51*$^{lox/lox}$ (n = 6; B-E, B'-E') and *Rad51*$^{lox/lox}$ (n = 5; F-I; F'-I') mice. The CST trajectory was similar in *Emx1::cre;Rad51*$^{lox/lox}$ and *Rad51*$^{lox/lox}$ mice: the CST axons crossed the midline at the decussation (C, C', G, G'), turned dorsally and continued their trajectory in the dorsal funiculus of the contralateral spinal cord (D-E, D'-E', H-I, H'-I'). (J, K) Quantification of the CST surface revealed that it was significant reduced in *Emx1::cre;Rad51*$^{lox/lox}$ mice as compared to controls in the medulla (Mann-Whitney test, p = 0.04) and in the spinal cord (Mann-Whitney test, p = 0.04). The scale bar represents 640 µm in B, C, D, F, G, H and 160 µm in E, I.

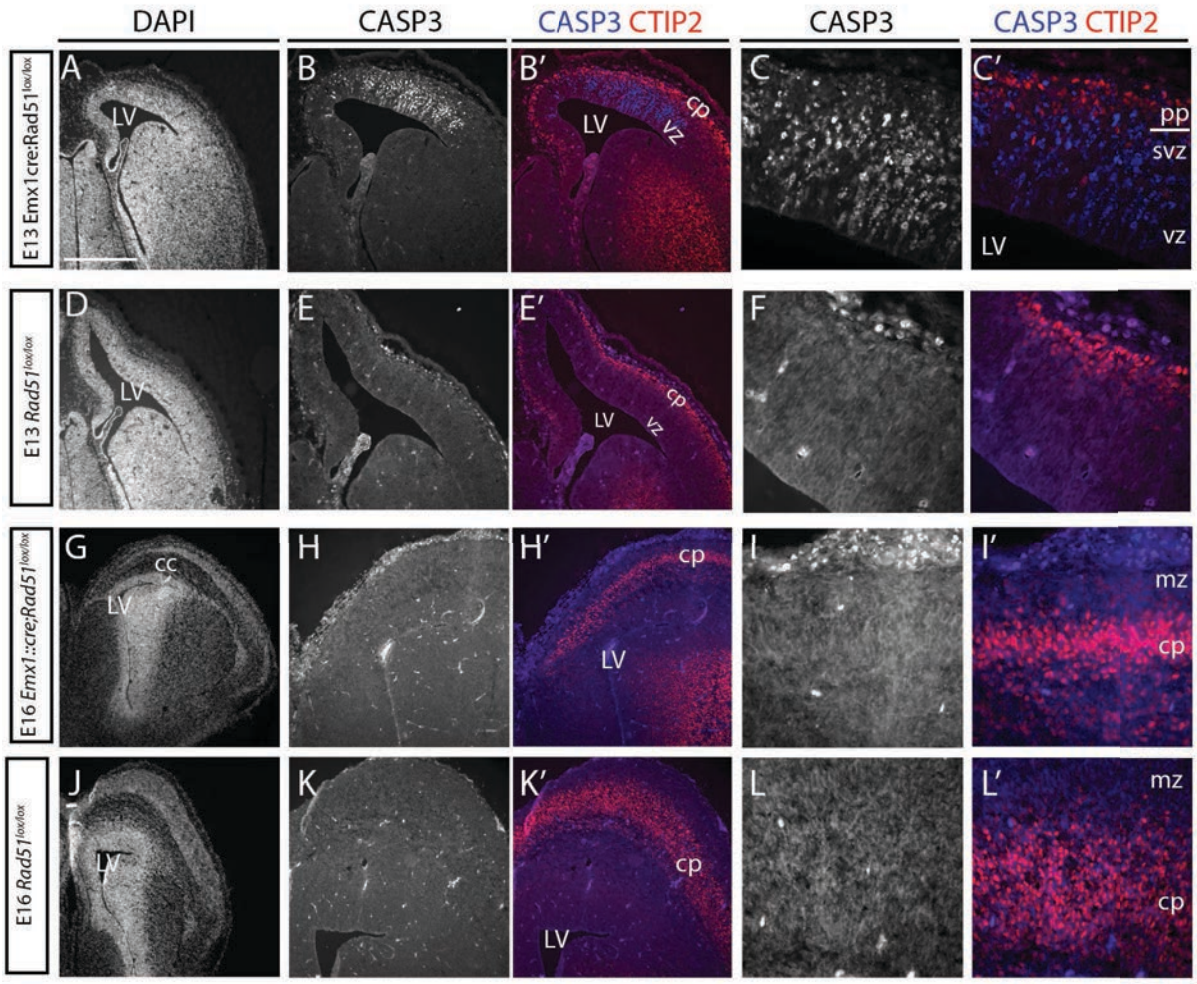

Figure 8. Massive apoptosis during the generation of deep-layers neocortical neurons in *Emx1::cre;Rad51*$^{lox/lox}$ mice. Coronal sections of *Emx1::cre;Rad51*$^{lox/lox}$ and *Rad51*$^{lox/lox}$ mice at E13 and E16 (n = 3) stained with anti-CASP3, anti-CTIP2 and DAPI.At E13, there was massive apoptosis in the progenitor neural layers of the neocortex of *Emx1::cre;Rad51*$^{lox/lox}$ mice (A-C). By contrast, very few cells underwent apoptosis in controls (D-F). At E16, very few CASP3 positive cells were detected in the progenitor layer of *Emx1::cre;Rad51*$^{lox/lox}$ (G-I) and *Rad51*$^{lox/lox}$ mice (J-L). However, the number of CASP3 positive cells appeared increased in the marginal zone of *Emx1::cre;Rad51*$^{lox/lox}$ mice (H-H', I-I'). cc: corpus callosum; cp: cortical plate; LV: lateral ventricule; mz: marginal zone; vz: ventricular zone. The scale bar represents 480 µm in A, D; 640 µm in G, J; 320 µm in B, E, H, K and 80 µm in C, F, I, L.

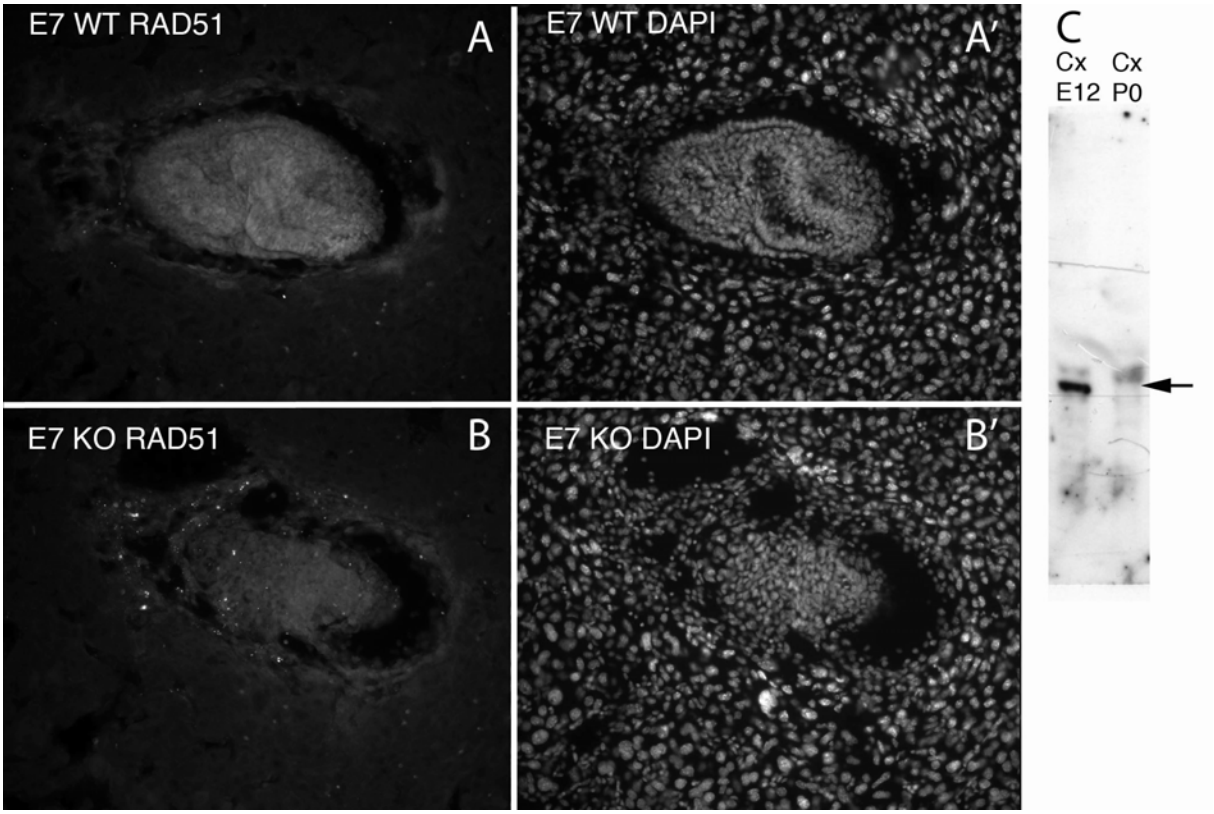

Supplementary Figure 1. Specificity of RAD51 antibody. (A-B) Sagittal sections of E7 *WT* and *Rad51*$^{-/-}$ embryos stained with anti-RAD51 and DAPI. RAD51 was detected in E7 *WT* embryos (A, A'), but not in Rad51$^{-/-}$ embryos (B, B'). (C) Western blot analysis on neocortex tissues from *WT* mice shows a single RAD51 band. Cx: cortex.

V. Article 4 : L'aire motrice supplémentaire intervient dans la préparation des mouvements latéralisés en modulant les interactions inter-hémisphériques (soumis)

Dans les sections précédentes, nous nous sommes principalement intéressés aux relations existant entre les mécanismes développementaux contrôlés par les gènes *DCC*, *NETRIN1* et *RAD51* d'une part et la physiopathologie des MMC d'autre part. En particulier, en utilisant des lignées de souris transgéniques variées, nous avons pu mettre en lumière le rôle de ces gènes dans le développement du système moteur. Par cette approche, nous avons appréhendé les aspects développementaux et anatomiques des MMC. En revanche, cela ne nous a pas permis d'aborder certains aspects fonctionnels de cette pathologie.

A notre sens, un aspect fondamental de la pathologie reste peu connu : celui des mécanismes responsables de l'activation anormale des aires motrices corticales lors de la réalisation d'un mouvement unimanuel. En effet, de nombreuses études ont décrit une activation bilatérale anormale des deux M1 lors de l'exécution de mouvements unimanuels par des patients atteints de MMC (Cohen et al., 1991; Mayer et al., 1995; Leinsinger et al., 1997; Gallea et al., 2013). Une première difficulté se pose à ce niveau : cette activation anormale du cortex ipsilatéral au mouvement est-elle une cause ou une conséquence des MM ? Par ailleurs, plusieurs éléments indiquent que la préparation motrice pourrait être anormale chez les patients atteints de MMC (voir la partie III. A de l'introduction). Cette perspective est intéressante, car les mécanismes sous-tendant la préparation de mouvements latéralisés sont mal connus. Ainsi, nous avons utilisé les MMC comme modèle dysfonctionnel de latéralisation motrice afin de mieux comprendre les mécanismes impliqués dans la préparation des mouvements latéralisés.

Nous avons pour cela étudié l'activation ainsi que les interactions inter-hémisphériques de différentes aires motrices et prémotrices corticales lors de la préparation de mouvements latéralisés par une double approche SMT/IRMf. Nous avons mené cette étude sur un groupe de patients atteints de MMC (n = 21), ainsi que sur des volontaires sains avant et après inhibition transitoire de l'AMS par SMT. Nous avons montré que les aires motrices et prémotrices corticales, notamment M1 et l'AMS, étaient activées de façon anormale lors de la préparation motrice chez les patients. Par ailleurs, les patients présentaient une diminution de l'IIH_c entre les deux M1. En procédant à une inhibition transitoire de l'AMS par SMT chez des volontaires sains, nous avons observé une diminution de l'IIH_c pendant la phase de préparation motrice, reproduisant ainsi la dysfonction observée chez les patients. Ces résultats suggèrent que l'AMS est impliquée dans la préparation des mouvements latéralisés, potentiellement en modulant les interactions inter-hémisphériques entre les deux M1.

The supplementary motor area underlies the preparation of lateralized movements by modulating interhemispheric interactions

Quentin Welniarz,[1,2] Cécile Gallea,[1] Jean-Charles Lamy,[1] Aurélie Méneret,[1,11] Traian Popa,[1] Romain Valabregue,[3] Vanessa Brochard,[4] Constance Flamand-Roze,[5,6] Oriane Trouillard,[1] Cécilia Bonnet,[1,11] Norbert Brüggemann,[7,8] Pierre Bitoun,[9] Bertrand Degos,[11] Cécile Hubsch,[1,11] Elodie Hainque,[1,11] Isabelle Dusart,[2] Marie Vidailhet,[1,11] Stéphane Lehéricy,[1,3] Jean-Louis Golmard,[10] Sabine Meunier,[1] and Emmanuel Roze[1,11]

[1] Sorbonne Universités, UPMC Univ Paris 06, INSERM U 1127, CNRS UMR 7225, Institut du Cerveau et de la Moelle épinière, F-75013, Paris, France

[2] Sorbonne Universités, UPMC Univ Paris 06, INSERM, CNRS, Institut de Biologie Paris Seine, Neuroscience Paris Seine, F-75005, Paris, France

[3] Centre de NeuroImagerie de Recherche CENIR, AP-HP, Hôpital de la Pitie Salpetrière, Paris, France

[4] Centre d'Investigation Clinique 14-22, INSERM/AP-HP, Paris, France

[5] IFPPC, centre CAMKeys, 7 rue des Cordelières, 75013, Paris, France

[6] Service de neurologie, unité cardiovasculaire, centre hospitalier Sud-Francilien, université Paris-Sud, 91100 Corbeille-Essonne, France

[7] Department of Neurology, University of Lübeck, Lübeck, Germany

[8] Institute of Neurogenetics, University of Lübeck, Lübeck, Germany

[9] Génétique Médicale, CHU Paris Nord, AP-HP, Hôpital Jean Verdier, Bondy, France

[10] Département de biostatistiques, AP-HP, Groupe Hospitalier Pitié-Salpêtrière Charles Foix, Paris, France

[11] Département de Neurologie, AP-HP, Hôpital Pitié Salpêtrière, Paris, France

Correspondance to: Emmanuel Roze

Département de Neurologie, Hôpital Pitié Salpêtrière,

47-83 boulevard de l'Hôpital, 75013 Paris

E-mail: flamand.roze.75012@gmail.com; Phone: +33142162748

Short title: Lateralization of movement preparation

Keywords: motor control, interhemispheric inhibition, mirror movements, movement preparation

ABSTRACT

Background: Execution of unimanual movements requires lateralized activation of the motor system. The motor areas involved in motor lateralization during movement preparation are poorly identified.

Objectives: To investigate: (i) motor lateralization during preparation of unimanual movements; (ii) the role of the supplementary motor area (SMA) in this process.

Methods: We studied the activation and interhemispheric interactions of motor/premotor areas during unimanual/bimanual movement preparation by means of functional MRI and transcranial magnetic stimulation in patients with congenital mirror movements, who cannot perform purely unimanual movements, and in healthy volunteers before and after transient SMA inhibition.

Results: Activation of motor/premotor areas and interhemispheric interactions during movement preparation differed between the patients and healthy volunteers. Transient SMA inhibition in the healthy volunteers resulted in abnormal interhemispheric interactions during movement preparation, reminiscent of the situation observed in the patients.

Conclusions: Preparation of unimanual movements is associated with lateralized activation of the motor network, a process that strongly involves the SMA.

INTRODUCTION

Unimanual movements require lateralized activation of the motor system (Welniarz, et al., 2015). Transcranial magnetic stimulation (TMS) and functional MRI (fMRI) studies have revealed activation of the primary motor cortex contralateral to the moving hand ($M1_c$) during unimanual tasks (Catalan, et al., 1998; Flament, et al., 1993; Leinsinger, et al., 1997). By contrast, the M1 ipsilateral to the moving hand ($M1_i$) is inhibited, even though ipsilateral cortical activations have been reported, depending on the movement's complexity, strength and laterality (dominant or non dominant hand) (Buetefisch, et al., 2014; Diedrichsen, et al., 2013; Nirkko, et al., 2001; Perez and Cohen, 2008; Tzourio-Mazoyer, et al., 2015; Ziemann and Hallett, 2001).

Execution of unimanual movements requires complex interactions between motor and premotor areas in the two hemispheres (Beaule, et al., 2012). Each M1 exerts "interhemispheric inhibition" (IHI) on its contralateral homologue via the corpus callosum. IHI directed towards $M1_i$ (IHI_i) is critical for restricting motor output to $M1_c$ (Duque, et al., 2007; Hubers, et al., 2008; Murase, et al., 2004; Perez and Cohen, 2008; Talelli, et al., 2008), while IHI towards $M1_c$ (IHI_c) is lifted during movement execution (Duque, et al., 2007; Hinder, et al., 2012). The dorsal premotor cortex (PMd) also modulates M1 activity during unimanual movements (Koch, et al., 2006; Kroeger, et al., 2010; O'Shea, et al., 2007), and inhibition of the contralateral PMd results in increased excitation of $M1_i$ (Cincotta, et al., 2004; Giovannelli, et al., 2006). The excitability of $M1_c$ and $M1_i$ (Klein, et al., 2016; Wilhelm, et al., 2016), as well as the inputs they receive from the contralateral M1 and PMd (Duque, et al., 2007; Koch, et al., 2006; Kroeger, et al., 2010; Liuzzi, et al., 2010; Murase, et al., 2004; O'Shea, et al., 2007), are differentially modulated during the preparation of unimanual movements in healthy volunteers, suggesting a lateralization of cortical activity during movement preparation. The supplementary motor area (SMA) is involved in

movement preparation and in bimanual coordination, potentially by modulating interhemispheric interactions (Brinkman, 1984; Chan and Ross, 1988; Deiber, et al., 1996; Gallea, et al., 2011; Grefkes, et al., 2008; Serrien, et al., 2002), mostly through the caudal part (SMA-proper) which projects directly to M1 in both hemispheres (Picard and Strick, 1996).

Mirror movements are involuntary symmetrical movements of one side of the body that mirror voluntary movements of the other side (Bonnet, et al., 2010). In patients with congenital mirror movements (CMM), the inability to perform lateralized movements is associated with bilateral M1 activation during the execution of intended unimanual movements, and with weak IHIi at rest (Cohen, et al., 1991; Gallea, et al., 2013; Leinsinger, et al., 1997; Mayer, et al., 1995). SMA activation and functional connectivity is abnormal during motor execution in CMM patients (Gallea, et al., 2013), suggesting that the SMA might be involved in motor lateralization during movement preparation.

Here, we investigated the role of the SMA in the lateralization of unimanual movement preparation by comparing whole-brain fMRI activation patterns during movement preparation in healthy volunteers and CMM patients. In addition, we used TMS to study interhemispheric interactions of motor/premotor areas during movement preparation. Finally, we focused on the role of the SMA in motor lateralization during movement preparation by performing the same protocol before and after transient inhibition of the SMA-proper in healthy volunteers.

MATERIAL AND METHODS

Subjects and experimental groups

Twenty-one right-handed CMM patients were matched for age, gender and handedness with healthy volunteers. All the participants gave their written informed consent and the protocol was approved by the Ile-de-France 6 ethics committee (2013-A00616-39).

Behavioral paradigm

We adapted a previously described delayed-response task (Kroeger, et al., 2010). A first visual cue (S1) informed the subjects to respond with the right hand alone or with both hands. Following S1 presentation, the subjects had to prepare the movement but to remain motionless. A second cue (S2) instructed the subjects either to react (Go) or to withhold the prepared movement (NoGo). In Go trials, the subjects had to tap the finger motor sequence 2-4-3 on a keyboard as fast and precisely as possible after S2. The second cue (S2) was a Go signal in 75% of the cases, and a NoGo signal in 25% of the cases. The S1-S2 interval was randomly chosen from 1.5 s, 2 s or 2.5 s. This procedure allowed the attention level to be maintained and the brain processes to be timed during motor preparation. This experimental design allowed us to distinguish two phases: (1) the preparation phase, between S1 and S2, during which the paraticipants were motionless but were preparing the movement according to S1; (2) the execution phase, after S2. In this study, we only investigated the preparation phase.

Data acquisition and procedure

MRI. The MRI device was a Siemens 3 T MAGNETOM Verio with a 32-channel head coil.

Echo planar images were acquired by multiband imaging (TE=30 ms, TR=1.31 s, flip angle=69°, voxel size=2x2x2 mm^3, 60 slices). The participants performed the task previously described in the MRI. This “event-related” paradigm allowed us to specifically study the brain activations during the preparation phase.

Study of interhemispheric interactions. EMG were recorded bilaterally from the first dorsal interosseous muscle (FDI) (active electrode over the motor point and reference electrode on the metacarpophalangeal joint) with disposable surface Ag/AgCl electrodes (Kendall, Covidien). Responses were amplified (1000x) and filtered (10-1000 Hz; Digitimer D360, Digitimer Ltd, Welwyn Garden City, UK), then digitally transformed at a sampling rate of 2000 Hz (CED Power 1401, CED Ltd., Cambridge, UK), and stored offline for further analysis (Signal 5.02, CED Ltd., Cambridge, UK). TMS test pulses (TP) were applied to the left M1, preceded by conditioning TMS pulses (CP) targeting cortical areas in the right hemisphere (M1, SMA-proper or PMd). TMS pulses were delivered through two figure-of-eight coils (70-mm and 25-mm coils for TP and CP, respectively) connected to two Magstim 200 units delivering monophasic current waveforms (Magstim, Dyfed, UK). For M1 stimulation, the coils were placed tangentially over the cortical representations of the hand areas, with the handle pointing backward, 45° from the midline, so that a posterior-anterior current was induced in the corresponding M1 (Gallea, et al., 2013). The SMA-proper and PMd stimulation sites were defined on the subjects' individual anatomical images. To stimulate the SMA-proper, the coil was centered on the midline, caudal to the VCA line (vertical line drawn through the anterior commissure and perpendicular to the anterior–posterior commissure line in the sagittal plane), and directed toward the right (Arai, et al., 2012; Vorobiev, et al., 1998). For stimulation of the PMd, the coil was positioned anterior to the M1 hotspot, at a distance corresponding to 8% of the distance from nasion to inion (typically around 3 cm) (Kroeger, et al., 2010). All the stimulation sites were stored in a MRI-

based neuronavigation system (Brainsight, Rogue Research, Montreal, Canada) fed with the subjects' individual MRIs, allowing us to maintain same stimulation conditions throughout the experimental sessions. Measurements of the active and resting motor threshold (AMT and RMT) were previously described (Gallea, et al., 2013).

At baseline, we measured the amplitude of the motor evoked potentials (MEPs) triggered by TPs delivered over the left M1 at 1.3xRMT (A_{MEP}[TP]). To measure interhemispheric interactions, TPs were preceded by CPs delivered as follows: (i) to the right M1, 40 ms before the TP (1.2xRMT) (Reis, et al., 2008); (ii) to the right SMA-proper, 6 ms before the TP (1.4xAMT) (Arai, et al., 2012); or (iii) to the right PMd, 8 ms before the TP (1.1xRMT) (Kroeger, et al., 2010). The amplitude of MEPs evoked by CP+TP are noted A_{MEP}[CP+TP]. TMS measurements were performed during the task previously described. TMS stimulations (TP alone or CP+TP) were delivered during the preparation phase, 300 ms after S1 (Fig. 2A). The outcome measure was the ratio of 15 A_{MEP}[CP+TP] to 15 A_{MEP}[TP].

Verification of motor activity during the task. To verify that the participants performed the task correctly, their hand movements were video-recorded and the EMG activity of the fingers extensor and flexor muscles was acquired during the MRI protocol. During the TMS experiments, the experimenters checked the hand movements and EMG traces of the two FDIs. In particular, the experimenters ensured that the subjects remained motionless during movement preparation.

Transient SMA inhibition. We used continuous theta-burst stimulation (cTBS) to transiently inhibit the SMA-proper in healthy volunteers: a total of 600 pulses were delivered at an intensity of 0.9xAMT, in bursts of 3 pulses at 50 Hz, with bursts repeated at a frequency of 5 Hz for a total duration of 40 s (Huang, et al., 2005). fMRI measurements were performed before and within 30 min after cTBS or SHAM stimulation of the right SMA-proper. The

SHAM stimulation was performed with a special coil (SHAM coil) that delivered low intensity stimulations. TMS measurements were made before and within 30 min after cTBS stimulation of the right SMA-proper (Fig. 1A, Fig. 2B).

Organization of the protocol. Each patient made one visit. The first part of the day was dedicated to the fMRI task. The second part of the day was dedicated to the TMS task. The three circuits ($M1_{right}$–$M1_{left}$; SMA_{right}–$M1_{left}$; PMd_{right}–$M1_{left}$) were tested in random order across the subjects.

Each volunteer made five visits. The first and last visits were dedicated to the fMRI task, which was performed before and after cTBS or SHAM stimulation of the SMA. The second, third and fourth visits (one for each tested circuit) were dedicated to the TMS protocol, which was performed before and after cTBS stimulation of the SMA-proper. For each visit, the second part of the protocol (after cTBS or SHAM) was performed within 30 min after SMA stimulation. The minimal interval between two visits was one week, to allow complete washout of the cTBS effects. The order of the visits was randomized across the subjects.

Statistical analysis

MRI. Data were processed and analyzed with statistical parametric mapping software (SPM8, http://www.fil.ion.ucl.ac.uk/spm) (Gallea, et al., 2013). Using individual global linear models, contrasts (unimanual right or bimanual versus implicit baseline) were defined to obtain individual Z-score maps over the whole brain. The Z-score maps of individual contrasts in each group were entered separately in a 2x2 ANOVA (Group: CMM patients, healthy volunteers; Movement: Unimanual right hand, bimanual) to test the hypothesis of abnormal brain activation during movement preparation in CMM patients. We used a 2x2x2 ANOVA (Procedure: cTBS, SHAM; Session: Pre, Post; Movement: Unimanual right hand, bimanual) to test whether cTBS over the SMA affected BOLD signal amplitude during movement

preparation in the healthy volunteers. ANOVA results were considered significant at $p<0.05$ with Family Wise Error (FWE) correction for multiple comparisons over the whole brain for main effects, and at $p<0.001$ uncorrected over the whole brain but with FWE correction at the cluster level for interaction effects.

TMS. The variables A_{MEP}[CP+TP] and A_{MEP}[TP] were entered separately for each circuit in a 2x2 ANOVA (Group: CMM patients, healthy volunteers; Movement: Unimanual right hand, bimanual) to test interhemispheric interactions in CMM patients during movement preparation. We then used a 2x2 ANOVA (Session: Pre, Post; Movement: Unimanual right hand, bimanual) to test whether cTBS over the SMA-proper affected interhemispheric interactions during movement preparation in the healthy volunteers.

RESULTS

MRI

The participants performed the task previously described in the MRI. This specific task allowed us to investigate whole-brain fMRI activation patterns during movement preparation (the period between S1 and S2, before the "Go" signal). In the 2x2 ANOVA (Group x Movement; Table 1), the preparation of bimanual movements as compared to right unimanual movements resulted in more activation of the right M1 and SMA in both groups (Effect of Movement; Fig. 1B). There was no effect of Group, but the Group x Movement interaction revealed stronger activation of the right M1 and right putamen in the CMM patients than in the healthy volunteers during preparation of right unimanual movements (Fig. 1C). Additionally, compared to the healthy volunteers, the CMM patients showed stronger activation of the anterior part of the left SMA (pre-SMA) during preparation of right unimanual and bimanual movements (Fig. 1D).

In the 2x2x2 ANOVA (Procedure x Session x Movement; Table 2), there was no significant effect of Procedure, and no Procedure x Session or Procedure x Session x Movement interaction with respect to the cortical motor/premotor areas. This suggested that cTBS of the SMA-proper did not affect the BOLD signal amplitude during motor preparation in the healthy volunteers.

Electrophysiological experiments

Using the task previously described, we then tested interhemispheric interactions between the right motor cortical areas ($M1_{right}$, PMd_{right}, SMA_{right}) and $M1_{left}$ during preparation (between S1 and S2) of right unimanual or bimanual movements in the CMM patients and healthy volunteers (Fig. 2A-B). For each circuit, we first verified that the A_{MEP}[TP] was similar in the patients and healthy volunteers ($M1_{right}$-$M1_{left}$: $F_{1,38} = 2.54$, $p = 0.12$; SMA_{right}-$M1_{left}$: $F_{1,38}$ =

3.67, p = 0.06; PMd_{right}-$M1_{left}$: $F_{1,38}$ = 0.01, p = 0.92). The 2x2 ANOVA (Group x Movement) showed less inhibition from $M1_{right}$ to $M1_{left}$ in the patients than in the healthy volunteers during both unimanual and bimanual movement preparation (Effect of Group: $F_{1,38}$ = 7.95, p = 0.0076; Fig. 2C). Interhemispheric interactions did not differ between the patients and healthy volunteers for the circuits SMA_{right}-$M1_{left}$ ($F_{1,38}$ = 0.22, p = 0.644; Fig. 2D) and PMd_{right}-$M1_{left}$ ($F_{1,38}$ = 0.01, p = 0.908; Fig. 2E).

We then measured interhemispheric interactions before and after cTBS stimulation of the right SMA-proper in the healthy volunteers (Fig. 1A, 2B). There was no difference in the A_{MEP}[TP] before versus after cTBS ($M1_{right}$-$M1_{left}$: $F_{1,21}$ = 0.16, p = 0.696; SMA_{right}-$M1_{left}$: $F_{1,21}$ = 0.29, p = 0.597; PMd_{right}-$M1_{left}$: $F_{1,21}$ = 0.15, p = 0.707). Similarly to the situation observed in the CMM patients, cTBS in the healthy volunteers diminished the inhibition from $M1_{right}$ to $M1_{left}$ (Effect of Session, $F_{1,21}$ = 4.83, p = 0.039; Fig. 2C), whereas interhemispheric interactions were unaltered for the circuits SMA_{right}-$M1_{left}$ ($F_{1,21}$ = 0.01, p = 0.941; Fig. 2D) and PMd_{right}-$M1_{left}$ ($F_{1,21}$ = 2.15, p = 0.158; Fig. 2E).

DISCUSSION

Using congenital mirror movements as a model of defective lateralization of motor control, we show here that the supplemental motor area is critical for the preparation of lateralized movements.

CMM patients have abnormal $M1_i$ activation during execution of unimanual movements (Cohen, et al., 1991; Gallea, et al., 2013; Leinsinger, et al., 1997; Mayer, et al., 1995). Here, we observed abnormal activation of the $M1_i$ and of the ipsilateral basal ganglia in CMM patients during the preparation of unimanual movement, despite the absence of any movement. This indicates that abnormal $M1_i$ activation during motor execution in CMM patients is not a mere sensory consequence of mirror movements, but is responsible, at least in part, for these patients' inability to produce purely unimanual movements.

Previous studies have revealed miscommunication between the SMA and $M1_i$ during attempted execution of unimanual movements in CMM patients (Gallea, et al., 2013). Here, we found abnormal pre-SMA activation associated with weaker IHI_c during movement preparation in CMM patients. Contrary to the SMA-proper, the pre-SMA has more cognitive properties, few anatomical connections to M1, and is involved in movement preparation (Picard and Strick, 1996). We found that transient inhibition of the SMA-proper by TMS in healthy volunteers resulted in weaker IHI_c during movement preparation, reminiscent of the situation observed in the CMM patients. Neurophysiological studies indicate a possible role of the SMA in motor lateralization during movement preparation (Brinkman, 1984; Gallea, et al., 2011; Gallea, et al., 2013; Grefkes, et al., 2008). Unilateral voluntary movements are preceded by slow-wave negativity on EEG recordings, consisting of two components: 1) the Bereitschaftspotential, starting 2 s before movement onset, is symmetrically distributed and reflects SMA activation; and 2) a subsequent late negative slope localized over the motor cortex contralateral to the moving hand (Shibasaki and Hallett, 2006). Two studies have

shown abnormal bilateral distribution of the late negative slope in patients with CMM (Cohen, et al., 1991; Shibasaki and Nagae, 1984). Our findings show that the SMA-proper modulates interhemispheric inhibition, potentially via direct projections to M1 in both hemispheres (Brinkman, 1984; Picard and Strick, 1996). The SMA thus appears to play a key role in motor lateralization during movement preparation.

ACKNOWLEDGMENTS

The authors thank the CENIR for MRI and TMS data acquisition.

FUNDING SOURCES

The study was supported by INSERM (COSSEC), Merz-Pharma, IP-santé, Djillali Mehri, and by the French Government (IHU-A-ICM) “Investissement d’avenir” ANR-10-IAIHU-06 program.

REFERENCES

Arai, N., Lu, M.K., Ugawa, Y., Ziemann, U. (2012): Effective connectivity between human supplementary motor area and primary motor cortex: a paired-coil TMS study. Exp Brain Res 220: 79-87.

Beaule, V., Tremblay, S., Theoret, H. (2012): Interhemispheric control of unilateral movement. Neural Plast 2012.

Bonnet, C., Roubertie, A., Doummar, D., Bahi-Buisson, N., Cochen de Cock, V., Roze, E. (2010): Developmental and benign movement disorders in childhood. Mov Disord 25: 1317-34.

Brinkman, C. (1984): Supplementary motor area of the monkey's cerebral cortex: short- and long-term deficits after unilateral ablation and the effects of subsequent callosal section. J Neurosci 4: 918-29.

Buetefisch, C.M., Revill, K.P., Shuster, L., Hines, B., Parsons, M. (2014): Motor demand-dependent activation of ipsilateral motor cortex. J Neurophysiol 112: 999-1009.

Catalan, M.J., Honda, M., Weeks, R.A., Cohen, L.G., Hallett, M. (1998): The functional neuroanatomy of simple and complex sequential finger movements: a PET study. Brain 121: 253-64.

Chan, J.L., Ross, E.D. (1988): Left-handed mirror writing following right anterior cerebral artery infarction: evidence for nonmirror transformation of motor programs by right supplementary motor area. Neurology 38: 59-63.

Cincotta, M., Borgheresi, A., Balestrieri, F., Giovannelli, F., Rossi, S., Ragazzoni, A., Zaccara, G., Ziemann, U. (2004): Involvement of the human dorsal premotor cortex in unimanual motor control: an interference approach using transcranial magnetic stimulation. Neurosci Lett 367: 189-93.

Cohen, L.G., Meer, J., Tarkka, I., Bierner, S., Leiderman, D.B., Dubinsky, R.M., Sanes, J.N., Jabbari, B., Branscum, B., Hallett, M. (1991): Congenital mirror movements. Abnormal organization of motor pathways in two patients. Brain 114 381-403.

Deiber, M.P., Ibanez, V., Sadato, N., Hallett, M. (1996): Cerebral structures participating in motor preparation in humans: a positron emission tomography study. J Neurophysiol 75: 233-47.

Diedrichsen, J., Wiestler, T., Krakauer, J.W. (2013): Two distinct ipsilateral cortical representations for individuated finger movements. Cereb Cortex 23: 1362-77.

Duque, J., Murase, N., Celnik, P., Hummel, F., Harris-Love, M., Mazzocchio, R., Olivier, E., Cohen, L.G. (2007): Intermanual Differences in movement-related interhemispheric inhibition. J Cogn Neurosci 19: 204-13.

Flament, D., Goldsmith, P., Buckley, C.J., Lemon, R.N. (1993): Task dependence of responses in first dorsal interosseous muscle to magnetic brain stimulation in man. J Physiol 464: 361-78.

Gallea, C., Popa, T., Billot, S., Meneret, A., Depienne, C., Roze, E. (2011): Congenital mirror movements: a clue to understanding bimanual motor control. J Neurol 258: 1911-9.

Gallea, C., Popa, T., Hubsch, C., Valabregue, R., Brochard, V., Kundu, P., Schmitt, B., Bardinet, E., Bertasi, E., Flamand-Roze, C., Alexandre, N., Delmaire, C., Meneret, A., Depienne, C., Poupon, C., Hertz-Pannier, L., Cincotta, M., Vidailhet, M., Lehericy, S., Meunier, S., Roze, E. (2013): RAD51 deficiency disrupts the corticospinal lateralization of motor control. Brain 136: 3333-46.

Giovannelli, F., Borgheresi, A., Balestrieri, F., Ragazzoni, A., Zaccara, G., Cincotta, M., Ziemann, U. (2006): Role of the right dorsal premotor cortex in "physiological" mirror EMG activity. Exp Brain Res 175: 633-40.

Grefkes, C., Eickhoff, S.B., Nowak, D.A., Dafotakis, M., Fink, G.R. (2008): Dynamic intra- and interhemispheric interactions during unilateral and bilateral hand movements assessed with fMRI and DCM. Neuroimage 41: 1382-94.

Hinder, M.R., Fujiyama, H., Summers, J.J. (2012): Premotor-motor interhemispheric inhibition is released during movement initiation in older but not young adults. PLoS One 7.

Huang, Y.Z., Edwards, M.J., Rounis, E., Bhatia, K.P., Rothwell, J.C. (2005): Theta burst stimulation of the human motor cortex. Neuron 45: 201-6.

Hubers, A., Orekhov, Y., Ziemann, U. (2008): Interhemispheric motor inhibition: its role in controlling electromyographic mirror activity. Eur J Neurosci 28: 364-71.

Klein, P.A., Duque, J., Labruna, L., Ivry, R.B. (2016): Comparison of the two cerebral hemispheres in inhibitory processes operative during movement preparation. Neuroimage 125: 220-32.

Koch, G., Franca, M., Del Olmo, M.F., Cheeran, B., Milton, R., Alvarez Sauco, M., Rothwell, J.C. (2006): Time course of functional connectivity between dorsal premotor and contralateral motor cortex during movement selection. J Neurosci 26: 7452-9.

Kroeger, J., Baumer, T., Jonas, M., Rothwell, J.C., Siebner, H.R., Munchau, A. (2010): Charting the excitability of premotor to motor connections while withholding or initiating a selected movement. Eur J Neurosci 32: 1771-9.

Leinsinger, G.L., Heiss, D.T., Jassoy, A.G., Pfluger, T., Hahn, K., Danek, A. (1997): Persistent mirror movements: functional MR imaging of the hand motor cortex. Radiology 203: 545-52.

Liuzzi, G., Horniss, V., Hoppe, J., Heise, K., Zimerman, M., Gerloff, C., Hummel, F.C. (2010): Distinct temporospatial interhemispheric interactions in the human primary and premotor cortex during movement preparation. Cereb Cortex 20: 1323-31.

Mayer, M., Botzel, K., Paulus, W., Plendl, H., Prockl, D., Danek, A. (1995): Movement-related cortical potentials in persistent mirror movements. Electroencephalogr Clin Neurophysiol 95: 350-8.

Murase, N., Duque, J., Mazzocchio, R., Cohen, L.G. (2004): Influence of interhemispheric interactions on motor function in chronic stroke. Ann Neurol 55: 400-9.

Nirkko, A.C., Ozdoba, C., Redmond, S.M., Burki, M., Schroth, G., Hess, C.W., Wiesendanger, M. (2001): Different ipsilateral representations for distal and proximal movements in the sensorimotor cortex: activation and deactivation patterns. Neuroimage 13: 825-35.

O'Shea, J., Sebastian, C., Boorman, E.D., Johansen-Berg, H., Rushworth, M.F. (2007): Functional specificity of human premotor-motor cortical interactions during action selection. Eur J Neurosci 26: 2085-95.

Perez, M.A., Cohen, L.G. (2008): Mechanisms underlying functional changes in the primary motor cortex ipsilateral to an active hand. J Neurosci 28: 5631-40.

Picard, N., Strick, P.L. (1996): Motor areas of the medial wall: a review of their location and functional activation. Cerebral cortex 6: 342-353.

Reis, J., Swayne, O.B., Vandermeeren, Y., Camus, M., Dimyan, M.A., Harris-Love, M., Perez, M.A., Ragert, P., Rothwell, J.C., Cohen, L.G. (2008): Contribution of transcranial magnetic stimulation to the understanding of cortical mechanisms involved in motor control. J Physiol 586: 325-51.

Serrien, D.J., Strens, L.H., Oliviero, A., Brown, P. (2002): Repetitive transcranial magnetic stimulation of the supplementary motor area (SMA) degrades bimanual movement control in humans. Neurosci Lett 328: 89-92.

Shibasaki, H., Hallett, M. (2006): What is the Bereitschaftspotential? Clin Neurophysiol 117: 2341-56.

Shibasaki, H., Nagae, K. (1984): Mirror movement: application of movement-related cortical potentials. Ann Neurol 15: 299-302.

Talelli, P., Ewas, A., Waddingham, W., Rothwell, J.C., Ward, N.S. (2008): Neural correlates of age-related changes in cortical neurophysiology. Neuroimage 40: 1772-81.

Tzourio-Mazoyer, N., Petit, L., Zago, L., Crivello, F., Vinuesa, N., Joliot, M., Jobard, G., Mellet, E., Mazoyer, B. (2015): Between-hand difference in ipsilateral deactivation is associated with hand lateralization: fMRI mapping of 284 volunteers balanced for handedness. Front Hum Neurosci 9.

Vorobiev, V., Govoni, P., Rizzolatti, G., Matelli, M., Luppino, G. (1998): Parcellation of human mesial area 6: cytoarchitectonic evidence for three separate areas. Eur J Neurosci 10: 2199-203.

Welniarz, Q., Dusart, I., Gallea, C., Roze, E. (2015): One hand clapping: lateralization of motor control. Frontiers in Neuroanatomy 9.

Wilhelm, E., Quoilin, C., Petitjean, C., Duque, J. (2016): A Double-Coil TMS Method to Assess Corticospinal Excitability Changes at a Near-Simultaneous Time in the Two Hands during Movement Preparation. Front Hum Neurosci 10.

Ziemann, U., Hallett, M. (2001): Hemispheric asymmetry of ipsilateral motor cortex activation during unimanual motor tasks: further evidence for motor dominance. Clin Neurophysiol 112: 107-13.

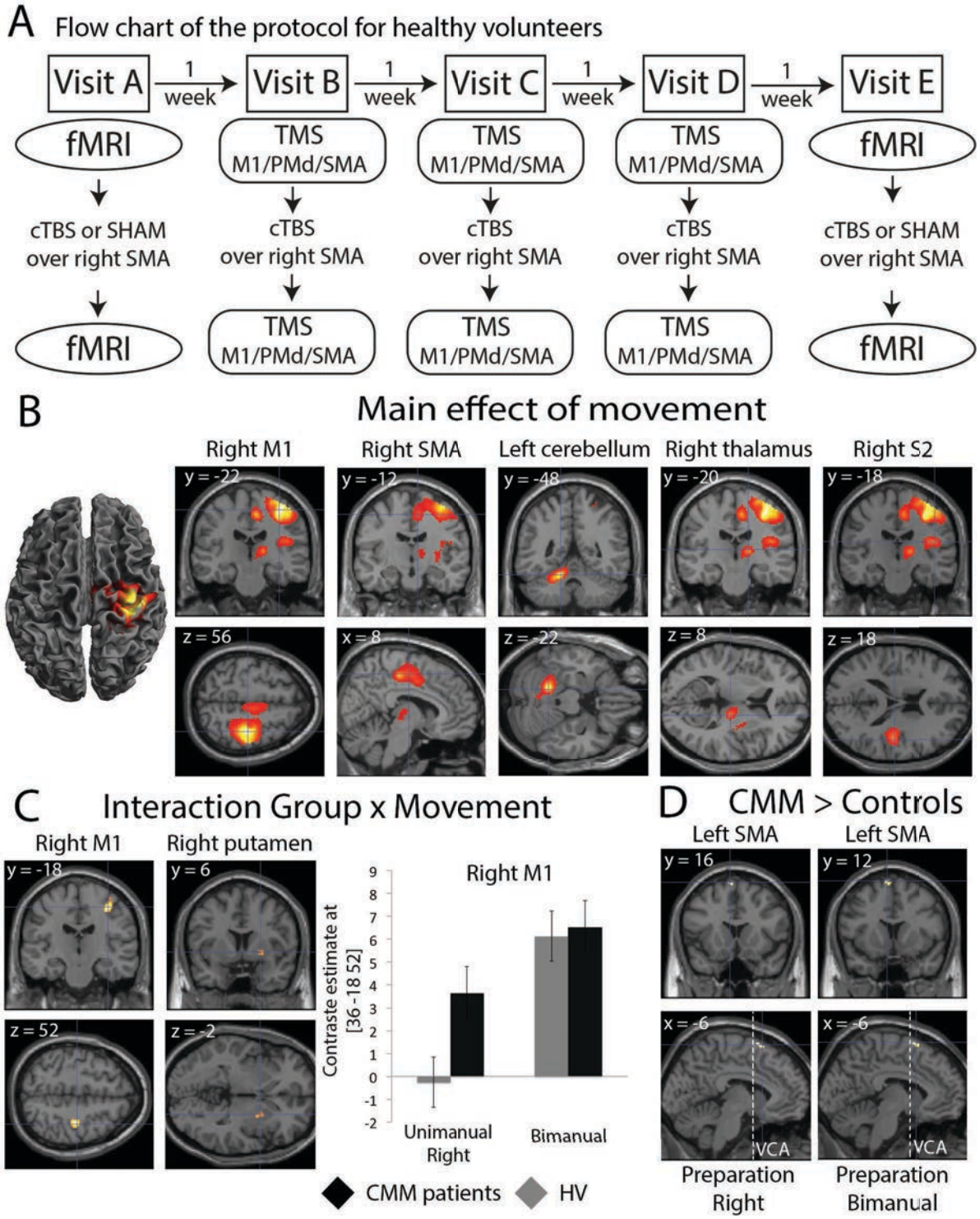

Figure 1. (A) Flow chart. (B-C) Results of 2x2 ANOVA (Group x Movement): sections showing the anatomical location of brain areas that are differently activated in CMM patients versus health volunteers during preparation of right unimanual or bimanual movements. (B) Effect of movement. (C) Group x Movement interaction. (D) Cortical regions more strongly activated in CMM patients than in healthy volunteers.

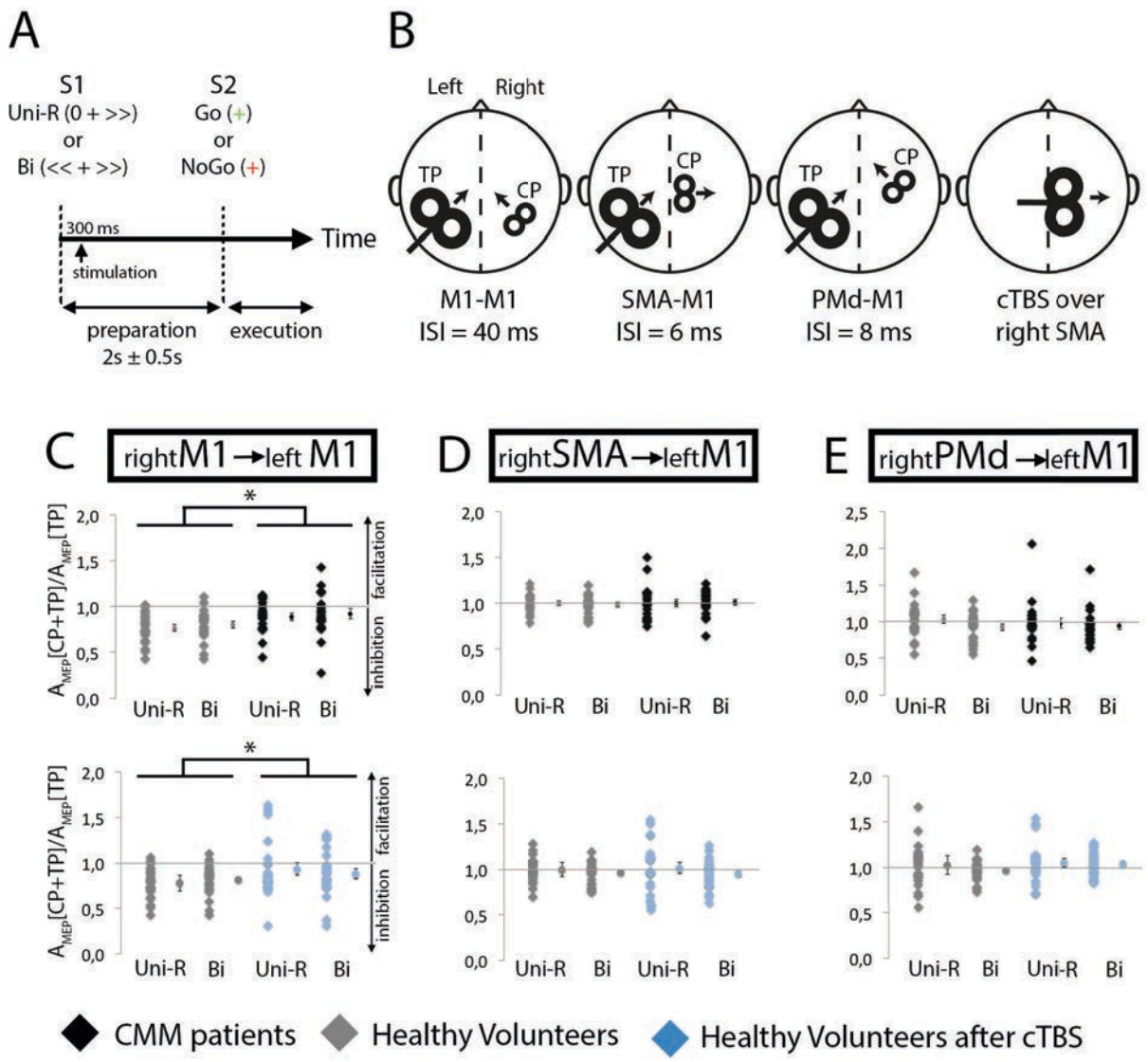

Figure 2. (A) Delayed-response task. (B) Schematic representation of the TMS experimental setup. (C-E) Interhemispheric interactions during preparation of right unimanual or bimanual movement in CMM patients and healthy volunteers (upper panel), and in healthy volunteers before and after inhibition of the SMA-proper (bottom panel). Individual data are presented as dot plots alongside the mean and SEM. ISI: inter-stimulus interval. Uni-R: unimanual right; Bi: bimanual.

Table 1. Comparison of BOLD response during right unimanual or bimanual movement preparation in CMM patients and healthy volunteers

Contrast/Anatomical location	MNI Coordinates	Z score (F score)	kE
Effect of Movement			
Right Precentral	36 -22 56	Inf (203.75)	3714
Right SMA	8 -12 52	6.85 (72.36)	
Left Cerebellum	-14 -48 -22	Inf (137.51)	648
Right Thalamus	16 -20 8	7.6 (97.56)	259
Right Rolandic Opercule	46 -18 18	7.48 (92.86)	546
Effect of Group			
-	-	-	-
Interaction Group x Movement			
Right Precentral	36 -18 52	4.54 (26.37)	170
Right Putamen	24 6 -2	3.35 (13.95)	28
Preparation unimanual			
Patients > Controls			
Left SMA	-6 16 68	3.9(4.47)	10
Preparation bimanual			
Patients > Controls			
Left SMA	-6 12 70	4.4(5.24)	10

MNI coordinates were derived from a 2x2 ANOVA Group (CMM patients; healthy volunteers) x Movement (unimanual right; bimanual). Contrasts for the main effect of Movement and Group were thresholded at a corrected threshold of $P < 0.05$, with a minimum cluster size of 100 voxels. Contrasts for the interaction Group x Movement were thresholded at an uncorrected threshold of $P < 0.001$, with a minimum cluster size of 25 voxels. We then used pairwise *t* test to compare the activations between CMM patients and healthy volunteers during the preparation of unimanual and bimanual movements. Contrasts were thresholded at an uncorrected threshold of $P < 0.001$, with a minimum cluster size of 10 voxels.

Table 2. Comparison of BOLD response during movement preparation before and after SMA-proper stimulation with cTBS or SHAM in healthy volunteers

Contrast/Anatomical location	MNI Coordinates	Z score (F score)	kE
Effect of Movement			
Right Precentral	36 -22 54	Inf(789.3)	7762
Right SMA	8 -22 52	Inf(314.82)	
Left Cerebellum	-16 -48 -20	Inf(310.19)	898
Right Thalamus	18 -20 6	Inf(214.48)	2369
Right Frontal Inferior	58 10 28	6.75(54.36)	220
Effect of time			
Right Parietal Inferior	44 -56 52	5.14(30.31)	52
Left Precuneus	-4 -64 54	5.11(29.93)	96
Effect of Procedure			
-	-	-	-
Effect of Session			
Right parietal inferior	44 -56 52	5.14(30.31)	52
Left precuneus	-4 -64 54	5.11(29.93)	96
Interaction Session x Movement			
-	-	-	-
Interaction Procedure x Session			
Right Occipital lobe	28 -76 4	4.04(18.65)	47
Left Temporal	-62 -48 4	3.96(17.97)	46
Left Insula	-38 -22 14	3.71(15.79)	64
Left frontal lobe	-22 -4 38	3.7(15.74)	42
Right Occipital Superior	28 -64 28	3.63(15.16)	49
Left Frontal Inferior	-48 20 4	3.35(13.02)	16
Interaction Procedure x Movement			
-	-	-	-
Interaction ProcedurexSessionxMovement			
Left parietal lobe	-20 -48 40	4(18.27)	64
Left temporal	-58 -44 0	3.54(14.47)	18
Left parietal inferior	-38 -54 44	3.34(12.97)	10

MNI coordinates were derived from a 2x2x2 ANOVA Procedure (cTBS; SHAM) x Session (Before stimulation; After stimulation) x Movement (unimanual right; bimanual). Contrasts for the main effect of Procedure, Session and Movement were thresholded at a corrected threshold of $P < 0.05$, with a minimum cluster size of 50 voxels. Contrasts for the interactions were thresholded at an uncorrected threshold of $P < 0.001$, with a minimum cluster size of 10 voxels.

Cette étude comporte plusieurs limites. Du fait de contraintes temporelles lors de la réalisation du protocole de SMT, nous avons fait des choix concernant le sens des interactions testées ainsi que les phases du mouvement que nous avons étudiées. Nous nous sommes spécifiquement intéressés aux interactions inter-hémisphériques dirigées vers le $M1_c$, alors que la physiopathologie des MMC fait intervenir une activation anormale du $M1_i$: il aurait donc été pertinent d'avoir des informations concernant l'IIH_i chez les patients. Nous justifions notre choix par le fait que l'inhibition dirigée vers le $M1_c$ est modulée de façon dynamique lors de la préparation motrice, tandis que celle dirigée vers le $M1_i$ reste constante (Murase et al., 2004; Duque et al., 2007; Perez and Cohen, 2008; Hinder et al., 2012). Il nous a donc semblé pertinent, en première approche, de nous intéresser à l'IIH_c.

Nous avons par ailleurs choisi d'étudier les interactions inter-hémisphériques durant la phase « précoce » de préparation motrice, 300 ms après la présentation de la première consigne (sachant que la durée totale de la phase de préparation était de 2 s en moyenne). Ce choix se justifie par les résultats de l'étude réalisée par Kroeger et al, qui décrivent une inhibition du $M1_c$ par le $M1_i$ et le PMd_i dès la phase précoce de préparation (300 ms après S1), tandis que ces inhibitions sont moins marquées au cours de la phase de préparation « tardive » (1800 ms après S1) (Kroeger et al., 2010).

L'absence d'effet de la stimulation conditionnante du PMd_i chez les volontaires sains lors de la phase de préparation peut sembler en contradiction avec les résultats d'études précédentes. Dans l'étude de Kroeger et al, la stimulation du PMd_i entraînait une inhibition du $M1_c$ dès la phase de préparation précoce, 300 ms après S1 (Kroeger et al., 2010). Cependant, les effets décrits dans cette étude ont été obtenus lors de la réalisation de mouvements unimanuels de la main non-dominante (gauche), tandis que dans notre étude, les participants devaient réaliser des mouvements unimanuels de la main dominante (droite). Ces résultats peuvent être expliqués par le fait que les mécanismes modulant l'excitabilité de la voie

corticospinale varient en fonction de la main utilisée (dominante ou non-dominante), comme nous l'avons illustré dans l'introduction. Dans notre étude, la stimulation conditionnante de l'AMS_i n'a pas eu d'effet sur l'hémisphère opposé lors de la phase de préparation motrice. Une modeste facilitation a été décrite entre l'AMS et M1 (Arai et al., 2012), mais dans des conditions différentes : en effet, dans cette étude, les interactions ont été testées au sein d'un même hémisphère et au repos.

Enfin, il peut sembler paradoxal d'avoir effectué une stimulation inhibitrice de l'AMS droite chez les volontaires sains, tandis que nous avons observé une activation anormale de l'AMS gauche chez les patients au cours de l'étude d'IRMf. Tout d'abord, l'activation anormale de l'AMS gauche chez les patients est un résultat qui a été obtenu *a posteriori*. Nous avions initialement fait le choix de stimuler l'AMS droite sur la base d'une étude de lésions unilatérales de l'AMS réalisées chez le singe (Brinkman, 1984). Dans cette étude, les effets de l'altération de l'AMS étaient maximaux lorsque la lésion était réalisée au niveau de l'hémisphère opposé à la main non-dominante. Tous nos sujets étant droitiers, il nous a donc semblé qu'une inhibition de l'AMS droite aurait des conséquences maximales. De plus, l'hypothèse que nous voulions étudier était que l'AMS puisse avoir un effet sur les interactions inter-hémisphériques par le biais du CC. En stimulant l'AMS gauche, nous n'aurions pas pu exclure un effet direct de l'AMS gauche sur le M1 gauche via des connexions intra-hémisphériques (Picard and Strick, 1996). Nous pouvons ajouter que sur le plan pratique, l'AMS étant une structure très médiale, il est probable que l'inhibition réalisée par SMT ait affecté non seulement l'AMS droite, mais aussi, dans une moindre mesure, l'AMS gauche.

DISCUSSION

Dans la première partie de la discussion, nous allons revenir sur l'ensemble des résultats de ce manuscrit (Articles 1-4 et résultats complémentaires) afin de répondre aux questions que nous avions posées en introduction : (i) l'homogénéité clinique des MM est-elle le reflet de mécanismes communs aux différentes formes génétiques de MMC ? (ii) quelles est l'importance relative du CC et du FCS dans la physiopathologie des MM ? (iii) existe-t-il d'autres mécanismes intervenant dans la physiopathologie des MM ? En particulier, quel est le lien entre la phase de préparation motrice et les MM ?

Dans un second temps nous reviendrons de façon plus précise sur les mécanismes développementaux responsables des MMC. Nous nous focaliserons sur le rôle du couple NETRIN1-DCC (Articles 2, 3 et résultats complémentaires) dans le développement du système moteur, et nous proposerons un mécanisme hypothétique pour expliquer les anomalies du FCS associées aux dysfonctions de ces deux protéines.

Pour conclure, nous nous demanderons si le cas des MM représente en effet un bon paradigme pour étudier la latéralisation du contrôle moteur, et en particulier si les anomalies observées chez les patients sont bien le reflet de fonctions physiologiques détériorées.

I. Les mouvements en miroir congénitaux : un modèle pour comprendre la latéralisation motrice

A. Des causes génétique hétérogènes aboutissant à un phénotype commun

Le syndrome des MMC est caractérisé par une hétérogénéité sur le plan génétique. Trois gènes en lien avec les MMC ont été identifiés à ce jour : *DCC, RAD51* et *DNAL4* (Meneret et al., 1993; Srour et al., 2010; Depienne et al., 2011; Depienne et al., 2012; Ahmed et al., 2014; Meneret et al., 2014a; Meneret et al., 2014b), et des travaux récents de l'équipe, présentés dans ce manuscrit, ont identifié de nouvelles mutations dans le gène *NETRIN1* (Article 2). Des études menées dans le laboratoire avaient permis d'explorer la physiopathologie des patients *RAD51*, et avaient identifié deux mécanismes, non exclusifs, expliquant les symptômes de ces patients : (i) une anomalie développementale du FCS aboutissant à la mise en place de projections bilatérales de chacun des hémisphères sur la moelle ; (ii) des défauts de communication inter-hémisphérique, responsables d'une activation bilatérale anormale des deux cortex moteurs lors de l'exécution d'un mouvement unimanuel (Gallea et al., 2013). Dans ce manuscrit, nous avons présenté les résultats provenant de l'étude de patients *DCC* et *NETRIN1* (Articles 1 et 2). Dans ces deux formes génétiques de MMC, nous avons retrouvé des altérations anatomiques de la décussation pyramidale associées à la présence de projections corticospinales anormales depuis chacun des hémisphères sur la moelle ipsilatérale. Chez les patients *DCC*, nous avons par ailleurs mis en évidence une diminution de l'IIH au repos, tandis que le faible nombre de patients *NETRIN1* étudiés ne nous permet pas de conclure sur une potentielle altération des interactions inter-hémisphériques (Articles 1 et 2).

Ainsi, des mutations des gènes *RAD51*, *DCC* et *NETRIN1* aboutissent à des anomalies anatomiques du FCS ainsi qu'à un phénotype moteur commun, les MM. Nos études chez la

souris ont permis de préciser le rôle de *DCC* et *NETRIN1* dans le développement du FCS (Article 1 et résultats complémentaires), et nous présenterons dans la partie suivante un mécanisme hypothétique expliquant la façon dont ce couple ligand/récepteur participe au guidage des axones corticospinaux à la ligne médiane. Le lien précis entre RAD51 et les anomalies décelées chez les patients *RAD51*-MMC demeure inconnu. Si nos études ont permis de démontrer que RAD51 assure le bon déroulement de la prolifération des progéniteurs néocorticaux grâce à son activité de réparation de l'ADN, la fonction de cette protéine en lien avec le développement du système moteur et les MMC reste inconnue (Article 3). En particulier, nous ne pouvons pas conclure quant à l'origine des anomalies du FCS observées chez les patients *RAD51*. Dans le cas des patients *DCC* et *NETRIN1*, la fonction connue de ces deux gènes dans le guidage des axones commissuraux chez la souris, ainsi que l'organisation aberrante des projections corticospinales chez les mutants Dcc^{kanga} et $Shh::cre;Netrin^{lox/lox}$ suggèrent que les anomalies anatomiques du FCS des patients sont la conséquence d'un défaut de guidage des axones corticospinaux au cours du développement (Articles 1, 2 et résultats complémentaires de la thèse). Dans le cas de RAD51, nous ne pouvons pas exclure la possibilité d'un mécanisme différent. Chez l'humain, des études de SMT ont démontré l'existence de projections corticospinales bilatérales sur la moelle chez les nouveau-nés et les jeunes enfants. Au cours des premières années de vie, les projections ipsilatérales aberrantes sont éliminées (Eyre et al., 2001; Eyre, 2007). Il est donc possible d'envisager qu'un défaut de maturation des projections corticospinales, et notamment un maintien anormal des projections ipsilatérales, puisse être responsable des anomalies observées chez ces patients.

Les mutations des gènes *RAD51*, *DCC* et *NETRIN1* aboutissent à des anomalies anatomiques du FCS ainsi qu'à un phénotype moteur semblable. Il est cependant très probable que les mécanismes sous-jacents soient différents. Il est intéressant de souligner que

le couple NETRIN1-DCC semble intervenir dans le guidage du FCS de façon non cellule-autonome (voir Article 1, résultats complémentaires et partie II de la discussion). En revanche, l'expression de RAD51 au niveau du FCS suggère un rôle direct, dont le mécanisme reste cependant à découvrir (Article 3). Ainsi nos travaux illustrent le fait que des phénotypes semblables peuvent avoir des origines différentes.

B. Importance relative du CC et du FCS dans la physiopathologie des MMC

Tout au long de ce travail, nous avons insisté sur l'existence de deux anomalies, non exclusives, pouvant expliquer les MM chez les patients atteints : (i) une anomalie de communication inter-hémisphérique, mettant en jeu le CC, aboutissant à une activation bilatérale des deux M1 lors de l'exécution d'un mouvement unimanuel ; (ii) une anomalie développementale du FCS aboutissant à la mise en place de projections bilatérales de chacun des hémisphères sur la moelle. Est-il possible de distinguer l'importance relative de ces deux processus dans la physiopathologie des MMC ?

Les anomalies anatomiques du FCS sont étroitement associées à la physiopathologie des MMC. A notre connaissance, tous les patients atteints de MMC présentent des projections corticospinales anormales. Réciproquement, l'existence de projections corticospinales bilatérales depuis un même cortex moteur est systématiquement associée à la présence de MM (Revues de la littérature 1 et 2). Le rôle connu du FCS dans le contrôle de la motricité volontaire suggère fortement que les projections corticospinales bilatérales observées chez les patients atteints de MMC sont responsables, du moins en partie, de leur incapacité à produire des mouvements latéralisés. A ce jour, une seule étude a véritablement remis en question le lien de cause à effet entre les projections corticospinales bilatérales et les MMC (Verstynen et al., 2007). Cette étude, réalisée sur un seul patient, a montré que les muscles qui étaient les

plus affectés par les MM n'étaient pas ceux qui recevaient les projections corticospinales conjointes (des deux M1) les plus fortes.

Il existe des MM dits « physiologiques », observés chez les jeunes enfants ou lors de la réalisation d'un effort particulièrement intense, qui surviennent chez des individus dont le FCS est complètement normal (Bonnet et al., 2010; Koerte et al., 2010). Des défauts de communication inter-hémisphérique, et en particulier d'IIH (normalement assurée par le CC), sont la principale explication des MM physiologiques (Hubers et al., 2008; Koerte et al., 2010; Welniarz et al., 2015). Une activation bilatérale des deux M1 lors de l'exécution de mouvements unimanuels a été décrite chez de nombreux patients atteints de MMC (Cohen et al., 1991; Mayer et al., 1995; Leinsinger et al., 1997; Verstynen et al., 2007; Gallea et al., 2013). De plus, cette activation anormale du $M1_i$ est corrélée à une diminution de l'IIH_i chez les patients *RAD51* (Gallea et al., 2013). Cependant, si les dysfonctions du CC et des interactions inter-hémisphériques étaient les principales causes des MMC, nous pourrions nous attendre à l'existence de liens forts entre les anomalies développementales du CC et les MMC. Or, bien que les AgCC sont associées le plus souvent à une altération profonde de la communication inter-hémisphérique (Meyer et al., 1995), l'activation des aires motrices corticales lors de la réalisation de mouvements unimanuels semble normale chez ces patients (Reddy et al., 2000; Hsu et al., 2013). Les MM ne sont pas un symptôme couramment associé aux AgCC (Paul et al., 2007), et très peu de patients présentant ces deux anomalies de façon conjointe ont été décrits (Lepage et al., 2012). Cependant, les AgCC sont une entité très hétérogène, ce qui représente probablement une limite de ces études. Lorsque l'AgCC n'est pas totale, il est difficile d'évaluer la proportion de fibres connectant encore les deux hémisphères, tandis qu'il existe probablement des mécanismes de compensation assurant la mise en relation des deux hémisphères par d'autres voies anatomiques (Hsu et al., 2013). De plus, nous avons souligné plus haut que les anomalies du CC observées chez les patients

MMC sont principalement fonctionnelles, tandis que les défauts anatomiques semblent réduits (Gallea et al., 2013).

La principale objection qui peut être faite quant à l'importance fonctionnelle de l'activation bilatérale des M1 observées chez les patients MMC est qu'il est difficile de déterminer si cette activation corticale anormale est la cause, ou simplement la conséquence sensorielle des MM. Notre protocole d'IRMf, réalisé sur un grand nombre de patients MMC, a montré une activation bilatérale des régions motrices corticales et des défauts d'interactions inter-hémisphériques dès la phase de préparation de mouvements unimanuels (Article 4), corroborant ainsi les données d'enregistrements EEG d'une étude antérieure (Cohen et al., 1991). Cette observation suggère fortement que l'activation anormale des deux M1 lors de la préparation et l'exécution de mouvements unimanuels chez les patients MMC n'est pas une conséquence des MM, mais participe activement (au moins en partie) à leur incapacité à réaliser des mouvements latéralisés.

Au vu de l'ensemble de ces données, il semble difficile de départager l'importance du CC et du FCS dans la physiopathologie des MMC. Cependant, il est possible que l'importance relative de ces deux mécanismes dépende de la forme génétique des MMC. Chez les patients *RAD51* et *DCC*, il semble que les deux processus soient à l'œuvre et qu'ils interviennent conjointement dans la génération des MM. A l'inverse, il est possible que chez d'autres patients, l'un des deux processus prédomine sur l'autre (Verstynen et al., 2007; Lepage et al., 2012).

C. Vers d'autres acteurs et mécanismes responsables des MMC ?

Les études précédentes menées dans le laboratoire (Gallea et al., 2013), ainsi que celle présentée dans ca manuscrit (Article 4), ont permis d'identifier un nouvel acteur dont le rôle est primordial dans la physiopathologie des MMC : l'AMS. Cécile Gallea avait observé que

l'activation et la connectivité fonctionnelle de l'AMS étaient anormales chez les patients *RAD51*-MMC au cours de l'exécution de mouvements unimanuels. L'hypothèse proposée était que cette activation anormale de l'AMS soit responsable d'une altération de la transmission du plan moteur depuis la SMA vers le cortex moteur, aboutissant ainsi à une activation bilatérale des deux M1 (Gallea et al., 2013). Etant donné le rôle connu de l'AMS dans la préparation motrice et dans la coordination bimanuelle, ces résultats ont suscité de nouvelles questions concernant la fonction de l'AMS dans la préparation des mouvements latéralisés. Dans l'étude présentée dans ce manuscrit, nous avons tout d'abord confirmé que l'activation de l'AMS était anormale lors de la phase de préparation motrice chez un grand nombre de patients, qui étaient, de plus, hétérogènes sur le plan génétique (Article 4). Ce résultat suggère donc que l'activation anormale de l'AMS n'est pas une spécificité liée à la mutation de *RAD51*. En outre, nous avons pu proposer des hypothèses sur le mécanisme d'action de l'AMS. En procédant à une inhibition transitoire de cette région par SMT chez des volontaires sains, nous avons observé une diminution de l'IIH_c pendant la phase de préparation motrice, reproduisant ainsi une dysfonction observée chez les patients. Il semble donc qu'il y ait un lien causal entre l'activation anormale de l'AMS et la diminution de l'IIH chez les patients MMC (Article 4). L'AMS pourrait donc moduler les interactions inter-hémisphériques, potentiellement par le biais de connexions cortico-corticales et transcalleuses avec les M1 des deux hémisphères (Brinkman, 1984; Picard and Strick, 1996).

Pour conclure cette partie, nous tenons à préciser que d'autres mécanismes, non encore connus, pourraient intervenir dans la physiopathologie des MMC. En particulier, nous avons souligné l'importance des interneurones commissuraux de la moelle pour la génération de mouvements alternés et asymétriques lors de la locomotion chez la souris (Revue de la littérature 1 ; Welniarz et al, 2015). La proportion de connexions excitatrices et inhibitrices établit un équilibre entre les deux moitiés de la moelle : lorsque l'équilibre est déplacé vers la

facilitation, des mouvements symétriques sont produits, et au contraire, des mouvements asymétriques sont produits lorsque l'inhibition prédomine. Il existe dans la moelle du singe des interneurones commissuraux établissant des connexions entre les motoneurones contrôlant les muscles des mains (Soteropoulos et al., 2013). En raisonnant par analogie avec le cas des souris *EphA4* (Kullander et al., 2001; Kullander et al., 2003; Borgius et al., 2014), il est possible d'imaginer qu'un défaut de guidage des axones spinaux puisse engendrer une augmentation des connexions excitatrices entre les motoneurones des deux mains, et par conséquent produire des MM. L'exploration des circuits spinaux représente donc une prochaine étape pour une compréhension plus complète de la physiopathologie des MM.

II. Le couple NETRIN1-DCC joue un rôle crucial dans le développement du système moteur

Nos études ont permis une meilleure compréhension de la fonction du couple NETRIN1-DCC dans le développement du système moteur et ont clarifié le lien entre la physiopathologie MMC et les dysfonctions de ces deux protéines. Nous avons tout d'abord montré que les patients *DCC* atteints de MMC présentent des anomalies anatomiques du FCS (Article 1). Nous avons identifié *NETRIN1*, le ligand de *DCC*, comme un nouveau gène responsable des MMC, et l'étude de ces patients a aussi révélé l'existence d'anomalies anatomiques du FCS (Article 2). Ainsi, DCC et NETRIN1 sont toutes deux nécessaires au développement du FCS chez l'humain.

L'analyse de différentes lignées de souris mutantes nous a permis de mieux comprendre le rôle de *Dc*c et *Netrin1* dans le développement du système moteur, et leur lien avec la pathologie des MMC. Le rôle de DCC dans le guidage du FCS au niveau de la ligne médiane était déjà connu (Finger et al., 2002). Nous avons montré que DCC contrôle ce processus de façon indirecte (non cellule-autonome), car la suppression totale de DCC dans le télencéphale dorsal, et donc dans le FCS, n'a pas reproduit les anomalies du FCS observées chez les souris Dcc^{kanga} (Article 1). Nous avons aussi démontré pour la première fois que la production de NETRIN1 au niveau de la plaque du plancher était nécessaire à la formation de la décussation pyramidale (résultats complémentaires).

Il est intéressant de remarquer que pour les mutants $Dcc^{kanga/-}$ comme pour les mutants $Shh::cre;Netrin^{lox/lox}$, il existe une association entre des défauts de guidage du FCS à la ligne médiane et des anomalies anatomiques de l'OI (Article 1 et résultats complémentaires). Chez les souris $Dcc^{kanga/-}$, seule la partie la plus caudale de l'OI était atteinte : des neurones de l'OI étaient présents à une position anormale, au niveau de la ligne médiane, à l'emplacement normal de la décussation pyramidale. Chez les souris $Shh::cre;Netrin^{lox/lox}$, la disposition des

cellules de l'OI vis-à-vis de la ligne médiane était normale. Cependant, au lieu d'être groupés à proximité de la ligne médiane, les neurones de l'OI étaient étalés latéralement (Figure 18B).

Il a été proposé que les neurones de l'OI interviennent dans le guidage du FCS par le biais de la sécrétion de SEMA6A. Cette molécule a un effet répulsif lorsqu'elle interagit avec ses récepteurs PLEXINA3/PLEXINA4, exprimés par les axones corticospinaux (Suto et al., 2005; Faulkner et al., 2008; Runker et al., 2008). La structure anatomique de l'olive permettrait donc potentiellement de contraindre les axones corticospinaux à adopter une position ventro-médiale dans le tronc cérébral. La disposition relative du FCS et de l'OI chez les souris sauvages est compatible avec cette hypothèse. En effet, le FCS est situé en-dessous de l'olive dans le tronc cérébral, et il n'y a pas de superposition entre les axones corticospinaux et les neurones de l'OI (Figure 18C). La décussation du FCS a lieu au niveau de l'extrémité caudale de l'olive, lorsque celle-ci adopte une position plus latérale, permettant ainsi le passage des axones vers la ligne médiane (Figure 18E).

Chez les souris *Dcc*$^{kanga/-}$ et *Shh::cre;Netrin*$^{lox/lox}$, la disposition relative de l'OI et du FCS était conservée, c'est-à-dire que nous n'avons pas observé de co-localisation d'axones corticospinaux et de cellules de l'OI. Il semble donc que le caractère répulsif de l'OI vis-à-vis du FCS soit conservé chez ces deux mutants. Etant donné que le positionnement des neurones de l'OI se fait avant P0 d'une part (Bourrat and Sotelo, 1988; 1990), et que *Netrin1* et *Dcc* sont tous deux impliqués dans le développement de l'OI d'autre part (Bloch-Gallego et al., 1999; Marcos et al., 2009), nous pouvons formuler l'hypothèse suivante : il est possible que des anomalies anatomiques de l'OI soient responsables de défauts de guidage du FCS lorsqu'il atteint la partie caudale du tronc cérébral à P0. Dans le cas des mutants *Dcc*^{kanga}, la présence de cellules de l'OI au niveau de la ligne médiane empêcherait donc l'ensemble des axones de décusser. Dans le cas des souris *Shh::cre;Netrin*$^{lox/lox}$, l'extension latérale anormale de l'OI serait responsable d'un « étalement » latéral du FCS dans le tronc cérébral, alors qu'il

est normalement regroupé en position médiale. Une fois arrivés au niveau de la décussation, les axones situés en position latérale seraient potentiellement trop éloignés pour percevoir les molécules de guidage sécrétées au niveau de la ligne médiane, ce qui expliquerait qu'ils restent au sein du cordon ventro-latéral de la moelle ipsilatérale. Cette hypothèse a été avancée dans le cas des mutants *Sema6A*$^{-/-}$, dont le phénotype est assez similaire à celui des souris *Shh::cre;Netrin*$^{lox/lox}$ (Faulkner et al., 2008; Runker et al., 2008). Cette hypothèse ne rend cependant pas compte de l'intégralité du phénotype des souris *Shh::cre ;Netrin*$^{lox/lox}$. En effet, nous avons observé chez ces dernière une composante du FCS située dans le cordon ventro-médial de la moelle ipsilatérale (Figure 19C). Ces axones, proches de la ligne médiane, devraient donc percevoir les molécules de guidage au niveau de la décussation, ce qui indique qu'un autre niveau de complexité, encore inconnu, est en jeu à ce niveau.

Cependant, il ne nous est pas actuellement possible d'exclure formellement l'hypothèse inverse, à savoir que les anomalies d'anatomie de l'OI soient la conséquence, et non pas la cause, des défauts de guidage du FCS. Afin de trancher, nous devrons générer des mutants présentant des altérations exclusivement au niveau de l'OI, et vérifier si ces anomalies sont suffisantes pour reproduire le phénotype des mutants que nous avons étudiés. L'équipe d'Alain Chédotal a généré des souris *Ptfa1::cre ;DCC*$^{lox/lox}$, chez qui le suppression de DCC est restreinte aux neurones de l'OI (Renier et al., 2010). Des analyses préliminaires n'ont révélé aucun défaut de l'anatomie du FCS chez ces souris. Cependant, de façon surprenante, ces souris ne présentent pas non plus de défauts de l'OI, ce qui ne nous permet donc pas d'écarter le rôle de cette structure dans le guidage du FCS. Comme perspective, nous proposons de comparer l'anatomie du tronc cérébral de nos mutants avec des souris contrôles à P0 afin d'identifier des structures, situées à proximité de la décussation pyramidale, dont la malformation chez les mutants pourrait expliquer les défauts de guidage du FCS au niveau de la ligne médiane.

III. Conclusion

Notre étude a-t-elle fait du tort aux conceptions héritées d'Auguste Comte et de Claude Bernard, ou les a-t-elle confortées ? Y a-t-il bien une continuité, une homogénéité entre les phénomènes normaux et les phénomènes pathologiques ?

En premier lieu, on peut remarquer que les MMC ont bien leur équivalent chez les individus dits « normaux ». Les MM physiologiques peuvent se manifester dans certaines situations ou à certains moments de la vie chez des sujets ne souffrant d'aucun trouble neurologique. On pourrait donc être tenté de dire que les MMC ne sont qu'une « exagération » des MM physiologiques, que les deux ne sont qu'une seule et même entité, qui serait simplement aggravée de façon considérable chez les patients. Cependant, l'examen plus précis des causes responsables des MM fait apparaître des différences fondamentales entre ces deux entités. Tandis que l'activation bilatérale des deux M1 lors de l'exécution d'un mouvement unimanuel est présente chez patients et parfois chez les sujets sains (dans une proportion moindre), les défauts de l'anatomie du FCS sont une caractéristique exclusive des patients. Chez les souris *Dcc*^{kanga} et *Shh::cre;Netrin*$^{lox/lox}$, la position du FCS ipsilatéral dans la moelle ne correspond pas à celle du FCS non-croisé « physiologique ». Cette observation suggère que chez les patients *DCC* et *NETRIN1*, le FCS ipsilatéral n'est probablement pas une simple exagération du FCS non-croisé existant chez les personnes saines. Il serait plutôt la conséquence d'une anomalie de guidage des axones corticospinaux, qui aboutirait à la mise en place d'une structure aberrante n'ayant pas son équivalent dans le développement normal. Chez ces patients, le FCS serait « altéré », ce terme renvoyant ici à une différence de nature, et non pas à une différence de degré, à une différence qualitative et non quantitative. Il semble donc que, contrairement à ce que pensait Auguste Comte, la pathologie soit bien capable de « produire des phénomènes vraiment nouveaux ».

Mais peut-être Claude Bernard aurait-il fait l'objection suivante : si les conséquences du diabète sur l'organisme n'ont pas leur équivalent chez les sujets sains, ses causes en revanche (une glycémie élevée) ne correspondent qu'à une simple dérégulation quantitative d'un processus qui existe dans le cas normal. Tout ne dépend-il pas de l'échelle à laquelle on se place ? Il est vrai que les anomalies anatomiques du FCS chez les patients MMC sont la conséquence d'une diminution de la quantité de protéine fonctionnelle produite (que ce soit *RAD51*, *DCC* ou *NETRIN1*) : il s'agit en somme d'une « simple » variation quantitative par rapport à une valeur normale. La subtilité se situe simplement dans le fait que des modifications pathologiques, en parfaite continuité avec les processus biologiques normaux, peuvent à un point donné créer une altération, une rupture qualitative.

Soit, mais nous aimerions pousser cette conception une dernière fois dans ses retranchements. Lorsqu'une mutation entraîne une diminution de la quantité de protéine produite, nous sommes bien dans le cadre des théories d'Auguste Comte et de Claude Bernard. Qu'en est-il dans le cas de mutations a effet dominant négatif, c'est-à-dire lorsqu'une mutation confère à la protéine une fonction totalement anormale, qui n'est pas observée chez le sujet sain ? Nous avons évoqué cette possibilité dans le cas des formes de MMC liées à des mutations de *RAD51* (voir la discussion de l'article 3).

Si les avancées de la biologie et la découverte de nouveaux niveaux de complexité questionnent cette approche, elle ne perd pas de sa puissance et de son caractère prédictif pour autant. C'est l'observation des anomalies d'activation de l'AMS chez les patients qui nous a poussés à supposer que cette aire avait un rôle dans la préparation motrice dans le cas normal, hypothèse que nous avons par la suite pu valider en créant une dysfonction transitoire et réversible de cette région. Tout notre raisonnement scientifique se fonde sur cette approche lorsque, pour connaître le rôle d'un gène, d'une protéine ou d'une structure, nous commençons par le modifier, l'altérer, le supprimer, afin d'en tirer des leçons sur sa fonction

normale. Ce paradigme demeure donc une façon puissante d'appréhender la complexité du vivant.

REFERENCES

REFERENCES

Aboitiz, F., and Montiel, J. (2003). One hundred million years of interhemispheric communication: the history of the corpus callosum. *Braz J Med Biol Res* 36**,** 409-420.

Aboitiz, F., Scheibel, A.B., Fisher, R.S., and Zaidel, E. (1992). Fiber composition of the human corpus callosum. *Brain Res* 598**,** 143-153.

Ahmed, G., Shinmyo, Y., Ohta, K., Islam, S.M., Hossain, M., Naser, I.B., et al. (2011). Draxin inhibits axonal outgrowth through the netrin receptor DCC. *J Neurosci* 31**,** 14018-14023.

Ahmed, I., Mittal, K., Sheikh, T.I., Vasli, N., Rafiq, M.A., Mikhailov, A., et al. (2014). Identification of a homozygous splice site mutation in the dynein axonemal light chain 4 gene on 22q13.1 in a large consanguineous family from Pakistan with congenital mirror movement disorder. *Hum Genet* 133**,** 1419-1429.

Alcamo, E.A., Chirivella, L., Dautzenberg, M., Dobreva, G., Farinas, I., Grosschedl, R., et al. (2008). Satb2 regulates callosal projection neuron identity in the developing cerebral cortex. *Neuron* 57**,** 364-377.

Alexander, G.E., and Crutcher, M.D. (1990). Preparation for movement: neural representations of intended direction in three motor areas of the monkey. *Journal of Neurophysiology* 64**,** 133-150.

Alisky, J.M., Swink, T.D., and Tolbert, D.L. (1992). The postnatal spatial and temporal development of corticospinal projections in cats. *Experimental brain research* 88**,** 265-276.

Amaniti, E.M., Hasenpusch-Theil, K., Li, Z., Magnani, D., Kessaris, N., Mason, J.O., et al. (2013). Gli3 is required in Emx1+ progenitors for the development of the corpus callosum. *Dev Biol* 376**,** 113-124.

Ameziane, N., May, P., Haitjema, A., Van De Vrugt, H.J., Van Rossum-Fikkert, S.E., Ristic, D., et al. (2015). A novel Fanconi anaemia subtype associated with a dominant-negative mutation in RAD51. *Nat Commun* 6**,** 8829.

Andrews, W., Liapi, A., Plachez, C., Camurri, L., Zhang, J., Mori, S., et al. (2006). Robo1 regulates the development of major axon tracts and interneuron migration in the forebrain. *Development* 133**,** 2243-2252.

Angevine, J.B., Jr., and Sidman, R.L. (1961). Autoradiographic study of cell migration during histogenesis of cerebral cortex in the mouse. *Nature* 192**,** 766-768.

Arai, N., Lu, M.K., Ugawa, Y., and Ziemann, U. (2012). Effective connectivity between human supplementary motor area and primary motor cortex: a paired-coil TMS study. *Exp Brain Res* 220**,** 79-87.

Arányi, Z., and Rösler, K.M. (2002). Effort-induced mirror movements. *Experimental Brain Research* 145**,** 76-82.

Arlotta, P., Molyneaux, B.J., Chen, J., Inoue, J., Kominami, R., and Macklis, J.D. (2005). Neuronal subtype-specific genes that control corticospinal motor neuron development in vivo. *Neuron* 45**,** 207-221.

Armand, J., Edgley, S.A., Lemon, R.N., and Olivier, E. (1994). Protracted postnatal development of corticospinal projections from the primary motor cortex to hand motoneurones in the macaque monkey. *Exp Brain Res* 101**,** 178-182.

Armand, J., Olivier, E., Edgley, S.A., and Lemon, R.N. (1997). Postnatal development of corticospinal projections from motor cortex to the cervical enlargement in the macaque monkey. *J Neurosci* 17**,** 251-266.

Ashwell, K.W., Marotte, L.R., Li, L., and Waite, P.M. (1996). Anterior commissure of the wallaby (Macropus eugenii): adult morphology and development. *J Comp Neurol* 366**,** 478-494.

Auerbach, A.D. (2009). Fanconi anemia and its diagnosis. *Mutat Res* 668**,** 4-10.

Bagri, A., Marin, O., Plump, A.S., Mak, J., Pleasure, S.J., Rubenstein, J.L., et al. (2002). Slit proteins prevent midline crossing and determine the dorsoventral position of major axonal pathways in the mammalian forebrain. *Neuron* 33**,** 233-248.

Baird, P.A., Robinson, G.C., and Buckler, W.S. (1967). Klippel-Feil syndrome. A study of mirror movement detected by electromyography. *Am J Dis Child* 113**,** 546-551.

Baranek, C., Dittrich, M., Parthasarathy, S., Bonnon, C.G., Britanova, O., Lanshakov, D., et al. (2012). Protooncogene Ski cooperates with the chromatin-remodeling factor Satb2 in specifying callosal neurons. *Proc Natl Acad Sci U S A* 109**,** 3546-3551.

Barkovich, A.J., Guerrini, R., Kuzniecky, R.I., Jackson, G.D., and Dobyns, W.B. (2012). A developmental and genetic classification for malformations of cortical development: update 2012. *Brain* 135**,** 1348-1369.

Bauman, G.I. (1932). Absence of the cervical spine. *Journal of the American Medical Association* 98**,** 129-132.

Beaule, V., Tremblay, S., and Theoret, H. (2012). Interhemispheric control of unilateral movement. *Neural Plast* 2012.

Belle, M., Godefroy, D., Dominici, C., Heitz-Marchaland, C., Zelina, P., Hellal, F., et al. (2014). A simple method for 3D analysis of immunolabeled axonal tracts in a transparent nervous system. *Cell Rep* 9**,** 1191-1201.

Benadiba, C., Magnani, D., Niquille, M., Morle, L., Valloton, D., Nawabi, H., et al. (2012). The ciliogenic transcription factor RFX3 regulates early midline distribution of guidepost neurons required for corpus callosum development. *PLoS Genet* 8**,** e1002606.

Berbel, P., and Innocenti, G.M. (1988). The development of the corpus callosum in cats: a light- and electron-microscopic study. *J Comp Neurol* 276**,** 132-156.

Bestmann, S., and Duque, J. (2015). Transcranial magnetic stimulation decomposing the processes underlying action preparation. *The Neuroscientist***,** 1073858415592594.

Bignami, A., and Dahl, D. (1974). Astrocyte-specific protein and neuroglial differentiation. An immunofluorescence study with antibodies to the glial fibrillary acidic protein. *J Comp Neurol* 153**,** 27-38.

Bloch-Gallego, E., Ezan, F., Tessier-Lavigne, M., and Sotelo, C. (1999). Floor plate and netrin-1 are involved in the migration and survival of inferior olivary neurons. *J Neurosci* 19**,** 4407-4420.

Bloom, J.S., and Hynd, G.W. (2005). The role of the corpus callosum in interhemispheric transfer of information: excitation or inhibition? *Neuropsychol Rev* 15**,** 59-71.

Bonnet, C., Roubertie, A., Doummar, D., Bahi-Buisson, N., Cochen De Cock, V., and Roze, E. (2010). Developmental and benign movement disorders in childhood. *Mov Disord* 25**,** 1317-1334.

Borgius, L., Nishimaru, H., Caldeira, V., Kunugise, Y., Low, P., Reig, R., et al. (2014). Spinal glutamatergic neurons defined by EphA4 signaling are essential components of normal locomotor circuits. *J Neurosci* 34**,** 3841-3853.

Bourrat, F., and Sotelo, C. (1988). Migratory pathways and neuritic differentiation of inferior olivary neurons in the rat embryo. Axonal tracing study using the in vitro slab technique. *Brain Res* 467**,** 19-37.

Bourrat, F., and Sotelo, C. (1990). Early development of the rat precerebellar system: migratory routes, selective aggregation and neuritic differentiation of the inferior olive and lateral reticular nucleus neurons. An overview. *Arch Ital Biol* 128**,** 151-170.

Brinkman, C. (1984). Supplementary motor area of the monkey's cerebral cortex: short- and long-term deficits after unilateral ablation and the effects of subsequent callosal section. *J Neurosci* 4**,** 918-929.

Brinkman, C., and Porter, R. (1983). Supplementary motor area and premotor area of monkey cerebral cortex: functional organization and activities of single neurons during performance of a learned movement. *Adv Neurol* 39**,** 393-420.

Britanova, O., De Juan Romero, C., Cheung, A., Kwan, K.Y., Schwark, M., Gyorgy, A., et al. (2008). Satb2 is a postmitotic determinant for upper-layer neuron specification in the neocortex. *Neuron* 57**,** 378-392.

Bronson, R.T., and Lane, P.W. (1990). Hydrocephalus with hop gait (hyh): a new mutation on chromosome 7 in the mouse. *Brain Res Dev Brain Res* 54**,** 131-136.

Brouns, M.R., Matheson, S.F., Hu, K.Q., Delalle, I., Caviness, V.S., Silver, J., et al. (2000). The adhesion signaling molecule p190 RhoGAP is required for morphogenetic processes in neural development. *Development* 127**,** 4891-4903.

Brouwer, B., Sale, M.V., and Nordstrom, M.A. (2001). Asymmetry of motor cortex excitability during a simple motor task: relationships with handedness and manual performance. *Exp Brain Res* 138**,** 467-476.

Buetefisch, C.M., Revill, K.P., Shuster, L., Hines, B., and Parsons, M. (2014). Motor demand-dependent activation of ipsilateral motor cortex. *J Neurophysiol* 112**,** 999-1009.

Carter, M.J., Maslovat, D., and Carlsen, A.N. (2015). Anodal transcranial direct current stimulation applied over the supplementary motor area delays spontaneous antiphase-to-in-phase transitions. *Journal of neurophysiology* 113**,** 780-785.

Catalan, M.J., Honda, M., Weeks, R.A., Cohen, L.G., and Hallett, M. (1998). The functional neuroanatomy of simple and complex sequential finger movements: a PET study. *Brain* 121**,** 253-264.

Chalupa, L.M., and Killackey, H.P. (1989). Process elimination underlies ontogenetic change in the distribution of callosal projection neurons in the postcentral gyrus of the fetal rhesus monkey. *Proc Natl Acad Sci U S A* 86**,** 1076-1079.

Chan, J.L., and Ross, E.D. (1988). Left-handed mirror writing following right anterior cerebral artery infarction: evidence for nonmirror transformation of motor programs by right supplementary motor area. *Neurology* 38**,** 59-63.

Chedotal, A. (2011). Further tales of the midline. *Curr Opin Neurobiol* 21**,** 68-75.

Chen, R. (2004). Interactions between inhibitory and excitatory circuits in the human motor cortex. *Experimental Brain Research* 154**,** 1-10.

Chen, R., Cohen, L.G., and Hallett, M. (1997a). Role of the ipsilateral motor cortex in voluntary movement. *Canadian Journal of Neurological Sciences/Journal Canadien des Sciences Neurologiques* 24**,** 284-291.

Chen, R., Gerloff, C., Hallett, M., and Cohen, L.G. (1997b). Involvement of the ipsilateral motor cortex in finger movements of different complexities. *Annals of neurology* 41**,** 247-254.

Chen, R., and Hallett, M. (1999). The time course of changes in motor cortex excitability associated with voluntary movement. *Canadian Journal of Neurological Sciences/Journal Canadien des Sciences Neurologiques* 26**,** 163-169.

Chiarello, C. (1980). A house divided? Cognitive functioning with callosal agenesis. *Brain Lang* 11**,** 128-158.

Chinn, G.A., Hirokawa, K.E., Chuang, T.M., Urbina, C., Patel, F., Fong, J., et al. (2015). Agenesis of the Corpus Callosum Due to Defective Glial Wedge Formation in Lhx2 Mutant Mice. *Cereb Cortex* 25**,** 2707-2718.

Ciani, L., and Salinas, P.C. (2005). WNTs in the vertebrate nervous system: from patterning to neuronal connectivity. *Nat Rev Neurosci* 6**,** 351-362.

Cincotta, M., Borgheresi, A., Balestrieri, F., Giovannelli, F., Rossi, S., Ragazzoni, A., et al. (2004). Involvement of the human dorsal premotor cortex in unimanual motor control:

an interference approach using transcranial magnetic stimulation. *Neurosci Lett* 367**,** 189-193.

Clegg, J.M., Conway, C.D., Howe, K.M., Price, D.J., Mason, J.O., Turnbull, J.E., et al. (2014). Heparan sulfotransferases Hs6st1 and Hs2st keep Erk in check for mouse corpus callosum development. *J Neurosci* 34**,** 2389-2401.

Cohen, L.G., Meer, J., Tarkka, I., Bierner, S., Leiderman, D.B., Dubinsky, R.M., et al. (1991). Congenital mirror movements. Abnormal organization of motor pathways in two patients. *Brain* 114 381-403.

Colamarino, S.A., and Tessier-Lavigne, M. (1995). The axonal chemoattractant netrin-1 is also a chemorepellent for trochlear motor axons. *Cell* 81**,** 621-629.

Colebatch, J.G. (2007). Bereitschaftspotential and movement‐related potentials: Origin, significance, and application in disorders of human movement. *Movement Disorders* 22**,** 601-610.

Conway, C.D., Howe, K.M., Nettleton, N.K., Price, D.J., Mason, J.O., and Pratt, T. (2011). Heparan sulfate sugar modifications mediate the functions of slits and other factors needed for mouse forebrain commissure development. *J Neurosci* 31**,** 1955-1970.

Corbin, J.G., and Butt, S.J. (2011). Developmental mechanisms for the generation of telencephalic interneurons. *Developmental neurobiology* 71**,** 710-732.

Cox, B.C., Cincotta, M., and Espay, A.J. (2012). Mirror movements in movement disorders: a review. *Tremor Other Hyperkinet Mov (N Y)* 2.

Cramer, S.C., Finklestein, S.P., Schaechter, J.D., Bush, G., and Rosen, B.R. (1999). Activation of distinct motor cortex regions during ipsilateral and contralateral finger movements. *J Neurophysiol* 81**,** 383-387.

Cubelos, B., Sebastian-Serrano, A., Kim, S., Moreno-Ortiz, C., Redondo, J.M., Walsh, C.A., et al. (2008). Cux-2 controls the proliferation of neuronal intermediate precursors of the cortical subventricular zone. *Cereb Cortex* 18**,** 1758-1770.

Cunnington, R., Windischberger, C., Deecke, L., and Moser, E. (2002). The preparation and execution of self-initiated and externally-triggered movement: a study of event-related fMRI. *Neuroimage* 15**,** 373-385.

Cunnington, R., Windischberger, C., and Moser, E. (2005). Premovement activity of the pre-supplementary motor area and the readiness for action: studies of time-resolved event-related functional MRI. *Hum Mov Sci* 24**,** 644-656.

Davidson, T., and Tremblay, F. (2013). Hemispheric differences in corticospinal excitability and in transcallosal inhibition in relation to degree of handedness. *PloS one* 8**,** e70286.

De Gennaro, L., Cristiani, R., Bertini, M., Curcio, G., Ferrara, M., Fratello, F., et al. (2004). Handedness is mainly associated with an asymmetry of corticospinal excitability and not of transcallosal inhibition. *Clinical Neurophysiology* 115**,** 1305-1312.

De Lacoste, M.C., Kirkpatrick, J.B., and Ross, E.D. (1985). Topography of the human corpus callosum. *J Neuropathol Exp Neurol* 44**,** 578-591.

Deiber, M.P., Ibanez, V., Sadato, N., and Hallett, M. (1996). Cerebral structures participating in motor preparation in humans: a positron emission tomography study. *J Neurophysiol* 75**,** 233-247.

Demeter, S., Rosene, D.L., and Van Hoesen, G.W. (1985). Interhemispheric pathways of the hippocampal formation, presubiculum, and entorhinal and posterior parahippocampal cortices in the rhesus monkey: the structure and organization of the hippocampal commissures. *J Comp Neurol* 233**,** 30-47.

Demyanenko, G.P., Tsai, A.Y., and Maness, P.F. (1999). Abnormalities in neuronal process extension, hippocampal development, and the ventricular system of L1 knockout mice. *J Neurosci* 19**,** 4907-4920.

Depienne, C., Bouteiller, D., Meneret, A., Billot, S., Groppa, S., Klebe, S., et al. (2012). RAD51 haploinsufficiency causes congenital mirror movements in humans. *Am J Hum Genet* 90**,** 301-307.

Depienne, C., Cincotta, M., Billot, S., Bouteiller, D., Groppa, S., Brochard, V., et al. (2011). A novel DCC mutation and genetic heterogeneity in congenital mirror movements. *Neurology* 76**,** 260-264.

Diedrichsen, J., Wiestler, T., and Krakauer, J.W. (2013). Two distinct ipsilateral cortical representations for individuated finger movements. *Cereb Cortex* 23**,** 1362-1377.

Ding, S.L., and Elberger, A.J. (2001). Postnatal development of biotinylated dextran amine-labeled corpus callosum axons projecting from the visual and auditory cortices to the visual cortex of the rat. *Exp Brain Res* 136**,** 179-193.

Dode, C., and Hardelin, J.P. (2010). Clinical genetics of Kallmann syndrome. *Ann Endocrinol (Paris)* 71**,** 149-157.

Dominguez, M.H., Ayoub, A.E., and Rakic, P. (2013). POU-III transcription factors (Brn1, Brn2, and Oct6) influence neurogenesis, molecular identity, and migratory destination of upper-layer cells of the cerebral cortex. *Cereb Cortex* 23**,** 2632-2643.

Donahoo, A.L., and Richards, L.J. (2009). Understanding the mechanisms of callosal development through the use of transgenic mouse models. *Semin Pediatr Neurol* 16**,** 127-142.

Donchin, O., Gribova, A., Steinberg, O., Mitz, A., Bergman, H., and Vaadia, E. (2002). Single-unit activity related to bimanual arm movements in the primary and supplementary motor cortices. *Journal of neurophysiology* 88**,** 3498-3517.

Dum, R.P., and Strick, P.L. (1996). Spinal cord terminations of the medial wall motor areas in macaque monkeys. *J Neurosci* 16**,** 6513-6525.

Duque, J., Davare, M., Delaunay, L., Jacob, B., Saur, R., Hummel, F., et al. (2010a). Monitoring coordination during bimanual movements: where is the mastermind? *J Cogn Neurosci* 22**,** 526-542.

Duque, J., Hummel, F., Celnik, P., Murase, N., Mazzocchio, R., and Cohen, L.G. (2005a). Transcallosal inhibition in chronic subcortical stroke. *Neuroimage* 28**,** 940-946.

Duque, J., and Ivry, R.B. (2009). Role of corticospinal suppression during motor preparation. *Cereb Cortex* 19**,** 2013-2024.

Duque, J., Lew, D., Mazzocchio, R., Olivier, E., and Ivry, R.B. (2010b). Evidence for two concurrent inhibitory mechanisms during response preparation. *The Journal of Neuroscience* 30**,** 3793-3802.

Duque, J., Mazzocchio, R., Dambrosia, J., Murase, N., Olivier, E., and Cohen, L.G. (2005b). Kinematically specific interhemispheric inhibition operating in the process of generation of a voluntary movement. *Cerebral Cortex* 15**,** 588-593.

Duque, J., Murase, N., Celnik, P., Hummel, F., Harris-Love, M., Mazzocchio, R., et al. (2007). Intermanual Differences in movement-related interhemispheric inhibition. *J Cogn Neurosci* 19**,** 204-213.

Eckler, M.J., Nguyen, T.D., Mckenna, W.L., Fastow, B.L., Guo, C., Rubenstein, J.L., et al. (2015). Cux2-positive radial glial cells generate diverse subtypes of neocortical projection neurons and macroglia. *Neuron* 86**,** 1100-1108.

Edwards, T.J., Sherr, E.H., Barkovich, A.J., and Richards, L.J. (2014). Clinical, genetic and imaging findings identify new causes for corpus callosum development syndromes. *Brain* 137**,** 1579-1613.

Elberger, A.J. (1994a). The corpus callosum provides a massive transitory input to the visual cortex of cat and rat during early postnatal development. *Behav Brain Res* 64**,** 15-33.

Elberger, A.J. (1994b). Transitory corpus callosum axons projecting throughout developing rat visual cortex revealed by Dil. *Cereb Cortex* 4**,** 279-299.

Eyre, J.A. (2007). Corticospinal tract development and its plasticity after perinatal injury. *Neurosci Biobehav Rev* 31**,** 1136-1149.

Eyre, J.A., Miller, S., Clowry, G.J., Conway, E.A., and Watts, C. (2000). Functional corticospinal projections are established prenatally in the human foetus permitting involvement in the development of spinal motor centres. *Brain* 123 (Pt 1)**,** 51-64.

Eyre, J.A., Taylor, J.P., Villagra, F., Smith, M., and Miller, S. (2001). Evidence of activity-dependent withdrawal of corticospinal projections during human development. *Neurology* 57**,** 1543-1554.

Fame, R.M., Macdonald, J.L., and Macklis, J.D. (2011). Development, specification, and diversity of callosal projection neurons. *Trends Neurosci* 34**,** 41-50.

Faulkner, R.L., Low, L.K., Liu, X.B., Coble, J., Jones, E.G., and Cheng, H.J. (2008). Dorsal turning of motor corticospinal axons at the pyramidal decussation requires plexin signaling. *Neural Dev* 3.

Fazeli, A., Dickinson, S.L., Hermiston, M.L., Tighe, R.V., Steen, R.G., Small, C.G., et al. (1997). Phenotype of mice lacking functional Deleted in colorectal cancer (Dcc) gene. *Nature* 386**,** 796-804.

Fearon, E.R., Cho, K.R., Nigro, J.M., Kern, S.E., Simons, J.W., Ruppert, J.M., et al. (1990). Identification of a chromosome 18q gene that is altered in colorectal cancers. *Science* 247**,** 49-56.

Ferbert, A., Priori, A., Rothwell, J., Day, B., Colebatch, J., and Marsden, C. (1992). Interhemispheric inhibition of the human motor cortex. *The Journal of physiology* 453**,** 525-546.

Ferland, R.J., Eyaid, W., Collura, R.V., Tully, L.D., Hill, R.S., Al-Nouri, D., et al. (2004). Abnormal cerebellar development and axonal decussation due to mutations in AHI1 in Joubert syndrome. *Nat Genet* 36**,** 1008-1013.

Finger, J.H., Bronson, R.T., Harris, B., Johnson, K., Przyborski, S.A., and Ackerman, S.L. (2002). The netrin 1 receptors Unc5h3 and Dcc are necessary at multiple choice points for the guidance of corticospinal tract axons. *J Neurosci* 22**,** 10346-10356.

Flament, D., Goldsmith, P., Buckley, C.J., and Lemon, R.N. (1993). Task dependence of responses in first dorsal interosseous muscle to magnetic brain stimulation in man. *J Physiol* 464**,** 361-378.

Fothergill, T., Donahoo, A.L., Douglass, A., Zalucki, O., Yuan, J., Shu, T., et al. (2014). Netrin-DCC Signaling Regulates Corpus Callosum Formation Through Attraction of Pioneering Axons and by Modulating Slit2-Mediated Repulsion. *Cereb Cortex* 24**,** 1138-1151.

Franco, S.J., Gil-Sanz, C., Martinez-Garay, I., Espinosa, A., Harkins-Perry, S.R., Ramos, C., et al. (2012). Fate-restricted neural progenitors in the mammalian cerebral cortex. *Science* 337**,** 746-749.

Frantz, G.D., and Mcconnell, S.K. (1996). Restriction of late cerebral cortical progenitors to an upper-layer fate. *Neuron* 17**,** 55-61.

Franz, E.A., Chiaroni-Clarke, R., Woodrow, S., Glendining, K.A., Jasoni, C.L., Robertson, S.P., et al. (2015). Congenital mirror movements: phenotypes associated with DCC and RAD51 mutations. *J Neurol Sci* 351**,** 140-145.

Frost, D.O., and Moy, Y.P. (1989). Effects of dark rearing on the development of visual callosal connections. *Exp Brain Res* 78**,** 203-213.

Galea, M.P., and Darian-Smith, I. (1995). Postnatal maturation of the direct corticospinal projections in the macaque monkey. *Cereb Cortex* 5**,** 518-540.

Gallea, C., Popa, T., Billot, S., Meneret, A., Depienne, C., and Roze, E. (2011). Congenital mirror movements: a clue to understanding bimanual motor control. *J Neurol* 258**,** 1911-1919.

Gallea, C., Popa, T., Hubsch, C., Valabregue, R., Brochard, V., Kundu, P., et al. (2013). RAD51 deficiency disrupts the corticospinal lateralization of motor control. *Brain* 136**,** 3333-3346.

Gibson, K.R. (1991). Myelination and behavioral development: A comparative perspective on questions of neoteny, altriciality and intelligence. *Brain maturation and cognitive development: Comparative and cross-cultural perspectives***,** 29-63.

Gil-Sanz, C., Espinosa, A., Fregoso, S.P., Bluske, K.K., Cunningham, C.L., Martinez-Garay, I., et al. (2015). Lineage Tracing Using Cux2-Cre and Cux2-CreERT2 Mice. *Neuron* 86**,** 1091-1099.

Giovannelli, F., Borgheresi, A., Balestrieri, F., Ragazzoni, A., Zaccara, G., Cincotta, M., et al. (2006). Role of the right dorsal premotor cortex in "physiological" mirror EMG activity. *Exp Brain Res* 175**,** 633-640.

Giovannelli, F., Borgheresi, A., Balestrieri, F., Zaccara, G., Viggiano, M.P., Cincotta, M., et al. (2009). Modulation of interhemispheric inhibition by volitional motor activity: an ipsilateral silent period study. *J Physiol* 587**,** 5393-5410.

Gorlin, R.J., and Goltz, R.W. (1960). Multiple nevoid basal-cell epithelioma, jaw cysts and bifid rib. A syndrome. *N Engl J Med* 262**,** 908-912.

Grefkes, C., Eickhoff, S.B., Nowak, D.A., Dafotakis, M., and Fink, G.R. (2008). Dynamic intra- and interhemispheric interactions during unilateral and bilateral hand movements assessed with fMRI and DCM. *Neuroimage* 41**,** 1382-1394.

Greig, L.C., Woodworth, M.B., Galazo, M.J., Padmanabhan, H., and Macklis, J.D. (2013). Molecular logic of neocortical projection neuron specification, development and diversity. *Nat Rev Neurosci* 14**,** 755-769.

Gu, C., Rodriguez, E.R., Reimert, D.V., Shu, T., Fritzsch, B., Richards, L.J., et al. (2003). Neuropilin-1 conveys semaphorin and VEGF signaling during neural and cardiovascular development. *Dev Cell* 5**,** 45-57.

Ha, H.Y., Cho, I.H., Lee, K.W., Lee, K.W., Song, J.Y., Kim, K.S., et al. (2005). The axon guidance defect of the telencephalic commissures of the JSAP1-deficient brain was partially rescued by the transgenic expression of JIP1. *Dev Biol* 277**,** 184-199.

Hakanen, J., and Salminen, M. (2015). Defects in neural guidepost structures and failure to remove leptomeningeal cells from the septal midline behind the interhemispheric fusion defects in Netrin1 deficient mice. *Int J Dev Neurosci* 47**,** 206-215.

Hamelin, M., Zhou, Y., Su, M.W., Scott, I.M., and Culotti, J.G. (1993). Expression of the UNC-5 guidance receptor in the touch neurons of C. elegans steers their axons dorsally. *Nature* 364**,** 327-330.

Hamzei, F., Dettmers, C., Rzanny, R., Liepert, J., Buchel, C., and Weiller, C. (2002). Reduction of excitability ("inhibition") in the ipsilateral primary motor cortex is mirrored by fMRI signal decreases. *Neuroimage* 17**,** 490-496.

Hanson, M.G., and Landmesser, L.T. (2004). Normal patterns of spontaneous activity are required for correct motor axon guidance and the expression of specific guidance molecules. *Neuron* 43**,** 687-701.

Harb, K., Magrinelli, E., Nicolas, C.S., Lukianets, N., Frangeul, L., Pietri, M., et al. (2016). Area-specific development of distinct projection neuron subclasses is regulated by postnatal epigenetic modifications. *Elife* 5**,** e09531.

Hasegawa, Y., Kasai, T., Tsuji, T., and Yahagi, S. (2001). Further insight into the task-dependent excitability of motor evoked potentials in first dorsal interosseous muscle in humans. *Exp Brain Res* 140**,** 387-396.

Haubensak, W., Attardo, A., Denk, W., and Huttner, W.B. (2004). Neurons arise in the basal neuroepithelium of the early mammalian telencephalon: a major site of neurogenesis. *Proc Natl Acad Sci U S A* 101**,** 3196-3201.

Heath, C.J., and Jones, E.G. (1971). Interhemispheric pathways in the absence of a corpus callosum. An experimental study of commissural connexions in the marsupial phalanger. *J Anat* 109**,** 253-270.

Heimer, L., Ebner, F.F., and Nauta, W.J. (1967). A note on the termination of commissural fibers in the neocortex. *Brain Res* 5**,** 171-177.

Hinder, M.R., Fujiyama, H., and Summers, J.J. (2012). Premotor-motor interhemispheric inhibition is released during movement initiation in older but not young adults. *PLoS One* 7.

Hofer, S., and Frahm, J. (2006). Topography of the human corpus callosum revisited--comprehensive fiber tractography using diffusion tensor magnetic resonance imaging. *Neuroimage* 32**,** 989-994.

Horenstein, C., Lowe, M.J., Koenig, K.A., and Phillips, M.D. (2009). Comparison of unilateral and bilateral complex finger tapping-related activation in premotor and primary motor cortex. *Hum Brain Mapp* 30**,** 1397-1412.

Houzel, J.C., Milleret, C., and Innocenti, G. (1994). Morphology of callosal axons interconnecting areas 17 and 18 of the cat. *Eur J Neurosci* 6**,** 898-917.

Hsu, Y.-T., Duann, J.-R., Chen, C.-M., Yang, Y.-W., Tsai, C.-H., and Lu, M.-K. (2013). Anatomical and electrophysiological manifestations in a patient with congenital corpus callosum agenesis. *Brain topography* 26**,** 171-176.

Hu, Z., Yue, X., Shi, G., Yue, Y., Crockett, D.P., Blair-Flynn, J., et al. (2003). Corpus callosum deficiency in transgenic mice expressing a truncated ephrin-A receptor. *J Neurosci* 23**,** 10963-10970.

Huang, Y., Song, N.N., Lan, W., Zhang, Q., Zhang, L., Zhang, L., et al. (2013). Sensory input is required for callosal axon targeting in the somatosensory cortex. *Mol Brain* 6**,** 53.

Hubers, A., Orekhov, Y., and Ziemann, U. (2008). Interhemispheric motor inhibition: its role in controlling electromyographic mirror activity. *Eur J Neurosci* 28**,** 364-371.

Immisch, I., Waldvogel, D., Van Gelderen, P., and Hallett, M. (2001). The role of the medial wall and its anatomical variations for bimanual antiphase and in-phase movements. *Neuroimage* 14**,** 674-684.

Inatani, M., Irie, F., Plump, A.S., Tessier-Lavigne, M., and Yamaguchi, Y. (2003). Mammalian brain morphogenesis and midline axon guidance require heparan sulfate. *Science* 302**,** 1044-1046.

Innocenti, G.M. (1981). Growth and reshaping of axons in the establishment of visual callosal connections. *Science* 212**,** 824-827.

Innocenti, G.M., and Caminiti, R. (1980). Postnatal shaping of callosal connections from sensory areas. *Exp Brain Res* 38**,** 381-394.

Innocenti, G.M., Clarke, S., and Kraftsik, R. (1986). Interchange of callosal and association projections in the developing visual cortex. *J Neurosci* 6**,** 1384-1409.

Innocenti, G.M., and Frost, D.O. (1979). Effects of visual experience on the maturation of the efferent system to the corpus callosum. *Nature* 280**,** 231-234.

Innocenti, G.M., and Frost, D.O. (1980). The postnatal development of visual callosal connections in the absence of visual experience or of the eyes. *Exp Brain Res* 39**,** 365-375.

Islam, S.M., Shinmyo, Y., Okafuji, T., Su, Y., Naser, I.B., Ahmed, G., et al. (2009). Draxin, a repulsive guidance protein for spinal cord and forebrain commissures. *Science* 323**,** 388-393.

Ivy, G.O., Akers, R.M., and Killackey, H.P. (1979). Differential distribution of callosal projection neurons in the neonatal and adult rat. *Brain Res* 173**,** 532-537.

Ivy, G.O., and Killackey, H.P. (1981). The ontogeny of the distribution of callosal projection neurons in the rat parietal cortex. *J Comp Neurol* 195**,** 367-389.

Jasin, M., and Rothstein, R. (2013). Repair of strand breaks by homologous recombination. *Cold Spring Harb Perspect Biol* 5**,** a012740.

Jones, E.G., Burton, H., and Porter, R. (1975). Commissural and cortico-cortical "columns" in the somatic sensory cortex of primates. *Science* 190**,** 572-574.

Joosten, E.A., Schuitman, R.L., Vermelis, M.E., and Dederen, P.J. (1992). Postnatal development of the ipsilateral corticospinal component in rat spinal cord: a light and electron microscopic anterograde HRP study. *J Comp Neurol* 326**,** 133-146.

Jouandet, M.L. (1982). Neocortical and basal telencephalic origins of the anterior commissure of the cat. *Neuroscience* 7**,** 1731-1752.

Jouandet, M.L., Garey, L.J., and Lipp, H.P. (1984). Distribution of the cells of origin of the corpus callosum and anterior commissure in the marmoset monkey. *Anat Embryol (Berl)* 169**,** 45-59.

Jouandet, M.L., and Gazzaniga, M.S. (1979). Cortical field of origin of the anterior commissure of the rhesus monkey. *Exp Neurol* 66**,** 381-397.

Karol, E.A., and Pandya, D.N. (1971). The distribution of the corpus callosum in the Rhesus monkey. *Brain* 94**,** 471-486.

Keeble, T.R., Halford, M.M., Seaman, C., Kee, N., Macheda, M., Anderson, R.B., et al. (2006). The Wnt receptor Ryk is required for Wnt5a-mediated axon guidance on the contralateral side of the corpus callosum. *J Neurosci* 26**,** 5840-5848.

Keino-Masu, K., Masu, M., Hinck, L., Leonardo, E.D., Chan, S.S., Culotti, J.G., et al. (1996). Deleted in Colorectal Cancer (DCC) encodes a netrin receptor. *Cell* 87**,** 175-185.

Kennedy, T.E., Serafini, T., De La Torre, J.R., and Tessier-Lavigne, M. (1994). Netrins are diffusible chemotropic factors for commissural axons in the embryonic spinal cord. *Cell* 78**,** 425-435.

Kermadi, I., Calciati, T., and Rouiller, E. (1998). Neuronal activity in the primate supplementary motor area and the primary motor cortex in relation to spatio-temporal bimanual coordination. *Somatosensory & motor research* 15**,** 287-308.

Kielan-Jaworowska, Z., Cifelli, R.L., and Luo, Z.-X. (2005). *Mammals from the age of dinosaurs: origins, evolution, and structure.* Columbia University Press.

Killackey, H.P., and Chalupa, L.M. (1986). Ontogenetic change in the distribution of callosal projection neurons in the postcentral gyrus of the fetal rhesus monkey. *J Comp Neurol* 244**,** 331-348.

Klein, P.A., Duque, J., Labruna, L., and Ivry, R.B. (2016). Comparison of the two cerebral hemispheres in inhibitory processes operative during movement preparation. *Neuroimage* 125**,** 220-232.

Koch, G., Franca, M., Del Olmo, M.F., Cheeran, B., Milton, R., Alvarez Sauco, M., et al. (2006). Time course of functional connectivity between dorsal premotor and contralateral motor cortex during movement selection. *J Neurosci* 26**,** 7452-7459.

Koeneke, S., Lutz, K., Wüstenberg, T., and Jäncke, L. (2004). Bimanual versus unimanual coordination: what makes the difference? *Neuroimage* 22**,** 1336-1350.

Koerte, I., Eftimov, L., Laubender, R.P., Esslinger, O., Schroeder, A.S., Ertl-Wagner, B., et al. (2010). Mirror movements in healthy humans across the lifespan: effects of development and ageing. *Dev Med Child Neurol* 52**,** 1106-1112.

Koester, S.E., and O'leary, D.D. (1994). Axons of early generated neurons in cingulate cortex pioneer the corpus callosum. *J Neurosci* 14**,** 6608-6620.

Koppel, H., and Innocenti, G.M. (1983). Is there a genuine exuberancy of callosal projections in development? A quantitative electron microscopic study in the cat. *Neurosci Lett* 41**,** 33-40.

Koralek, K.A., and Killackey, H.P. (1990). Callosal projections in rat somatosensory cortex are altered by early removal of afferent input. *Proc Natl Acad Sci U S A* 87**,** 1396-1400.

Kowalczyk, T., Pontious, A., Englund, C., Daza, R.A., Bedogni, F., Hodge, R., et al. (2009). Intermediate neuronal progenitors (basal progenitors) produce pyramidal-projection neurons for all layers of cerebral cortex. *Cereb Cortex* 19**,** 2439-2450.

Krams, M., Quinton, R., Mayston, M.J., Harrison, L.M., Dolan, R.J., Bouloux, P.M., et al. (1997). Mirror movements in X-linked Kallmann's syndrome. II. A PET study. *Brain* 120 (Pt 7)**,** 1217-1228.

Krimpenfort, P., Song, J.Y., Proost, N., Zevenhoven, J., Jonkers, J., and Berns, A. (2012). Deleted in colorectal carcinoma suppresses metastasis in p53-deficient mammary tumours. *Nature* 482**,** 538-541.

Kroeger, J., Baumer, T., Jonas, M., Rothwell, J.C., Siebner, H.R., and Munchau, A. (2010). Charting the excitability of premotor to motor connections while withholding or initiating a selected movement. *Eur J Neurosci* 32**,** 1771-1779.

Kullander, K., Butt, S.J., Lebret, J.M., Lundfald, L., Restrepo, C.E., Rydstrom, A., et al. (2003). Role of EphA4 and EphrinB3 in local neuronal circuits that control walking. *Science* 299**,** 1889-1892.

Kullander, K., Croll, S.D., Zimmer, M., Pan, L., Mcclain, J., Hughes, V., et al. (2001). Ephrin-B3 is the midline barrier that prevents corticospinal tract axons from recrossing, allowing for unilateral motor control. *Genes Dev* 15**,** 877-888.

Kunzle, H. (1976). Alternating afferent zones of high and low axon terminal density within the macaque motor cortex. *Brain Res* 106**,** 365-370.

Lamantia, A.S., and Rakic, P. (1990a). Axon overproduction and elimination in the corpus callosum of the developing rhesus monkey. *J Neurosci* 10**,** 2156-2175.

Lamantia, A.S., and Rakic, P. (1990b). Cytological and quantitative characteristics of four cerebral commissures in the rhesus monkey. *J Comp Neurol* 291**,** 520-537.

Laplane, D., Talairach, J., Meininger, V., Bancaud, J., and Orgogozo, J. (1977). Clinical consequences of corticectomies involving the supplementary motor area in man. *Journal of the neurological sciences* 34**,** 301-314.

Lee, K.M., Chang, K.H., and Roh, J.K. (1999). Subregions within the supplementary motor area activated at different stages of movement preparation and execution. *Neuroimage* 9**,** 117-123.

Leinsinger, G.L., Heiss, D.T., Jassoy, A.G., Pfluger, T., Hahn, K., and Danek, A. (1997). Persistent mirror movements: functional MR imaging of the hand motor cortex. *Radiology* 203**,** 545-552.

Leocani, L., Cohen, L.G., Wassermann, E.M., Ikoma, K., and Hallett, M. (2000). Human corticospinal excitability evaluated with transcranial magnetic stimulation during different reaction time paradigms. *Brain* 123**,** 1161-1173.

Leone, D.P., Heavner, W.E., Ferenczi, E.A., Dobreva, G., Huguenard, J.R., Grosschedl, R., et al. (2015). Satb2 Regulates the Differentiation of Both Callosal and Subcerebral Projection Neurons in the Developing Cerebral Cortex. *Cereb Cortex* 25**,** 3406-3419.

Lepage, J.F., Beaule, V., Srour, M., Rouleau, G., Pascual-Leone, A., Lassonde, M., et al. (2012). Neurophysiological investigation of congenital mirror movements in a patient with agenesis of the corpus callosum. *Brain Stimul* 5**,** 137-140.

Li, Q., and Martin, J.H. (2000). Postnatal development of differential projections from the caudal and rostral motor cortex subregions. *Exp Brain Res* 134**,** 187-198.

Li, Q., and Martin, J.H. (2002). Postnatal development of connectional specificity of corticospinal terminals in the cat. *J Comp Neurol* 447**,** 57-71.

Liang, N., Murakami, T., Funase, K., Narita, T., and Kasai, T. (2008). Further evidence for excitability changes in human primary motor cortex during ipsilateral voluntary contractions. *Neurosci Lett* 433**,** 135-140.

Liepert, J., Dettmers, C., Terborg, C., and Weiller, C. (2001). Inhibition of ipsilateral motor cortex during phasic generation of low force. *Clin Neurophysiol* 112**,** 114-121.

Lim, J.W., Donahoo, A.L., Bunt, J., Edwards, T.J., Fenlon, L.R., Liu, Y., et al. (2015). EMX1 regulates NRP1-mediated wiring of the mouse anterior cingulate cortex. *Development* 142**,** 3746-3757.

Lindwall, C., Fothergill, T., and Richards, L.J. (2007). Commissure formation in the mammalian forebrain. *Curr Opin Neurobiol* 17**,** 3-14.

Liu, J., Morel, A., Wannier, T., and Rouiller, E.M. (2002). Origins of callosal projections to the supplementary motor area (SMA): A direct comparison between pre‐SMA and SMA‐proper in macaque monkeys. *Journal of Comparative Neurology* 443**,** 71-85.

Liuzzi, G., Horniss, V., Hoppe, J., Heise, K., Zimerman, M., Gerloff, C., et al. (2010). Distinct temporospatial interhemispheric interactions in the human primary and premotor cortex during movement preparation. *Cereb Cortex* 20**,** 1323-1331.

Lopez-Bendito, G., Flames, N., Ma, L., Fouquet, C., Di Meglio, T., Chedotal, A., et al. (2007). Robo1 and Robo2 cooperate to control the guidance of major axonal tracts in the mammalian forebrain. *J Neurosci* 27**,** 3395-3407.

Lose, F., Lovelock, P., Chenevix-Trench, G., Mann, G.J., Pupo, G.M., Spurdle, A.B., et al. (2006). Variation in the RAD51 gene and familial breast cancer. *Breast Cancer Res* 8**,** R26.

Luppino, G., Matelli, M., Camarda, R., and Rizzolatti, G. (1993). Corticocortical connections of area F3 (SMA‐proper) and area F6 (pre‐SMA) in the macaque monkey. *Journal of Comparative Neurology* 338**,** 114-140.

Luppino, G., Matelli, M., Camarda, R.M., Gallese, V., and Rizzolatti, G. (1991). Multiple representations of body movements in mesial area 6 and the adjacent cingulate cortex: an intracortical microstimulation study in the macaque monkey. *J Comp Neurol* 311**,** 463-482.

Magnani, D., Hasenpusch-Theil, K., Benadiba, C., Yu, T., Basson, M.A., Price, D.J., et al. (2014). Gli3 controls corpus callosum formation by positioning midline guideposts during telencephalic patterning. *Cereb Cortex* 24**,** 186-198.

Marcorelles, P., and Laquerriere, A. (2010). Neuropathology of holoprosencephaly. *Am J Med Genet C Semin Med Genet* 154C**,** 109-119.

Marcos, S., Backer, S., Causeret, F., Tessier-Lavigne, M., and Bloch-Gallego, E. (2009). Differential roles of Netrin-1 and its receptor DCC in inferior olivary neuron migration. *Mol Cell Neurosci* 41**,** 429-439.

Martin, G.F., Jr. (1967). Interneocortical connections in the opossum, Didelphis virginiana. *Anat Rec* 157**,** 607-615.

Masu, M. (2015). Proteoglycans and axon guidance: a new relationship between old partners. *J Neurochem*.

Matsunami, K., Kawashima, T., Ueki, S., Fujita, M., and Konishi, T. (1994). Topography of commissural fibers in the corpus callosum of the cat: a study using WGA-HRP method. *Neurosci Res* 20**,** 137-148.

Matsuzaka, Y., Aizawa, H., and Tanji, J. (1992). A motor area rostral to the supplementary motor area (presupplementary motor area) in the monkey: neuronal activity during a learned motor task. *Journal of Neurophysiology* 68**,** 653-662.

Mayer, M., Botzel, K., Paulus, W., Plendl, H., Prockl, D., and Danek, A. (1995). Movement-related cortical potentials in persistent mirror movements. *Electroencephalogr Clin Neurophysiol* 95**,** 350-358.

Mayston, M.J., Harrison, L.M., and Stephens, J.A. (1999). A neurophysiological study of mirror movements in adults and children. *Ann Neurol* 45**,** 583-594.

Mcconnell, S.K. (1988). Fates of visual cortical neurons in the ferret after isochronic and heterochronic transplantation. *J Neurosci* 8**,** 945-974.

Mcevilly, R.J., De Diaz, M.O., Schonemann, M.D., Hooshmand, F., and Rosenfeld, M.G. (2002). Transcriptional regulation of cortical neuron migration by POU domain factors. *Science* 295**,** 1528-1532.

Mehlen, P., Rabizadeh, S., Snipas, S.J., Assa-Munt, N., Salvesen, G.S., and Bredesen, D.E. (1998). The DCC gene product induces apoptosis by a mechanism requiring receptor proteolysis. *Nature* 395**,** 801-804.

Mendes, S.W., Henkemeyer, M., and Liebl, D.J. (2006). Multiple Eph receptors and B-class ephrins regulate midline crossing of corpus callosum fibers in the developing mouse forebrain. *J Neurosci* 26**,** 882-892.

Meneret, A., Depienne, C., Riant, F., Trouillard, O., Bouteiller, D., Cincotta, M., et al. (2014a). Congenital mirror movements: mutational analysis of RAD51 and DCC in 26 cases. *Neurology* 82**,** 1999-2002.

Meneret, A., Trouillard, O., Depienne, C., and Roze, E. (1993). "Congenital Mirror Movements," in *GeneReviews(R)*, eds. R.A. Pagon, M.P. Adam, H.H. Ardinger, S.E. Wallace, A. Amemiya, L.J.H. Bean, T.D. Bird, C.T. Fong, H.C. Mefford, R.J.H. Smith & K. Stephens. (Seattle (WA)).

Meneret, A., Trouillard, O., Vidailhet, M., Depienne, C., and Roze, E. (2014b). Congenital mirror movements: no mutation in DNAL4 in 17 index cases. *J Neurol* 261**,** 2030-2031.

Meyer, B.U., Roricht, S., Grafin Von Einsiedel, H., Kruggel, F., and Weindl, A. (1995). Inhibitory and excitatory interhemispheric transfers between motor cortical areas in normal humans and patients with abnormalities of the corpus callosum. *Brain* 118 (Pt 2)**,** 429-440.

Mire, E., Mezzera, C., Leyva-Diaz, E., Paternain, A.V., Squarzoni, P., Bluy, L., et al. (2012). Spontaneous activity regulates Robo1 transcription to mediate a switch in thalamocortical axon growth. *Nat Neurosci* 15**,** 1134-1143.

Mizuno, H., Hirano, T., and Tagawa, Y. (2007). Evidence for activity-dependent cortical wiring: formation of interhemispheric connections in neonatal mouse visual cortex requires projection neuron activity. *J Neurosci* 27**,** 6760-6770.

Mizuno, H., Hirano, T., and Tagawa, Y. (2010). Pre-synaptic and post-synaptic neuronal activity supports the axon development of callosal projection neurons during different post-natal periods in the mouse cerebral cortex. *Eur J Neurosci* 31**,** 410-424.

Moldrich, R.X., Gobius, I., Pollak, T., Zhang, J., Ren, T., Brown, L., et al. (2010). Molecular regulation of the developing commissural plate. *J Comp Neurol* 518**,** 3645-3661.

Molyneaux, B.J., Arlotta, P., Hirata, T., Hibi, M., and Macklis, J.D. (2005). Fezl is required for the birth and specification of corticospinal motor neurons. *Neuron* 47**,** 817-831.

Molyneaux, B.J., Arlotta, P., Menezes, J.R., and Macklis, J.D. (2007). Neuronal subtype specification in the cerebral cortex. *Nat Rev Neurosci* 8**,** 427-437.

Moynahan, M.E., and Jasin, M. (2010). Mitotic homologous recombination maintains genomic stability and suppresses tumorigenesis. *Nat Rev Mol Cell Biol* 11**,** 196-207.

Muellbacher, W., Facchini, S., Boroojerdi, B., and Hallett, M. (2000). Changes in motor cortex excitability during ipsilateral hand muscle activation in humans. *Clinical Neurophysiology* 111**,** 344-349.

Mueller, K.L.O., Marion, S.D., Paul, L.K., and Brown, W.S. (2009). Bimanual motor coordination in agenesis of the corpus callosum. *Behavioral neuroscience* 123**,** 1000.

Muller, K., Kass-Iliyya, F., and Reitz, M. (1997). Ontogeny of ipsilateral corticospinal projections: a developmental study with transcranial magnetic stimulation. *Ann Neurol* 42**,** 705-711.

Murase, N., Duque, J., Mazzocchio, R., and Cohen, L.G. (2004). Influence of interhemispheric interactions on motor function in chronic stroke. *Ann Neurol* 55**,** 400-409.

Nachev, P., Kennard, C., and Husain, M. (2008). Functional role of the supplementary and pre-supplementary motor areas. *Nat Rev Neurosci* 9**,** 856-869.

Newton, J.M., Sunderland, A., and Gowland, P.A. (2005). fMRI signal decreases in ipsilateral primary motor cortex during unilateral hand movements are related to duration and side of movement. *Neuroimage* 24**,** 1080-1087.

Nicol, X., Voyatzis, S., Muzerelle, A., Narboux-Neme, N., Sudhof, T.C., Miles, R., et al. (2007). cAMP oscillations and retinal activity are permissive for ephrin signaling during the establishment of the retinotopic map. *Nat Neurosci* 10**,** 340-347.

Nieto, M., Monuki, E.S., Tang, H., Imitola, J., Haubst, N., Khoury, S.J., et al. (2004). Expression of Cux-1 and Cux-2 in the subventricular zone and upper layers II-IV of the cerebral cortex. *J Comp Neurol* 479**,** 168-180.

Niquille, M., Garel, S., Mann, F., Hornung, J.P., Otsmane, B., Chevalley, S., et al. (2009). Transient neuronal populations are required to guide callosal axons: a role for semaphorin 3C. *PLoS Biol* 7**,** e1000230.

Niquille, M., Minocha, S., Hornung, J.P., Rufer, N., Valloton, D., Kessaris, N., et al. (2013). Two specific populations of GABAergic neurons originating from the medial and the caudal ganglionic eminences aid in proper navigation of callosal axons. *Dev Neurobiol* 73**,** 647-672.

Nirkko, A.C., Ozdoba, C., Redmond, S.M., Burki, M., Schroth, G., Hess, C.W., et al. (2001). Different ipsilateral representations for distal and proximal movements in the sensorimotor cortex: activation and deactivation patterns. *Neuroimage* 13**,** 825-835.

Noctor, S.C., Flint, A.C., Weissman, T.A., Dammerman, R.S., and Kriegstein, A.R. (2001). Neurons derived from radial glial cells establish radial units in neocortex. *Nature* 409**,** 714-720.

Noctor, S.C., Martinez-Cerdeno, V., Ivic, L., and Kriegstein, A.R. (2004). Cortical neurons arise in symmetric and asymmetric division zones and migrate through specific phases. *Nat Neurosci* 7**,** 136-144.

Noctor, S.C., Martinez-Cerdeno, V., and Kriegstein, A.R. (2007). Contribution of intermediate progenitor cells to cortical histogenesis. *Arch Neurol* 64**,** 639-642.

O'leary, D.D., Stanfield, B.B., and Cowan, W.M. (1981). Evidence that the early postnatal restriction of the cells of origin of the callosal projection is due to the elimination of axonal collaterals rather than to the death of neurons. *Brain Res* 227**,** 607-617.

O'shea, J., Sebastian, C., Boorman, E.D., Johansen-Berg, H., and Rushworth, M.F. (2007). Functional specificity of human premotor-motor cortical interactions during action selection. *Eur J Neurosci* 26**,** 2085-2095.

Olavarria, J., Malach, R., and Van Sluyters, R.C. (1987). Development of visual callosal connections in neonatally enucleated rats. *J Comp Neurol* 260**,** 321-348.

Olavarria, J., and Van Sluyters, R.C. (1985). Organization and postnatal development of callosal connections in the visual cortex of the rat. *J Comp Neurol* 239**,** 1-26.

Olavarria, J., and Van Sluyters, R.C. (1986). Axons from restricted regions of the cortex pass through restricted portions of the corpus callosum in adult and neonatal rats. *Brain Res* 390**,** 309-313.

Pandya, D.N., Karol, E.A., and Heilbronn, D. (1971). The topographical distribution of interhemispheric projections in the corpus callosum of the rhesus monkey. *Brain Res* 32**,** 31-43.

Paul, L.K., Brown, W.S., Adolphs, R., Tyszka, J.M., Richards, L.J., Mukherjee, P., et al. (2007). Agenesis of the corpus callosum: genetic, developmental and functional aspects of connectivity. *Nat Rev Neurosci* 8**,** 287-299.

Payne, B.R., and Siwek, D.F. (1991). The visual map in the corpus callosum of the cat. *Cereb Cortex* 1**,** 173-188.

Peng, J., and Charron, F. (2013). Lateralization of motor control in the human nervous system: genetics of mirror movements. *Curr Opin Neurobiol* 23**,** 109-118.

Perez, M.A., and Cohen, L.G. (2008). Mechanisms underlying functional changes in the primary motor cortex ipsilateral to an active hand. *J Neurosci* 28**,** 5631-5640.

Picard, N., and Strick, P.L. (1996). Motor areas of the medial wall: a review of their location and functional activation. *Cerebral cortex* 6**,** 342-353.

Piper, M., Moldrich, R.X., Lindwall, C., Little, E., Barry, G., Mason, S., et al. (2009a). Multiple non-cell-autonomous defects underlie neocortical callosal dysgenesis in Nfib-deficient mice. *Neural Dev* 4**,** 43.

Piper, M., Plachez, C., Zalucki, O., Fothergill, T., Goudreau, G., Erzurumlu, R., et al. (2009b). Neuropilin 1-Sema signaling regulates crossing of cingulate pioneering axons during development of the corpus callosum. *Cereb Cortex* 19 Suppl 1**,** i11-21.

Pont-Lezica, L., Beumer, W., Colasse, S., Drexhage, H., Versnel, M., and Bessis, A. (2014). Microglia shape corpus callosum axon tract fasciculation: functional impact of prenatal inflammation. *Eur J Neurosci* 39**,** 1551-1557.

Quinton, R., Duke, V.M., De Zoysa, P.A., Platts, A.D., Valentine, A., Kendall, B., et al. (1996). The neuroradiology of Kallmann's syndrome: a genotypic and phenotypic analysis. *J Clin Endocrinol Metab* 81**,** 3010-3017.

Rabe Bernhardt, N., Memic, F., Gezelius, H., Thiebes, A.L., Vallstedt, A., and Kullander, K. (2012). DCC mediated axon guidance of spinal interneurons is essential for normal locomotor central pattern generator function. *Dev Biol* 366**,** 279-289.

Raedler, E., and Raedler, A. (1978). Autoradiographic study of early neurogenesis in rat neocortex. *Anat Embryol (Berl)* 154**,** 267-284.

Rakic, P. (1971). Guidance of neurons migrating to the fetal monkey neocortex. *Brain Res* 33**,** 471-476.

Rakic, P. (1974). Neurons in rhesus monkey visual cortex: systematic relation between time of origin and eventual disposition. *Science* 183**,** 425-427.

Rakic, P., and Yakovlev, P.I. (1968). Development of the corpus callosum and cavum septi in man. *J Comp Neurol* 132**,** 45-72.

Rash, B.G., and Richards, L.J. (2001). A role for cingulate pioneering axons in the development of the corpus callosum. *J Comp Neurol* 434**,** 147-157.

Reddy, H., Lassonde, M., Bemasconi, N., Bemasconi, A., Matthews, P.M., Andermann, F., et al. (2000). An fMRI study of the lateralization of motor cortex activation in acallosal patients. *Neuroreport* 11**,** 2409-2413.

Reis, J., Swayne, O.B., Vandermeeren, Y., Camus, M., Dimyan, M.A., Harris-Love, M., et al. (2008). Contribution of transcranial magnetic stimulation to the understanding of cortical mechanisms involved in motor control. *J Physiol* 586**,** 325-351.

Ren, T., Anderson, A., Shen, W.B., Huang, H., Plachez, C., Zhang, J., et al. (2006). Imaging, anatomical, and molecular analysis of callosal formation in the developing human fetal brain. *Anat Rec A Discov Mol Cell Evol Biol* 288**,** 191-204.

Renier, N., Schonewille, M., Giraudet, F., Badura, A., Tessier-Lavigne, M., Avan, P., et al. (2010). Genetic dissection of the function of hindbrain axonal commissures. *PLoS Biol* 8**,** e1000325.

Richter, W., Andersen, P.M., Georgopoulos, A.P., and Kim, S.G. (1997). Sequential activity in human motor areas during a delayed cued finger movement task studied by time-resolved fMRI. *Neuroreport* 8**,** 1257-1261.

Robichaux, M.A., Chenaux, G., Ho, H.Y., Soskis, M.J., Greenberg, M.E., Henkemeyer, M., et al. (2016). EphB1 and EphB2 intracellular domains regulate the formation of the corpus callosum and anterior commissure. *Dev Neurobiol* 76**,** 405-420.

Rochefort, N.L., Buzas, P., Quenech'du, N., Koza, A., Eysel, U.T., Milleret, C., et al. (2009). Functional selectivity of interhemispheric connections in cat visual cortex. *Cereb Cortex* 19**,** 2451-2465.

Roebuck, T.M., Mattson, S.N., and Riley, E.P. (1998). A review of the neuroanatomical findings in children with fetal alcohol syndrome or prenatal exposure to alcohol. *Alcohol Clin Exp Res* 22**,** 339-344.

Romani, M., Micalizzi, A., and Valente, E.M. (2013). Joubert syndrome: congenital cerebellar ataxia with the molar tooth. *Lancet Neurol* 12**,** 894-905.

Rouiller, E.M., Babalian, A., Kazennikov, O., Moret, V., Yu, X.H., and Wiesendanger, M. (1994). Transcallosal connections of the distal forelimb representations of the primary and supplementary motor cortical areas in macaque monkeys. *Exp Brain Res* 102**,** 227-243.

Royal, S.A., Tubbs, R.S., D'antonio, M.G., Rauzzino, M.J., and Oakes, W.J. (2002). Investigations into the association between cervicomedullary neuroschisis and mirror movements in patients with Klippel-Feil syndrome. *AJNR Am J Neuroradiol* 23**,** 724-729.

Runker, A.E., Little, G.E., Suto, F., Fujisawa, H., and Mitchell, K.J. (2008). Semaphorin-6A controls guidance of corticospinal tract axons at multiple choice points. *Neural Dev* 3.

Sacher, G.A., and Staffeldt, E.F. (1974). Relation of gestation time to brain weight for placental mammals: implications for the theory of vertebrate growth. *American Naturalist***,** 593-615.

Sadato, N., Yonekura, Y., Waki, A., Yamada, H., and Ishii, Y. (1997). Role of the supplementary motor area and the right premotor cortex in the coordination of bimanual finger movements. *The Journal of neuroscience* 17**,** 9667-9674.

Sag, E., Gocmen, R., Yildiz, F.G., Ozturk, Z., Temucin, C., Teksam, O., et al. (2016). Congenital Mirror Movements in Gorlin Syndrome: A Case Report With DTI and Functional MRI Features. *Pediatrics* 137**,** 1-5.

Salerno, A., and Georgesco, M. (1996). Interhemispheric facilitation and inhibition studied in man with double magnetic stimulation. *Electroencephalography and Clinical Neurophysiology/Electromyography and Motor Control* 101**,** 395-403.

Sánchez‐Camacho, C., Ortega, J.A., Ocaña, I., Alcántara, S., and Bovolenta, P. (2011). Appropriate Bmp7 levels are required for the differentiation of midline guidepost cells involved in corpus callosum formation. *Developmental neurobiology* 71**,** 337-350.

Schell-Apacik, C.C., Wagner, K., Bihler, M., Ertl-Wagner, B., Heinrich, U., Klopocki, E., et al. (2008). Agenesis and dysgenesis of the corpus callosum: clinical, genetic and neuroimaging findings in a series of 41 patients. *Am J Med Genet A* 146A**,** 2501-2511.

Schwartz, M.L., and Goldman-Rakic, P.S. (1984). Callosal and intrahemispheric connectivity of the prefrontal association cortex in rhesus monkey: relation between intraparietal and principal sulcal cortex. *J Comp Neurol* 226**,** 403-420.

Segraves, M.A., and Rosenquist, A.C. (1982). The distribution of the cells of origin of callosal projections in cat visual cortex. *J Neurosci* 2**,** 1079-1089.

Serafini, T., Colamarino, S.A., Leonardo, E.D., Wang, H., Beddington, R., Skarnes, W.C., et al. (1996). Netrin-1 is required for commissural axon guidance in the developing vertebrate nervous system. *Cell* 87**,** 1001-1014.

Serafini, T., Kennedy, T.E., Galko, M.J., Mirzayan, C., Jessell, T.M., and Tessier-Lavigne, M. (1994). The netrins define a family of axon outgrowth-promoting proteins homologous to C. elegans UNC-6. *Cell* 78**,** 409-424.

Serradj, N., Paixao, S., Sobocki, T., Feinberg, M., Klein, R., Kullander, K., et al. (2014). EphA4-mediated ipsilateral corticospinal tract misprojections are necessary for bilateral voluntary movements but not bilateral stereotypic locomotion. *J Neurosci* 34**,** 5211-5221.

Serrien, D.J., Strens, L.H., Oliviero, A., and Brown, P. (2002). Repetitive transcranial magnetic stimulation of the supplementary motor area (SMA) degrades bimanual movement control in humans. *Neurosci Lett* 328**,** 89-92.

Sessa, A., Mao, C.A., Hadjantonakis, A.K., Klein, W.H., and Broccoli, V. (2008). Tbr2 directs conversion of radial glia into basal precursors and guides neuronal amplification by indirect neurogenesis in the developing neocortex. *Neuron* 60**,** 56-69.

Shen, Q., Wang, Y., Dimos, J.T., Fasano, C.A., Phoenix, T.N., Lemischka, I.R., et al. (2006). The timing of cortical neurogenesis is encoded within lineages of individual progenitor cells. *Nat Neurosci* 9**,** 743-751.

Shibasaki, H., and Hallett, M. (2006). What is the Bereitschaftspotential? *Clin Neurophysiol* 117**,** 2341-2356.

Shibasaki, H., and Nagae, K. (1984). Mirror movement: application of movement-related cortical potentials. *Ann Neurol* 15**,** 299-302.

Shu, T., Butz, K.G., Plachez, C., Gronostajski, R.M., and Richards, L.J. (2003a). Abnormal development of forebrain midline glia and commissural projections in Nfia knock-out mice. *J Neurosci* 23**,** 203-212.

Shu, T., Li, Y., Keller, A., and Richards, L.J. (2003b). The glial sling is a migratory population of developing neurons. *Development* 130**,** 2929-2937.

Shu, T., and Richards, L.J. (2001). Cortical axon guidance by the glial wedge during the development of the corpus callosum. *J Neurosci* 21**,** 2749-2758.

Shu, T., Sundaresan, V., Mccarthy, M.M., and Richards, L.J. (2003c). Slit2 guides both precrossing and postcrossing callosal axons at the midline in vivo. *J Neurosci* 23**,** 8176-8184.

Shu, T., Valentino, K.M., Seaman, C., Cooper, H.M., and Richards, L.J. (2000). Expression of the netrin-1 receptor, deleted in colorectal cancer (DCC), is largely confined to projecting neurons in the developing forebrain. *J Comp Neurol* 416**,** 201-212.

Silver, J., Lorenz, S.E., Wahlsten, D., and Coughlin, J. (1982). Axonal guidance during development of the great cerebral commissures: descriptive and experimental studies, in vivo, on the role of preformed glial pathways. *J Comp Neurol* 210**,** 10-29.

Smith, G.E. (1937). A Preliminary Communication upon the Cerebral Commissures of the Mammalia, with Special Reference to the Monotremata and Marsupialia. *J Anat* 71**,** 528-543.

Smith, K.M., Ohkubo, Y., Maragnoli, M.E., Rasin, M.R., Schwartz, M.L., Sestan, N., et al. (2006). Midline radial glia translocation and corpus callosum formation require FGF signaling. *Nat Neurosci* 9**,** 787-797.

Sohn, Y.H., Jung, H.Y., Kaelin-Lang, A., and Hallett, M. (2003). Excitability of the ipsilateral motor cortex during phasic voluntary hand movement. *Exp Brain Res* 148**,** 176-185.

Soteropoulos, D.S., Edgley, S.A., and Baker, S.N. (2013). Spinal commissural connections to motoneurons controlling the primate hand and wrist. *The Journal of Neuroscience* 33**,** 9614-9625.

Squarzoni, P., Thion, M.S., and Garel, S. (2015). Neuronal and microglial regulators of cortical wiring: usual and novel guideposts. *Front Neurosci* 9**,** 248.

Srivatsa, S., Parthasarathy, S., Britanova, O., Bormuth, I., Donahoo, A.L., Ackerman, S.L., et al. (2014). Unc5C and DCC act downstream of Ctip2 and Satb2 and contribute to corpus callosum formation. *Nat Commun* 5**,** 3708.

Srour, M., Riviere, J.B., Pham, J.M., Dube, M.P., Girard, S., Morin, S., et al. (2010). Mutations in DCC cause congenital mirror movements. *Science* 328**,** 592.

Stańák, A., Cohen, E.R., Seidler, R.D., Duong, T.Q., and Kim, S.-G. (2003). The size of corpus callosum correlates with functional activation of medial motor cortical areas in bimanual and unimanual movements. *Cerebral Cortex* 13**,** 475-485.

Steele-Perkins, G., Plachez, C., Butz, K.G., Yang, G., Bachurski, C.J., Kinsman, S.L., et al. (2005). The transcription factor gene Nfib is essential for both lung maturation and brain development. *Mol Cell Biol* 25**,** 685-698.

Stephan, K., Binkofski, F., Halsband, U., Dohle, C., Wunderlich, G., Schnitzler, A., et al. (1999). The role of ventral medial wall motor areas in bimanual co-ordination. *Brain* 122**,** 351-368.

Steyvers, M., Etoh, S., Sauner, D., Levin, O., Siebner, H.R., Swinnen, S.P., et al. (2003). High-frequency transcranial magnetic stimulation of the supplementary motor area reduces bimanual coupling during anti-phase but not in-phase movements. *Exp Brain Res* 151**,** 309-317.

Suarez, R., Fenlon, L.R., Marek, R., Avitan, L., Sah, P., Goodhill, G.J., et al. (2014a). Balanced interhemispheric cortical activity is required for correct targeting of the corpus callosum. *Neuron* 82**,** 1289-1298.

Suarez, R., Gobius, I., and Richards, L.J. (2014b). Evolution and development of interhemispheric connections in the vertebrate forebrain. *Front Hum Neurosci* 8**,** 497.

Sugitani, Y., Nakai, S., Minowa, O., Nishi, M., Jishage, K., Kawano, H., et al. (2002). Brn-1 and Brn-2 share crucial roles in the production and positioning of mouse neocortical neurons. *Genes Dev* 16**,** 1760-1765.

Suto, F., Ito, K., Uemura, M., Shimizu, M., Shinkawa, Y., Sanbo, M., et al. (2005). Plexin-a4 mediates axon-repulsive activities of both secreted and transmembrane semaphorins and plays roles in nerve fiber guidance. *J Neurosci* 25**,** 3628-3637.

Talelli, P., Ewas, A., Waddingham, W., Rothwell, J.C., and Ward, N.S. (2008). Neural correlates of age-related changes in cortical neurophysiology. *Neuroimage* 40**,** 1772-1781.

Tanji, J. (1996). New concepts of the supplementary motor area. *Curr Opin Neurobiol* 6**,** 782-787.

Tanji, J., and Mushiake, H. (1996). Comparison of neuronal activity in the supplementary motor area and primary motor cortex. *Cognitive Brain Research* 3**,** 143-150.

Tarabykin, V., Stoykova, A., Usman, N., and Gruss, P. (2001). Cortical upper layer neurons derive from the subventricular zone as indicated by Svet1 gene expression. *Development* 128**,** 1983-1993.

Terashima, T., Inoue, K., Inoue, Y., Mikoshiba, K., and Tsukada, Y. (1985). Distribution and morphology of callosal commissural neurons within the motor cortex of normal and reeler mice. *J Comp Neurol* 232**,** 83-98.

Thacker, J. (2005). The RAD51 gene family, genetic instability and cancer. *Cancer Lett* 219**,** 125-135.

Thapa, R., and Mukherjee, K. (2010). Seckel syndrome with asymptomatic tonsillar herniation and congenital mirror movements. *J Child Neurol* 25**,** 231-233.

Tole, S., Gutin, G., Bhatnagar, L., Remedios, R., and Hebert, J.M. (2006). Development of midline cell types and commissural axon tracts requires Fgfr1 in the cerebrum. *Dev Biol* 289**,** 141-151.

Tomasch, J. (1954). Size, distribution, and number of fibres in the human corpus callosum. *Anat Rec* 119**,** 119-135.

Toyokura, M., Muro, I., Komiya, T., and Obara, M. (1999). Relation of bimanual coordination to activation in the sensorimotor cortex and supplementary motor area: analysis using functional magnetic resonance imaging. *Brain research bulletin* 48**,** 211-217.

Tzourio-Mazoyer, N., Petit, L., Zago, L., Crivello, F., Vinuesa, N., Joliot, M., et al. (2015). Between-hand difference in ipsilateral deactivation is associated with hand lateralization: fMRI mapping of 284 volunteers balanced for handedness. *Front Hum Neurosci* 9.

Uhl, F., Kornhuber, A., Wartberger, P., Lindinger, G., Lang, W., and Deecke, L. (1996). Supplementary motor area in spatial coordination of bilateral movements: a new aspect to 'the SMA debate'? *Electroencephalography and Clinical Neurophysiology/Electromyography and Motor Control* 101**,** 469-477.

Ullen, F., Forssberg, H., and Ehrsson, H.H. (2003). Neural networks for the coordination of the hands in time. *J Neurophysiol* 89**,** 1126-1135.

Unni, D.K., Piper, M., Moldrich, R.X., Gobius, I., Liu, S., Fothergill, T., et al. (2012). Multiple Slits regulate the development of midline glial populations and the corpus callosum. *Dev Biol* 365**,** 36-49.

Utsunomiya, H., Yamashita, S., Takano, K., Ueda, Y., and Fujii, A. (2006). Midline cystic malformations of the brain: imaging diagnosis and classification based on embryologic analysis. *Radiation medicine* 24**,** 471-481.

Verstynen, T., Diedrichsen, J., Albert, N., Aparicio, P., and Ivry, R.B. (2005). Ipsilateral motor cortex activity during unimanual hand movements relates to task complexity. *J Neurophysiol* 93**,** 1209-1222.

Verstynen, T., Spencer, R., Stinear, C.M., Konkle, T., Diedrichsen, J., Byblow, W.D., et al. (2007). Ipsilateral corticospinal projections do not predict congenital mirror movements: a case report. *Neuropsychologia* 45**,** 844-852.

Verzijl, H.T., Van Der Zwaag, B., Cruysberg, J.R., and Padberg, G.W. (2003). Mobius syndrome redefined: a syndrome of rhombencephalic maldevelopment. *Neurology* 61**,** 327-333.

Vorobiev, V., Govoni, P., Rizzolatti, G., Matelli, M., and Luppino, G. (1998). Parcellation of human mesial area 6: cytoarchitectonic evidence for three separate areas. *Eur J Neurosci* 10**,** 2199-2203.

Wahl, M., Strominger, Z., Jeremy, R., Barkovich, A., Wakahiro, M., Sherr, E., et al. (2009). Variability of homotopic and heterotopic callosal connectivity in partial agenesis of the corpus callosum: a 3T diffusion tensor imaging and Q-ball tractography study. *American Journal of Neuroradiology* 30**,** 282-289.

Wahlsten, D., Bishop, K.M., and Ozaki, H.S. (2006). Recombinant inbreeding in mice reveals thresholds in embryonic corpus callosum development. *Genes Brain Behav* 5**,** 170-188.

Wang, A.T., Kim, T., Wagner, J.E., Conti, B.A., Lach, F.P., Huang, A.L., et al. (2015). A Dominant Mutation in Human RAD51 Reveals Its Function in DNA Interstrand Crosslink Repair Independent of Homologous Recombination. *Mol Cell* 59**,** 478-490.

Wang, C.L., Zhang, L., Zhou, Y., Zhou, J., Yang, X.J., Duan, S.M., et al. (2007). Activity-dependent development of callosal projections in the somatosensory cortex. *J Neurosci* 27**,** 11334-11342.

Wang, X., Tsai, J.W., Lamonica, B., and Kriegstein, A.R. (2011). A new subtype of progenitor cell in the mouse embryonic neocortex. *Nat Neurosci* 14**,** 555-561.

Wang, Y., Thekdi, N., Smallwood, P.M., Macke, J.P., and Nathans, J. (2002). Frizzled-3 is required for the development of major fiber tracts in the rostral CNS. *J Neurosci* 22**,** 8563-8573.

Webb, B.D., Frempong, T., Naidich, T.P., Gaspar, H., Jabs, E.W., and Rucker, J.C. (2014). Mirror movements identified in patients with moebius syndrome. *Tremor Other Hyperkinet Mov (N Y)* 4**,** 256.

Welniarz, Q., Dusart, I., Gallea, C., and Roze, E. (2015). One hand clapping: lateralization of motor control. *Frontiers in Neuroanatomy* 9.

Wilhelm, E., Quoilin, C., Petitjean, C., and Duque, J. (2016). A Double-Coil TMS Method to Assess Corticospinal Excitability Changes at a Near-Simultaneous Time in the Two Hands during Movement Preparation. *Front Hum Neurosci* 10.

Woods, B.T., and Teuber, H.-L. (1978). Mirror movements after childhood hemiparesis. *Neurology* 28**,** 1152-1157.

Wyss, J.M., Swanson, L.W., and Cowan, W.M. (1980). The organization of the fimbria, dorsal fornix and ventral hippocampal commissure in the rat. *Anat Embryol (Berl)* 158**,** 303-316.

Yorke, C.H., Jr., and Caviness, V.S., Jr. (1975). Interhemispheric neocortical connections of the corpus callosum in the normal mouse: a study based on anterograde and retrograde methods. *J Comp Neurol* 164**,** 233-245.

Zang, Y., Jia, F., Weng, X., Li, E., Cui, S., Wang, Y., et al. (2003). Functional organization of the primary motor cortex characterized by event-related fMRI during movement preparation and execution. *Neurosci Lett* 337**,** 69-72.

Zhao, H., Maruyama, T., Hattori, Y., Sugo, N., Takamatsu, H., Kumanogoh, A., et al. (2011). A molecular mechanism that regulates medially oriented axonal growth of upper layer neurons in the developing neocortex. *J Comp Neurol* 519**,** 834-848.

Zhou, J., Wen, Y., She, L., Sui, Y.N., Liu, L., Richards, L.J., et al. (2013). Axon position within the corpus callosum determines contralateral cortical projection. *Proc Natl Acad Sci U S A* 110**,** E2714-2723.

Ziemann, U., and Hallett, M. (2001). Hemispheric asymmetry of ipsilateral motor cortex activation during unimanual motor tasks: further evidence for motor dominance. *Clin Neurophysiol* 112**,** 107-113.

Résumé

Le syndrome des mouvements en miroir congénitaux (MMC) est une maladie génétique caractérisée par l'existence de mouvements involontaires symétriques d'une main qui reproduisent à l'identique les mouvements volontaires de l'autre main. Deux structures sont impliquées dans la physiopathologie de cette maladie : le corps calleux (CC) et le faisceau corticospinal (FCS). Deux gènes ont été liés aux MMC à ce jour : *DCC* et *RAD51*. Tandis que *DCC* joue un rôle crucial dans le guidage des axones commissuraux, *RAD51* intervient dans la réparation de l'ADN, et son rôle dans le développement du système moteur était inattendu.

Chez la souris, nous avons étudié le rôle de *RAD51* et *DCC* dans le développement du FCS et du CC, ainsi que l'implication de ces deux structures dans la latéralisation du contrôle moteur. Nous avons prouvé que DCC contrôle le guidage du FCS à la ligne médiane de façon indirecte. RAD51 intervient dans le développement du neocortex, mais son rôle précis dans le développement du système moteur demeure inconnu.

Nous avons par ailleurs comparé un groupe de patients MMC à des volontaires sains afin d'étudier la latéralisation de l'activité corticale lors de la préparation motrice. L'activation et les interactions inter-hémisphériques des aires motrices sont anormales dès la préparation du mouvement chez les patients MMC. L'inhibition de l'aire motrice supplémentaire (AMS) chez les volontaires sains reproduit les défauts d'interactions inter-hémisphériques observés chez les patients. Ces résultats suggèrent que l'AMS est impliquée dans la préparation des mouvements latéralisés, potentiellement en modulant les interactions entre les deux hémisphères via le CC.

Abstract

Mirror movements are involuntary symmetrical movements of one side of the body that mirror voluntary movements of the other side. Congenital mirror movements (CMM) is a rare genetic disorder transmitted in autosomal dominant manner, in which mirror movements are the only clinical abnormality. Two structures are involved in the physiopathology of CMM: the corpus callosum (CC) and the corticospinal tract (CST). The two main culprit genes identified so far are *DCC* and *RAD51*. While the role of DCC in commissural axons guidance during development is well known, RAD51 is involved in DNA repair, and its link with CMM was totally unexpected.

In mice, we investigated the role of RAD51 and DCC in the development of the CC and CST, as well as the role of these two structures in motor lateralization. We showed that DCC controls CST midline crossing in an indirect manner. Our work clarified the role of RAD51 in neocortex development, but how RAD51 influences motor system development remains unknown.

We compared a group of CMM patients with healthy volunteers to investigate the lateralization of cortical activity during movement preparation. We showed that activation of motor/premotor areas and interhemispheric interactions during movement preparation differed between the CMM patients and healthy volunteers. Transient inhibition of the supplementary motor area (SMA) in the healthy volunteers resulted in abnormal interhemispheric interactions during movement preparation, reminiscent of the situation observed in the patients. These results suggest the SMA is involved in lateralized movements preparation, potentially by modulating interhemispheric interactions via the CC.